University of Huddersfield Repository

Al-Jasmin, Ammar

Synthesis and Characterisation of Novel Sophorolipids and Their Applications

Original Citation

Al-Jasmin, Ammar (2016) Synthesis and Characterisation of Novel Sophorolipids and Their Applications. Masters thesis, University of Huddersfield.

This version is available at http://eprints.hud.ac.uk/id/eprint/29193/

http://eprints.hud.ac.uk/

SYNTHESIS AND CHARACTERISATION OF NOVEL SOPHOROLIPIDS AND THEIR APPLICATIONS

Ammar A. M. AL-Jasim BSc (Hons), MSc

University of
HUDDERSFIELD
Inspiring tomorrow's professionals

A thesis submitted to the University of Huddersfield in partial
fulfilment of the requirements for the degree of Doctor of Philosophy

Departments of Chemical and Biological Sciences
School of Applied Sciences
The University of Huddersfield

June 2016

Dedication

This thesis is dedicated to the memory of my father, Abdulsahib AL-Jasim and to my beloved mother, Fareeda ALrade, who has been a source of encouragement and inspiration throughout my life.

I also dedicate it to my sister Zainab AL-Jasim and my dear loving Sabrine Bousoutine. Without their sacrifices, support and love, I would have never accomplished what I have been able to. I am forever grateful for everything they have done for me.

Ammar AL-Jasim

Acknowledgments

Abstract

The present study investigated the structural characterisation of the fermentation products (sophorolipids) produced by *Candida. bombicola.* The analysis included the use of 1D- and 2D-NMR, FT-IR, HPLC-MS, monomer and linkage analysis employing HPAEC-PAD and GC-MS to fully characterise the main fermentation products: sophorolipids lactone and acid forms. The characterisation also looked at materials present in waste streams. Interestingly, free sophorose was identified in a number of the waste streams. The composition of the lactone waste stream was investigated utilizing HPAEC-PAD and NMR techniques. The results indicated the presence of glucose, sophorose and trace amount of isomaltose; these were separated using a liquid-liquid extraction technique followed by the isolation of each sugar using carbon: celite 535 column chromatography. Attempts were made to determine the origin of sophorose in the waste streams. In aqueous alkali, sophorose was observed to undergo an epimerisation reaction and was converted to 2-*O*-β-D-glucopyranosyl-D-mannose. Another experiment was performed to investigate if enzyme(s) were present in the spent fermentation liquors, which were capable of hydrolysing sophorolipids to produce sophorose. The result suggested that sophorolipids were being converted into sophorose, glucose, isomaltose, and a glucolipid.

A number of novel sophorolipids were synthesised starting from sophorose and using both enzyme and chemical glycosylation reactions. The lipase Novozyme 435 was used to catalyse the synthesis of the sophorolipid derivatives: 1′,6″-sophorolactone, 1′,6″-sophorolactone-6′-acetate and methyl ester-6′,6″-sophorose dibutyrate. Sophorose was used in the preparation of 2″,3′,3″,4′,4″,6′,6″-hepta-*O*-acetyl-α-D-sophoryl bromide, which was coupled to a range of different fatty alcohols. Finally, the interfacial properties, enzyme inhibition effect and biological activity of a number of novel sophorolipids were explored.

Contents

Abbreviations

$Å^2$	Area per surface molecule
CMC	Critical micelle concentration
CPR	Cytochrome P450 reductase
CoA	Acetyl-coenzyme A
$CDCl_3$	Deuterated chloroform
DMSO	Dimethyl sulfoxide
D_2O	Deuterium oxide
FTIR	Fourier Transform Infrared
GC-MS	Gas Chromatography-Mass spectrometry
HPAEC-PAD	High-Performance Anion Exchange Chromatography-Pulsed Amperometric Detector
HPLC-MS	High-pressure Liquid Chromatography-Mass Spectrometry
MEL	Mannosylerthritol lipids
MPLC	Medium pressure liquid chromatography
MALDI-TOF	Matrix assisted laser desorption ionization-time of flight
mN/m	Millinewton per metre
mL	Millilitres
NaOD	Sodium deuteroxide
NMR	Nuclear magnetic resonance
NADPH	Nicotinamide Adenine dinucleotide phosphate
PPL	Porcine pancreatic lipase
ppm	Part per million
PMAA	Permethylated alditol acetates
pH	Hydrogen ion concentration
SL-Crude	Crude (initial) sophorolipid
SL-Lactone	Lactone sophorolipid
SL-Acid	Acid sophorolipid
SL-Me	Methyl ester sophorolipid
SL-Et	Ethyl ester sophorolipid
TFA	Trifluoroacetic acid
THF	Tetrahydrofuran
TLC	Thin layer chromatography
µL	Microlitre
UV	Ultraviolet spectroscopy
UPD	Uridine diphosphate glucose
v/v	Volume per volume
w/v	Weight per volume
γ_{cmc}	Surface tension
Γ_{max}	Surface excess

Chapter one: General Introduction

1. General Introduction

Sophorolipids (sophorose-lipids) are classified as biological surface-active compounds, which have been known for almost 45 years as biosurfactants. Sophorolipids can be produced by some yeast strains and they display low ecotoxicity and are considered biodegradable. [1,2] These characteristics make them commercially attractive. Millions of tons of chemical-based surfactants are produced each year, and these are used in a wide range of applications: in cleaning, in the manufacture of food and paper, cosmetics, and as health care products. [3,4] However, the majority of chemically synthesised surfactants display some degree of toxicity, especially to the environment and their frequent use and release into the environment, especially when used in washing application, is of growing concern. [5,6] The ecotoxicity and biodegradability are of significant concern to our current society. In contrast, sophorolipids are considered to be green glycolipid-surfactants and can be viewed as natural products. [7] Glycolipids are composed of sugar (carbohydrate part) and a fatty acid part. They are classified as nonionic surfactants and have seen an increased interest in their use during the last twenty years. They are environmentally compatible and still retain functional surface properties comparable to those chemical-based surfactants. Glycolipid biosurfactants, particularly rhamnolipids and sophorolipids also demonstrate improved skin compatibility, which is a characteristic that is highly desirable for personal care and cosmetic applications. The production of glycolipid biosurfactants via the fermentation pathway has led to the replacement of first generation glycolipids (*i.e.,* alkyl poly glucosides), substituting those generated by chemical methods.[8] The production of sophorolipids is also attractive from a substantial consideration. It has been estimated that in the Europe, 50% of current surfactant production derives the hydrophobic component from palm or coconut oil [9] diverting these materials away from food production. Glycolipds includes sophorolipids, rhamnolipids, mannosylerthritol lipids and cellobiolipids. These are produced in high yield by nonpathogenic yeasts or bacteria where the most productive strains (Table 1-1) are belonging to different species. [10]

Table 1-1: Microbial source of important types of biosurfactants [8]

Biosurfactant type	Producing organism
(Low molecular weight) Glycolipids	
Rhamnolipids	*Pseudomonas aeruginosa, Pseudomonas* sp.
Trehalolipids	*Rhodococus Erythropolis, Nocardia erythropolis Mycobacterium* sp.
Sophorolipids	*Candida. bombicola, Camdida. apicola, and Rhodotorula bogoriensis*
Mannosylerythritol lipids	*Pseudozyma antarctica*
Cellobiolipids	*Ustilago zeae, U. maydis*
Lipopeptides and lipoproteins	
Peptide-lipid	*Bacillus licheniformis*
Serrawettin	*Serratia marcescens*
Viscosin	*Ps. fluorescens*
Surfactin	*Bacillus. subtilis*
Gramicidins	*Bacillus. brevis*
Polymyxins	*Bacillus. polymyxa*
Fatty acids, neutral lipids and phospholipids	
Fatty acids	*C. lepus*
Neutral lipids	*R. erythropolis*
Phospholipids	*Thiobacillus thiooxidans*
Polymeric surfactants	
Emulsan	*Acinetobacter calcoaceticus*
Biodispersan	*Acinetobacter. calcoaceticus*
Mannan-lipid-protein	*Candida. tropicalis*
Carbohydrate-protein-lipid	*Pseudomonas. fluorescens Debaryomyces polymorphis*
Protein PA	*Pseudomonas. aeruginosa*

1.1 Surfactants

1.1.1 Definition of surfactants and their applications

Surfactants are defined as surface-active agents capable of decreasing the surface tension between two different phases *e.g.,* liquids, solids, and gases, allowing them to disperse readily in liquids. Most surfactants are produced by organic chemical reactions and are considered as amphiphilic molecules (Figure 1-1) *i.e.,* they are composed of a hydrophilic and a hydrophobic part that interact with the phase boundary in liquid systems. The hydrophobic, non-polar "part" is usually a hydrocarbon chain whereas the hydrophilic, polar "head" can be derived from a variety of different polar entities including carbohydrates, alcoholalkoxylates, amino acids, phosphates, carboxylates, sulphates, and sulphonates. [11]
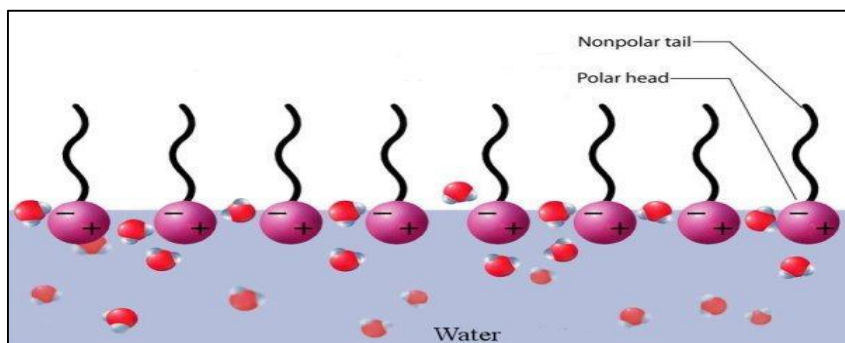
Figure 1-1: Surfactant molecules organised on an air–water interface

Surfactants are the most important products of industrial chemicals with a current total global production exceeding 10 million tons a year and is estimated half of that is used in household and laundry detergents, while the other half involved in a variety of industrial sectors, such as the chemical and food industry, cosmetics and personal care and paper industry. [12-14] In addition to their use as surface-active agents, a number of surfactants possess biological activity including antimicrobial, antitumor, and antiviral properties. [15-18]

3

Currently, a number of commercial surfactants are petroleum-based products around 80%. These surfactants are not very biodegradable and possess high levels of ecotoxicity, therefore, there is an increasing concern about the large-scale use of a number of common chemical-surfactants. [5,6,19]

1.1.2 Characteristics of surfactants

The activity of a surfactant can be evaluated by determining its ability to lower the surface tension between either oil and water inter-phases or water and air interface. The symbols γ or σ are detonated for the surface tension, which is the force (F) along a line with length (L), where the force is parallel to the surface and perpendicular to the line. Surface tension is defined as the force per unit length ($\gamma = F/L$) and the SI unit of surface tension is N/m. Another characteristic of surfactants which is used to determine their performance is their critical micelle concentration (CMC, Figure 1-2) which is referred to as the concentration above which the micelles are formed. Surfactant molecules can align themselves with the surface of the air-water interface such that the polar group interacts with water and the non-polar group are arranged above the water surface. The way these molecules present at the interfacial surface will disrupt the surface's cohesive force, thus reducing the surface tension.
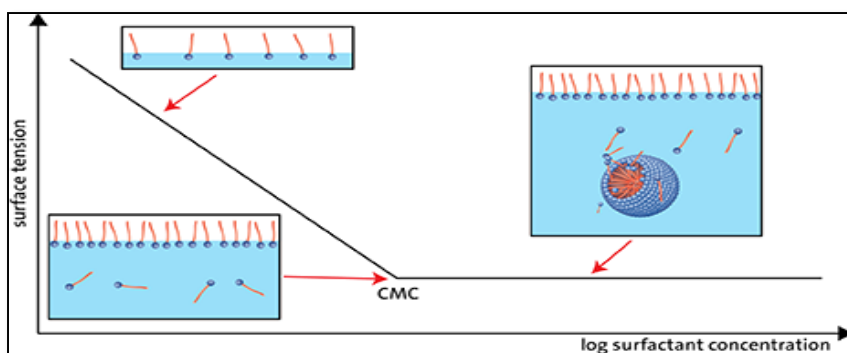
Figure 1-2: A plot of log surfactant concentration versus surface tension showing the CMC formation point established when the micelles start to form. [20]

The surface tension decreases after the addition of the surfactant to the water until the CMC is reached. Beyond the CMC point, the addition of surfactant will cause no further decrease in surface tension as micelles are already formed, meaning that hydrophobic groups are oriented within the micelles and hydrophilic groups are exposed to the water. To determine the surface excess **Γmax** of a surfactant component, Gibbs derived a mathematical equation, which explains the relationship between the surface tension γ and the surface excess **Γmax**, which is defined as the adsorption per unit area. [21] The equation is **dγ /dlog C= −2.303 Γ RT…. (1-1)**, where **C**: the concentration of surfactant, **R**: the gas constant, and **T**: the absolute temperatures. Thus, the amount of the adsorbed surfactant **Γmax** (mol/m^2) [21] can be determined using this adsorption equation.

1.2 Biosurfactants

1.2.1 Introduction

Biosurfactants are biologically produced molecules, which are synthesised using microorganisms (yeast, fungi and bacteria) when they are grown in an aqueous media and supplied with a carbon source as a feedstock, such as mixtures of carbohydrates, hydrocarbons, oils and fats. [22] Biosurfactants are usually composed of a lipophilic part *e.g.* a carbohydrate, protein, or peptide and a hydrophobic chain *e.g.*, a hydrocarbon chain of a fatty acid with 10 to 18 carbon atoms. The hydrophilic head can be an amino acid, ester, hydroxyl, carboxylate, mono-, di-, or polysaccharides. [23,24] As this research project focuses on the glycolipid sophorolipids, this group will be discussed in more detail.

The chemical structure of biosurfactants is mainly determined by the producing organism and is also influenced by the culture conditions. Biosurfactants are classified according to their structure into one of four groups based on their chemical composition: (1) glycolipids, (2) oligopeptides and lipopeptides, phospholipids, (3) fatty acids and neutral lipids and (4) polymeric biosurfactants. The most important microbial surfactants are listed in (Table 1-1).

1.2.2 Glycolipids

Glycolipids are biosurfactants which are composed of polar head groups derived from simple sugars which are connected to either fatty acids, hydroxy fatty acids or fatty alcohols as the non-polar hydrocarbon tail. The sugar component can be mono-, di-, tri- or tetrasaccharides. [25,26] Glycolipids are usually produced in high yield and can use renewable resources for their carbon feeds and for this reason they are considered as desirable surfactants for commercial production. [27] The most studied glycolipids (Table 1-1) are rhamnolipids produced by *Pseudomonas* sp., [28] mannosylerythriol lipids produced by *Pseudozyma Antarctica,* [29] trehalose lipids produced by *Rhodococcus* sp., *Nocardia* sp., [30] and sophorolipids produced by *Candida bombicola and Candida apicola.* [30,31]

1.2.2.1 Rhamnolipids

Rhamnolipids are synthesised by the bacteria, *P. aeruginosa,* [32-34] which can generate materials with yields higher than 100 g/L. Rhamnolipids are a combination of a number of similar molecules. To form the most important types of rhamnolipids, either one or two rhamnose molecules linked to one or two β-hydroxydecanoic acids. [33,35] Figure (1-3) shows the structure of a rhamnolipid with two rhamnose molecules and two β-hydroxydecanoic acid units.
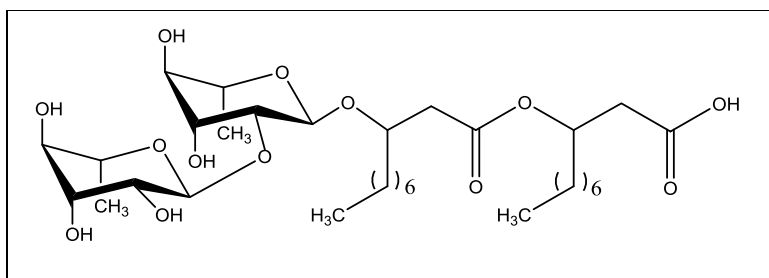
Figure 1-3: Chemical structure of rhamnolipid

1.2.2.2 Sophorolipids

Sophorolipids (SLs) are glycolipid surfactants, which are composed of the disaccharide sophorose (2-*O*-β-D-glucopyranosyl-α-D-glucose) linked by a β-glycosidic bond to a hydroxyl fatty acid chain of between 10 to 18 carbon atoms (Figure 1-4). Sophorolipids are produced by various microorganisms, such as; *Torulopsis sp.* or *Candida sp.,* such as *C.bombicola*, *C.apicola and Wickerhamiella domercqiae* has also been shown to produce sophorolipids. [36,37]

(a): 17-L-((2'-O-D-glucopyranosyl)-oxy)-9-octadecenoic acid 1',4"-lactone 6',6"-diacetate
(b): 17-L-((2'-O-D-glucopyranosyl)-oxy)-9-octadecenoic acid
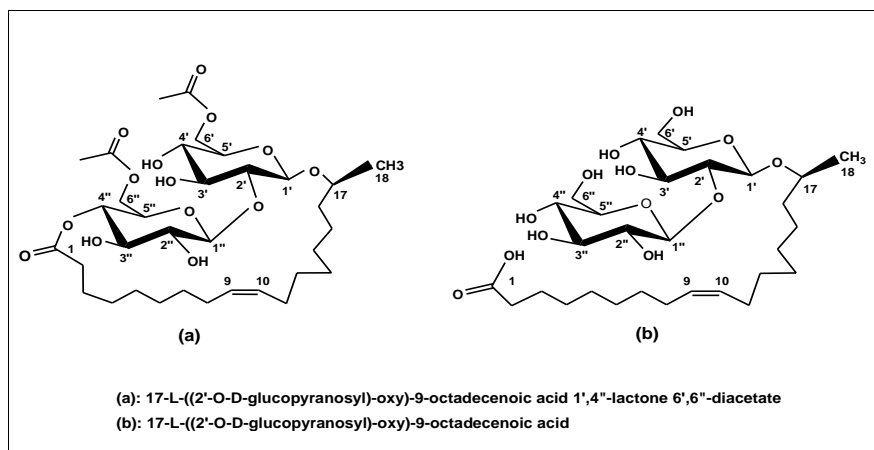
Figure 1-4: Chemical structure of natural sophorolipids

Natural (classical) sophorolipids are of two types namely, the acidic and the lactonic form. The hydroxylated fatty acid chain of the acid form sophorolipid possesses a free carboxylic acid (COOH) functional group. In contrast, the fatty acid chain of the lactone sophorolipid forms a macrocyclic lactone ring in which the 4″-hydroxyl group of the sophorose is attached to the lipid by intramolecular esterification. [38,39]

1.2.2.3 Mannosylerythritol lipids

The mannosylerythritol lipids (MEL) are classified into four types: MEL-A and B as major classes, MEL C and D as minor products (Figure 1-5). The mannose-erythritol moiety is the main sugar component of these glycolipids on which either a short chain fatty acid of C-2 to C-8 or longer chain of C-10 to C-18 carbon atoms are acetylated. [29,30,41]

MELs demonstrate excellent interfacial surface-activity. They were produced by *Pseudozyma siamensis* and capable of reducing the water surface tension to 35 mN/m at 25 [0] C. They also possess biological activity, such as protein binding towards immunoglobulin G and lectin. [22, 42]
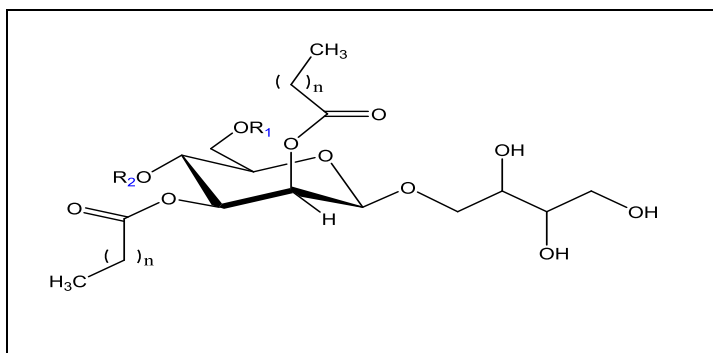
Figure 1-5: **Chemical structure of mannosylerythritol lipids (MEL): Type A: $R_1 = R_2 =$ acetyl, Type B: $R_1 =$ acetyl and $R_2 =$ H, type C: $R_1 =$ H, $R_2 =$ acetyl, type D: $R_1 = R_2 =$ H, n = 6-12.** [30]

1.2.2.4 Trehalose lipids

Trehalose glycolipids, possess the α-1,1 linked glucoses as a disaccharide and are attached to mycolic acids at C-6 and C-6′ position. Mycolic acid is long chain α-branched-β-hydroxy fatty acids (Figure 1-6). Trehalose lipids are produced by bacteria such as *Mycobacterium* sp., and *Rhodococcus* sp. However, *R. erythropolis* was found the most productive strain that synthesises a mixture of surfactants. [24] The major components are trehalose mycolates.

8

It was demonstrated that specific growth conditions, nitrogen deficiency, can lead to the production of anionic trehalose tetra-esters. [24,43]
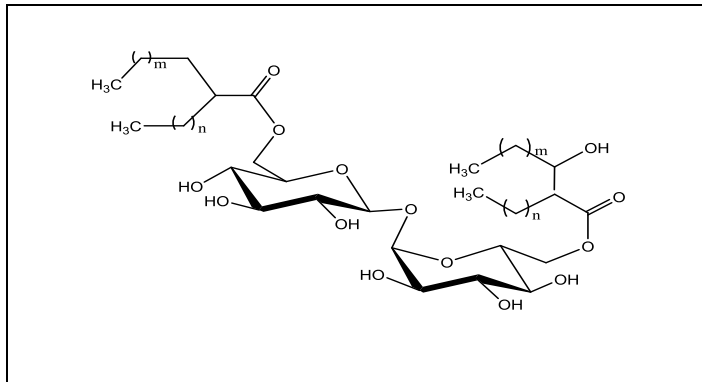
Figure 1-6: Chemical structure of trehalose-dicorynomycolates. n + m = 27 to 30.[8]

1.2.3 Lipopeptides

The chemical structures of lipopeptides are composed of amino acids linked to fatty acids chain. There are many types of lipopeptides synthesised by bacteria, among them *Bacillus subtilus*, which produces surfactin, that comprises of seven amino acids attached to a carboxyl (COOH) and hydroxyl (OH) groups of a C-14 fatty acid chain (Figure 1-7). Lipopeptides possesses antibacterial, antifungal and antiviral activities. [44] The antibiotic activity is linked to the lipopeptides ability to reduce the surface tension of water from 72.8 to 27.9 mN/m. [45]
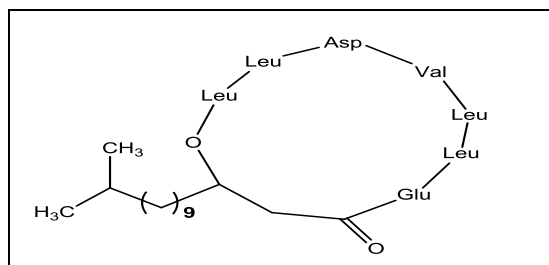
Figure 1-7: Structure of surfactin

1.2.4 Fatty acids

These biosurfactants are composed entirely of a carboxyl group with a long methylene hydrocarbon chain; some examples are spiculisporic acids and corynomycolic acids. Alkanes hydrophobic substrates are necessary for the growth of significant number of yeasts, fungi and bacteria (*Aspergillus* sp. and *Acinetobacter* sp.) to secrete considerable amount of fatty acids, phospholipids or neutral lipids to assist the utilization of the carbon source. [46]

1.2.5 Phospholipids

A number of particular bacterial strains, such as *Aspergillus* sp.,[47] and *Thiobacillus thiooxidans* [48] are capable of synthesising phospholipid based biosurfactants. For instance, phospholipid-based biosurfactants were produced by *acinetobacter* sp., when grown on hexadecane as a substrate. The phosphatidylethanolamine, structure shown in (Figure 1-8) was produced by *Rhodococcus erythropolos* when grown on an n-alkane substrate.
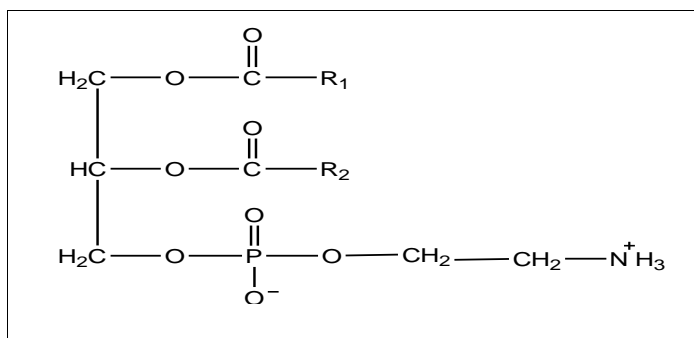
Figure 1-8: Structure of phosphatidylethanolamine, R_1 and R_2 are fatty acid chain [24]

1.2.6 Polymeric biosurfactant

Polymeric biosurfactants are composed of several components. Emulsan is a known studied example of a polymeric surfactant, which is produced by *Acinetobacter calcoaceticus*. The structure of emulsan composed of a polysaccharide backbone to which fatty acids are linked covalently. [49] Another example synthesised by the yeast *Yarrowia lipolytica* is liposan, a complex of carbohydrate and protein. [50]
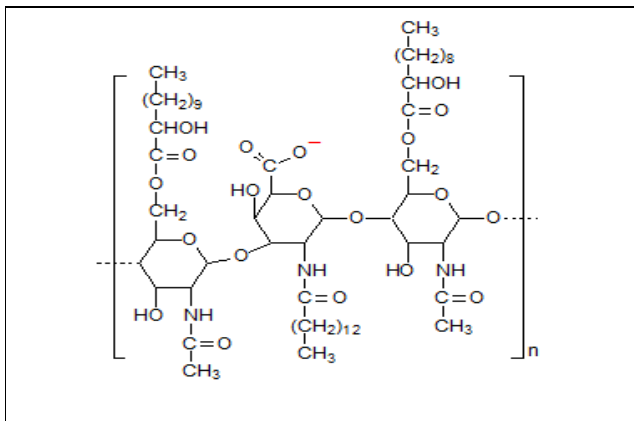
Figure 1-9: Structure of emulsan [51-52]

1.3 Sophorolipid production

1.3.1 Introduction

As was stated above, sophorolipids are biosurfactants in which the disaccharide sophorose is linked to a hydroxy fatty acid. As sophorolipids are the main focus of the current research programme more details about the organisms producing these biosurfactants and the biosynthetic pathway leading to sophorolipid production will be provided in section 1.3.4.

11

1.3.2 Sophorolipids producing microorganisms

Gorin *et al.,* [53] were one of the first researchers who described sophorolipids as extracellular glycolipids produced by the yeast *Torulopsis magnoliae*. In 1968, Tulloch and Spencer confirmed that the secreting strain was *T. apicola*, which is recently known as *Candida apicola*. During the same year, the authors also reported the use of *Candida bogoriensis* in the production of a new sophorolipids. [54] The sophorolipids chemical structure is analogous to that of sophorolipid produced by *Candida apicola*, however, it differs only at the point where the sophorose moiety is linked to a 13-hydroxydodecanoic acid moiety.

The species, *Candida bombicola* (or *Torulopsis bombicola*); *was* the third productive yeast strain, which was also discovered by Tulloch and Spencer. The production yield and structure characteristics were nearly identical to those of *C. apicola.* [55] In 1998, the yeast species *Starmerella bombicola* was described by Rosa and Lachance and presented it as *C.bombicola.* Later on, in 2006, Chen *et al.,* confirmed the production of sophorolipid using a newly discovered strain of *Wickerhamiella domericqiae.* [40,18] In their study, they confirmed the production of more than six sophorolipids, one of the three major products was identified as 17-L-(-oxy)-octadecenoic acid 1,4″-lactone-6′,6″-diacetate, which is identical to the main sophorolipid form produced by the strain; *C. bombicola* and *C. apicola*.

The yeast *Candida bombicola* ATCC 22214 (Figure 1-10) is known to produce high yields of sophorolipids, approximately, 400 g/L. [56] Therefore, it is considered as the preferred strain for commercial production.
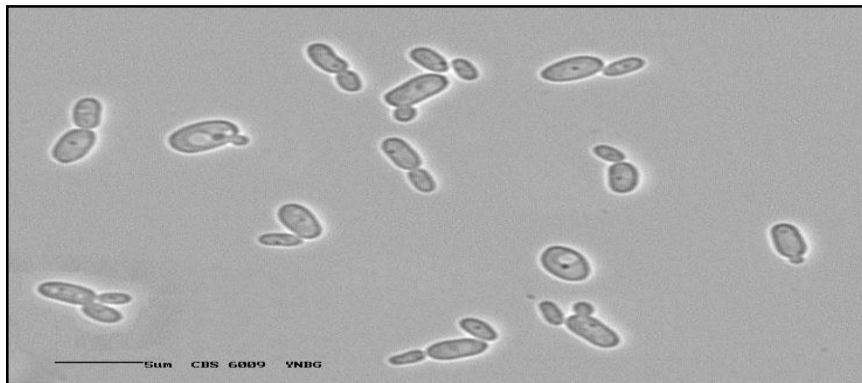
Figure 1-10: Microscopic image of *C. bombicola* cells, the length of the bar is 5 µm. [57]

1.3.3 Structure, properties and nomenclature

Sophorolipids are composed of a terminal or subterminal hydroxylated fatty acid, sophorose (2′-*O*-β-D-glucopyranosyl-β-D-glucopyranose) is a molecule containing two glucose joined with the β-1,2-glycosidic bond. The lactone sophorolipid is acetylated on the C-6′ & C-6″ position of sophorose moiety (Figure 1-4). The fatty acid is usually hydroxylated on C-17 position (terminal of subterminal), which is β-glycosidically linked to the sophorose moiety. The carboxylic functional group of the fatty acid is either remains unreacted (acidic form) or esterified internally at position C-4″ of sophorose moiety (lactonic form). In general, the hydroxy fatty acid chain length is between 16 to 18 carbon atoms with one or more double bonds. [37,58] *C.bombicola* synthesized a mixture of sophorolipids with variation in the fatty acid moiety, such as the length of chain, degree of unsaturation, and point of hydroxylation as well as the lactonization and acetylation. The structural variation of sophorolipids was first studied by Asmer and co-worker. [37] Their study showed that the sophorolipid mixture could be separated using medium pressure liquid chromatography (MPLC) and TLC.

The results confirmed the separation of 14 components based on their lactonisation and acetylation pattern. Though, the length and hydroxylation pattern of the fatty acid chain were not investigated. Another study by Davila et al., [58] reported the separation of sophorolipid mixture using gradient elution HPLC and employing the detector evaporative light scattering for the identification of individual sophorolipids. The authors separated over 20 components. These different structural variations in sophorolipids impart wide variation in their interfacial properties. Sophorolipids are reported to reduce the surface tension of water from 72.80 mN/m to 40-30 mN/m, with a critical micelle concentration (CMC) of 40 to 250 mg/L. [59] The ratio of acid to lactone forms has a significant effect on the hydrophilic/lipophilic balance, foam formation, and antimicrobial activity. The lactones sophorolipid have improved interfacial properties and antimicrobial activity; whereas the acid form demonstrates better foam formation and good solubility. Furthermore, the substituted acetyl groups have a significant effect on the properties of sophorolipids. It has found that acetyl groups reduce the hydrophilicity of the molecules and improve their antiviral, surface tension and cytokine effects. [60]

The nomenclature of sophorolipids was introduced by Gorin et al., [53] however, most authors have used the nomenclature introduced by Davila et al., [58] Table (1-2), shows the conventional as well as common nomenclature used with the major sophorolipids. Figure (1-11) matches the nomenclature with the structure of the corresponding sophorolipid. During the synthesis, the sophorose fragment of the sophorolipid is not affected by the use of different glucosidic substrates. [61] Glucose is the preferred sugar source for the biosynthesis of sophorose, although *C.bombicola* can grow in various carbohydrates. Glucosidic substrates that have been used in the production of sophorolipids include glucose, sucrose, fructose and mannose. [62,63] Oleic acid is also the preferred fatty acid for the incorporation into the lipidic backbone of the sophorolipids; however, other fatty acids can comprise the lipidic backbone. Moreover, the position of the attachment of the carbohydrate component occurs on the penultimate (ω-1) carbon of the fatty acid with minor bonding occurring to the ultimate carbon. [53, 54, 55]

14

Table 1-2: Nomenclature of major sophorolipids. [46]

Common name	Traditional (IUPAC)	Link (Fig.1-11)
Sophorose	2-O-β-glucopyranosyl-β-D-glucopyranose	
Diacetylated acidic sophorolipids or acid 6',6"-diacetate	17-L-((2'-O-β-D-glucopyranosyl)-oxy)-9-octadecenoic acid 6',6"-diacetate	v, R_1=R_2=Ac
Acetylated acidic sophorolipids or acid 6'-monoacetate	17-L-((2'-O-β-D-glucopyranosyl)-oxy)-9-octadecenoic acid 6'-monoacetate/6"-monoacetate	vi, R_1=Ac, R_2=H vii, R_1=H, R_2=Ac
Non-acetylated acidic sophorolipids or acid sophorolipids	17-L-((2'-O-β-D-glucopyranosyl)-oxy)-9-octadecenoic acid	viii, R_1=R_2=H
Diacetylated lactones or 1',4"-lactone 6',6"-diacetate	17-L-((2'-O-β-D-glucopyranosyl)-oxy)-9-octadecenoic acid 1',4"-lactone 6',6"-diacetate	i, R_1=R_2=Ac
6'-acetylated lactones or 1',4"-lactone 6'-monoacetate	17-L-((2'-O-β-D-glucopyranosyl)-oxy)-9-octadecenoic acid 1',4"-lactone 6'monoacetate/6"-monoacetate	ii, R_1=Ac, R_2=H iii, R_1=H, R_2=Ac
Non-acetylated lactones or 1',4"-lactone sophorolipids	17-L-((2'-O-β-D-glucopyranosyl)-oxy)-9-octadecenoic acid 1',4"-lactone	vi, R_1=R_2=H
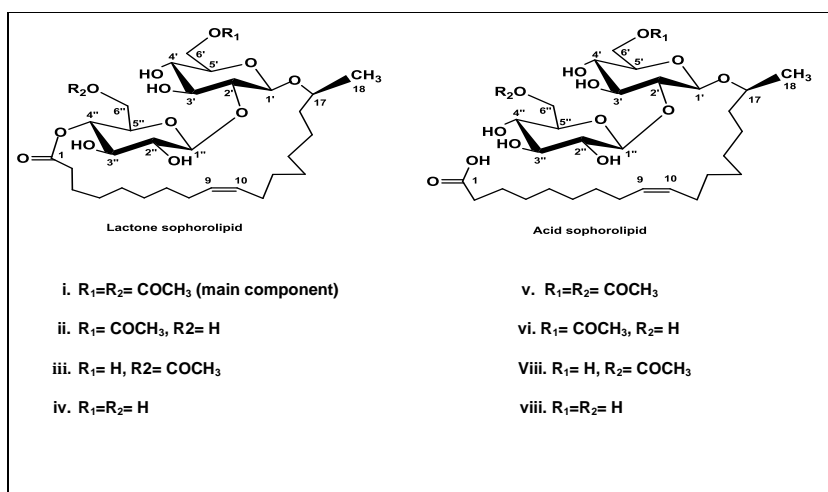
Figure 1-11: Structural classes of possible forms of lactone and acid sophorolipids

1.3.4 Biosynthesis of sophorolipids

The proposed biochemical pathway of sophorolipids is outlined in (Figure 1-12). The synthesis of natural sophorolipid involves the presence of a hydrophilic carbohydrate source and a lipophilic hydrocarbon source, such as an alkane, a fatty acid alcohol or a fatty acid. For high production yield, both carbon sources should be provided in the production medium, or other substrates, such as triglycerides, methyl or ethyl esters fatty acids were also frequently utilized. The *C. bombicola* and *C. apicola* species can grow on hydrocarbons as they possess the necessary enzymes for the β-oxidation step of alkanes on the terminal carbon C-17, to produce hydroxyl fatty acids. Therefore, alkanes or the terminally oxidised intermediates can act as feedstock with bioconversion to the hydroxy fatty acid.

The initial step of biosynthesis involves the conversion of lipophilic hydrocarbon source (fatty acids) to a terminal (ω) or subterminal (ω-1) hydroxy fatty acids based on the action of (NADPH) monooxygenase enzyme-dependent, cytochrome P450. [63] The P450 is capable of hydroxylating fatty acids or alkanes at the terminal (ω) or sub-terminal (ω-1) positions. [64,65] In 2007, a study by Van Bogaert *et al.,* [66] on sophorolipids produced by *C. bombicola* confirmed the isolation and identification of the cytochrome P450 reductase gene (CPR). The cytochrome P450 reductase function reduces the heme centre of cytochrome P450 monooxygenase, which is then activated molecular oxygen. The study also reported the involvement of the glucosyltransferase enzyme in the sophorolipid synthesis by *C. bombicola*. Further to the Bogaert study, it was confirmed by Saerens *et al.,* [25,26] that there are two independent glucosyltransferases in *C.bombicola,* which are responsible for sophorolipid synthesis. As shown in the pathway (Figure 1-12) the first glucose molecule is coupled with position C-1′ glycosidically to the fatty acid hydroxyl group. This reaction involved a specific glucosyltransferase I action and requires nucleotide-activated glucose (UDP-glucose) as glucosyl donor. [27] The second step involves the addition of another glucose molecule, which is glycosidically coupled on C-2′ position to the first glucose moiety by the action of glucosyltransferase II. [66,67]
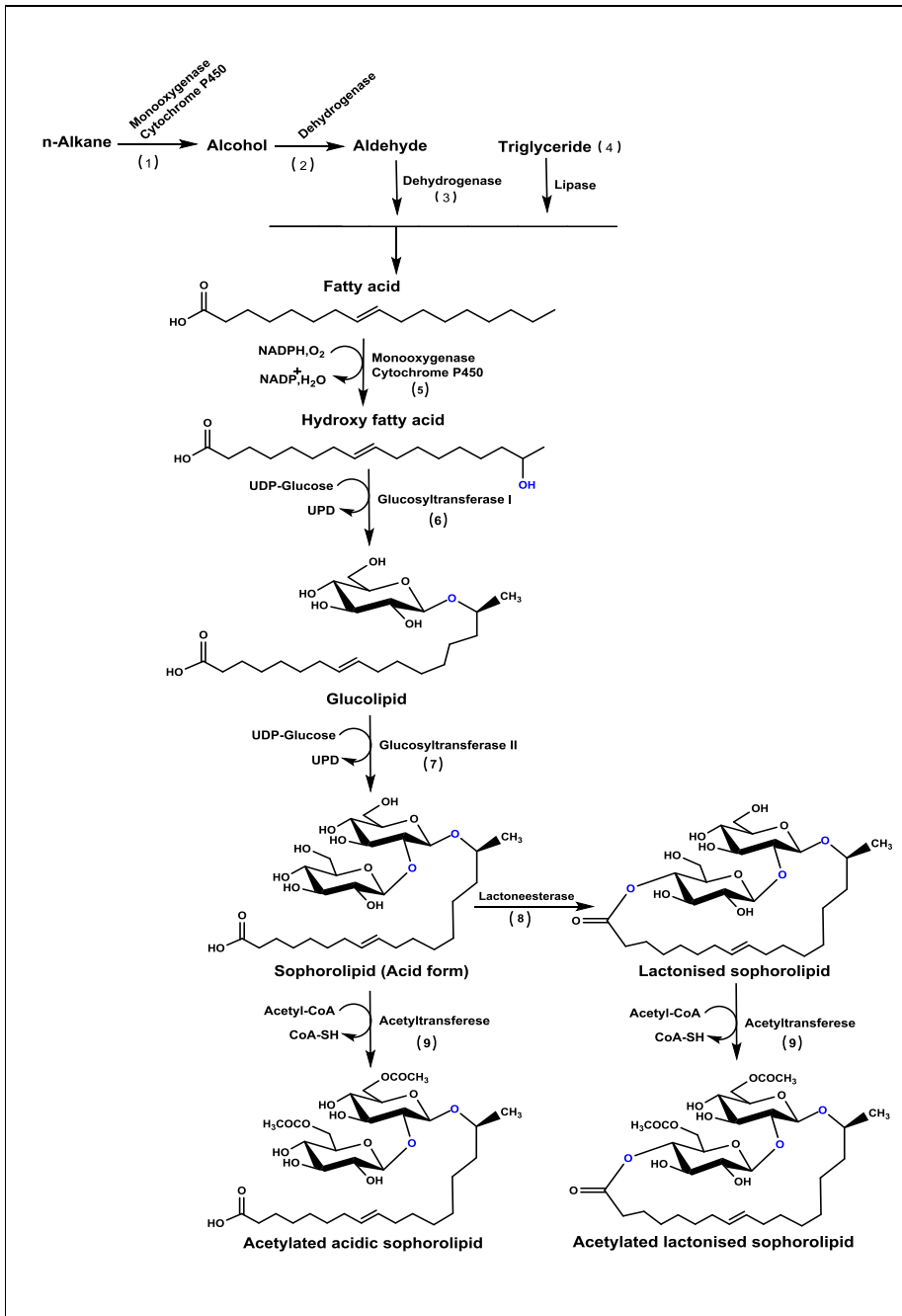
Figure 1-12: Proposed sophorolipid biosynthetic pathway given by Bogaert and coworkers. [66]

After the action of glycosyltransferase II, the sophorolipid formed and detected in the mixture as non-acetylated acidic molecules. After this step, modifications in the sophorolipid structure (lactonization) also occur through the internal esterification action followed by substitution of the acetyl groups on the sophorose moiety. Thus, the esterification process involved the reaction of the COOH-group of the hydroxy fatty acid with an O-H group at the C-4" position on sophorose, produced the lactone form by the action of a specific lactone esterase. [37] The (CoA) dependent acetyltransferase catalysed the acetylation of the C-6s position on sophorose moiety. [28,29]

1.4 Physiological role of sophorolipids

A study on glycolipids reported that the microbial surface-active compounds are produced by the assimilation of hydrophobic or water insoluble substrates by microorganisms.[30] Sophorolipids emulsify the hydrocarbon substrates in the water phase and thus make them accessible to the microorganisms; [31] it was also proposed that the production of sophorolipids by *C.bombicola* is associated with uptake of carbon sources. [32] Another study suggested that sophorolipids can be utilized as a feedstock (carbon source) during the starvation period (lag phase) of sophorolipids fermentation. [33] Moreover, sophorolipids demonstrate an antibacterial activity against particular *Candida* and *Pichia* yeasts species [30] and this may provide the parent strain with a competitive advantage. The mono- and diacetylated lactonic forms possess the strongest inhibitory effect. [68]

1.5 Application of sophorolipids

Currently, sophorolipids are considerable as desirable as they are biodegradable, they have good foaming properties and are effective emulsifiers. Sophorolipids are being used by the Belgian company Ecover NV [69] as ecological detergents, cleaning agents, and cosmetics.

The same company has formulated sophorolipids into products for use as hard surface cleaners for floor and window cleaning. [59]

In 2002, the Japanese company Saraya Co, Ltd., developed products for applications in dishwasher which employ sophorolipids as cleaning agents. [70] Sophorolipids have also been applied in laundry detergents. [38] Sophorolipids based products were approved by the Food and Drug administration (FDA) and commercially available, for use in cosmetics and skin care products. The chemical modification of sophorose moiety via the substitution of hydroxyl alkyl groups resulted in the formation of hydroxyl propyl-etherified glycolipid ester. The later has been used in the production of lip rouge and cream as well as powdered cosmetic formulations. [41,71]

Sophorolipids act as an emulsifying as well as bactericidal agents and are used in the treatment of skin rash, in anti-dandruff shampoos and to combat body odours. The lactone form is used as an emulsifier in cosmetic formulations. [72] It has been confirmed that sophorolipids exhibit a lower cytotoxicity than the existing commercial cosmetic biosurfactant surfactin and other chemical surfactants. [73] The emulsifying properties of sophorolipids have found uses in the petroleum-based industry, being effective in the field of oil recovery, and cleaning of drill material. [74,75] Sophorolipids have been involved in environmental bioremediation *e.g.*, for the treatment of soils contaminated by hydrocarbons and in the elimination of heavy metals from dirty soils. [76] The sophorolipids emulsification properties were applied in food manufacturing to improve the quality of bakery-based products and in the air conditioning storage system for the prevention of ice particle formation. [77]

Sophorolipids have important biological properties. They can be formulated in germicidal mixtures which are appropriate for cleaning vegetables and fruits. [78] Sophorolipids also possess antifungal activity against pathogenic fungi, such as *Pythium* sp. and *Phytophthora* sp. Sophorolipids are reported to have sperm-immobilizing activities and are active against the human immunodeficiency virus. [15,16] Sophorolipids also have anticancer properties and activity against a number of cancer cell lines including the human leukemia cell line HL60 and human liver cancer cells H7402. [17,79]

Sophorolipids acts as septic shock antagonists [80] and can act as anti-inflammatory agents. [81]

Furthermore, sophorolipids are capable of inducing several enzymes. Research conducted on sophorolipids revealed that sophorolipid can act as an inducer for cellulase production. [82] Sophorolipids are reported to induce the production of amylase in *Bacillus subtilis* and manganese peroxidase production in *Pleurotus ostreatus.* [83]

Sophorolipids have numerous applications in nanotechnology, such as in the manufacture of metal nanoparticles; nanoparticles were stabilized using sophorolipids as a capping agent to stop their accumulation and allowed their distribution in water of organic solvents. For example, acidic sophorolipids was used to encapsulate silver or cobalt particles, the fatty acid part interacting with the metal particle either through the terminal carboxylic group or through the double bond while the sophorose moiety is exposed to the solvent; therefore, nanoparticles acquire hydrophilic properties and are easily dispersible in water. [84]

1.6 Enzymatic or chemical modification of sophorolipids

The chemical / enzymatic modification of natural sophorolipids has been used in the production of new compounds with improved biological and surface tension properties. These modifications reduced the structural variability of sophorolipids. For example, the alkaline hydrolysis of natural lactone SLs, which is esterified on C-6s position, is a usual practice to produce the deacetylated acid form sophorolipid. Therefore, the aqueous alkaline or acidic hydrolysis can convert the lactone form into the non-acetylated acidic form. [85] Moreover, deacetylated sophorolipids have also been generated using acetylesterase (EC.3.1.1.6) to remove both acetyl groups, whereas cutinase (EC.3.1.1.74) from *Fusarium solani* can specifically hydrolyse the acetate group on C-6' position only. [37,66,86]

Sophorolipids *have also been* enzymatically modified using glycosidases and lipases, for example, several glycosidases (hesperidinase EC.3.2.1.40,

pectolyase EC 3.2.1.15 and naringinase EC 3.2.1.40); have been used to remove one glucose molecule from sophorose moiety to produce the glucolipids. [87] Another study reported the use of the porcine pancreatic lipase (PPL, EC 3.1.1.3) to stimulate polymerization and de-acetylation of the lactone form. [88]

Other modifications include the conversion of the carboxylic-COOH group of the fatty acid chain into alkyl ester. The preparation of alkyl esters sophorolipid was first reported in attempts to improve the properties of commercial products, such as bread and oily emulsions based-products. [89] In 2004, a study [90] of the synthesis of alkyl esters sophorolipids inspected the physical properties of methyl, ethyl, propyl and butyl ester and confirmed that the surface-tension ability reduced by approximately a 1/2 per every additional methyl group added to the ester terminal. Novozyme 435 (EC 232-619-9) has been used to re-acetylate the hydroxyl groups on the C-6s position of sophorolipid esters as well as to promote the lactonization of the acidic form into the lactonic form at C-6" position of the sophorose moiety. [91,92] In 2003 Carr and Bisht reported the peracetylation of the free hydroxyl groups on sophorose moiety of the methyl ester sophorolipids as a way of blocking -OH groups. [93]

Finally, recently a number of newly synthesised amino acid derivatives have been prepared. Some amino acids have been attached to the sophorolipid carboxylic group using di-carbodiimide as an activator. In this reaction, the non-ionic sophorolipids can be modified into cationic or anionic surfactants, which improve the molecule water solubility and the head group (amino acids) provide an opportunity for further chemical derivatisation. [94]

1.7 Structure characterisation and analysis of sophorolipids

Different analytical techniques have been used for the structure elucidation and characterisation of sophorolipids including ^{1}H- and ^{13}C-NMR, GC-MS, MS, chromatography and FT-IR. One of the first most frequently used techniques for sophorolipid analysis is MS.

This technique provided data, such as the molecular mass and, through the observation of fragmentation ions, vital structural information of sophorolipids. Examples of the use of MS include the identification of sophorolipids using (MALDI-TOF) MS in the work of Bisht *et al.*, [91] and Kurtzman *et al.* [95] Atmospheric pressure chemical ionization (APCI) and electrospray ionization (ESI+/-) are the usual HPLC-MS interfaces utilized in the characterisation of sophorolipids. [96-100] A high resolution chromatographic and fast liquid method coupled with APCI-mass detection (UHPLC/APCI-MS) was used and applied for the quantitative separation of sophorolipids analogues synthesised by *C.bombicola*. [101]

The second beneficial analytical technique utilized for the characterisation of the hydroxylated lipid moiety incorporated in the sophorolipids backbone is GC-MS. GC-MS is particularly useful for sophorolipids which display variations in their lipid moiety: Fatty Acid Methyl Ester (FAMEs) analysis offers essential structural information for the identification of the sophorolipid's fatty acid. To carry out this analysis, it is necessary to perform an acid catalysed methanolysis of the bond that links the sugar moiety to the lipid chain followed by the esterification of the lipid chain. This technique was used by Davila and colleagues [58] to analyse a number of sophorolipids. The same method was also used with slight variations by Cooper and Cavalero [102] and Ma and colleagues. [103]

The third technique which has been used to characterise sophorolipids is NMR and can provide complete identification, facilitating the structural characterisation of functional groups and the degree of acetylation within the sophorolipids. [37,86] The 1D- & 2D-NMR analysis has been conducted on pure sophorolipids and their derivatives by several researchers. [90,91,93,104]

The final analytical technique which is routinely used for the analysis of sophorolipids is FT-IR. Studies conducted by Hu & Ju in 2001 and Davery & Pakshirajan have reported the use of FT-IR to characterise the sophorolipid functional groups permitting the confirmation of acidic and lactonic structures. [105-107]

1.7.1 Analysis of carbohydrates

The analysis of the carbohydrate components of sophorolipids has not received a lot of attention. Monomer analysis is a technique which is frequently employed to determine the monosaccharides in glcoconjgates including in glycolipids, in monomer analysis the glycol-conjugate is subjected to a hydrolysis reaction, generally employing trifluoroacetic acid (TFA) as a catalyst to promote the release of neutral sugars which are then analysed using GC-MS and HPAEC-PAD, in the GC-MS methods, after the conventional hydrolysis [108,109] derivatisation is undertaken to form alditol acetates, which are then analysed by GC, this technique has been progressively replaced by direct analysis of monomers using HPAEC-PAD which avoids the need for a derivatization step. [110] The acid role is to cleave the glycosidic bond between monosaccharide residues and the lipid portion of the sophorolipids. TFA is the preferred acid, being volatile and can be removed easily prior to HPAEC-PAD and GC-MS analysis. The monomer analysis reaction scheme is shown in (Figure 1-13) below:
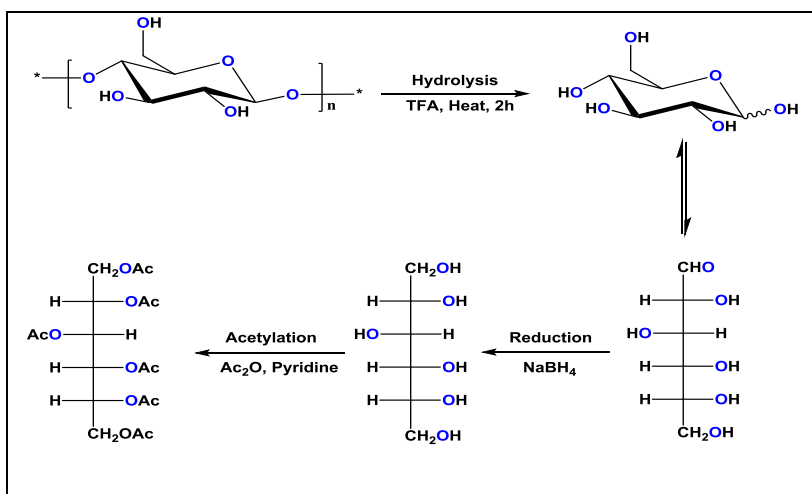
Figure 1-13: Monomer analysis reaction scheme

23

1.7.1.1 High-Performance Anion-Exchange Chromatography with pulsed Amperometric Detection (HPAEC-PAD) analysis

The HPAEC-PAD is a modern technique, which is commonly used to determine anionic analytes without derivatisation, combined with high selectivity and sensitivity. It is a valuable method for the identification and quantification of sugars: mono-, di-, tri-, and oligosaccharides. [111-114] This chromatographic technique is sensitive for the analysis of monosaccharides and disaccharides. [112-115] HPAEC is used to separate analytes that can be ionized at high pH values (*i.e.,* carbohydrate > pH12) carbohydrate in a suitable alkaline condition will ionize; thus, separation occurs via an ion exchange mechanism within a positively charged anion exchange column and using sodium hydroxide eluents at high pH. Detection is accomplished by monitoring the electrical current change resulting from the oxidation of sugars on the surface of a working electrode (gold or platinum) located in the pulsed amperometric detector (PAD). This detector offers low detection and its suitability for gradient elution. [116] Overall, HPAEC-PAD has the advantage of assisting the separation of carbohydrate and their quantification with low detection limits and using NaOH as an inexpensive and relatively safe eluent. [116]

1.7.1.2 Gas Chromatography-Mass Spectrometry (GC-MS) analysis

This technique is considered as the most valuable technique for the analysis of the monomer composition and linkage analysis of sugars. The key advantage of GC-MS compared to liquid chromatography is the much higher separation power of the GC in relatively short retention times. Although the resolution in GC is very effective compared to other separation techniques, a derivatisation step is essential. In GC analysis, the sugars need to be converted into volatile and stable derivatives prior to analysis. The typical derivatisation techniques involve the substitution of the polar groups of carbohydrates. The most common derivatives for GC analysis of saccharides [117-119] are methyl ethers, acetates, trifluoroacetate, and trimethylsilyl ethers. [109,120]

The main elements of derivatisation method involve the conversion of neutral sugars to alditols via reduction and their subsequent acetylation. The product is then dissolved in a volatile solvent prior for analysis by GC-MS. [121]

1.7.1.3 Linkage analysis method

The methylated alditol acetate method is a technique which is routinely applied for the determination of the linkage patterns in carbohydrates and will be employed for this purpose in the current project. The method which is frequently called linkage analysis involves the conversion of carbohydrates into their per-O-methylated derivatives which are then hydrolysed, reduced and converted into permethylated alditol acetates (PMAAs), followed by analysis by GC-MS. A schematic representation of the method can be observed in (Figure 1-14) below:
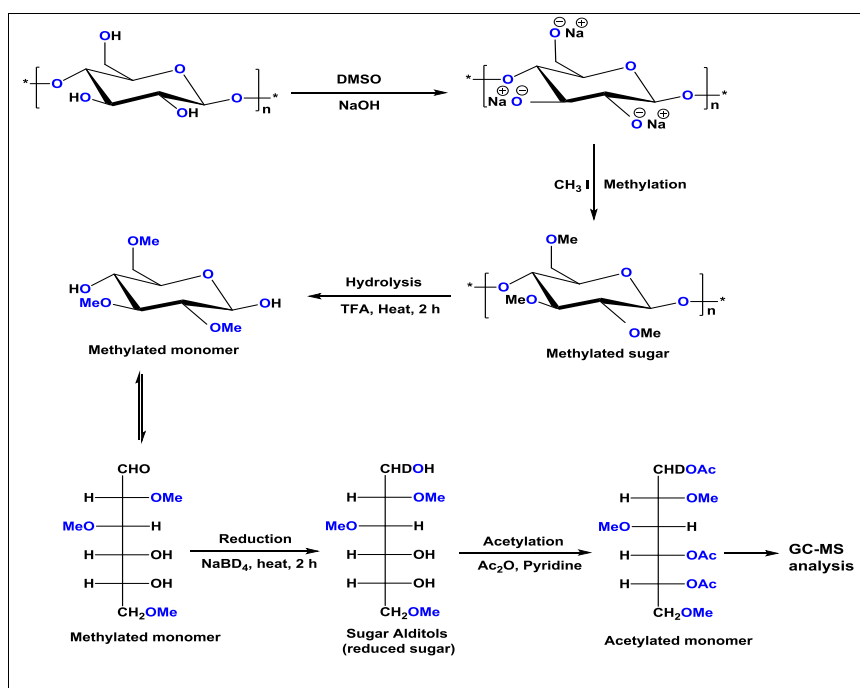
Figure 1-14: Linkage analysis reaction scheme

25

The linkage analysis techniques used in this study was originally developed by Stellner and co-workers, [122] and the main aim is to find the linkage patterns in the repeating sugar units. Generally, in this method the methylated alditol acetate (Figure 1-14) are analyzed by GC-MS. [123,124] The methoxy groups identify where a free hydroxyl group was present and the acetylated sites display where there was a glycosidic linkage to another monosaccharide or where ring formation was present.

The per-*O*-methylation of carbohydrates is a crucial step for determining the position of the glycosidic links. [125] In 1903, Purdie and Irvine [126] were the first to prepare *O*-methylated sugar by treating carbohydrates in methanol with methyl iodide (CH_3I) in the presence of silver oxide (Ag_2O). Later on, Denham and Woodhouse, [127] subjected aqueous carbohydrates to a solution of sodium hydroxide (NaOH) and dimethyl sulphate (Me_2SO_4). Both methods produced *O*-methylated carbohydrates. In 1964, Hakomori, [128] prepared the per-*O*-methylation of polysaccharides in a single step, by mixing a solution of sodium methyl sulfinyl carbanion (Na dimsyl or NaDMSO) to methyl iodide (MeI) which was added to the carbohydrate dissolved in dimethyl sulfoxide. The preparation of the dimsyl reagent is found to be hazardous and laborious. Another method involves adding a small amount of solid sodium hydride into the carbohydrate dimethylsulfoxide solution [19,129] however the formation of Na dimsyl cannot be avoided. The methylation in dimethyl sulfoxide and treatment with powdered (NaOH) and methyl iodide was developed by Ciucanu for per-*O*-methylation of carbohydrates. [130,131] This method is not sensitive to moisture and gives complete *O*-methylation in a single step with high yields, no side products are observed and a very short reaction time is required.

1.8 Glycosidase catalysed glycoside hydrolysis

Glycosidases, also known as α- and β-glycoside hydrolases are one of the groups of enzymes capable of hydrolysing the glycosidic bonds in complex sugars, between two or more sugars or between a carbohydrate and an aglycone (non-carbohydrate moiety).

Glycosidases are able to catalyse both the synthesis and cleavage of glycosidic bonds [132] and display varying degrees of specificity for the structural components either side of the glycosidic bond. They are considered specific for specific glycosyl moieties and only tolerate a limited range of derivatisation within the parent monosaccharide. [133] These enzymes are very specific towards the orientation of the glycosidic bond, which means they require an exclusive axial or equatorial orientated glycosidic bond. The enzyme's stereochemical specificity results in an absolute distinction between anomers of an individual substrate.
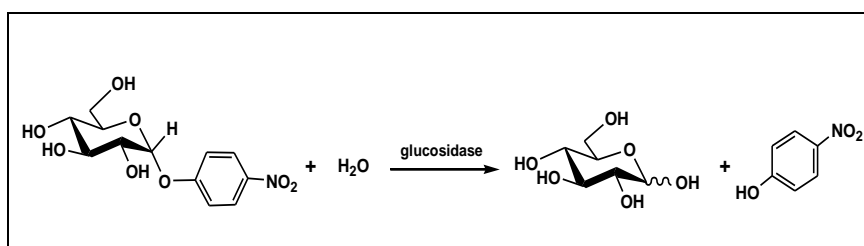
Figure 1-15: Scheme represents substrate specificity of glycosidases.

Glycosidases are categorized as either retaining or inverting enzymes. [133, 134] Glycosidases are also classified on the basis of the regioselectivity of their reactions and termed as being capable of acting as exo or endo, *i.e.*, acting at the reducing or non-reducing end of an oligo/polysaccharide chain.

1.8.1 Proposed glycoside hydrolase mechanism

The catalytic action of glycosidases is considered to follow a mechanism equivalent to that of the acid hydrolysis and proceeds via an oxocarbenium ion intermediate. Generally, the hydrolysis of the glycosidic link is catalysed by two enzymatic carboxylate residues; one work as a proton donor (acid) and the other as a (base). [135-137]

The enzyme-stabilised intermediate (transition state) of the hydrolysis strongly differs depending on the type of glycosidase used: glycosidases proceeding either through retention or inversion of configuration at the anomeric centre, do not share the same mechanism. Both mechanisms (Figure 1-16) involve the oxocarbenium ion formation, like transition state with flattened ring structure at the active site. [138]

In inverting glycoside hydrolases, two enzymatic residues are involved in a single-displacement mechanism, where the first carboxylate residue donate a H^{+} (proton) to the central anomeric carbon while the second carboxylate base residue eliminates a H^{+} (proton) from the available H_2O molecule, enabling its attack on the central anomeric carbon. [139]

In the retaining mechanism, the hydrolysis reaction proceeds through a double displacement mechanism, where a carboxylic residue first acts as proton donor (acid) and secondly a base involving two steps: in the first step (glycosylation), the anomeric carbon is attacked by a nucleophile resulting in a glycosyl-enzyme intermediate formation, thus facilitating the leaving group departure via providing a proton to the glycosyl oxygen atom. In the second step (deglycosylation), the carboxylate acid residue works as a base to initiate a water molecule to carry out a nucleophilic attack to hydrolyse the glycosyl-enzyme intermediate. These steps lead to the retention of the stereochemistry at the anomeric carbon centre. [136,137]
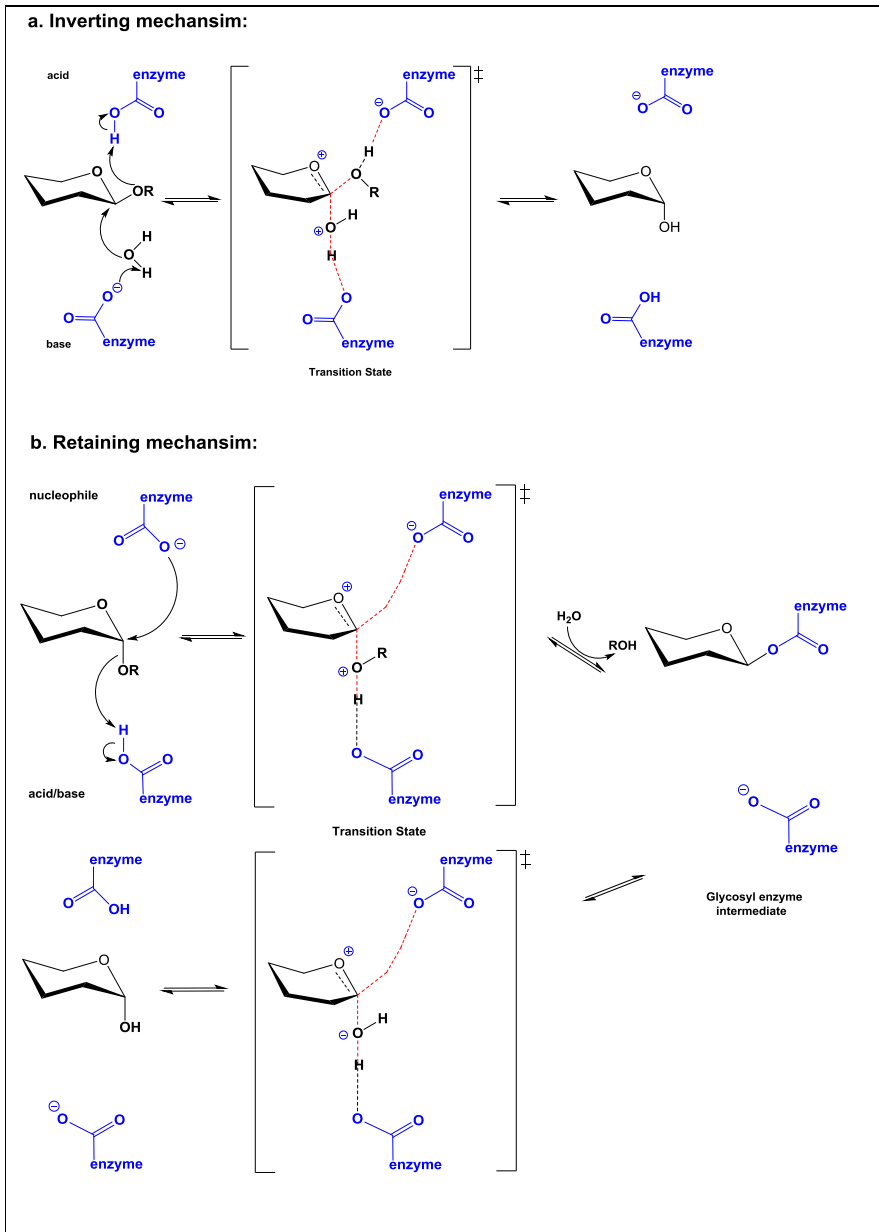
Figure 1-16: Schematic represents the proposed glycosidase mechanism for (a) an inverting mechanism and (b) a retaining mechanism proceeding via a glycosyl enzyme intermediate. [138]

1.9 Aims of research

The first aim of this project was to study in details the nature of the products formed during the synthesis of sophorolipid by microbial fermentation. A full and detailed characterisation of both sophorolipids and of materials found in the waste streams generated during the fermentation and during the processing of the sophorolipids was undertaken and full analysis explained in chapter 3 & 4. It was hoped that the detailed investigation of all these products would provide novel information about the microbial biosynthetic pathways that are active during the fermentation process. A range of sophorolipids samples was provided by Industrial collaborators working in Croda Biotechnology, UK, (Dr. Douglas Cossar and Dr. Timothy Miller). The main techniques used were, 1D- & 2D-NMR, FT-IR, HPLC-MS, HPAEC-PAD (monomer analysis), and GC-MS (monomer & linkage analysis).

The second aim (see-chapter 4) was to investigate the origin of components identified in various products in the lactone waste stream; these studied included trying to determine the origin of the disaccharides; sophorose and isomaltose. This work was to include a study of the stability of sophorolipids in acid and alkaline solutions and in the fermentation liquors generated at the end of a fermentation reaction.

The third aim (see-chapter 5) was to prepare a range of novel sophorolipids by their synthesis from sophorose using both enzymes and chemical coupling reactions. It was decided to attempt to synthesis a number of activated sophoryl-substrates for use in detecting the hydrolase activity of enzymes able to utilize sophorolipids as substrates. The chemical structures of these derivatives were investigated using NMR, FT-IR and HPLC-MS.

Finally, the last aim of the project (see-chapter 6) was to study the application of the newly synthesized sophorolipids derivatives, namely their surface properties, their potential as substrates for monitoring enzyme activity and also to investigate their biological activity.

Chapter two: Experimental

2. Experimental

The experimental chapter is divided into four sections; the first section outlines the production, characterisation and structure elucidation of sophorolipids (Initial sophorolipid products, lactone form and acid form) and their derivatives (methyl ester and ethyl ester) as well as the synthesis of esterified sophorolipid derivatives via a lipase-catalysed regioselective acylation. The second part details the isolation and structure elucidation of sophorose from sophorolipid process wastes, sophorolipid chemical reactivity and the epimerization of sophorose. The third section outlines the synthesis of new sophorolipids from sophorose via a glycosylation reaction. The last section details the study of the surface tension properties and biological activity of sophorolipids and their derivatives.

2.1 Materials and reagents

The chemicals, reagents and enzymes utilized throughout the experiments were all purchased from Sigma-Aldrich Co. Ltd (Gillingham, Kent, UK), Fisher Scientific UK (Loughborough, Leicestershire, UK) and Goss Scientific Instruments Ltd (Nantwich, Cheshire, UK). Monosaccharides, disaccharides sugar standards and 4-nitrophenyl-α-D-glucopyranoside were purchased from Carbosynth (Compton, West Berkshire, UK). The breast and prostate cancer cell lines were purchased from ATCC (LGC Standards, Teddington, Middlesex, UK). Unless otherwise stated reagents were used as supplied.

2.1.1 Sophorolipids and sophorolipid process waste

Samples of sophorolipids and sophorolipid process waste streams were provided by Croda Biotechnology Group (Foundry Lane, Widnes, Cheshire, UK). Those were generated from a large-scale fermentation process as part of an ongoing commercial production of sophorolipid biosurfactants.

2.2 Production of sophorolipids and sophorolipid process wastes-fermentation process carried out by Croda Biotechnology

Croda uses a fermentation process employing the yeast *C.bombicol* ATCC 22214 for sophorolipid production. In brief, the process employed by Croda includes the cultivation of the yeast on glucose as the main carbon source and oleic acid as the lipid source. The oleic acid is an enriched fraction of vegetable oil origin, which has primarily 9-octadecenoic acid, but also contains some hexadecanoic acid, octadecenoic acid and 9,12-octadecadienoic acid (total composition: C16:0 (4%), C18:0 (4%), C18:1 (80%), and C18:2 (11%)).

The specific conditions under which the fermentations are performed include the use of yeast extract (2.0% w/v), urea (0.2% w/v), glucose (10% w/v), DC1510 antifoam (0.5% v/v) as a medium, a temperature of 27 °C, a pH range of 3.5-5.7 and the fermentation is run for 7 days.

2.2.1 Production of the Lactone sophorolipid, (2) from the initial crude sophorolipid product (1)

After the performance of the fermentation process, Croda allows the broth to settle generating two phases: a lipid-rich phase containing sophorolipids (crude sophorolipid mixture (1)) and an aqueous phase. Adjustment of the pH to 5.5 of the crude sophorolipid by the addition of aqueous alkali [0.1 M] at room temperature provides, after washing with water, the sophorolipid lactone (2) (Figure 2-1).

Furthermore, the alkaline treatment of the crude sophorolipid and after neutralization with acid to pH 5.5 resulted in the generation of a solid lactone (2) and an aqueous phase. The aqueous phase contained the free sugar sophorose and also free lipid. This aqueous phase is subsequently referred to as 'lactone-waste, 4'.

2.2.2 Production of acid sophorolipid (3) from the lactone sophorolipid (2)

The acidic sophorolipid (3) was produced by the alkaline treatment (hydrolysis) of the lactone sophorolipid (2). Basically, the lactone sophorolipid was heated at 50-70 °C in an aq.KOH solution (a fixed volume of 20 % KOH per volume of fermentation harvest was used by Croda), this resulted in the lactone ring opening and the deacetylation of the C-6' and C-6" positions (Figure 2-1):
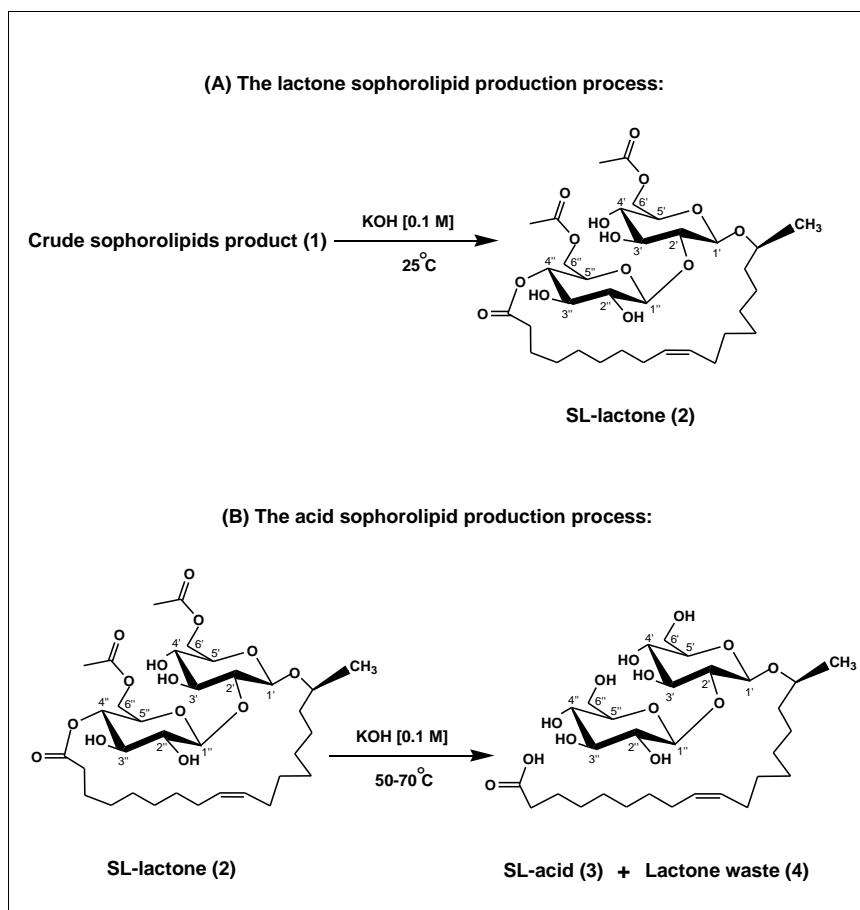
Figure (2-1): Scheme representing the chemical processes of sophorolipids production. (A) The lactone sophorolipid production and (B) The acid sophorolipid production.

2.3 Analytical techniques and structural characterisation

Sophorolipids samples and their derivatives were analysed and their chemical structures were characterised by various analytical approaches. This section will describe different analytical techniques that have been used to investigate the chemical structure and composition of sophorolipids (from Croda Biotechnology) and the esterified sophorolipids derivatives

2.3.1 NMR analysis of sophorolipids

The chemical structures of sophorolipids were characterised using 1D- and 2D-NMR spectroscopy. All NMR spectra for sophorolipids and their derivatives were run on either a Bruker Avance DPX400, 400.13 MHz unshielded magnet or a Bruker Avance DPX500, 500.13 MHz with an 11.7 Tesla Ultra Shield TM magnet. All spectra were acquired at either room temperature or at 70 °C. NMR samples (10 or 20 mg) were prepared in deuterated chloroform $CDCl_3$ (600 μl), and DMSO-d_6 (600 μl), or using deuterium oxide D_2O (600 μl) solvent. Bruker TopSpin version 3.1 was used for acquiring and structural analysis of NMR spectra. A specific set of 2D-experiments were also carried out, which showed the environment in which each carbon & hydrogen is positioned, and the possible structure of sophorolipids was determined. These experiments are:

2D-COSY	Two-dimensional correlated spectroscopy, which shows the correlation between neighbouring protons.
2D-HSQC	Two-dimensional heteronuclear single quantum coherence, which shows the correlation between protons and carbons.
2D-HMBC	Two-dimensional heteronuclear multiple bond correlation, which shows long range coupling between protons and carbons.
^{13}C-DEPT 135	Distortionless Enhancement by Polarization Transfer. Displays negative signals for CH_2 groups, while CH- and -CH_3 groups have positive signals.
TOCSY	Total Correlated Spectroscopy
HSQC-TOCSY	Heteronuclear Single Quantum Coherence-Total Correlation Spectroscopy

2.3.2 FTIR analysis of sophorolipids

FTIR Spectra for sophorolipids were recorded using a Nicolet 380, FT-IR spectrometer (Thermo Electron Corporation, UK) in the range of 400-4000 cm^{-1}. A small amount of sophorolipid (2-5 mg) was placed on the Attenuated Total Reflection (ATR) plate of the FT-IR spectrometer. Spectrometer background scans (background correction) were carried out before each replicate analysis. Isopropanol was used to clean the ATR plate before each measurement.

2.3.3 HPLC-MS analysis of sophorolipids

Electrospray ionization technique was used with HPLC for the analysis of sophorolipids and their derivatives. The LC-MS analysis and chromatographic conditions employed for the sophorolipid analysis are listed as follows:

Chromatographic conditions for sophorolipids mass detection	
Instrument	Agilent 6210 TOF MS
Mass Spectrometry	LC-MS
Flow Rate	0.8 ml.min^{-1}
Binary Pump Model	G4220 A
Injection Volume	1.0 µl
Column	ACE 3 C18-Ar (150 mm X 4.6 mm)
Mass component name	LC-MS
Ionisation	ESI (+ve)
Detector	DAD
Column Oven Temperature	40 °C
LC run time	10 mins

LC Solvent Composition				
Channel	Ch.1 Solvent	Eluent additive	Ch.2 Solvent	Solvent ratio %
A	100% Water	0.1% TFA or 0.1% FA, pH 3	100% Water	20% or 40%
B	100% Acetonitrile	Methanol	100% Acetonitrile	80% or 60%

2.4 Structural characterisation of sophorolipid samples: crude sophorolipid fermentation product (1), lactone form (2) and acid form (3)

The chemical structure of the crude, lactone and acid sophorolipids provided by Croda Biotechnology were fully characterised and elucidated using a number of different analytical techniques; FT-IR,[18,37] ^{1}H-, ^{13}C-NMR and mass spectrometry. [140,141]

2.4.1 The analytical data of crude sophorolipid product (1)

Crude sophorolipid product (1)

SL-lactone (2)   +   SL-acid (3)
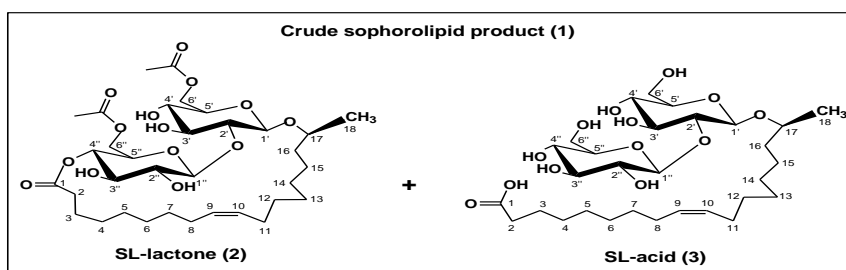
FT-IR: (cm^{-1}) 3390, 2923, 2854,1742,1651,1435, 1239, 1170 and 1035.

^{1}H-NMR: (D$_2$O, 500 MHz, ppm) δ 1.22 (3 H, d, J = 7.3 Hz, H-18), 1.28 -1.34 (14 H, brs, H-4-7 and 12-14), 1.58 (2 H, m, H-15), 1.61 (4 H, m, H-3 and H-16), 2.01 (4 H, m, H-8 and H-11), 2.07 (3 H, s, lactone form -OCOCH_3) , 2.10 (3 H, s, lactone form - OCOCH_3), 2.18 (3 H, s, acid form-O-COCH_3), 2.24 (2 H, t, J = 7.16 Hz, H-2-acid form), 2.30 (2 H, t, J = 6.0 Hz, H-2-lactone form), 3.26 - 3.85 (7 H, m, H-3″, H-3′, H-5′, H-5″, H-2′, H-2″ and H-4′), 4.06-4.10 (1 H, m, H-17), 4.24 (2 H, m, H-6′), 4.40 (2 H, d, J = 7.5, H-6″), 4.53 (1 H, d, J = 7.5 Hz, H-1″), 4.61 (1 H, J = 7.5 Hz, H-1'), 4.67 (1 H, t , J = 9.5, lactone form-H-4″) and 5.42-5.28 (2 H, m, H-9 and H-10).

^{13}C-NMR: (D$_2$O, 500 MHz, ppm) δ 20.70 & 20.95 (C-18-lipid chains for acid and lactone form), 24.73 (C-3), 25.42 (C-15), 26.82 (C-8), 27.14 (C-11), 28.20, 28.41, 28.96, 29.75, 30.14, 30.21, 33.95 (C-4-7 & C-12-14), 34.31 (C-16), 37.50 (C-2), 62.12 (C-6′), 63.83 (C-6″), 69.74 (C-4′), 70.18 (C-4″), 72.34 (C-2″), 73.06 (C-5′), 73.45 (C-5″), 75.09 (C-3″), 75.55 (C-3′), 79.16 (C-17), 82.64 (C-2′), 102.25 (C-1″), 103.98 (C-1′), 129.72 and 129.99 (C-9 & C-10), 170.63 and 171.69 (2 x OCOCH_3), 173.3 (*C*OOR, lactone).

2.4.2 The analytical data of the lactone sophorolipid 17-L-([2′-*O*-β-D-glucopyranosyl-1-β-D-glucopyranosyl]-oxy)-9-octadecenoic acid 1, 4″-lactone 6′, 6″-diacetate, SL-lactone (2)

Scheme 1
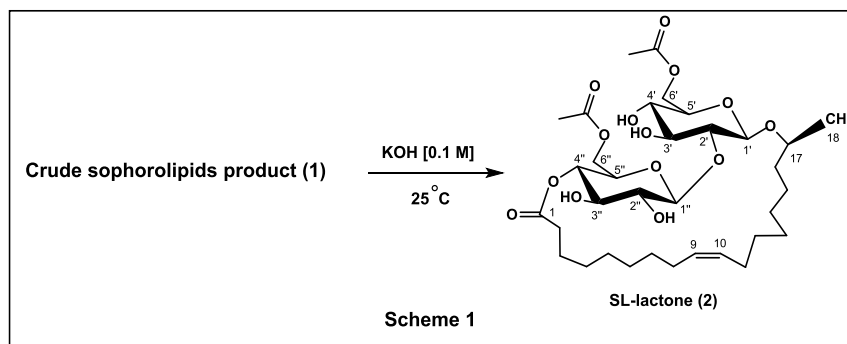
FT-IR: (cm^{-1}) 3369, 2925, 2854, 1744, 1741, 1651, 1234, 1170, and 1035.

^{1}H-NMR: (CDCl$_3$, 500 MHz, ppm) *δ* 1.25 (3 H, d, *J* = 4.3 Hz, H-18), 1.25-1.41 (14 H, brs, H-4-7 and -12-14), 1.59 (2 H, m, H-15), 1.65 (4H, m, H-3 and H-16), 2.03 - 2.13 (6H, s, 2 x OCOC*H$_3$*), 2.30 (4 H, m, H-8 and H-11), 2.45 (2 H, t, *J* = 6.5 Hz, H-2), 3.36-3.81 (7 H, m, H-3″, H-3′, H-5′, H-5″, H-2′, H-2″ and H-4′), 4.06-4.15 (1H, M, H-17), 4.17 (2 H, d, *J* = 1.8, H-6′), 4.26 (2 H, d, *J* = 1.6, H-6″), 4.48 (1 H, d, *J* = 7.6 Hz, H-1″), 4.55 (1 H, *J* = 8.1 Hz, H-1′), 4.97 (1 H, t, *J* = 9.5, lactone form-H-4″) and 5.36 (2 H, m, H-9 and H-10).

^{13}C-NMR: (CDCl$_3$, 500 MHz, ppm) *δ* 20.78 (C-18), 21.10, 22.20 (2 x OCOCH$_3$), 24.71 (C-3), 25.28 (C-15), 26.93 (C-8), 27.21 (C-11), 28.13, 28.22, 28.26, 28.99, 29.65, 29.98, 30.09 (C-4-7, C-12-14), 34.37 (C-16), 37.44 (C-2), 62.20 (C-6′), 63.70 (C-6″), 69.74 (C-4′), 70.38 (C-4″), 72.62 (C-2″),73.33 (C-5′), 73.95 (C-5″), 75.11 (C-3″), 75.74 (C-3′), 79.39 (C-17), 81.91 (C-2′), 102.30 (C-1″), 103.85 (C-1′),129.78, 130.01 (C-9, C-10), 170.62, 171.71 (2 x O*C*OCH$_3$), 173.38 (C-1 carbon-lactone carbonyl).

m/z (HPLC-ESI$^+$, ACN:H$_2$O (8:2): [M+Na]$^+$ for C$_{34}$H$_{56}$O$_{14}$ calculated 688.3690, measured 688.3697.

2.4.3 The analytical data of the acid sophorolipid 2-L-([2′-*O*-β-D-glucopyranosyl-1-β-D-glucopyranosyl]-oxy)-9-octadecenoic acid, SL-acid (3)

Scheme 2
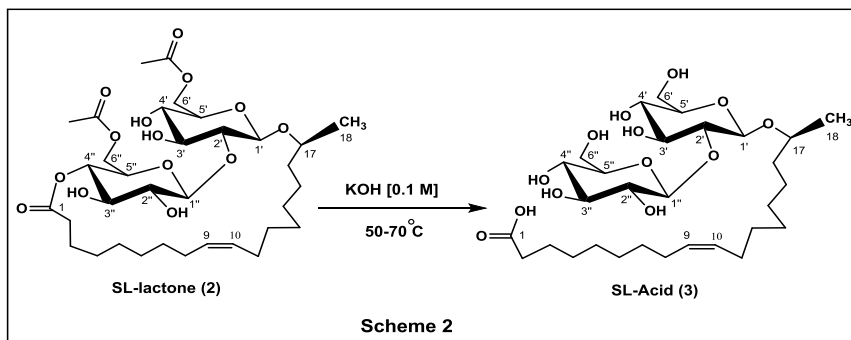
FT-IR: (cm⁻¹) 3368, 2924, 2853,1643,1643,1556, 1410, and 1263.

¹H-NMR: (D_2O, 500 MHz, ppm) δ 1.62 (3 H, d, *J* = 6.3 Hz, H-18), 1.7 (14 H, brs, H-4-7 and H-12-14), 1.97 (2 H, m, H-15), 2.04 (4H, m, H-3 and-16), 2.32 (3H, s, OCOC*H₃*), 2.40 (4 H, dt, H-8 and -11), 2.65 (2 H, t, *J* = 7.8 Hz, H-2), 3.68 - 3.94 (7 H, m, H-3″, H-3′, H-5′, H-5″, H-2′, H-2″ and H-4′), 4.06-4.10 (1H, m, H-17), 4.20 (2 H, d, *J* = 2.6, H-6′), 4.26 (2 H, d, *J* = 2.2, H-6″), 4.89 (1 H, d, *J* = 7.8 Hz, H-1″), 5.09 (1 H, *J* = 7.8 Hz, H-1′), 5.72 (2 H, m, H-9 and -10).

¹³C-NMR: (D_2O, 500 MHz, ppm) δ 20.80 (C-18), 22.20 (OCOC*H₃*), 22.49 (C-3), 25.49 (C-15), 25.58 (C-8), 27.45 (C-11), 27.55, 27.61, 29.50, 29.54, 29.65, 29.84, 30.05 (C-4-7, C-12-14), 35.17 (C-16), 36.66 (C-2), 61.50 (C-6′), 62.07 (C-6″), 70.03 (C-4′), 70.71 (C-4″), 74.70 (C-2″), 76.19 (C-5′), 76.42 (C-5″), 76.81 (C-3″), 76.86 (C-3′), 77.80 (C-17), 81.23 (C-2′), 101.22 (C-1″), 103.43 (C-1′), 130.16, 130.34 (C-9, C-10), 179.34 (carboxylate ion, *C*OO⁻K⁺).

m/z ((HPLC-ESI⁺, ACN:H_2O (8:2): [M+Na]⁺ for $C_{30}H_{54}O_{13}$ calculated 623.3448, measured 623.3459.

2.5 Synthesis of ester sophorolipid derivatives (Esterification)

The lactone sophorolipid (2) was used as the substrate for the production of the methyl ester, SL-Me (4) and ethyl ester, SL-Et (5) sophorolipids.

2.5.1 Synthesis of methyl 17-L-([2'-O-β-D-glucopyranosyl-β-D-glucopyranosyl]-oxy)-cis-9-octadecenoate, SL-Me (4)

Scheme 3
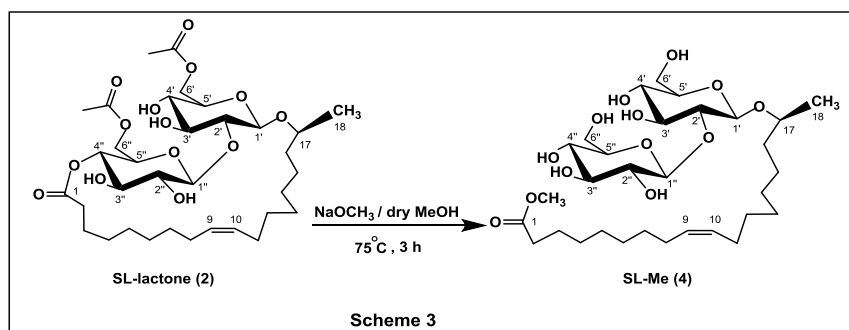
To a round-bottomed flask (100 ml) equipped with a reflux condenser were added lactone sophorolipid (2) (5.0 g) (dried over P_2O_5 for 24 h) and sodium methoxide (0.022 N) in methanol solution (10.0 ml). The reaction mixture was protected from atmospheric moisture by a calcium chloride guard tube. The reaction mixture was refluxed for 3 h at 75 $^{\circ}$C then cooled down to room temperature and acidified using glacial acetic acid to pH 5.5. The reaction mixture was concentrated by rotary evaporation under vacuum and was poured with stirring into ice-cold H_2O (35.0 ml) resulting in the precipitation of the sophorolipid methyl ester as a white solid. This was filtered washed with ice-water and dried (3.78 g, yield 75.5%).[91,93,142]

M.P.: 130 -133 ºC. (No literature M.P., has been reported)
FT-IR: (cm^{-1}) 3323, 2923, 2951,1740,1591,1156, 1066 and 1027.

¹H-NMR: (CD$_3$OD, 500 MHz, ppm) δ 1.27 (3H, d, J = 6.0 Hz, H-18), 1.34 (14 H, brs, H-4-7 and 12-14), 1.48 (2 H, m, H-15), 1.62 (4H, m, H-3 and H-16), 2.06 (4 H, m, H-8 and -11), 2.34 (2 H, t, J =7.5 Hz, H-2), 3.23 - 3.38 (4 H, m, H-2″,-4″,-4′, and -5′), 3.40 (1 H, t, J = 8.4 Hz, H-3″), 3.47 (1H, t, J = 8.8 Hz, H-2′), 3.58 (1H, t, J = 8.85 Hz, H-3′), 3.65 - 3.73 (3 H, m, H-6′a, -6″a, and H-5″), 3.68 (3 H, s, OCH_3), 3.80 -3.90 (3- H, m, H-6′b, -6″b, and H-17), 4.47 (1 H, d, J = 7.6 Hz, H-1′), 4.66 (1 H, J = 7.8 Hz, H-1″) and 5.38 (2 H, m, H-9 and -10).

¹³C-NMR: (CD$_3$OD, 500 MHz, ppm) δ 20.51 (C-18), 24.71 (C-3), 25.00 (C-15), 26.71 (C-8), 26.76 (C-11), 28.75, 28.76, 28.86, 29.02, 29.46, 29.44, 29.53 (C-4-7 & C-12-14), 33.43 (C-16), 36.43 (C-2), 50.59 (-O-CH$_3$), 61.75 (C-6′), 61.41 (C-6″), 70.11 (C-4′), 70.42 (C-4″), 74.52 (C-2″), 76.37 (C-5′), 76.40 (C-5″), 76.88 (C-3″), 76.97 (C-3′), 77.50 (C-17), 80.54 (C-2′), 101.43 (C-1″), 103.33 (C-1′), 129.42, 129.52 (C-9, C-10), 175.04 (OCOCH$_3$).

m/z (HPLC-ESI⁺, ACN:H$_2$O (8:2): [M+Na]⁺ for C$_{31}$H$_{56}$O$_{13}$ calculated 636.3748, measured 636.3753.

2.5.2 Synthesis of ethyl 17-L-([2'-*O*-β-D-glucopyranosyl-β-D-glucopyranosyl]-oxy)-cis-9-octadecenoate, SL-Et (5)

Scheme 4
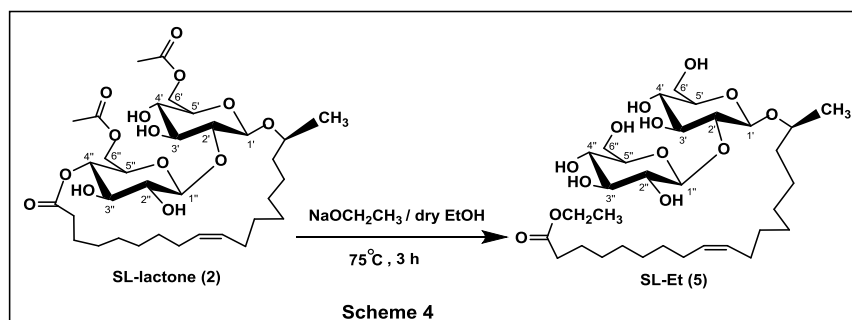
The same procedure as mentioned in (section 2.5.1) for the production of the sophorolipid methyl ester was used to prepare the sophorolipid ethyl ester (SL-Et). Lactone sophorolipid (5.0 g) (dried over P$_2$O$_5$ for 24 h) was dissolved in sodium ethoxide (0.021 N) (10.0 ml) in ethanol solution and refluxed for 3 h at 75 °C using a constant temperature oil bath.

The identical work-up as for the analogue methyl ester (SL-Me) gave total weight (4.11 g, yield 82 %) of sophorolipid ethyl ester as a white solid. [91]

M.P.: 138 -141 °C. (No literature M.P., has been reported)
FT-IR: (cm^{-1}) 3324, 2924, 2853,1738,1574,1156, 1067 and 1028.

^{1}H-NMR: (DMSO- d_6, 400 MHz, ppm) δ 1.13 (3H, t, J = 6.1 Hz, OCH$_2$CH_3), 1.17 (3 H, d, J = 7.1 Hz, H-18), 1.25 (14H, brs, H-4-7 and -12-14), 1.29 (2 H, m, H-15), 1.51 (4 H, m, H-3 and H-16), 2.00 (4 H, m, H-8 and -11), 2.28 (2 H, t, J = 7.4 Hz, H-2), 2.99 - 3.65 (13 H, m, H-sug. and -17), 4.05 (2 H, q, J = 7.1 Hz, OCH_2CH$_3$), 4.31 (1 H, d, J = 7.7 Hz, H-1'), 4.398 (1 H, d, J= 7.7 Hz, H-1″) and 5.33 (2 H, m, H-9 and -10).

^{13}C-NMR (DMSO-d_6, 400 MHz, ppm) δ 21.60 (C-18), 21.78 (-O-CH$_2$CH$_3$), 22.60 (C-3), 24.46 (C-15), 27.04 (C-8), 27.11 (C-11), 28.88, 28.90, 29.00, 29.23, 29.40, 29.53, 29.67 (C- 4-7, C-12-14), 34.11(C-16), 36.63 (C-2), 59.78 (-O-CH$_2$CH$_3$), 60.35 (C-6'), 61.51 (C-6″), 69.98 (C-4'), 70.33 (C-4″), 75.48 (C-2″), 76.39 (C-5'), 76.50 (C-5″), 76.65 (C-3″), 76.92 (C-3'), 77.45 (C-17), 82.53 (C-2'), 101.62 (C-1″), 104.50 (C-1'), 130.02, 130.15 (C-9, C-10) 173.20 (C-1).

m/z (HPLC-ESI$^+$, ACN:H$_2$O (8:2): [M+Na]$^+$ for C$_{32}$H$_{58}$O$_{13}$ calculated 650.3898, measured 650.3906.

2.6 Lipase-catalysed regioselective acylations

The methyl ester, (4) was used as the substrate for the production of 1′,6″-sophorolactone, 1′,6"-sophorolactone-6'-acetate and the methyl ester-6′,6″-sophorose dibutyrate) using the lipase Novozyme 435 from *C. antarctica.*

2.6.1 Novozyme 435 catalyzed synthesis of 17-L-([2'-*O*-β-D-glucopyranosyl-β-D-glucopyranosyl]-oxy)-cis-9-octadecenoic acid-1′,6″-lactone (6)

Scheme 5
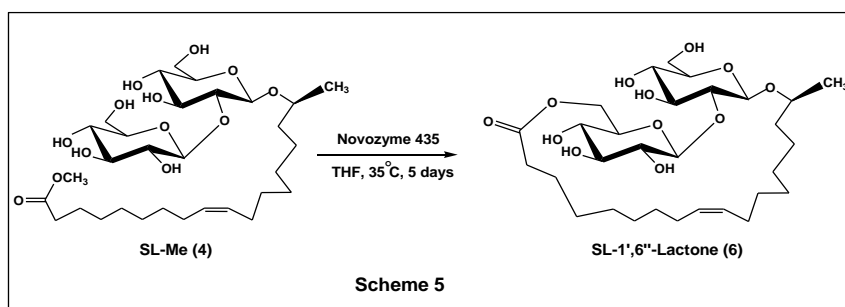
To an oven dried round-bottomed flask (100 ml) were transferred (SL-Me, 4) (1.0 g), Novozyme 435, (2.0 g), molecular sieve 4 Å (2.0 g) and THF (35.0 ml). The round-bottomed flask was immediately stoppered and the reaction assembly was protected from the atmosphere using N_2 gas and placed in a constant temperature oil bath and maintained at 35 °C for 5 days and the contents of the flask were stirred magnetically. After 5 days, the reaction mixture was centrifuged at 4000 rpm for 10 min to remove the Novozyme and molecular sieves. The supernatant containing the desired product was rotary-evaporated under vacuum to remove the solvent (THF). The resulting pale green coloured solid was recrystallised from chloroform / methanol (4:2) and dried for 5 h to give (0.74 g, yield 72 %) of sophorolipid-1', 6"-lactone. [93]

M.P.: 92 - 94 ºC. (No literature M.P., has been reported)

FT-IR: (cm⁻¹) 3348, 2931, 2858, 1728, 1455, 1375, 1169, 1069.

¹H-NMR: (DMSO-d_6, 400 MHz, ppm) δ 1.12 (3 H, d, J = 6.0 Hz, H-18), 1.30 (14 H, brs, H-4-7 and -12-14), 1.51 (2 H, m, H-15), 1.62 (4 H, m, H-3 and H-16), 2.01 (4H, t, J = 6.6 Hz, H-8 and -11), 2.43 (2 H, t, J = 8.2 Hz, H-2), 3.10 - 3.40 (4H, m, H-2″,- 4″,-2″, and -5′), 3.65 (2 H, m, H-3′ and -5″), 3.70 (2 H, m, H-3″ and -4′), 3.73 (1H, m, H-6′ a), 3.80 (2 H, m, H-6′ b and H-17), 3.80 (1 H, m, H-6″a), 3.84 (1 H, m, H-6″ b), 4.02 (1 H, d, J = 4.4 Hz, H-1′), 4.05 (1 H, d, J = 4.3 Hz, H-1″) and 5.34 (2 H, m, H-9 and -10).

¹³C-NMR (DMSO-d_6, 400 MHz, ppm) δ 21.68 (C-18), 22.60 (C-3), 24.46 (C-15), 27.04 (C-8), 27.11 (C-11), 28.88, 28.90, 29.00, 29.23, 29.40, 29.53, 29.67 (C-4-7, C-12-14), 34.11(C-16), 36.63 (C-2), 59.78 (-O-CH_2CH_3), 61.39 (C-6′), 63.85 (C-6″), 69.84 (C-4′), 70.27 (C-4″), 75.48 (C-2″), 75.47 (C-5′), 76.50 (C-5″), 76.30 (C-3″), 76.77(C-3′), 76.98 (C-17), 84.53 (C-2′), 100.72 (C-1″), 105.65 (C-1′), 129.95, 130.54 (C-9, C-10) 173.60 (C-1).

m/z (HPLC-ESI⁺, ACN:H$_2$O (8:2): [M+Na]⁺ for $C_{30}H_{52}O_{12}$ calculated 604.3462, measured 604.3475.

2.6.2 Novozyme 435 catalysed synthesis of 17-L-([2'-O-β-D-glucopyranosyl-β-D-glucopyranosyl]-oxy)-cis-9-octadecenoic acid-1′,6″-lactone-6′-acetate (7)

Scheme 6
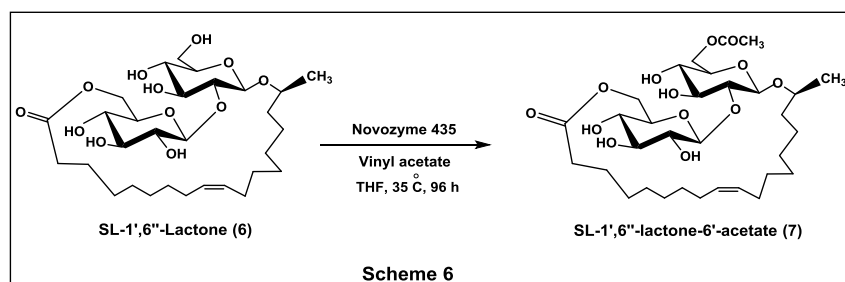
To an oven dried round-bottomed flask (100 ml) were added (1',6"-sophorolactone, 6) (0.40 g), immobilized Novozyme 435 (0.80 g), molecular sieve 4 Å (2 g) and THF (30.0 ml). The round-bottomed flask was immediately stoppered. Vinyl acetate (1.50 ml) was added and the reaction assembly was protected from the atmosphere using N$_2$ gas and the round bottomed flask was covered with aluminium foil to seclude it from light then was placed in a constant temperature oil bath maintained at 35 °C for 96 h and the contents were stirred magnetically. After 96 h, the reaction mixture was centrifuged at 4000 rpm for 10 min to remove the Novozyme and molecular sieve. The supernatant containing the desired product was rotary-evaporated at reduced pressure to remove the solvent (THF).

The resulted yellowish solid was recrystallised from chloroform / methanol (4:2) and dried for 5 h to give (0.36 g, yield 70 %) of sophorolipid-1',6"-lactone-6'-acetate (7). [142]

M.P.: 126 -128 ºC. (No literature M.P. has been reported)
FT-IR: (cm^{-1}) 3468, 2980, 2933, 2860, 1731, 1698, 1455, 1367, 1238, 1067.

^{1}H-NMR: (DMSO-d_6, 400 MHz, ppm) δ 1.12 (3 H, d, J = 6.1 Hz, H-18), 1.30 (14 H, brs, H-4-7 and -12-14), 1.42 (2 H, m, H-15), 1.52 (4 H, m H-3 and H-16), 2.01 (4 H, t, J = 6.6 Hz, H-8 and -11), 2.09 (3 H, s, COCH_3) 2.30 (2 H, t, J = 7.2 Hz, H-2), 3.02 - 3.40 (4 H, m, H-2″,- 4″,- 2″, and - 5′), 3.63 (2 H, m, H-3′ and -5″), 4.03 (2 H, m, H-3″ and-4′), 4.10 (1 H, m, H-6′ a), 4.20 (2 H, m, H-6′ b and H-17), 4.28 (1 H, m, H-6″), 4.36 (1 H, d, J = 4.2 Hz, H-1′), 4.43 (1 H, d, J = 4.2 Hz, H-1″) and 5.32 (2 H, m, H-9 and -10).

^{13}C-NMR (DMSO-d_6, 400 MHz, ppm) δ 21.10 & 21.50 (double, C-18), 24.50 (C-3), 25.26 (C-15), 26.05 (C-8), 27.16 (C-11), 27.65, 28.03, 28.44, 29.40, 29.47, 29.72, 29.80 (C-4-7, and C-12-14), 31.15 (OCOCH_3), 33.79 (C-16), 36.63 (C-2), 61.39 (C-6′), 63.85 (C-6″), 69.88 (C-4′), 70.26, (C-4″), 73.60 (C-2″), 74.36 (C-5′), 75.562 (C-5″), 76.10 (C-3″), 76.3 (C-3′), 76.48 (C-17), 84.17 (C-2′), 100.72 (C-1″), 105.65 (C-1′), 129.96, 130.54 (C-9, C-10), 170.72 (OCOCH$_3$), 173.32 (Lactone-OCOR).

m/z (HPLC-ESI$^+$, ACN:H$_2$O (8:2): [M+Na]$^+$ for $C_{32}H_{54}O_{13}$ calculated 646.34780, measured 646.3480.

2.6.3 Novozyme 435 catalyzed synthesis of 17-L-([2'-*O*-β-D-glucopyranosyl-β-D-glucopyranosyl]-oxy)-cis-9-octadecenoic acid 6′,6″-dibutyrate (8)

Scheme 7
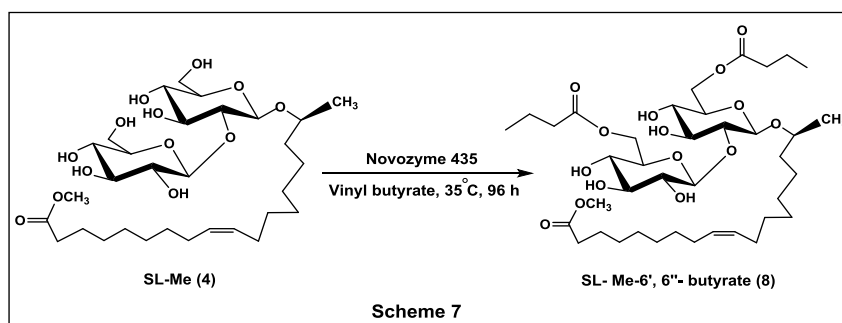
To an oven dried round-bottomed flask (100 ml) were transferred (SL-Me, 4) (0.710 g), immobilized Novozyme 435 (0.80 g), molecular sieve 4 Å (2.0 g) and THF (30.0 ml).

The round-bottomed flask was immediately stoppered. Excess of vinyl butyrate (1.0 ml) was added and the reaction assembly was protected from the atmosphere using N_2 gas then placed in a constant temperature oil bath and maintained at 35 $^{\circ}$C for 96 h and the contents were stirred magnetically. After 96 h, the reaction mixture was centrifuged at 4000 rpm for 10 min to remove both the solid supported Novozyme and the molecular sieves. The supernatant containing the desired product was rotary-evaporated to remove the solvent (THF). The resulting yellowish oily product was washed with hexane (2 x 10.0 ml) to give (0.53 g, yield 72 %) of the product (8).

FT-IR: (cm^{-1}) 3346, 2928, 2853, 1736, 1722, 1651, 1556, 1455, 1255, 1047, 1022.

^{1}H-NMR: (CDCl$_3$, 500 MHz, ppm) δ 0.93 - 0.99 (6 H, m, 2 x butyrate H-4), 1.22 (3 H, d, J = 6.1Hz, H-18), 1.31 (14 H, brs, H-4-7 and -12-14), 1.43 (2 H, m, H-15), 1.57-1.62 (4H, m, H-3 and -16), 1.63 - 1.72 (4 H, m, 2 x butyrate H-3), 1.86 (2 H, m, 2 x butyrate H-2), 2.06 (4 H, dt, J = 6.0 Hz, H-8 and -11), 2.32 (2 H, t, J = 7.7 Hz, H-2), 3.33-3.51 (4 H, m, H-2″,- 4″,- 2″, and -5′), 3.55 - 3.63 (2 H, m, H-3′ and -5″), 3.66 (3H, s, -O-C*H*$_3$), 3.70-3.79 (2 H, m, H-3″ and H-4′), 4.27 (1H, m, H-6′ a), 4.33 (1 H, m, H-6″), 4.38 (2 H, m, H-6′ b and -17), 4.44 (1 H, d, J = 7.5 Hz, H-1′), 4.51(1 H, d, J = 8.0 Hz, H-1″) and 5.33 (2 H, m, H-9 and -10).

^{13}C-NMR: (CDCl$_3$, 500 MHz, ppm) δ 13.53, 13.57 (2 x butyrate-*C*H$_3$) 20.06 (C-18), 25.23 (C-3), 25.49 (C-15), 27.08 (C-8), 27.13 (C-11), 28.99, 29.01, 29.06, 29.25, 29.57, 29.66, 29.70 (C-4-7 & C-12-14), 33.99 (C-16), 35.86, 35.98 (2 x OCOC*H*$_2$CH$_2$CH$_3$) 36.20 (C-2), 51.47 (-O-*C*H$_3$), 63.703 (C-6′), 63.29 (C-6″), 67.83 (2 X OCO*C*H$_2$CH$_2$CH$_3$), 69.71 (C-4′), 70.41 (C-4″), 73.18 (C-2″), 73.36 (C-5′), 74.64 (C-5″), 75.59 (C-3″), 75.93 (C-3′), 77.16 (C-17), 81.10 (C-2′), 100.40 (C-1″), 103.30 (C-1′), 129.68, 129.76 (C-9 and C10), 175.04 (O*C*OCH$_3$), 174.03, 174.31 (2 x O*C*OCH$_2$CH$_2$CH$_3$).

m/z (HPLC-ESI$^+$, ACN:H$_2$O (8:2), FA (0.1%): [M+Na]$^+$ for C$_{39}$H$_{68}$O$_{15}$ calculated 776.4592, measured 776.4618.

2.7 Monomer analysis using HPAEC-PAD and GC-MS

This section is concerned with the analysis of the monosaccharide compositions of sophorolipids by chromatographic techniques (HPAEC-PAD and GC-MS). The direct analysis of the monosaccharides released by acid catalysed hydrolysis of the sophorolipids, using trifluoroacetic acid (TFA), was performed using HPAEC-PAD. Monomer analysis via derivatisation to their alditol acetates involved three chemical steps, namely; acid hydrolysis, reduction and acetylation and GC-MS analysis. [143]

2.7.1 Acid hydrolysis reaction of sophorolipids

An amount of sophorolipid (3.0 mg) was added to a pressure tube containing TFA (2.0 ml of 2 M); the tube was heated to 120 $^{\circ}$C for 2 h.

After the 2 h period had elapsed, the sample solution was cooled to room temperature and the cap of the pressure tube was removed. The solution was evaporated to dryness under a constant stream of nitrogen gas at 60 $^{\circ}$C to give monomers that can be analysing by HPAEC. Ultra-pure water (3.0 ml) was then added to the dry residue in order to give a sample concentration of 1000 ppm. Half of this volume (1.5 ml) was used for HPAEC-PAD analysis after a further dilution to suit the concentration required for the monomer analysis by HPAEC, whereas the other (1.5 ml) was used in the next reduction step.

2.7.2 Reduction

In this step, the hydrolysed monomer sample (1.5 ml) was treated with sodium borohydride (40.0 mg), in order to reduce the sugar monomers; the tube was sealed and heated at 40 °C for 2 h. After 2 h the solution was evaporated to dryness as previously detailed. Glacial acetic acid (1.0 ml) was then added to destroy any excess borohydride present; the solution was then evaporated under a stream of nitrogen. Methanol (3 x 1.0 ml) was added and repeatedly evaporated to remove the borate complex and give the sugar alditols.

46

2.7.3 Acetylation

For the acetylation, pyridine (2.0 ml) and acetic anhydride (2.0 ml) were then added to the dry residue (sugar alditols) in the pressure tube; the sample was heated at 100 °C for 2 h. After 2 h the resulting solution was evaporated to dryness. The dried acetylated monomers (alditol acetates) were suspended in deionised water (5.0 ml) and extracted with chloroform (3 x 5.0 ml); the total organic layer was then washed with deionised water (5.0 ml). The solution was then dried over anhydrous sodium sulphate for 30 mins before being filtered and the resulting solution evaporated as previously described. The dried residue was reconstituted by dissolution in acetone (2.0 ml) in preparation for GC-MS analysis.

2.8 High-Performance Anion Exchange Chromatography-Pulsed Amperometric Detection (HPAC-PAD)

The prepared solutions, which were obtained after the hydrolysis reactions, were transferred into small glass vials for preparation for HPAEC-PAD analysis. The HPAEC instrument used was a Dionex ICS-3000 Ion Chromatography System (Dionex Corporation, CA, USA), which consists of Dionex AS (Autosampler), Dionex ICS 3000 DP-Dual Pump System, Dionex ICS-3000, (EG-Eluent Generator, RFIC-Reagent-Free Ion Chromatography). The Chromeleon® Xpress software was used for the processing of the data.

The monosaccharide and disaccharide standards used as controls were prepared to the specific concentrations in ultra-pure water (UPW) and were run as triplicate using the chromatographic conditions listed below:

Chromatographic Conditions	
Instrument	Dionex ICS-3000 Ion Chromatography System (Dionex Corp. CA, USA)
Pump	Dionex ICS-3000 DP-Dual Pump System
Column	CarboPac PA 20 analytical column, 3 x 150 mm, 6.0µm particle size
Flow Rate	0.30 ml. min^{-1}
Mobile Phase	10 mM NaOH
Injection Volume	25.0 µL
Temperature	30 ºC
Detector	PAD
Run Time	25 mins

2.9 Gas Chromatography-Mass Spectrometry GC-MS

GC-MS analysis was performed on an Agilent 7890A GC system, coupled with an Agilent 7683B Injector and Agilent 5975B Inert XL EI/CI MSD (Agilent Technologies UK Ltd. Cheshire, UK). Samples were eluted from an Agilent HP5-MS (30 m x 250 µm-id, 0.25 µm) column (Agilent Technologies UK Ltd.) eluting with helium (1 ml/min).

The chromatographic conditions for the monomer analysis of the components derived from sophorolipids by GC-MS are listed below and samples were run in triplicates.

Chromatographic Conditions	
Instrument	Agilent 7890A GC system (Agilent Technologies, Edinburgh, UK)
Column	Agilent 19091S-433, 30 m x 250 µM x 0.25 µM
Carrier Gas	Helium
Mass Spectrometer	Agilent 5975B Inert XL EI/CI MSD
Mode	Split (split ratio of 10:1)
Injection Volume	0.25 µL
Ionisation	Electron Impact (EI)
Flow Rate	1.0 ml/min
Monosaccharide method program	180 °C for 1 min, 1 °C/min to 220 °C, hold 5 min
Oven Temperature	220 °C
Pressure	14.992 psi
Run Time	46 mins

2.9.1 Linkage analysis (Methylated Alditol Acetate Method)

This section is concerned with the conversion of sophorolipids compounds into per-*O*-methylated alditol acetates (PMAAs), followed by analysis by GC-MS. The linkage analysis is very similar to the monomer characterisation method but employs an initial methylation step first to generate the methylated sugars:

An amount of sophorolipid sample (3 mg) was added to a pressure tube containing anhydrous dimethyl sulfoxide (DMSO) (0.7 ml) and was stirred at room temperature until the formation of the slurry was observed. Dried and crushed NaOH (50 mg) was added with stirring along with methyl iodide (60 µl).

After 25 mins the resulting solution was suspended in UPW (1.0 ml) and extracted with dichloromethane (1.0 ml), the organic layer was then washed with UPW (3 x 5.0 ml). The resulting liquid was then evaporated to dryness under a stream of nitrogen gas at 40 °C. To give the methylated disaccharide as a solid, this was used directly in the next step.

The dried residue (methylated disaccharide) was then subjected to the same procedure as previously described for GC-MS monomer analysis (Sections 2.7.1, 2.7.2 & 2.7.3) the only difference to the method being the substitution of sodium borohydride with sodium borodeuteride in the reduction reaction (section 2.7.2). Samples were run in triplicates.

2.9.2 GC-MS analysis of PMAAs

GC-MS analysis and chromatographic conditions for analysis of the prepared PMAAs for sophorose and disaccharide samples are listed as follows:

Chromatographic Conditions	
Instrument	Agilent 7890A GC system (Agilent Technologies, Edinburgh, UK)
Column	Agilent 19091S-433, 30 m x 250 µM x 0.25 µM
Carrier Gas	Helium
Mode	Split (split ratio of 10:1)
Injection Volume	0.25 µL
Flow Rate	1.0 ml/ min
Sophorose Method Program	150 °C for 1 min, 5 °C/min to 300 °C
Oven Temperature	220 °C
Pressure	14.992 psi
Run Time	44 mins

2.10 Extraction of isomaltose and sophorose from the lactone waste

Lactone waste (100 ml, 98 g, and pH 1.57) was suspended in ultra-pure water (200 ml) and left to stir at 35-40 °C for 1h. The resulting brown suspension was centrifuged (4200 rpm for 10 mins) and the supernatant was collected. After completion of the separation process, the aqueous phase was rotary evaporated at a temperature of 45 °C to give a crude mixture of salts and sugars as brown syrup (5.50 g). The resulting brown syrup was stored at -18 °C before being used directly in the next step.

2.10.1 Isolation and separation of glucose, isomaltose and sophorose using a carbon: celite 535 column

The isolated crude sugar mixture was subjected to a carbon: celite column chromatography as follows:

2.10.1.1 Preparation of a carbon: celite column

The adsorbent dry charcoal (Darco G-60, 200 g, 100 mesh and Celite 535, 200 g) was mixed carefully and slurried in UPW (1 L). After thorough mixing, the mixture was allowed to settle for 1h and fine carbon particles were removed by decantation. A layer of sand (1-2 cm) deep was added to a fritted glass chromatography column (5 cm x 50 cm). The carbon: celite slurry was suspended in UPW and carefully poured into the column and the UPW (1 L) eluted through the column under gravity to pack the bed thoroughly. After packing the column, another layer of sand (2 cm) was added on the top surface of the column. The salt and sugar mix (5.50 g) was dissolved in UPW (3.0 ml) and the sample sonicated for 5 min before being applied to the top of the column. Elution of sugars was carried out with an increasing concentration of aqueous ethanol (from 0 to 20 % in UPW in 5 % incremental steps of 2 L). Sample fractions (45.0 ml) were collected and subjected to analysis.

HPAEC-PAD analysis of the different fractions identified salt plus glucose in the fractions eluting with 5 % ethanol (4 g) isomaltose (9) in the fractions eluting with 10 % ethanol (0.5 g) and sophorose (10) from the fractions eluting with 20 % ethanol (1 g).

2.11 Isolation of 2-*O*-β-D-glucopyranosyl-α/β-D-mannose (11)

Sophorose (50 mg) was treated with aqueous sodium hydroxide (100 mM, 20 ml at pH 13) in a pressure tube and was held at 60 °C for 24 h. The progress of the reaction was monitored using HPAEC; small samples (1.0 ml) were removed every 3 h and the pH of the sample was adjusted to 6 using glacial acetic acid. Samples were then transferred to small glass vials and injected into the HPAEC using sodium hydroxide (50 mM) as the mobile phase.

HPEAC analysis suggested that the reaction had reached equilibrium after 24 h at which time the remaining solution was neutralised with glacial acetic acid and the solvent removed under vacuum to give a crude mixture of sugars and sodium acetate as a yellow solid. The sample was re-dissolved in ultrapure water (1.0 ml) and was applied to the top of a carbon: celite column (2.5 x 20 cm). Elution of sugars was carried out with an increasing concentration of aqueous ethanol (from 0 to 20% ethanol in UPW in 5 % incremental steps each of 200.0 ml). The desired product eluted with 20 % aqueous ethanol and the combined fractions were rotary evaporated to give a pure sample of 2-*O*-β-D-glucopyranosyl-α/β-D-mannopyranose (11) as a white solid (10 mg, 40 % overall yield based on the volume of solution remaining at the end of the reaction). The identity and anomeric purity of the product were determined by 1D- and 2D-NMR.

2.12 Monitoring the base catalysed hydrolysis of sophorolipids

Acid sophorolipid (200 mg, 0.322 mM) was dissolved in aqueous sodium hydroxide (10 mM, 20 ml at pH 12) in a pressure tube at a temperature of 50 °C for around 270 min.

Samples (1.0 ml) were taken at 30 min intervals and the pH of the samples was adjusted to pH 6 using glacial acetic acid. Samples were then transferred into small glass vials and injected into the HPAEC.

2.13 Monitoring the stability of sophorose in aqueous alkaline solution

Sophorose (5 mg, 0.015 mM) was treated with aq. sodium hydroxide (100 mM, 20 ml at pH 13) in a pressure tube at room temperature for 32 h. Samples (1.0 ml) were taken out every 1 h and the pH of the sample was adjusted to 6 using glacial acetic acid. Samples were then transferred into small glass vials and injected into the HPAEC using sodium hydroxide (50 mM) as the mobile phase.

The same experiment was carried out on sophorose (8 mg), but in an alkaline solution of NaOD (100 mM, 600 µl in D_2O) at room temperature. The progress of the reaction was followed by running ^{1}H-NMR spectra after 1, 12 & 24 h. A sophorose standard was used as a control for the reaction.

2.14 Hydrolysis of sophorolipids by spent fermentation broth

A sample of a fermentation broth (250 ml, pH 3.5) recovered at the end of the fermentation process was supplied by Croda Biotechnology and was stored in a cold-room for 24 h before being used to test for the presence of enzyme activity that may hydrolyse sophorolipids. In separate experiments, both lactone and acid sophorolipids (0.5 g) were added to a 250 ml clean and autoclaved conical flask containing fermentation broth (50.0 ml, pH 3.5) and a third flask without any sophorolipid was used as a control. The newly prepared mixtures were kept in a shake–flask incubator. The incubator conditions were set as follows: 30 ºC, under agitation at 120 rev/min for 3 days (Stuart Orbital Incubator, SI 500). After 24 h intervals, samples (1.0 ml) were taken and filtered through (0.45 µl disk filter) and the supernatant was diluted with UPW (2.0 ml) then transferred into small vials. The sugar composition of the flasks was assayed by HPAEC-PAD.

2.15 Monitoring the acid catalysed hydrolysis of sophorolipids

Acid sophorolipid (500 mg, 0.804 mM) was dissolved in aqueous sulphuric acid (2 M, 20.0 ml at pH 0.30) in a round-bottomed flask and refluxed at a temperature of 92 °C for 24 h. Brown oil droplets were observed suspended in the reaction mixture. [144] The reaction vessel was allowed to cool down to room temperature; the mixture was transferred to a separating funnel and was extracted with hexane (2 x 25.0 ml). The hexane layer was reduced using a rotary-evaporator and the resulting yellowish oil (300 mg) was analysed by NMR.

Scheme 8
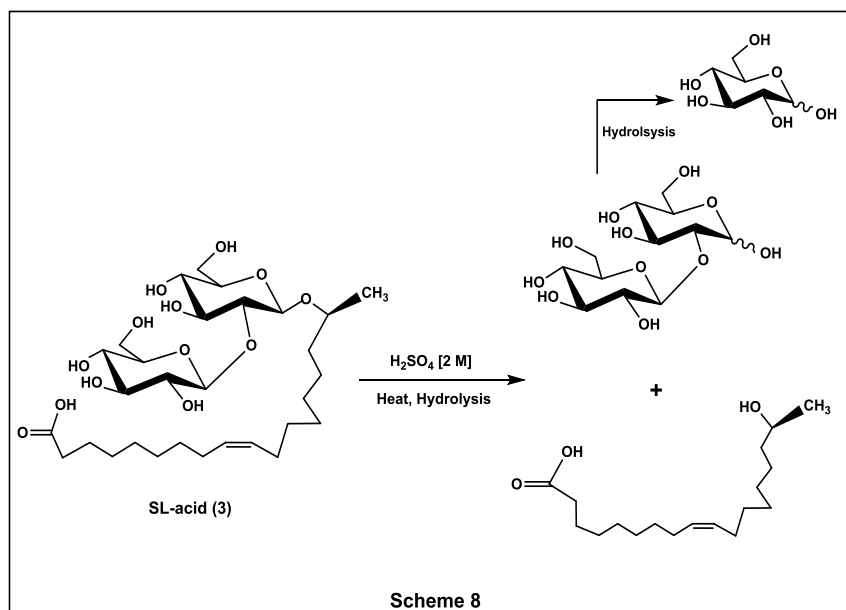
2.16 Synthesis of sophorose derivatives (glycosylation reaction)

The sophorose isolated form the lactone waste has been used as the sugar substrate for the chemical synthesis of a number of novel sophorolipids as follows:

54

2.16.1 Synthesis of 1′, 2″, 3′, 3″, 4′, 4″, 6′, 6″-octa-*O*-acetyl-β-D-sophorose (12)

Scheme 9
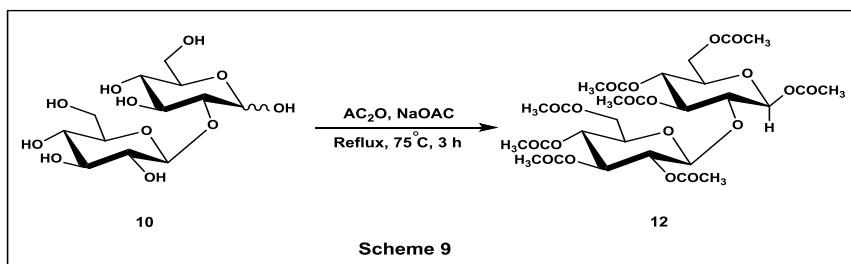
In a dry porcelain mortar, sophorose (0.61 g, 1.75 mM) was ground with anhydrous sodium acetate (0.4 g, 4.87 mM) and the powdered mixture was placed in a 100 ml round bottomed flask. Acetic anhydride (8.0 ml) was added and the mixture was allowed to reflux for 3 h at a temperature of 75 °C. The reaction mixture was then poured into ice-cold water 30.0 ml in a beaker and allowed to stand with occasional stirring for about 3 h. The resulting white crystals were filtered under vacuum and washed with cold water and the product recrystallised from methylated spirits (20.0 ml) to give the product (12) as a white powder of (0.48 g, yield 85%).[145-147]

M.P.: 193-194 ºC. (Literature M.P.: 191-192 ºC) [148]

FT-IR: (cm^{-1}) 2957, 2851, 1764, 1373, 1213, 1030.

^{1}H-NMR: (CDCl$_3$, 400 MHz, ppm) *δ* 5.68 (1 H, d, *J*= 7.9 Hz, H-1′), 5.25 (1 H, AK$_2$, *J*= 9.6, H-3′), 5.15 (1H, AK$_2$, *J* = 9.6 Hz, H-3″), 5.06 (1H, AK$_2$, *J* = 8.4 Hz, H-4′), 5.02 (1H, m, H-4″), 4.94 (1 H, AK$_2$, *J* = 9.2 Hz, H-2″), 4.64 (1 H, d, *J* = 8.08, H-1″), 4.37 (1 H, m, H-6′a), 4.34 (1H, m, H-6″a), 4.17 (1H, m , H-5′), 4.10 (1H, d, *J* = 9.2 Hz, H-6′b), 4.08 (1 H, m, H6″b), 3.84 (3 H, t, *J* = 8.8 Hz, H-2′), 3.69 (1H, m, H-5″), 2.15, 2.13, 2.12, 2.11, 2.09, 2.04, 2.02, 2.00, (24 H, 8 s, -OCOC*H*$_3$).

^{13}C-NMR: (CDCl$_3$, 400 MHz, ppm) *δ* 170.58, 170.53, 170.33, 169.827, 169.78, 169.36, 169.30, 168.74 (8 x C=O), 100.95 (C-1″), 91.73 (C-1′), 77.08 (C-2), 74.47 (C-3′), 72.83 (C-3″), 72.45 (C-5″), 71.83 (C-2″), 71.03 (C-5′), 68.06 (C-4″), 67.95 (C-4′), 61.83 (C-6″), 61.49 (C-6′), 20.79, 20.72, 20.67, 20.56, 20.56, 20.56, 20.39, 20.32 (8 x -OCOC*H*$_3$).

m/z (HPLC-ESI$^+$, ACN: H$_2$O (6:4): [M+NH$_4$]$^+$ for C$_{28}$H$_{38}$O$_{19}$ calculated 678.2007, measured 678.2006.

2.16.2 Synthesis of 2″, 3′, 3″, 4′, 4″, 6′, 6″- hepta-*O*-acetyl-α-D-sophoryl bromide (13)

Scheme 10
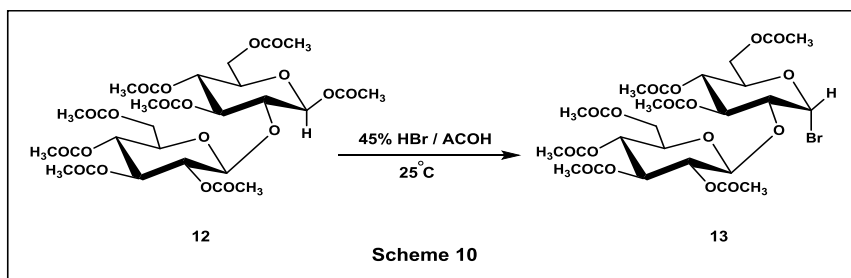
The β-D-sophorose octaacetate, 12 (0.92 g, 1.34 mM) was added to a round-bottomed flask containing HBr in acetic acid (45% w/v, 6.0 ml) at room temperature and the mixture was left stirring for 1 h at room temperature. After 1 h, the reaction mixture was poured into a beaker containing ice-cold water (25.0 ml) and left to cool to room temperature before adding dichloromethane (20.0 ml) to the flask. The two layers were separated; the organic layer was washed with four portions of water (10.0 ml) until the aqueous phase was close to neutral pH 6. The organic layer was dried over anhydrous sodium sulphate and filtered. The product was obtained by removing the solvent on a rotary evaporator at 40 °C to give a crude white solid product (13) of (0.78 g, yield 76%). [149-150]

M.P.: 168 -170 ºC. (No literature M.P., has been reported)

FT-IR: (cm^{-1}) 2961, 2953, 1738, 1366, 1208, 1030 and 557.

^{1}H-NMR: (CDCl$_3$, 400 MHz, ppm) *δ* 6.45 (1 H, d, *J* = 4 Hz, H-1′α), 5.48 (1 H, AK$_2$, *J* = 9.6, H-3′), 5.15 (1H, AK$_2$, *J* = 9.2 Hz, H-3″), 5.11 (1H, AK$_2$, *J* = 7.0 Hz, H-4′), 5.08 (1 H, m, H-4″), 4.94 (1 H, t, *J* = 8.8 Hz, H-2″), 4.70 (1 H, d, *J* = 7.80, H-1″ β), 4.38 (1 H, m, H-6″a), 4.34 (1H, m, H-6″a), 4.25 (1H, m, H-5′), 4.20 (1H, d, *J* = 4.5 Hz, H-6′b), 4.17 (1 H, m, H6″b), 4.09 (1H, m, H-2′), 3.81(1H, dd, H-5″), 2.13, 2.10, 2.08, 2.05, 2.04, 2.02, 2.01 (21 H, 7 s, -OCOC*H*$_3$).

^{13}C-NMR: (CDCl$_3$, 400 MHz, ppm) *δ* 170.65, 170.47, 170.37, 169.70, 169.47, 169.27, 169.00, (7 x C=O), 100.93 (C-1″), 88.77 (C-1′), 77.08 (C-2′), 72.53 (C-3′), 72.09 (C-3″), 72.45 (C-5″), 71.90 (C-2″), 70.99 (C-5′), 68.09 (C-4″), 67.10 (C-4′), 61.12 (C-6″), 61.08 (C-6′), 20.76, 20.75, 20.69, 20.60, 20.58, 20.58, 20.33 (7 X -OCOC*H*$_3$).

m/z (HPLC-ESI$^+$, ACN:H$_2$O (6:4): [M+Na]$^+$ for C$_{26}$H$_{35}$O$_{17}$Br calculated 698.1058, measured 698.1045.

2.16.3 Synthesis of oleyl 2″, 3′, 3″, 4′, 4″, 6′, 6″-hepta-*O*-acetyl-β-D-sophoroside (14)

Scheme 11
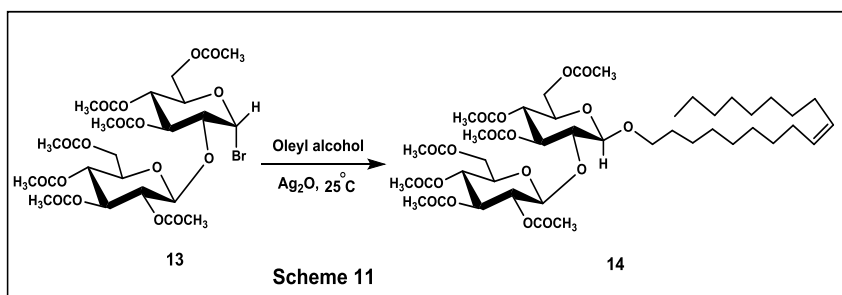
In a dry round bottom flask (100 ml), the product 13 (0.90 g, 1.28 mM) was added along with oleyl alcohol (0.41 ml, 1.28 mM). Dichloromethane (30.0 ml) was used as the solvent and silver oxide (200 mg) along with of pre-dried molecular sieves 4 Å, 2.5 g. The reaction was carried out at 25 °C for 45 h and the flask was sealed with a calcium chloride guard tube. Once completed, the reaction mixture was diluted with dichloromethane (15.0 ml) and stirred for further 30 min and then filtered through a pad of celite, and the filtrate was evaporated under vacuum. The residue was recrystallised from ethanol to give the final product (14) as white flocks (0.58 g, 64.4 %). [151-153]

FT-IR: (cm^{-1}) 2923, 2853, 1741, 1569, 1366, 1217, 1030.

^{1}H-NMR: (CDCl$_3$, 500 MHz, ppm) *δ* 5.34 (2 H, m, H-9 & H-10), 5.17 (1H, AK$_2$, *J* = 9.2 Hz, H-3′), 5.14 (1 H, AK$_2$, *J* = 9.6, H-3″), 5.07 (1 H, AK$_2$, *J* = 8.9 Hz, H-4′), 4.90 (1H, t, *J* = 7.8 Hz, H-4″), 4.50 (1H, d, *J* = 7.7, H-1′), 4.43 (1 H, d, *J* = 7.9 Hz, H-1″), 4.37 (1 H, m, H-6′a), 4.09 (1 H, m, H-6″a), 4.05 (1H, d, H-5′), 4.02 (1H, d, *J* = 2.9, H-6′b), 3.82 (1H, m, H-6″b), 3.76 (2 H, t, *J* = 9.4, sugar-O-C*H$_2$*-), 4.17 (1H, m, H6″b), 3.65 (1H, m, H-2′), 3.57 (1H, m, H-5″), 2.12, 2.08, 2.03, 2.02, 2.01, 1.98, 1.96 (21 H, 7 s, -OCOC*H$_3$*), 1.54 (4 H, m, H-8 & H-11), 1.26 (24 H, brs, H-2-7 & H-12-17), 0.87 (3 H, t, *J* = 6.9, H-18). **α/β ratio:** 1.7:1.

^{13}C-NMR: (CDCl$_3$, 500 MHz, ppm) *δ* 170.52, 170.55, 170.24, 169.85, 169.57, 169.32, 169.05, (7 x C=O), 130.01, 129.80 (C-9 & C-10), 100.81 (C-1″), 100.69 (C-1′), 76.59(C-2′), 72.97 (C-3′), 72.64 (C-3″), 72.55 (C-5″), 71.96 (C-2″), 71.63 (C-5′), 70.28 (sugar-O-CH$_2$-), 68.09 (C-4″), 67.80 (C-4′), 61.93 (C-6″), 61.55 (C-6′), 31.92 (C-3), 29.77 (C-8), 29.55 (C-11), 29.739, 29.32, 29.27, 27.12, 27.20, 25.60, 25.50, 23.42,

22.67, 22.52 (C-4-7 & C-12-17), 20.89, 20.68, 20.68, 20.57, 20.55, 20.51, 20.30 (7 x -OCOCH_3), 14.14 (C-18).

m/z (ESI$^+$): [M+NH$_4$]$^+$ for C$_{44}$H$_{70}$O$_{18}$ calculated 886.4562, measured 886.4562.

2.16.4 Synthesis of oleyl β-D-sophoroside (15)

Scheme 12
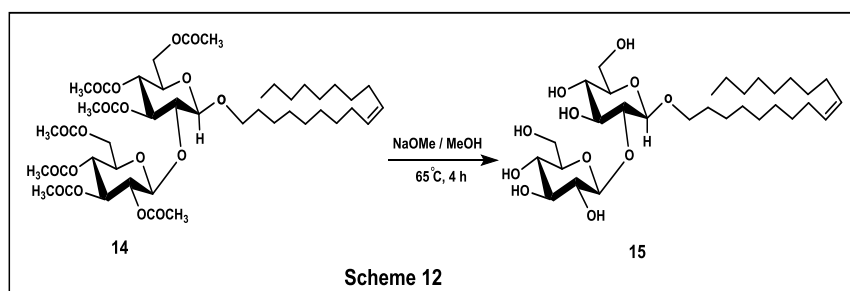
The product 14 (0.53 g, 0.59 mM) and sodium methoxide (0.032 g, 0.59 mM) were added to a round-bottomed flask with dry methanol (10.0 ml). The reaction mixture was left to stir for 4 h at a temperature of 65 °C. The reaction mixture was protected from atmospheric moisture by the use of calcium chloride guard tube. On completion, the reaction mixture was cooled down to room temperature and acidified using glacial acetic acid to pH 6, then concentrated by rotary evaporation to (10.0 ml) then was poured with stirring into ice-cold d.H$_2$O (25.0 ml) resulting in the precipitation of the product as a white solid, which was recrystallised from hot methanol (10.0 ml). The product (15) was recovered as a white powder (0.36 g, yield 70.1 %).

FT-IR: (cm^{-1}) 3433-3377, 2921, 2853, 1569, 1376, 1058, 1026.

^{1}H-NMR: (DMSO, 500 MHz, ppm) *δ* 5.34 (2H, m, H-9 & H-10), 4.26 (1H, d, *J* = 7.1 Hz, H-1'), 4.15 (1H, d, *J* = 6.95, H-1″), 3.73 (1H, m, H-3'), 3.70 (1H, m, H-3″), 3.68 (1H, m, H-4'), 3.61 (1H, m, H-6'a), 3.41 (1H, m, H-6'b), 4.09 (1H, m, H-6″a), 3.39 (1H, m, H-5'), 3.30 (1H, m, H-6'b), 3.28 (1H, m, H-6″b), 3.24 (1H, m, H-2'), 3.17 (2H, t, *J* = 8.0 Hz, Sugar-O-CH_2-), 3.03 (1H, m, H-5″), 1.50 (4H, m, H-8 & H-11), 1.24 (24 H, brs, H-2-7 & H-12-17), 0.85 (3 H, t, *J* = 6.5, H-18). **α/β ratio:** 1.1:1

^{13}C-NMR: (CDCl$_3$, 500 MHz, ppm) *δ*, 130.07, 130.03 (C-9 & C-10), 103.68 (C-1″), 103.04 (C-1'), 80.98 (C-2'), 77.27 (C-3'), 76.77 (C-3″), 75.44 (C-5″), 75.25 (C-2″), 73.67 (C-5'), 73.47 (C-4″), 70.36 (C-4'), 69.19 (Sugar-O-CH_2-), 61.34 (C-6″), 60.81

(C-6′), 31.79 (C-3), 29.73 (C-8), 29.64 (C-11), 29.57, 29.42, 29.32, 29.18, 29.14, 29.07, 27.11, 27.05, 20.01, 22.56 (C-4-7 & C-12-17), 23.72 (C-18).

m/z: (ESI$^+$): [M+NH$_4$]$^+$ for C$_{30}$H$_{56}$O$_{11}$ calculated 592.3823, measured 592.3816.

2.16.5 Synthesis of stearyl 2", 3′, 3", 4′, 4", 6′, 6"-hepta-*O*-acetyl-β-D-sophoroside (16)

Scheme 13
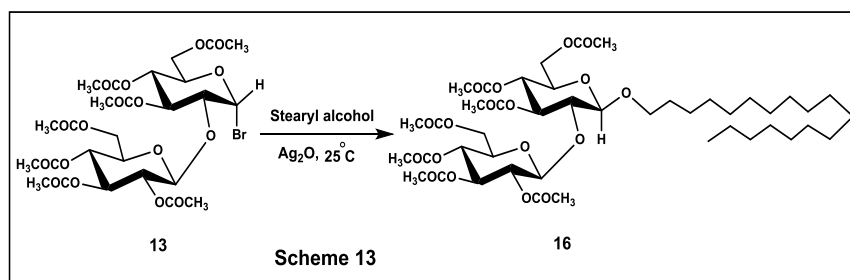
In a dry round bottom flask (100 ml), the product 15 (0.40 g, 0.572 mM) was added to stearyl alcohol (0.155 g, 0.572 mM). Dichloromethane (25.0 ml) was used as the solvent and silver oxide (220 mg) was added along with of pre-dried molecular sieve 4 Å, 2.5 g. The reaction was carried out at 25 $^\circ$C for 45 h and the flask was sealed with calcium chloride guarding tube and secluded from light. After that, the reaction mixture was diluted with dichloromethane (15.0 ml) and the solution stirred for a further 30 min before being filtered through a pad of celite. The filtrate was evaporated under vacuum. The residue was recrystallised from hot methanol (20.0 ml) to give white flocks of the desired product (16) (0.32 g, 76.5%).

FT-IR: (cm^{-1}) 2919, 2850, 1741, 1367, 1215, 1034.

^{1}H-NMR: (CDCl$_3$, 500 MHz, ppm) *δ* 5.20 (1H, m, H-3′), 5.16 (1H, m, H-3″), 5.08 (1H, t, *J* = 8.9 Hz, H-4′), 4.93 (1H, m, H-4″), 4.52 (1H, d, *J* = 7.95, H-1′), 4.46 (1 H, d, *J* = 7.91 Hz, H-1″), 4.39 (1H, dd, H-6′a), 4.11 (1 H, dd, H-6″a), 4.06 (1H, m, H-5′), 3.86 (1H, m, H-6′b), 3.82 (1H, m, H-6″b), 3.78 (2 H, t, *J* = 9.4, Sugar-O-C*H₂*-), 3.67 (1H, m, H-2′), 3.60 (1H, m, H-5″), 2.14, 2.11, 2.06, 2.04, 2.03, 2.02, 2.00 (21H, 7s, OCOC*H₃*),

1.56 (2H, m, H-2-chain), 1.27 (31H, brs, H-3-17), 0.89 (3H, t, *J* = 7.05, H-18). **α/β ratio:** 1:1.5

¹³C-NMR: (CDCl₃, 500 MHz, ppm) *δ* 170.71, 170.29, 170.23, 169.67, 169.40, 169.31, 169.18, (7 x C=O), 101.94 (C-1″), 100.77 (C-1′), 77.70 (C-2′), 73.01 (C-3′), 72.48 (C-3″), 71.97 (C-5″), 71.91 (C-2″), 71.33 (C-5′), 69.68 (C-4″), 68.13 (C-4′), 63.16 (Sugar-O-*C*H₂-), 61.90 (C-6″), 61.57 (C-6′), 32.78 (C-2), 31.89 (C-3), 29.92, 29.80, 29.739, 29.32, 29.27, 27.12, 27.20, 25.60, 25.50, 23.42, 22.67, 22.52 (C-4-17), 21.00, 20.88, 20.84, 20.66, 20.59, 20.54, 20.30 (7 x -OCO*C*H₃), 14.19 (C-18).

m/z: (ESI⁺): [M+NH₄]⁺ for C₄₄H₇₂O₁₈ calculated 888.4719, measured 888.4703.

2.16.6 Synthesis of 2″, 3′, 3″, 4′, 4″, 6′, 6″-hepta-*O*-acetyl-α/β-D-sophorose (17)

Scheme 14
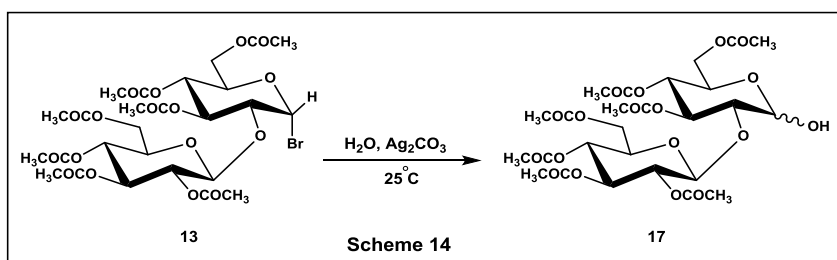
The product 13 (0.73 g, 1.04 mM) was reacted with UPW (0.019 ml, 1.04 mM). Dichloromethane (20.0 ml) was used as the solvent to which silver oxide (200 mg) was added. The reaction was carried out at 25 °C for 36 h and the flask was sealed with calcium chloride guarding tube and secluded from light. After that, the reaction mixture was diluted with dichloromethane (15.0 ml) and stirred for a further (30 min) before being filtered through a pad of celite and the filtrate was evaporated under vacuum. The residue was rotary evaporated and recrystallised from hot methanol to give the product as a mixture of anomers as white flocks (0.61 g, 83.56 %).

M.P.: 188 -190 ºC.

FT-IR: (cm⁻¹) 3478, 2961, 1738, 1366, 1212, 1031.

¹H-NMR: (CDCl₃, 400 MHz, ppm) *δ* 5.46 (1 H, t, *J* = 9.6, H-3′), 5.37 (1 H, d, *J* = 3.3 Hz, H-1′α) and 4.96 (1 H, m, H-1′α), 5.17 (1 H, t, *J* = 9.4 Hz, H-3″), 5.06 (1H, t, *J* = 8.9 Hz, H-4′), 5.00 (1 H, t, *J* = 6.5, H-4″), 4.98 (1 H, t, *J* = 8.8 Hz, H-5′), 4.72 (1 H, d, *J* = 7.06, H-1″ β) and 4.64 (1 H, d, *J* = 7.9, H-1″ β) 4.31 (1H, m, H-6′a), 4.29 (1H, m, H-

6″a), 4.20 (1H, d, J = 3.5 Hz, H-2″), 4.08 (1H, m, H-6′b), 3.78 (1H, m, H6″b), 3.72 (1H, d, J = 7.0 Hz, H-2′), 3.70 (1H, m, H-5″), 2.11, 2.09, 2.06, 2.04, 2.02, 2.01, 2.00 (21 H, 7 s, -OCOCH_3). **α/β ratio:** 1:1.2

^{13}C-NMR: (CDCl3, 400 MHz, ppm) δ 170.82, 170.76, 170.30, 169.92, 169.77, 169.37, 169.32, (7 x C=O), 101.01 (C-1″) and 100.50 (C-1″) 90.90 (C-1′) and 95.07 (C-1″), 77.79 (C-2′), 72.52 (C-3′), 72.15 (C-3″), 71.51 (C-5″), 70.69 (C-2″), 68.33 (C-5′), 68.17 (C-4″), 67.25 (C-4′), 61.96 (C-6″), 61.59 (C-6′), 20.82, 20.78, 20.76, 20.64, 20.58, 20.58, 20.38 (7 x -OCOCH_3).

m/z (HPLC-ESI$^+$, ACN:H_2O (6:4): [M+Na]$^+$ for $C_{26}H_{36}O_{18}$ calculated 636.1902, measured 636.1885.

2.16.7 Synthesis of 2″, 3′, 3″, 4′, 4″, 6′, 6″-hepta-*O*-acetyl-1'-*O*-palmitoyl-β-D-sophoroside (18)

Scheme 15
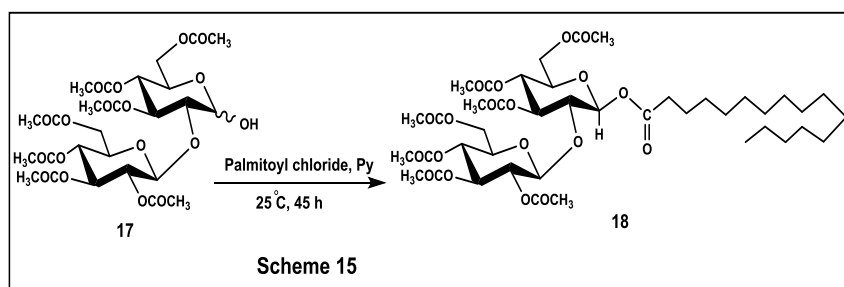
The product 17 (0.400 g, 0.62 mM, 1 eq.), palmitoyl chloride (0.208 g, 0.755 mM, 1.2 eq.) and pyridine (0.30 ml, 4 eq.) were added along with dichloromethane (20.0 ml). The reaction was carried out at 25 ºC for 45 h. After that the reaction mixture was concentrated and extracted with DCM (10.0 ml) and UPW (20.0 x 2 ml). The organic layer was back washed with brine water (20.0 ml x 2).

The organic phase was dried over anhydrous sodium sulphate. The crude product was filtered and rotary-evaporated and recrystallised from ethanol (30.0 ml) to give the product (18) as white flocks (0.281 g, 70.25 %).

M.P.: 114 -116 ºC.

FT-IR: (cm^{-1}) 2916, 2848, 1740, 1703, 1366, 1214, 1033.

¹H-NMR: (CDCl₃, 400 MHz, ppm) δ 5.68 (1 H, d, J = 8.2 Hz, H-1′), 5.24 (1 H, t, J = 9.3, H-3′), 5.15 (1H, t, J = 9.3 Hz, H-3″), 5.06 (1H, m, H-4′), 5.06 (1 H, m, H-4″), 4.98 (1 H, t, J = 8.8 Hz, H-5′), 4.52 (1 H, d, J = 7.8, H-1″), 4.40 (1H, dd, H-6′a), 4.37 (1H, m, H-6″a), 4.15 (1H, m, H-6′b), 4.12 (1H, m, H6″b), 3.83 (1H, d, J = 9.0 Hz, H-2′), 3.67 (1H, m, H-2″), 2.45 (1H, d, J = 7.9 Hz, H-5″), 2.35 (2 H, m, sugar-O-COCH_2), 2.14, 2.11, 2.05, 2.04, 2.02, 2.01, 2.00 (21 H, 7 s, -OCOCH_3), 1.61 (2 H, m, H-3-chain), 1.27 (24 H, brs, H-4-15), 0.89 (3 H, t, J= 6.96, H-16). **α/β ratio**: 1:1.6

¹³C-NMR: (CDCl3, 400 MHz, ppm) δ 171.75 (sugar-O-CO-CH₂), 170.29, 170.27, 169.70, 169.67, 169.49, 169.33,169.05 (7 x C=O), 100.73 (C-1″), 92.36 (C-1′), 75.96 (C-2′), 73.52 (C-3′), 72.89 (C-3″), 72.31 (C-5″), 70.01 (C-2″), 71.52 (C-5′), 70.41 (C-4″), 67.77 (C-4′), 61.61 (C-6″), 61.56 (C-6′), 47.34 (C-2 chain), 34.05 (C-3 chain), 31.64 (C-4 chain), 29.70, 29.67, 29.63, 29.60, 29.41, 27.37, 29.20, 28.94, 28.88, 24.35, 22.71 (C-5-15), 20.86, 20.82, 20.77, 20.67, 20.57, 20.56, 20.51 (7 x -OCOCH_3).

m/z (ESI+): [M+NH₄]⁺ for C₄₄H₇₂O₁₈ calculated 874.4198, measured 874.4208.

2.16.8 Synthesis of 2″, 3′, 3″, 4′, 4″, 6′, 6″-hepta-*O*-acetyl-α-(4-nitrophenyl)-D-sophorose (19)

Scheme 16
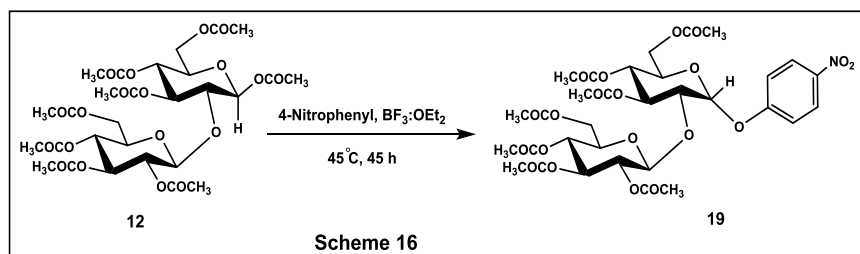
The product 12 (0.611 g, 0.900 mM, 1 eq.) was added to a solution of dichloromethane (25.0 ml) containing 4-nitrophenol (0.250 g, 1.80 mM, 2 eq.) under N₂ gas.

The mixture was cooled to 0 ºC for 30 min before adding boron trifluoride etherate (0.332 ml, 2.70 mM, 3 eq.), the reaction mixture was left to stir for 2 h at room temperature with N₂ gas flowing through. The mixture was kept under

reflux at 45 ºC for 48 h then quenched by adding a saturated NaHCO$_3$ solution (15.0 ml), diluted with dichloromethane (10.0 ml) and stirring was continued for 20 min. The organic layer was then washed with Na$_2$CO$_3$ (2 × 20.0 ml) and with brine water (2 x 20.0 ml).

The combined organic phase was dried over anhydrous sodium sulphate. The crude product was filtered and rotary-evaporated then recrystallised from hot methanol to give the product as a pure white solid (0.421 g, 68.90%).[154-156]

M.P.: 98-100 ºC.
FT-IR: (cm^{-1}) 3119, 2943, 1738, 1613, 1593, 1366, 1209, 1026.

^{1}H-NMR: (CDCl$_3$, 400 MHz, ppm) *δ* 8.24 (2 H, d, *J* = 9.1Hz, ortho Ar-H substituted), 7.25 (2 H, d, *J* = 9.2, meta Ar-H substituted), 5.73 (1H, d, *J* = 4.01 Hz, α H-1′) 5.61 (1 H, t, *J* = 9.3 Hz, H-3′), 5.14 (1H, m, H-3″), 5.03 (1 H, t, *J* = 9.7 Hz, H-4′), 4.95 (1H, t, *J* = 9.0, H-4″), 4.68 (1H, d, *J* = 8.0 Hz, β H-1″), 4.25 (1H, dd, H-6′a), 4.20 (1H, dd, H-6″a), 4.11(1H, dd, H-6′b), 4.03 (1H, m, H-6″b), 4.05 (1H, m, H-5″), 3.97 (1H, t, *J* = 3.6, H-5′), 3.85 (1H, m, H-2′), 3.60 (1H, dd, H-2″), 2.13, 2.11, 2.08 , 2.04, 2.03, 2.02, 2.00 (21H,7 s, -OCOC*H*$_3$). **α/β ratio**: 1.4:1

^{13}C-NMR: (CDCl$_3$, 400 MHz, ppm) *δ* 170.43, 170.37, 170.31, 169.72, 169.71, 169.25, 169.07 (7 x C=O), 161.2, 143.2, 125.80, 117.00 (-C=C- phenyl ring), 101.41 (C-1″), 97.00 (C-1′), 76.27 (C-2′), 72.55 (C-3″), 72.18 (C-5″), 71.26 (C-3′), 71.04 (C-2″), 68.47 (C-5′), 68.03 (C-4″), 67.97 (C-4′), 61.47 (C-6″), 61.34 (C-6′), 20.81, 20.71, 20.65, 20.58, 20.56, 20.55, 20.37 (7 x -OCOC*H*$_3$).

m/z (ESI$^+$): [M+NH$_4$]$^+$ for C$_{32}$H$_{39}$NO$_{20}$ calculated 757.2065, measured 757.2061.

2.16.9 Synthesis 4-nitrophenyl-α-D-sophoroside (20)

Scheme 17
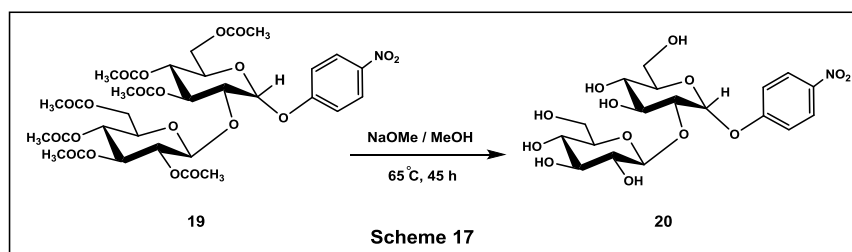
The product 19 (0.350 g, 0.46 mM) and sodium methoxide (0.032 g, 0.59 mM) were added to a round-bottomed flask with dry methanol (10.0 ml). The reaction mixture was left to stir for 4 h at a temperature of 65 °C and was protected from the atmospheric moisture by the use of a calcium chloride guard tube. On completion, the reaction mixture was cooled down to room temperature and acidified using glacial acetic acid to pH 6, then concentrated by rotary evaporation (to 10.0 ml) then was poured with stirring into ice-cold d.H_2O (25.0 ml) resulting in the precipitation of the product as a white solid, which was recrystallised from hot methanol (10.0 ml). The product (20) was recovered as white solid (0.245 g, yield 70.0%).

M.P.: 90-92 °C.

FT-IR: (cm^{-1}) 3430-3320, 2931, 2787, 2701, 1697, 1562, 1519, 1365, 1058, 1075.

^{1}H-NMR: (CD$_3$OD, 400 MHz, ppm) δ 8.22 (2 H, d, J = 8.9, ortho Ar-H substituted), 7.31 (2 H, d, J = 9.2, meta Ar-H substituted), 6.05 (1H, d, J = 3.0 Hz, α H-1′) and 6.10 (1H, d, J = 3.6 Hz, α H-1″), 5.73 (1 H, m, H-3′), 5.49 (1H, m, H-3″), 5.38 (1 H, m, H-4′), 5.30 (1H, d, J = 6.5, H-4″), 4.67 (1H, m, H-2″), 4.56 (1H, d, J = 7.6 Hz, β H-1′) and 4.65 (1H, d, J =7.5 Hz, β H-1″), 4.09 (1H, m, H-6′a), 3.92 (1H, m, H-6″a), 3.77 (1H,m, H-6′b), 3.62 (1H, m , H-6″b), 3.53 (1H, dd, H-5′), 3.45 (1H, t, J = H-2′), 3.32 (1H, m, H-5 **). α/β ratio**: 1.6:1

^{13}C-NMR: (CD$_3$OD, 400 MHz, ppm) δ 162.1, 142.4, 125.30, 116.80 (-C=C- phenyl ring), 104.50 (C-1″), 97.64 (C-1′), 80.63 (C-2′), 76.64 (C-3″), 76.15 (C-5″), 73.69 (C-3′), 73.40 (C-2″), 71.80 (C-5′), 70.20 (C-4″), 67.97(C-4′), 61.41 (C-6″), 60.30 (C-6′).

m/z (ESI$^+$): [M+Na]$^+$ for C$_{18}$H$_{25}$NO$_{13}$ calculated 463.1326, measured 463.1332.

2.16.10 Synthesis of 2″, 3′, 3″, 4′, 4″, 6′, 6″-hepta-*O*-acetyl-β-(4-nitrophenyl)-D-sophorose (21)

Scheme 18
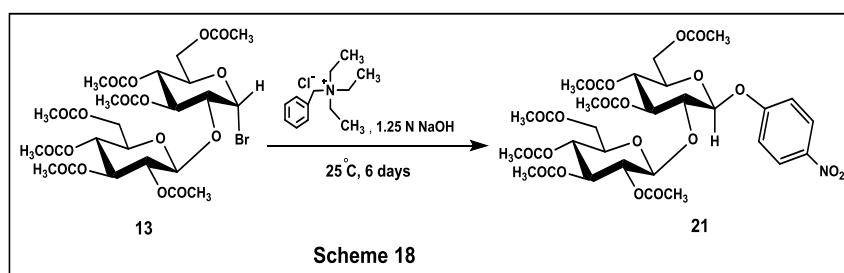
In a dry round bottom flask (250 ml), the product 13 (0.670 g, 0.96 mM, 1eq.), 4-nitrophenol (0.066 g, 0.479 mM, 0.5 eq.) and dry chloroform (40.0 ml) were added under N_2 gas and the mixture was kept under stirring. Triethylbenzylammonium chloride (1.03 g) dissolved in an aqueous sodium hydroxide solution (36.0 ml, 1.25 N) was added dropwise. The reaction mixture was left to stir at 25 ºC for 6 days. Then UPW (60 ml) was added and the reaction mixture was further extracted with dichloromethane (2 x 50.0 ml). The organic layer was then washed with UPW, dried over anhydrous sodium sulfate and concentrated under reduced pressure. The residue was then purified by silica gel column chromatography [(kiesel gel 60= 150 g, dimensions: 5.5 cm length and the eluent mixture was n-hexyl/ethyl acetate (1:1)] to obtain the desired compound (0.450 g, 68.1%) as white crystals. [157-159]

M.P.: 96-98 ºC.

FT-IR: (cm^{-1}) 3110, 2943, 1735, 1593, 1519, 1366, 1211, 1031.

¹H-NMR: (CDCl₃, 400 MHz, ppm) *δ* 8.14 (2 H, d, *J* = 8.8 Hz, ortho Ar-H substituted), 7.04 (2 H, d, *J* = 8.8, meta Ar-H substituted), 5.48 (1H, d, *J* = 3.1 Hz, H-4″), 5.08 (1 H, m, H-4′), 5.00 (1H, dd, H-2″), 5.22 (1 H, t, *J* = 9.2 Hz, H-3″), 4.87 (1H, t, *J* = 8.7, H-5′), 5.12 (1H, d, *J* = 7.9 Hz, α H-1′) and 4.98 (1H, d, *J* = 7.0 Hz, α H-1′), 4.68 (1H, *J* = 8.0 Hz, β H-1″) and 4.57 (1H, *J* = 7.7 Hz, β H-1″), 4.36 (1H, dd, H-6′a), 4.19 (1H, m, H-6′b), 4.17 (1H, m, H-3′), 4.02 (1H, m, H-6″b), 4.04 (1H, m, H-6″a), 3.95 (1H, dd, H-2′), 3.69 (1H, m, H-5″), 2.05, 2.02, 2.01, 1.98, 1.96, 1.93, 1.92 (21 H, 7 s, -OCOC*H₃*).

α/β ratio: 1:4.

13C-NMR: (CDCl$_3$, 400 MHz, ppm) δ 170.47, 170.35, 170.11, 169.70, 169.38, 169.29, 169.12 (7 x C=O), 161.50, 143.2, 125.77, 116.39 (-C=C- phenyl ring), 101.40 (C-1″) and 101.25 (C-1″), 100.70 (C-1′) and 98.28 (C-1′), 73.96 (C-2′), 73.52 (C-3′), 72.37 (C-3″), 71.93 (C-5′), 70.79 (C-5″), 68.09 (C-2″), 67.54 (C-4′), 67.35 (C-4″), 61.63 (C-6″), 60.57 (C-6′), 20.95, 20.78, 20.66, 20.61, 20.59, 20.48, 20.33 (7 x -OCOCH$_3$).

m/z (HPLC-MS, ACN:H$_2$O (5:5): (ESI$^+$): [M+Na]$^+$ for C$_{32}$H$_{39}$NO$_{20}$ calculated 757.2065, measured 757.2034.

2.16.11 Synthesis 4-Nitrophenyl-β-D-sophoroside (22)

Scheme 19
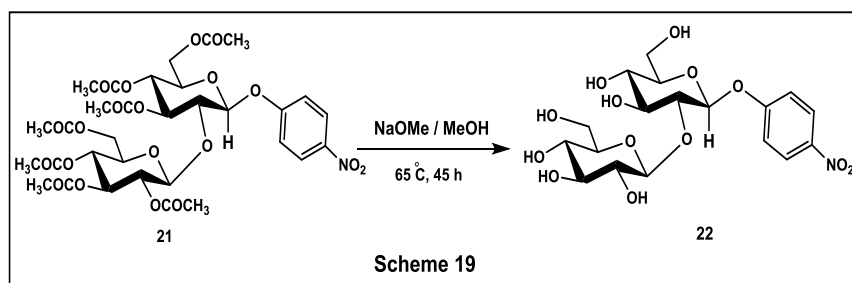
The product 21 (0.320 g, 0.42 mM) and sodium methoxide (0.032 g, 0.59 mM) were added to a round-bottomed flask with dry methanol (10.0 ml). The reaction mixture was left to stir for 4 h at a temperature of 65 °C and was protected from the atmospheric moisture by the use of calcium chloride guard tube. On completion, the reaction mixture was cooled down to room temperature and acidified using glacial acetic acid to pH 6, concentrated by rotary evaporation to (10.0 ml) and then was poured with stirring into ice-cold d.H$_2$O (25.0 ml) resulting in the precipitation of the product as a white solid, which was recrystallised from hot methanol (10.0 ml). The product (22) was recovered as a white solid (0.270 g, yield 74%).

M.P.: 91-93 ºC.

FT-IR: (cm^{-1}) 3430-3267, 2981, 2891, 1622, 1592, 1346, 1074, 1020.

1H-NMR: (DMSO-d_6, 400 MHz, ppm) δ 8.19 (2 H, d, J = 8.9, ortho Ar-H substituted), 7.28 (2 H, d, J = 9.2, meta Ar-H substituted), 5.22 (1 H, d, J = 6.8 Hz, H-1′α) and 5.20 (1 H, d, J = 6.1 Hz, H-1′α), 4.47 (1 H, d, J = 7.6, H-1′β) and 4.24 (1 H, d, J = 6.8, H-

66

1′β), 3.70 (1H, m, H-6′a), 3.57 (1H, m, H-6′b), 3.52 (1H, m, H-3″), 3.50 (1 H, m, H-2′), 3.47 (1 H, d, J = 8.5, H-3′), 3.46 (1H, m, H-6″b), 3.34 (1H, m, H-6a″), 3.25 (1H, m, H-4″), 3.17(1 H, m, H-5″), 3.12 (1 H, m, H-5′), 3.09 (1 H, m , H-4′), 2.98 (1 H, m, H-2″). **α/β ratio**: 1:4.

^{13}C-NMR: (DMSO-d_6, 400 MHz, ppm) δ 153.0, 142.50, 125.60, 117.50 (-C=C- phenyl ring), 105.32 (C-1″), 99.5 (C-1′), 83.31 (C-2′), 77.45 (C-3″), 77.39 (C-3′), 76.62 (C-5″), 75.16 (C-2″), 76.11 (C-5′), 70.06 (C-4″), 67.57 (C-4′), 61.15 (C-6″), 60.84 (C-6′).

m/z (ESI+): [M+Na]$^+$ for $C_{18}H_{25}NO_{13}$ calculated 486.1326, measured 486.1339.

2.17 Measurement of the critical micelle concentration (CMC) of sophorolipids

The minimum surface tension and critical micelle concentration (CMC) of sophorolipids and their derivatives were measured at 25 ºC using the dynamometer 0.1N surface tensiometer (Leybold® Didactic GMBH, Germany). The experiment (break-away method) was carried out with an assembly used for measuring surfactant surface tension. The apparatus used consists of a light-alloy ring with a knife edge of approximately 60 mm diameter and connected to a hook by means of three threads. When the edge is dipped into sophorolipid solution the surface tension can be determined when withdrawing the ring. The force at which the ring loses contact with the surface is equivalent to the surface tension of the liquid. The liquid level should be lowered at a constant rate by lowering the laboratory stand.

The surface tensions of different concentration of sophorolipids and their derivatives from (5 to 1000 mg/L) in UPW were measured. Sodium dodecyl sulfate (SDS) was used as the control. The data were presented as the mean of three readings. The CMC [mM] and γ_{cmc} (mN/m) values were obtained from the relationship curve between the sophorolipid's concentration and their corresponding surface tension. [160,161]

The CMC values were obtained from a plot of the surface tension as a function of the biosurfactant concentration.

The concentration at which micelles began to form was taken to be the CMC. Above this concentration, no increment was detected in the reduction of surface tension of sophorolipids.

2.18 Substrate studies: Is the sophorose derivative, 4-nitrophenyl-α-D-sophoroside a substrate for the α-glucosidase enzyme

The sophorose derivative; 4-nitrophenyl-α-D-sophoroside were tested as a substrate of the α-glucosidase (EC.3.2.1.20) from *Saccharomyces cerevisiae.* The compound 4-nitrophenyl-α-D-glucoside was used as a control substrate during the experiment.

The enzyme activity was determined by measuring the increase in the absorbance of the released 4-nitophenol at 400 nm as a function of time. The reactions were performed in a UV-spectrophotometer, Biowave ll UV spectrophotometer (Biochrom Ltd., Cambridge, UK) at room temperature.

2.18.1 UV-spectrophotometric (colorimetric) determination method

The enzyme catalysed hydrolysis reaction was studied using 4-nitrophenyl-α-D-glucopyranoside (pNP-Glc) as a substrate in the absence and presence of 4-nitrophenyl-α-D-sophoroside and using the α-glucosidase enzyme from *Saccharomyces cerevisiae.*

The reaction conditions were conducted at 37 ºC, pH 6.8 and Λ_{max} 400 nm.

Scheme 20
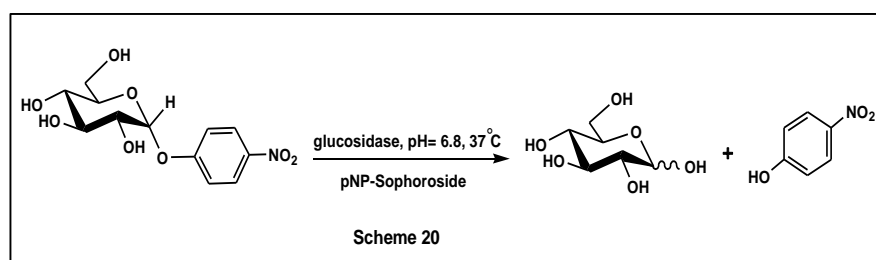
2.18.1.1 General working procedure

Separate stock solutions were prepared for the substrate, the inhibitor and the enzyme:

- 4-nitrophenyl-α-D-glucopyranoside (pNP-Glc)   0.01 M
- 4-nitrophenyl-α-D-sophoroside (pNP-Soph)   0.01 M
- α-glucosidase from *Saccharomyces cerevisiae*:   1 mg/ml
  in potassium phosphate buffer, pH 6.8, 0.067 M at 37 °C.
- Glutathione, reduced solution (GSH)   0.003 M

The reaction system was prepared as follows:

1) Test-solution: Consisted of reagent A (buffer pH 6.8, 10.0 ml), reagent B (GSH, 0.40 ml) and reagent C (enzyme solution 0.40 ml).

2) Blank-solution: Consisted of UPW (0.40 ml), reagent A (buffer pH 6.8, 10.0 ml) and reagent B (GSH, 0.40 ml).

The test and blank solutions were pipetted into a separate clean universal glass vial (20.0 ml) and mixed by inversion then equilibrated to 37 °C for 10 min. After that substrate solution (pNP-Glc, 1.0 ml) was added to each vial, which was then mixed and incubated for exactly 20 mins at 37 °C. In a separate experiment, the substrate (pNP-Soph, 1.0 ml) was added to the test and blank solution vials and also incubated for 20 min at 37 ºC.

Before quantifying the amount of p-nitrophenol released to the test solution (1.0 ml) was added a solution of Na_2CO_3, (0.1 M, 4.0 ml) and the mixture was pipetted into a clean vial (5 ml) and mixed by inversion. The same procedure was repeated for the blank solution (1.0 ml).

The solutions (1.0 ml) were then transferred into a UV cuvettes and the absorbance recorded at 400 nm for using the UV spectrophotometer. All measurements were performed in triplicate and values were averaged.

2.19 Inhibitor studies: Is the sophorose-derivative, 4-nitrophenyl-α-D-sophoroside an inhibitor of the α-glucosidase enzyme

The effect of the addition of 4-nitrophenyl-α-D-sophoroside (pNP-Soph) to the enzyme substrate 4-nitrophenyl-α-D-glucopyranoside (pNP-Glc) was studied and the reaction conditions were conducted based on the following procedure:

2.19.1 Non-competitive inhibition procedure

The working concentrations of the substrate pNP-Glc and inhibitor pNP-Soph were tested in the presence of the enzyme α-glucosidase. Three experiments with different concentrations of the inhibitor of 4-nitrophenyl-α-D-sophoroside (pNP-Soph) were conducted to test the effect on substrate hydrolysis (pNP-Glc). In the first experiment, the same colorimetric method was conducted (section 2.18.1.1) with a concentration of the pNP-Glc, (5 mM) without the inhibitor. In the second experiment, the conditions utilized were pNP-Glc, (5 mM) mixed with an equal concentration of pNP-Soph (5 mM, 1.0 ml) in the third experiment, the concentration of substrate pNP-Glc (5 mM) was kept constant while increasing the concentration of the inhibitor (10 mM). During these experiments, the colorimetric method was used to monitor the formation of *p*-nitrophenolate.

2.20 Cell viability and cytotoxicity assays of sophorolipids

The cytotoxic effect (anticancer activity) of sophorolipid derivatives against human breast MCF7 and prostate PC3 carcinoma cell lines were investigated using the following techniques: MTT assay and cell-lysis method.

The work was conducted at the University of Huddersfield and was carried out by the postgraduate researcher Mr. Glenn Robinson and the project students; Hanna White and Emily Roddy.

Results and Discussion

3. Production, structure elucidation and characterisation of natural sophorolipids.

4. Isolation & structure elucidation of sophorose from the lactone waste and the conversion of sophorose to the isomeric 2-O-β-D-glucopyranosyl-D-mannose.

5. Synthesis of novel sophorolipids using the lipase-catalysed trans-esterification and using chemical glycosylation coupling reactions.

6. Application of novel sophorolipids: Surface tension properties, enzyme substrate studies and biological activity.

3. Production, structure elucidation and characterisation of natural sophorolipids

3. Production, structure elucidation and characterisation of natural sophorolipids

3.1 General introduction

Sophorolipids are extracellular-biosurfactants, which have been known for over four decades as environmentally friendly surface-active compounds. Sophorolipids can be produced using a number of different yeast strains in a fermentation process and starting from either renewable resources or materials recovered from existing waste streams (spent oils and sugars derived from agricultural wastes). Sophorolipids usually show low ecotoxicity and are biodegradable; these characteristics make them highly desirable in our society with growing environmental awareness. Surfactants are widely used in a range of industrial sectors and have a number of applications: including in food production, as cleaning products, as chemical raw materials, as cosmetics, in health care and as personal care products. The large majority of surfactants that are in use are produced by chemical methods and are classified as chemical surfactants. [13,23] These chemical surfactants when applied, for example, in washing applications, inevitably end up in the environment where they are not always easily degradable compared to biosurfactants. [5]

3.2 Production of sophorolipid biosurfactants

Sophorolipid surfactants are synthesized by nonpathogenic yeasts and can be produced in high yields and have wide applications due to either their emulsifying, antimicrobial or other beneficial properties. The yeast *Candida bombicola* is considered as one of the most widely used strains of microorganism in the production of sophorolipid biosurfactants. [55] The sophorolipid products are composed of the disaccharide sophorose linked by a glycosidic bond to the terminal (ω) or sub-terminal (ω-1)-hydroxy group of a hydroxy-fatty acid. [37]

SL-Crude (1)

SL-lactone (2)   +   SL-acid (3)
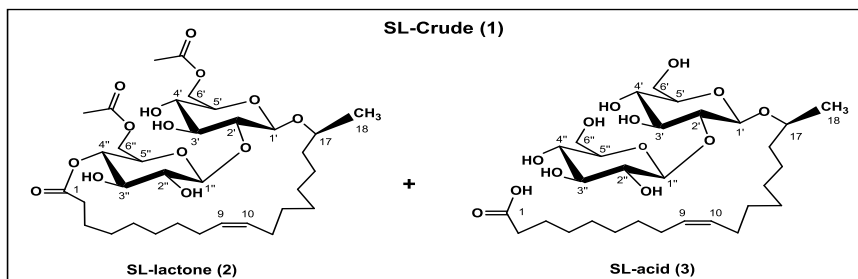
The carbon chain length of these hydroxy fatty acids varies: normally between 16 to 18 carbon atoms. The yeasts, *Candida bombicola* (ATCC 22214) and *Candida apicola* (ATCC 96134) synthesize a mixture of sophorolipids: an acidic form (3) and a diacetylated lactonic form (2) with the lactone form representing the majority of the material present in the mixture when *C.bombicola* is used. [96,162] In contrast, the *domercqia* strain is a different sophorolipid producer which is known for the synthesis of acid sophorolipids. [99]

A study of sophorolipid production showed that the composition of the fatty acid portion of sophorolipid varies according to the substrate added into the medium. [163] The study was based on the use of fatty acid esters of palmitic C16, stearic C18:0, oleic C18:1 and linoleic acid C18:1. Using these carbon sources, maximum incorporation was observed with using stearic and oleic acid. The identity of the fatty acid being determined using the acid methanolysis method and gas liquid chromatography. [54] Other products with different lipid chain lengths have been reported, a recent study by Ribeiro and *et.al.,* demonstrated the production of a C24:0 monoacetylated/diacetylated acidic sophorolipid using the *yeast Rodotorula bogoriensis.* [164] The yeast secretes sophorolipids when grown on media containing glucose supplemented with long-chain fatty acids as a carbon source. [165]

Whilst a large number of studies on sophorolipid production have identified that both sugar and fatty acid carbon sources are required for maximum production of sophorolipids, production can occur in the absence of a lipid source, but at a much-reduced amount. [61,102,163,166]

These studies showed that the glucose was used primarily for cellular metabolism and the formation of sophorose moiety while the other carbon source (fatty acids) was used for the synthesis of the hydroxy-carboxylic acid part, which is linked to the sophorose. It has also been reported that the glucose present in the culture medium is not incorporated directly into the sophorolipid molecule and that the glucose required for sophorolipid production is formed during gluconeogenesis. [167] This fact explained the inability to modify the carbohydrate composition of sophorolipids by adding different sugars to the culture medium, it also explains why it is possible to get sophorolipid production when glucose is not present in the media, but at lower yield.

3.3 Analysis and structure characterisation of sophorolipids

A number of different analytical methods and instrumental techniques have been used by researchers for the structural elucidation of sophorolipids. Thin layer chromatography and medium pressure liquid chromatography have been the most extensively used techniques. [37] Historically, the identification of the sophorolipid structures *e.g.* those derived using oleic acid as a lipophilic substrate have been determined with the help of a range of mass spectrometry techniques including: fast atom bombardment mass spectrometry (FAB-MS),[99] atmospheric pressure chemical ionization mass spectrometry (APCI-MS) [86] and electro-spray ionization mass spectrometry (ESI-MS). [37,62] More recently, a wider variety of structural analysis methods have been used for the analysis of sophorolipids and their derivatives including 1D- and 2D-NMR, [102,166,167] FT-IR , HPLC-MS, [92,93,97,168] GC and MS. [106,107] The hydroxyl fatty acid type incorporated into the sophorose moiety was routinely identified by GC-MS and using Fatty Acid Methyl Ester (FAMEs) analysis. [54,102,166]

In the commercial production of sophorolipids, a number of different unit processes are needed in order to isolate products suitable for use in specific applications. Many of these processes involve exposing materials to acidic and basic conditions and to elevated temperatures.

Little is known about how these processes can alter the distribution of the different products. For this reason, it was decided to perform a detailed analysis of the products formed at various points in the processing of sophorolipid fermentation products. It was also hoped that by identifying minor components present in the reaction system more information could be learnt about sophorolipid biosynthesis and if there was any evidence for product catabolism. It is not immediately obvious why microorganisms such as *C. bombicola* should produce sophorolipids as this would remove a valuable carbon feed. A number of authors have suggested that during starvation the sophorolipids can be used as a carbon feed-stock but to date there is very little evidence to support this theory.

Therefore, the aims of this part of the current research project were to study the products of the fermentation process in detail and to determine if it is possible to observe the production catabolic products such as glucolipids and free sugars including sophorose. In doing so, it was also of interest to determine if new analytical methods, those that are routinely used for sugar analysis such as monomer and linkage analysis; can be applied to gain a detailed structural analysis of sophorolipids.

3.4 Production and isolation of sophorolipids

In the commercial production of sophorolipids, after the completion of the fermentation process, the initial product is a crude mixture of lactone & acid sophorolipids. The crude product is dense brown oil which settles as one of two phases: a lipid-rich bottom layer containing the sophorolipids and an upper aqueous phase (spent liquors).

74

3.5 Structural analysis of the initial sophorolipids mixture using NMR spectroscopy

In this study, the chemical structures of sophorolipids and their derivatives were investigated using 1D- and 2D-NMR spectroscopy and spectra were recorded at either 400 or 500 MHz as discussed in the experimental section 2.3.1. To simplify the analysis of the ^{1}H-NMR spectra, the spectra can be considered as being composed of three main sections; the high chemical shift region (Section A; 5.5-4.4 ppm), the region containing the sugar ring protons (Section B; 4.3-3.1 ppm) and the low chemical shift region *i.e.*, below 3.05 ppm (Section C).

3.5.1 Structural analysis of the initial crude fermentation products (1)

- **Section (A)**: The high chemical shift region includes the anomeric sugar protons and the alkene protons (4.4-5.5 ppm), which has signals from the H-1' and H-1''-protons of the sugars, signals from the lipid alkene protons (H-9 and H-10) and the H-4''-proton of the lactone sophorolipid.
- **Section (B)**: This section covers the region between (4.3-3.1 ppm) and consists of signals belonging to the sugar ring protons (H-2 to H-6) and the lipid H-17 proton.
- **Section (C)**: This section covers the region below (3 ppm), which consists of signals from the lipid methylene and methyl groups, the acetyl groups (O(CO)CH_3) and acetate either in the form of acetic acid or sodium acetate.

Inspection of the ^{1}H-NMR spectrum of the initial fermentation products (Figure 3-1) identified that it is a mixture of the acid and lactone forms of the sophorolipids. With the lactone form as the major component: in section (A), the integral value for the resonance attributed to the alkene signals of the lipid chain resonating at (-CH$_9$=CH$_{10}$- ; 5.42-5.28 ppm) was close to 2 whereas the triplet signal at 5.0-4.9 ppm, is for lactone-H-4″ signal, *i.e.,* the point of lactone esterification on the sophorose moiety integrated to 0.66.
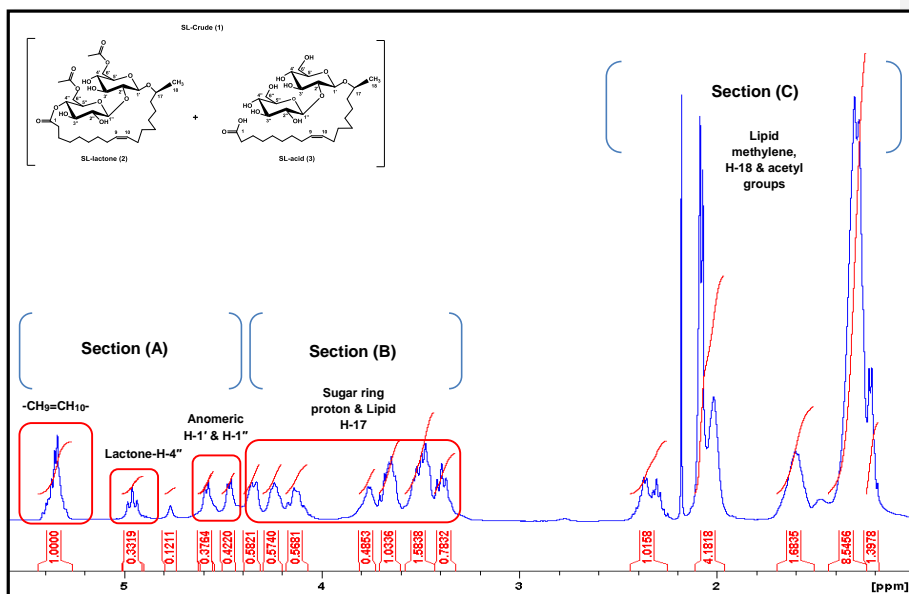
Figure 3-1: ^{1}H-NMR spectrum of the initial sophorolipid product (1) recoded at 25 ºC using CDCl$_3$.

The protons for the glucopyranose-H-1' and glucopyranose-H-1" resonate at 4.61-4.53 ppm and 4.50-4.43 ppm respectively. In *section* (B) of the spectrum, the resonances attributed to the signals of (H-6' and H-6") of the sophorose moiety were located at 4.40-4.20 ppm, and appear as two sets of peaks indicating the presence of acetylated and non-acetylated C6s for both acid and lactone sophorolipids, while the multiplet signal which was at 4.10-4.06 ppm, (integral 1 H) belongs to the H-17 of the lipid chain.

Furthermore, the resonance signals within the range (3.85-3.25 ppm, 8 H) represents the sophorose ring protons, namely H-3', H-3", H-5', H-5", H-2', H-2" and H-4' and H-4" for the acid form of the sophorolipids, which is present in a small amount (approximately 33%) in the crude.

Finally, section (C), includes the signals from the lipid chain protons. The multiplet peak resonating at (2.43-2.25 ppm, 4 H) represents the methylene attached to carbon (C-2) in the lipid chain (adjacent to the carbonyl group) in both the acidic and lactone form, whereas the two sharp singlet peak, resonating at (2.10-2.05 ppm, 6 H) represent the resonance of the acetyl

methyl groups (O(CO)CH_3) attached to the position C-6' and C-6" on the sophorose moiety for the lactone form in the crude sample. The peak at (2.05 and 1.65 ppm, 4 H) is due to the methylene protons (CH_2-CH=CH-CH_2) adjacent to the alkene protons. The multiple signals for protons which were present at (1.40-1.24 ppm, 21 H) were assigned to the lipid methylene protons as well as the doublet peak, which resonated at (1.20 ppm, 3 H) was derived from the methyl group on (C-18) of the lipid chain.

The composition of the crude products, specifically the presence of both the lactone and acid forms of the sophorolipid, was determined by examination of a series of 2D-NMR spectra. Analysis of the 2D-HMBC spectrum (Figure 3-2) of the initial products, (1) confirmed that the major component is the lactone form (66%, 2) of the sophorolipid and this was deduced through identification of the long-range coupling (on the HMBC spectrum) of the H-4″ proton (4.9 ppm) with the ester carbonyl carbon (173.3 ppm). Also, the protons at H-6′ & H-6″ were correlated with the acetyl groups at (171.70 and 170.60 ppm), which confirms the presence of two acetyl groups on positions C-6s. The presence of two acetyl methyl groups (O(CO)CH_3) at (2.20-2.00 ppm) which were correlated to the acetyl carbonyl signals at (171.70 and 170.60 ppm) confirmed the presence of the acetylated lactone form in the initial products.
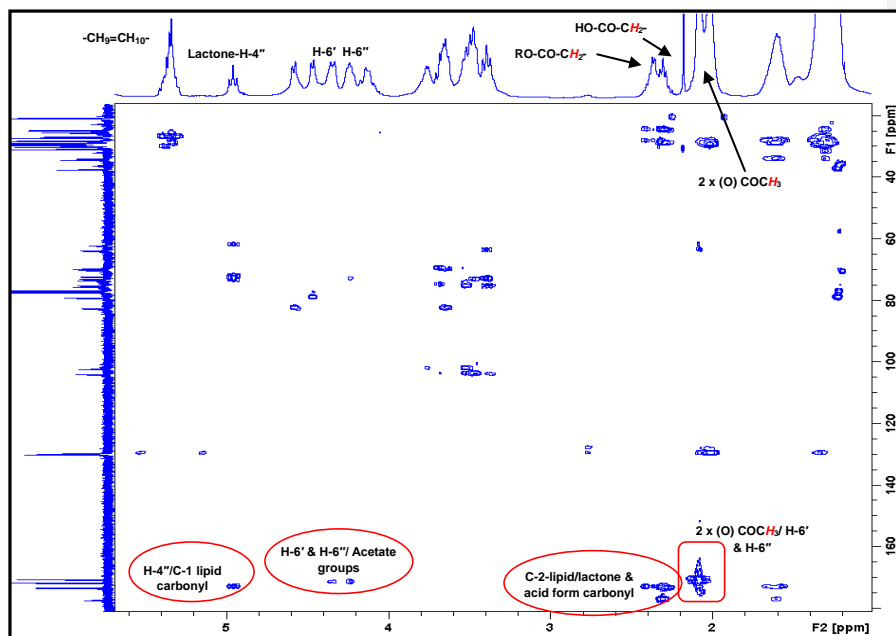
Figure 3-2: ^{1}H-^{13}C-HMBC spectrum of the initial sophorolipid product (1).

3.6 Structural analysis of the initial sophorolipid mixture using FT-IR spectroscopy

The chemical structures of sophorolipids and their derivatives were also investigated using FT-IR spectroscopy. The methods employed to record the spectra are reported in the experimental section 2.3.2. The initial sophorolipid product (1) showed a broad absorption band at 3361-3377 cm^{-1} (Figure 3-3) corresponding to the O-H stretching for the sugar ring hydroxyls and for the carboxylic O-H group in the case of the acid sophorolipid form. The absorption due to the asymmetrical and symmetrical stretching of the methylene (-CH$_2$-) occurred at 2924-2854 cm^{-1} as medium strength bands, whereas the strong absorption band occurred at 1743 cm^{-1}, was attributed to the C=O stretching of the lactone ester and the acetate ester carbonyls located on the C-6 positions of the sophorose moiety; this confirmed the acetylation of the lactone form.

78

The medium absorption band at 1644 cm^{-1} was assigned to the stretching vibration of the unsaturated alkene group (-CH=CH-) present in the fatty acid chain. The strong C-O absorption band of the acetyl esters was observed at 1240 cm^{-1} while the weak bands at 1440 cm^{-1} corresponded to the C-O-H in the plane bending of the carboxylic acid (-COOH) in the structure of both lactone and acid sophorolipid products. Finally, the C-O stretch from the C-O-H groups of the sugar (sophorose moiety) was observed at 1080-1035 cm^{-1}.
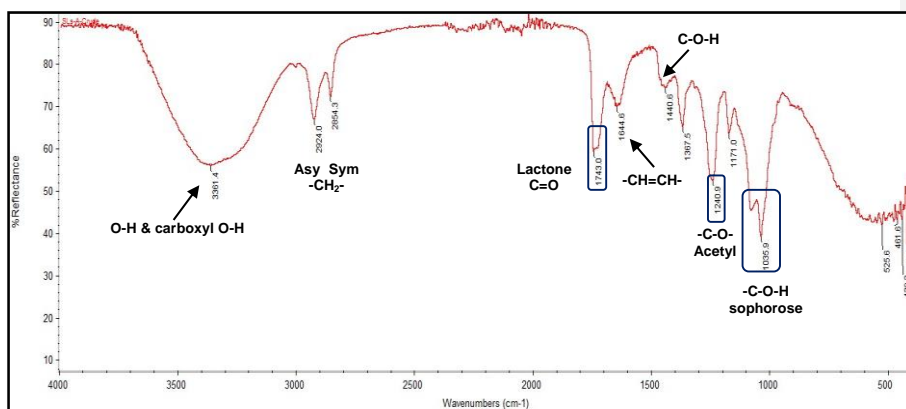
Figure 3-3: FT-IR spectrum of the initial sophorolipid product, (1)

3.7 Structural analysis of sophorolipids using GC-MS and HPAEC-PAD

After identifying the structural information from the NMR and FT-IR interpretation, monomer and linkage analysis were performed to confirm that the sugar monomers present in the sophorolipids were glucose and that the glucose monomers were joined by a β (1→2)-linkage. Both GC-MS and HPAEC-PAD techniques were used to identify the linkage pattern present in the sophorolipids samples.

3.7.1 Monomer analysis of the initial sophorolipid product using HPAE-PAD

HPAEC–PAD is frequently utilized to determine the monomer composition of carbohydrate-containing molecules. The process is rapid and only requires acid hydrolysis to remove glycoside links and aglycones (lipids) for investigation; the detailed procedure is discussed earlier in section 2.7.1.

All the products recovered from the commercial manufacture of sophorolipids were analysed. A series of standards, glucose, galactose, and mannose were run in order to identify the relevant retention times of the monomers. Each standard was run in triplicate to minimize the variation in the retention times (Table 3-1). The peak's retention times (RT) were used to confirm the presence of the monomers.

Table 3-1: HPAEC-PAD retention times of standard sugars

Standards	pKa	Average Retention Time (RT) min.	Standard Deviation (SD)
Galactose	12.39	6.55	0.082
Glucose	12.28	7.00	0.130
Mannose	12.08	9.78	0.073

After acid hydrolysis of sophorolipids, samples were run immediately along with the standards. Galactose and mannose were included as standards in order to investigate the possible presence of small amounts of any components that may be generated from the yeast extract, cell-wall mannan and glucans, added as part of the media employed in the fermentation process, which may present in sophorolipids composition.

The analysis of the initial sophorolipid mixture sample (1) gave just one peak, which was observed with a retention time of 6.97 min. (Figure 3-4). This observed retention time was compared with the standard analysis chromatogram; the monomer type in the crude sample was similar to glucose.
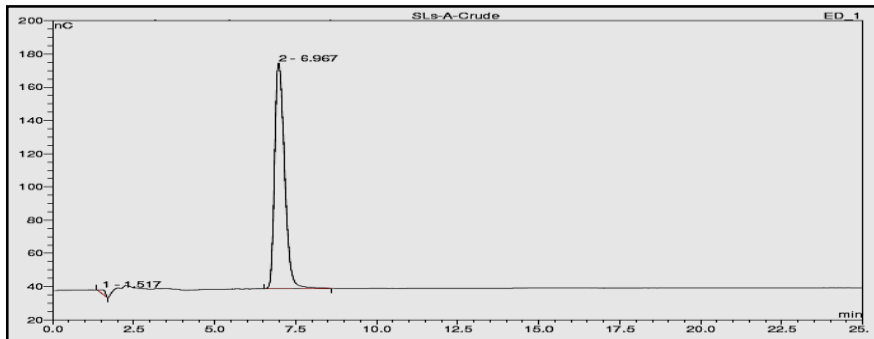
Figure 3-4: HPAEC-PAD chromatogram for the initial sophorolipid product (1) sample after acid hydrolysis.

In order to get further confirmation, initial sophorolipid sample was spiked with the monosaccharide and the sample was assayed by HPAEC-PAD and the resulting chromatograms showed that the sugar present is exclusively glucose and trace amounts of other sugars were not detected.

3.7.2 Monomer analysis using GC-MS

The sophorolipids monosaccharide composition was also investigated using GC-MS. Trifluoroacetic acid was employed for the hydrolysis of the glycosidic linkage in sophorolipids to obtain the monomer components, which were then converted to alditol acetates using the method described in section 2.7. The resulting reaction products were then subjected to GC-MS analysis using the GC-MS column oven temperature program listed in section 2.9.

The GC-chromatogram obtained (Figure 3-5) for the initial sophorolipid products contained a distinct peak around 13.54 min, this peak had a very similar retention time to that the monomer glucose, which was run as a control 13.58 min. The mass spectrometry fragmentation pattern generated by this peak was analysed (Figure 3-6). The fragmentation observed for these peaks were identical to that generated by glucitol hexaacetate.
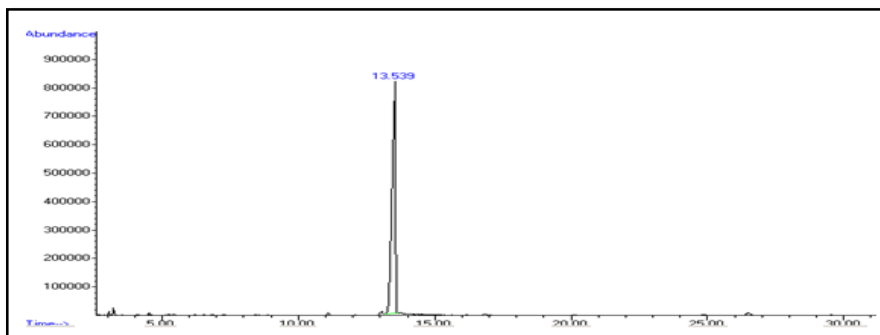
Figure 3-5: GC-chromatogram for initial sophorolipid products (1) after acid hydrolysis.
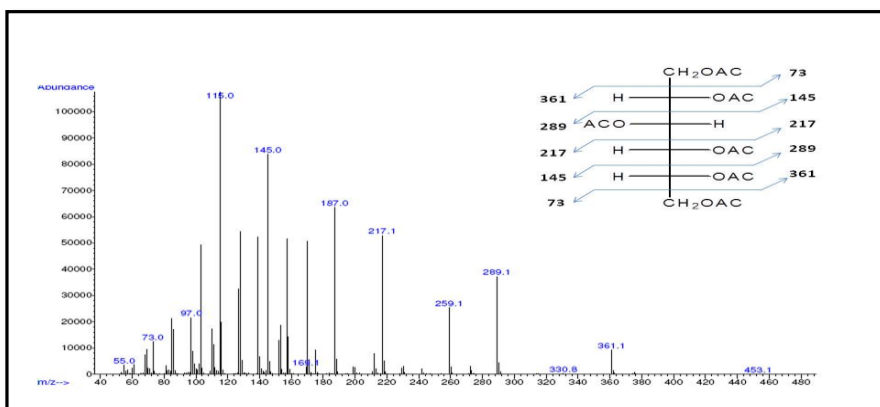
Figure 3-6: EI-mass spectrum of the glucitol hexaacetate generated from the initial sophorolipid product (1) and the mass fragmentation interpretation pattern (inset MS adapted from analysis of carbohydrates by GLC-MS) [169]

The monomer analysis results by GC-MS further confirmed that there is no an impurity or contamination from the media present in the crude product and glucose is the only sugar presents after the acid hydrolysis process. As a result, the monomer analysis methods performed by HPAEC-PAD and GC-MS both gave identical results.

3.7.3 Linkage analysis of the initial sophorolipid products (1)

The type of linkage present in the sophorolipids samples was investigated using GC-MS. The sugars present in the sophorolipid samples were converted to their permethylated alditol acetates (PMAAs), which were analysed using the GC-MS method described in section 2.9.1. The permethylation analysis was used to establish the point of attachment of the glycosidic linkages between each of the monomer residues. Typically, the sophorolipids were derivatized to form acid stable methyl ethers, the glycosidic bonds were hydrolysed, the C-1 carbonyls were reduced with sodium deuterioborohydride and free hydroxyls were peracetylated, and the products analysed by GC-MS. The linkage analysis method was also used to determine the extent of acetylation on the C-6 positions on the sophorose moiety. The PMAA derivatisation of the crude sophorolipid sample produced peaks observed in the GC-MS chromatogram (Figure 3-7) at 12.37, 15.25, 15.41, 16.32 and 19.59 min with a peak area ratio of 74.52, 100.00, 17.14, 23.25, 83.17 % respectively, in addition to other minor peak at 23.84 min with a ratio of 5.33 %. For interpretation of the mass spectrometry data for the PMAA fragmentation patterns for these peaks were (Figure 3-8 & 9) compared to literature MS, [169] it was found that the first peak was for 1,5-di-*O*-acetyl-(1-deuterio)-2,3,4,6-tetra-*O*-methyl glucitol, derived from a terminally linked glucose moiety (T-glucose).
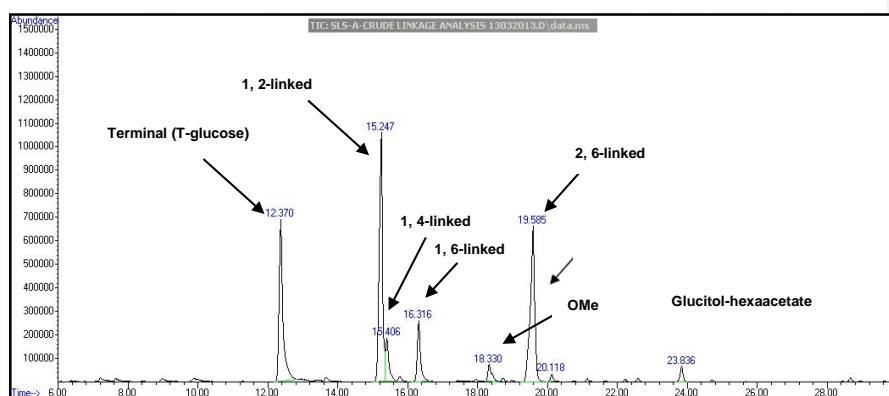
Figure 3-7: GC-chromatogram represents the linkage pattern for the initial sophorolipid products (1)
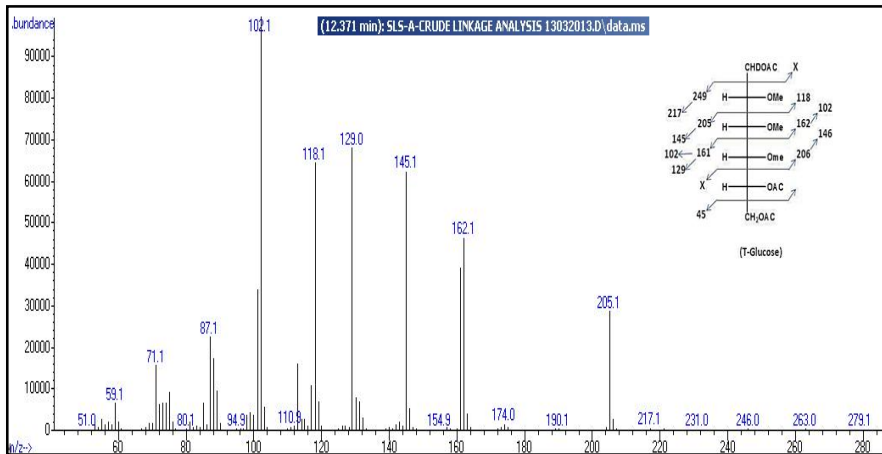
Figure 3-8: EI-mass spectrum for derivative 1,5-di-*O*-acetyl-(1-deuterio)-2,3,4,6-tetra-*O*-methyl glucitol (T-Glucose) derived from the 12.37 min GC-peak (inset MS adapted from analysis of carbohydrates by GLC-MS) [169]

Whereas the second peak at 15.25 min was identified as 1,2,5-tri-*O*-acetyl-(1-deuterio)-3,4,6-tri-*O*-methyl glucitol (1-2-glucose), derived from a 1→2 linked glucose moiety (1-2-glucose). These are the linkage that we were expecting to find in a deacetylated sophorolipids sample *i.e.* in a sample which is composed of two glucose molecules linked by a 1→2 glycosidic bond. The other peaks in the GC chromatogram, at 15.41 and 16.32 min, were determined to be: 1,4,5-tri-*O*-acetyl-(1-deuterio)-2,3,6-tri-*O*-methyl glucitol, derived from a 1→4 linked glucose moiety (1-4-glucose; generated from the lactone);1,5,6-tri-*O*-acetyl-(1-deuterio)-2,3,4-tri-*O*-methyl glucitol, derived from a 1-6 linked glucose moiety (1-6-glucose-acetylated), (Figure 3-10 & 11).

The last peaks in GC chromatogram are at 19.59 min was determined for 1,2,5,6-tetra-*O*-acetyl-(1-deuterio)-,3,4-di-*O*-methyl glucitol (2→6-glucose) as shown in (Figure 3-12). This is expected for an acetylated sophorolipid product which is mainly the lactone form presents in the initial (crude) sophorolipid products sample.
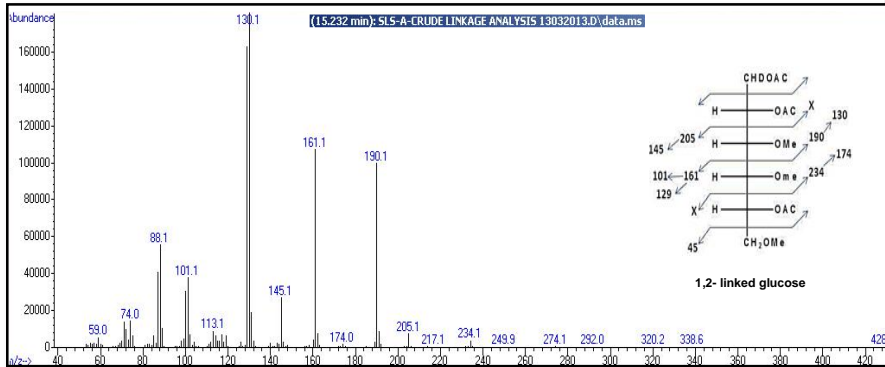
Figure 3-9: EI-mass spectrum for derivative of 1,2,5-tri-*O*-acetyl-(1-deuterio)-3,4,6-tri-*O*-methy glucitol (1→2 Linked glucose) derived from the 15.25 min GC-peak (inset MS adapted from analysis of carbohydrates by GLC-MS) [169]
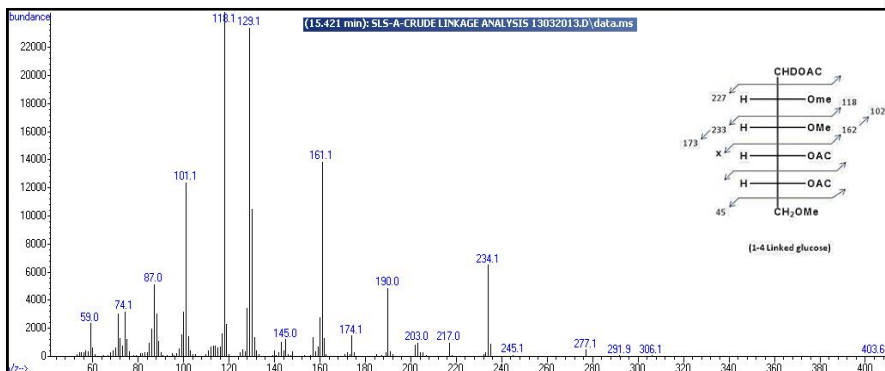
Figure 3-10: EI-mass spectrum for derivative of 1,4,5-tri-*O*-acetyl-(1-deuterio)-2,3,6-tri-*O*-methyl glucitol (1→4 Linked glucose) derived from the 15.41 min GC-peak.
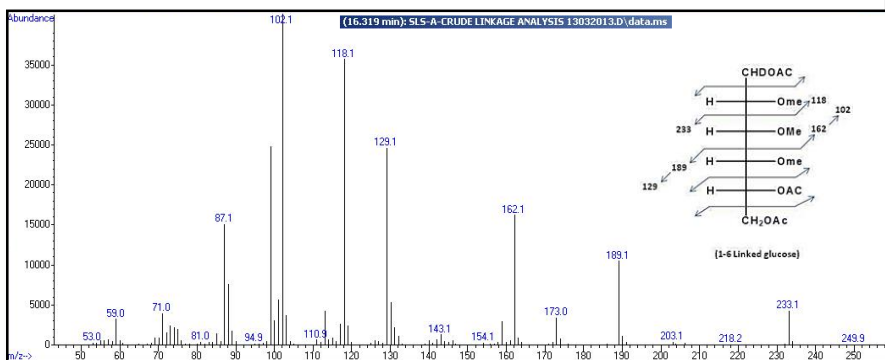
Figure 3-11: EI-mass spectrum for derivative of 1,5,6-tri-*O*-acetyl-(1-deuterio)-2,3,4-tri-*O*-methyl glucitol, alternatively denoted as a 1→6 linked glucose moiety (1→6 Linked glucose) derived from the 16.31 min GC-peak.

85
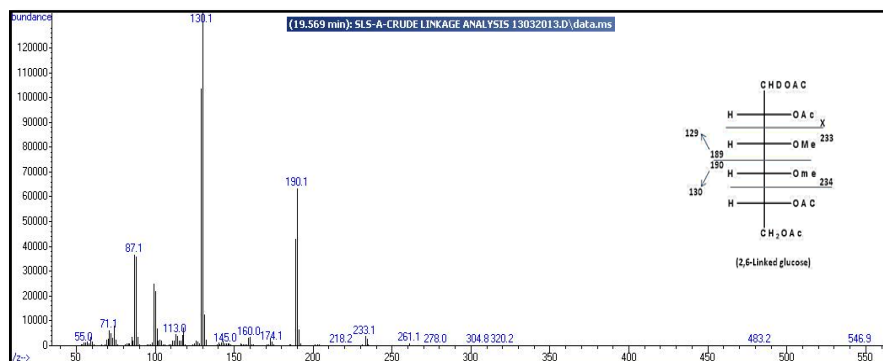
Figure 3-12: Mass spectrum for derivative of 1,2,5,6-tetra-*O*-acetyl-(1-deuterio)-,3,4-di-*O*-methyl glucitol, alternatively denoted as a 2→6 linked glucose moiety (2→6 Glucose) derived from the 19.54 min GC-peak. (inset MS adapted from analysis of carbohydrates by GLC-MS) [169]

3.8 Production of the lactone form of the sophorolipid

In order to isolate the lactone form of the sophorolipid, the pH of the lipid-rich layer is increased using cold aqueous alkaline solution [0.1 M] resulting in the dissolution of the acid sophorolipid (3) and leaving the lactone form (2) as a white solid material (Figure 3-13) which is further cleaned by treatment with water.

To isolate the deacetylated acid form (3), it is normal practice to recover the pure lactone sophorolipid from the crude product and then to convert it to the acid form via a based catalysed hydrolysis reaction [65,87,170] which involves heating with an aqueous alkaline solution at 50-70 ⁰C. The hot alkaline treatment gives two phases, an upper aqueous phase from which the acid form is precipitated on reacidification and a brown lipid-phase (lactone waste). The acid form was generated as a result of the hydrolysis reaction of the lactone form which resulted in the opening of the lactone ring and the deacetylation of the acetyl esters at positions C-6′ & C-6″, the product recovered is a colourless viscous liquid.

(A) The lactone sophorolipid production process:

Initial sophorolipids products (1) →[KOH [0.1 M], 25°C]

Lactone form (2)

(B) The acid sophorolipid production process:

Lactone form (2) →[KOH [0.1 M], 50-70°C]

Acid form (3)

+

Lactone waste
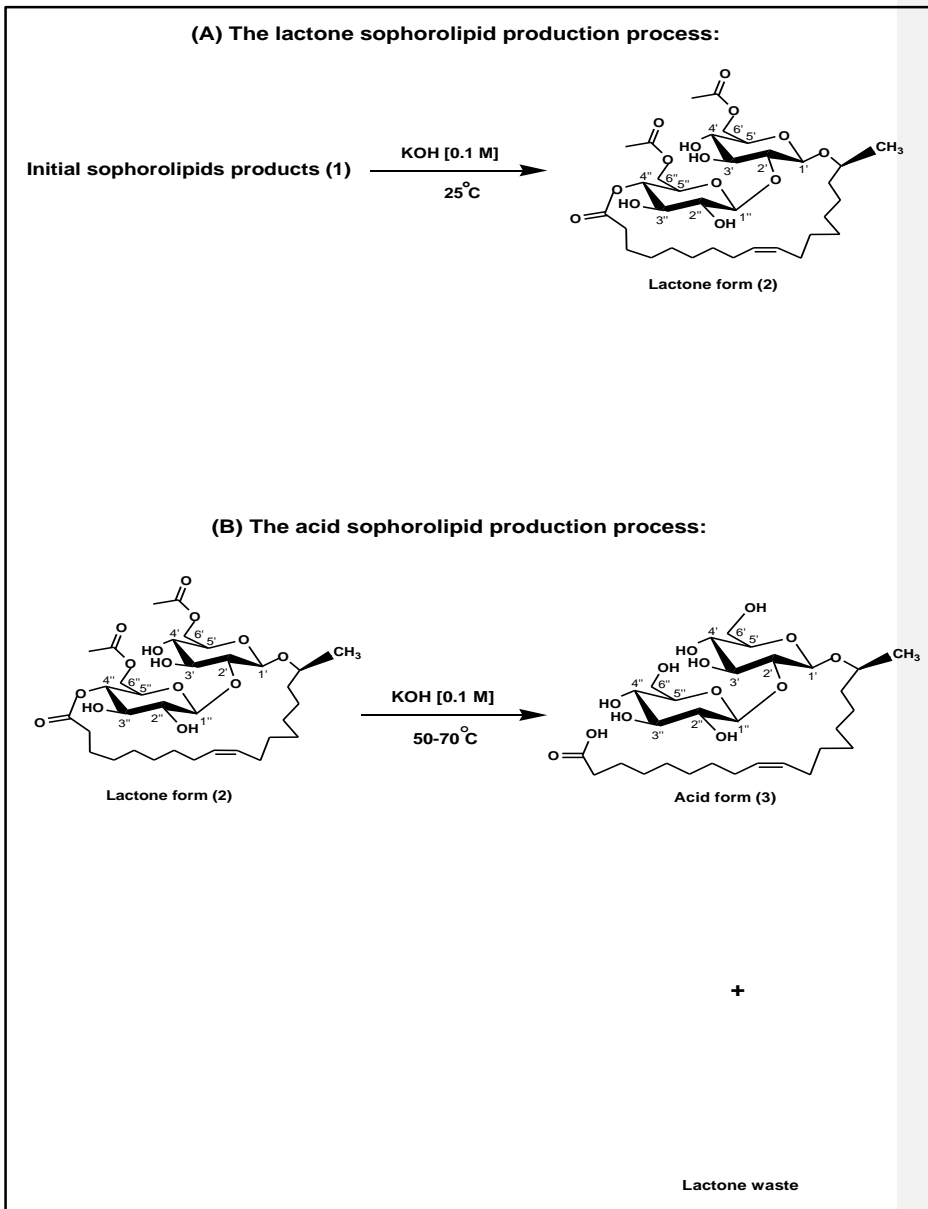
Figure 3-13: Scheme representing (A) the lactone sophorolipid production and (B) the acid sophorolipid production.

3.8.1 Structural analysis of the sophorolipid lactone, (2) and acid, (3) using NMR spectroscopy

The ^{1}H-NMR spectra for the pure lactone and acid sophorolipids are both shown in (Figure 3-14). The ^{1}H-NMR spectra were recorded in different solvents, D_2O for the acid and $CDCl_3$ for the lactone form using 400 MHz NMR spectrometer at 25 $^{\circ}$C. The assignments of signals are also based on the same three sections as for the initial sample, (1). The distinct difference between the two forms is the absence of the triplet peak resonating at 5.0-4.9 ppm, in the acid form (3) which is for the H-4" proton *i.e.* the point of lactone esterification in the lactone form. The ^{1}H-NMR spectrum for the lactone sample showed the presence of small peaks at (4.04, 5.10 & 5.13 ppm) which belong to the sophorose hydroxyl groups. Those peaks were absent in the case of the acid form (3), which was recorded in D_2O where they undergo exchange.
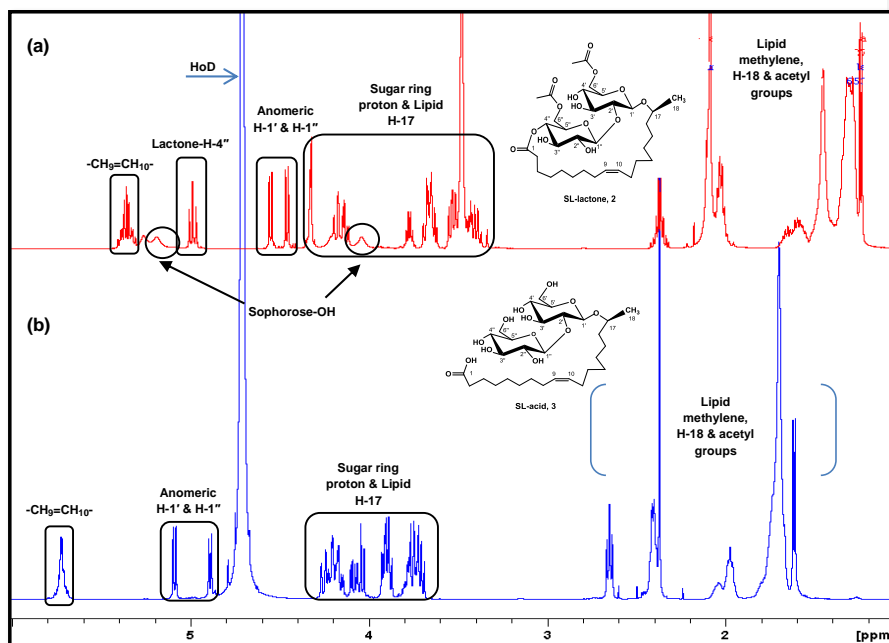
Figure 3-14: ^{1}H-NMR spectra of sophorolipids (a) lactone form, (2) and (b) acid form, (3) recoded at 25 ^{0} C.

The difference between the two forms was also seen in the ^{13}C-NMR spectrum acid form (Figure 3-15), which showed the presence of a signal at (178.0 ppm) that was assigned to the carboxylate ion (COO⁻K⁺). In contrast, the lactone form has three signals (173.3, 171.7 and 170.7 ppm) which were all assigned to the lactone carbonyl and for the two acetyl groups O(CO)CH_3. The ^{1}H- and ^{13}C-NMR chemical shifts for the individual resonances were similar to the NMR data of the SLs compounds reported by other researchers.[18,106,171,172]
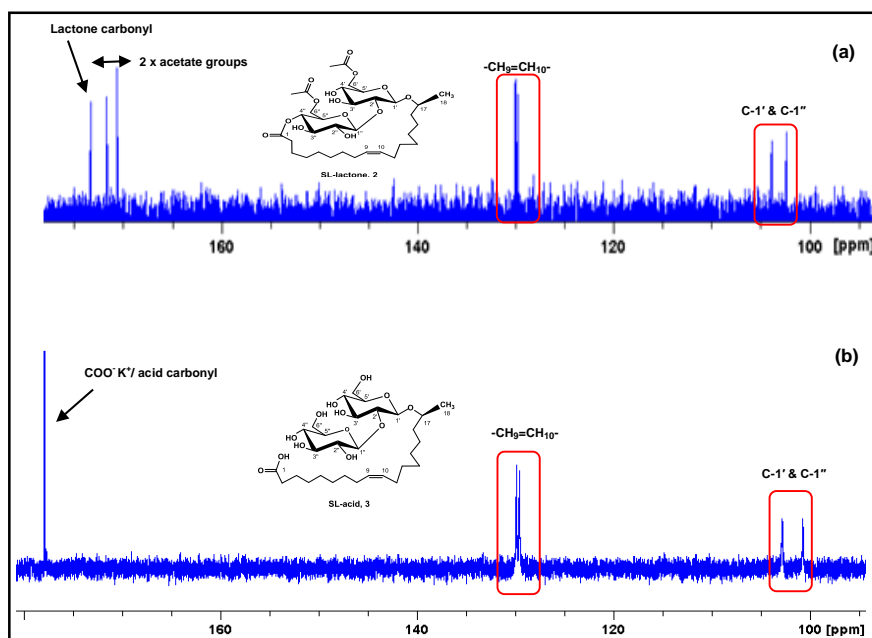
Figure 3-15: The ^{13}C–NMR spectra for sophorolipids (a) lactone, (2) recoded in CDCl$_3$ and (b) acid (3) in D$_2$O solvent.

3.8.2 Structural analysis of lactone, (2) and acid, (3) sophorolipids using FT-IR spectroscopy.

The structures of the sophorolipids were investigated using FT-IR spectroscopy. The spectra for the lactone and acid form both included a broad absorption band around 3361-3377 cm⁻¹ (Figure 3-16, a & b) corresponding to

the O-H stretching for the sugar hydroxyls and the carboxylic O-H groups in the case of the acid/lactone form sophorolipids.

The medium strength absorption bands for asymmetrical and symmetrical stretching of the methylene CH_2's occurred at 2924-2854 cm^{-1}, whereas the 1651 cm^{-1} & 1558 cm^{-1} medium strength absorption bands were for the stretching of the unsaturated -CH=CH- in the case of the lactone (a) and the acid (b) sophorolipids. This -CH=CH-, the band was shifted to 1558 cm^{-1} in the acid form due to the opening of the lactone ring.

The lactone sophorolipid sample showed a strong C=O band for the lactone carbonyl at 1744 cm^{-1} and the acetate carbonyls located on the C-6 positions of the sophorose moiety; this confirmed the acetylation of the lactone. This band was weaker and shifted to 1643 cm^{-1} for the acid form which confirmed the opening of the lactone ring and the formation of the carboxylic acid or (carboxylate salt, $COO^- K^+$) after treatment with KOH. The absence of the small shoulder attached to the carbonyl absorption band confirmed the removal of the acetate groups (through solvolysis) on the C-6 positions of the acid sophorolipid sample.

The acetyl groups on the C-6 positions generated a strong C-O stretching band at 1234 cm^{-1} in the lactone sample confirming the presence of acetates on the C6s (these results agree with the ^{13}C-NMR data, which also confirmed the presence of the acetate groups on the C-6s). This band became very weak or had disappeared in the case of the acid sophorolipid; this is further evidence of the deacetylation of the C-6 positions. The weak bands at 1453 cm^{-1} and 1410 cm^{-1} corresponding to the C-O-H in-plane bending of carboxylic acid (-COOH) in the structure of both SLs samples also the C-O stretch from C-O-H groups of sugar (sophorose moiety) are observed at 1075-1034 cm^{-1}.

The FT-IR spectral data of the lactone and acid sophorolipids were found similar to data reported in previous studies. [106,173,174]
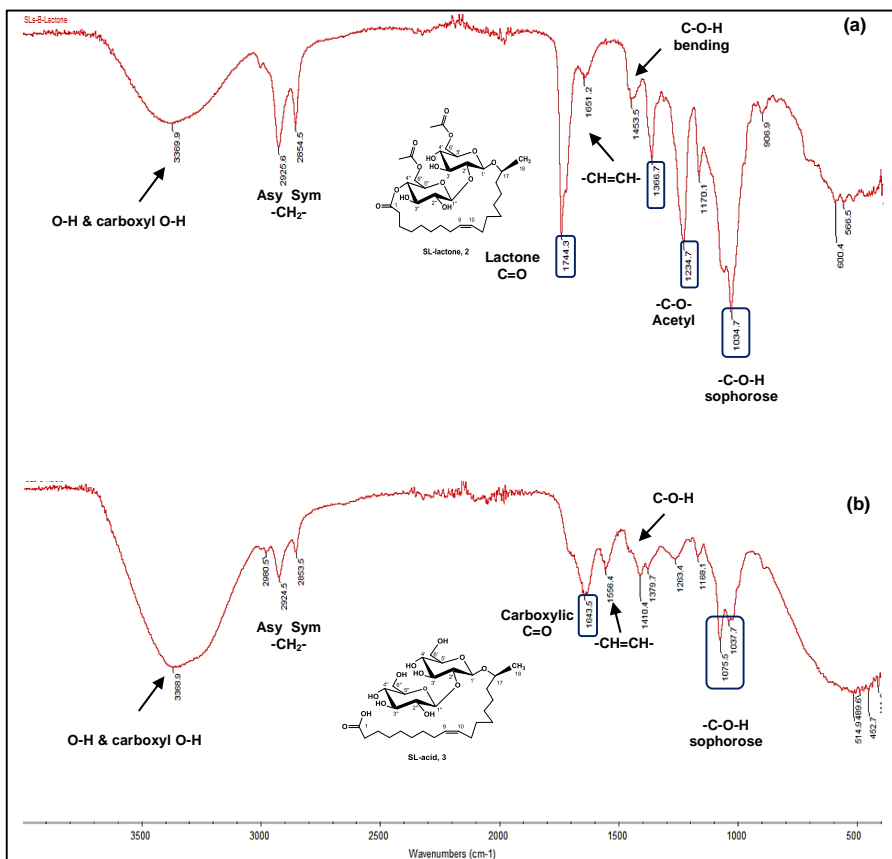
Figure 3-16: Comparison of FT-IR spectra for sophorolipids: (a) lactone, (2) and (b) acid, (3).

3.8.3 Monomer analysis of lactone, (2) and acid, (3) sophorolipids using HPAEC–PAD

The lactone and acid form were subjected to monomer analysis in order to investigate the sugar type involved in their carbohydrate components. After acid hydrolysis of sophorolipids, samples were run on the HPAEC-PAD along with standards (glucose, galactose and mannose) to identify the relevant retention times of monomers.

The analysis of samples gave just one peak as was the case for the initial sophorolipid sample, which was observed with a retention time between

7.25-7.30 min (Figure 3-17, a & b). The observed retention time was compared with the standard analysis chromatogram (Table 3-1); all samples were identical to glucose and no evidence of other impurities were present in both samples.
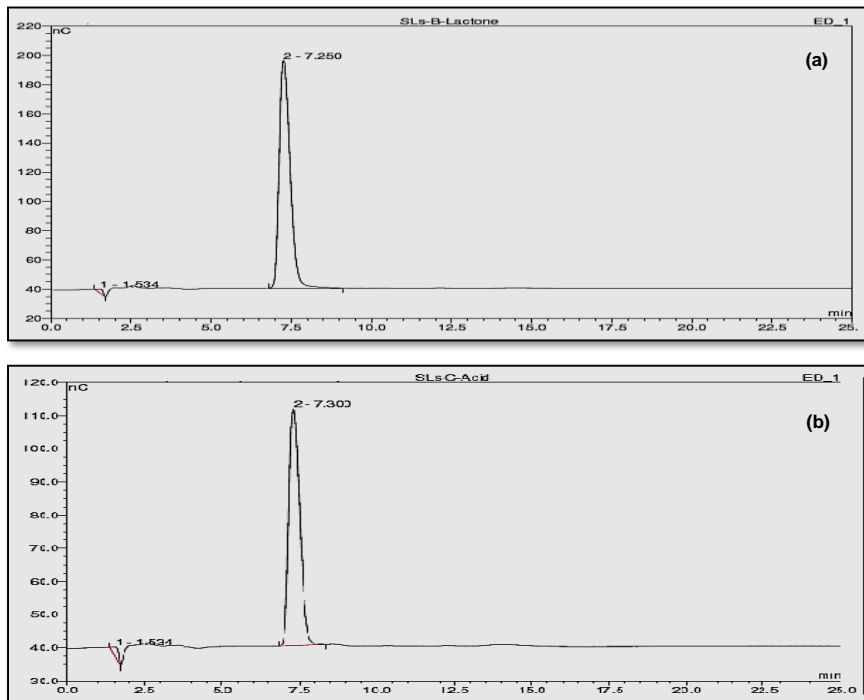
Figure 3-17: HPAEC-PAD chromatograms after acid hydrolysis for (a) lactone, (2) and (b) acid, (3)

To further confirm the identity of the monomers present in the lactone and acid sophorolipids, the samples were spiked with glucose and the samples were assayed by HPAEC-PAD. The resulting chromatograms showed that the sugar present was glucose. The monomer analysis results confirmed that there is no evidence for other impurities associated with or incorporated into the products.

3.8.4 Monomer analysis of lactone, (2) and acid, (3) sophorolipids using GC-MS

The lactone and acid sophorolipids' monosaccharide composition were further investigated utilizing GC-MS. The GC-chromatograms obtained (Figure 3-18, a & b) for both samples contained distinct peaks at 13.52 and 13.42 min for the lactone and the acid samples respectively. The peaks had a very similar retention time to that of the monomer glucose, which was run as a control *i.e.* 13.58 min. The mass spectrometry fragmentation pattern generated by these peaks was analysed (Figure 3-19). The fragmentation observed for the peaks were identical to that generated by glucitol hexaacetate.
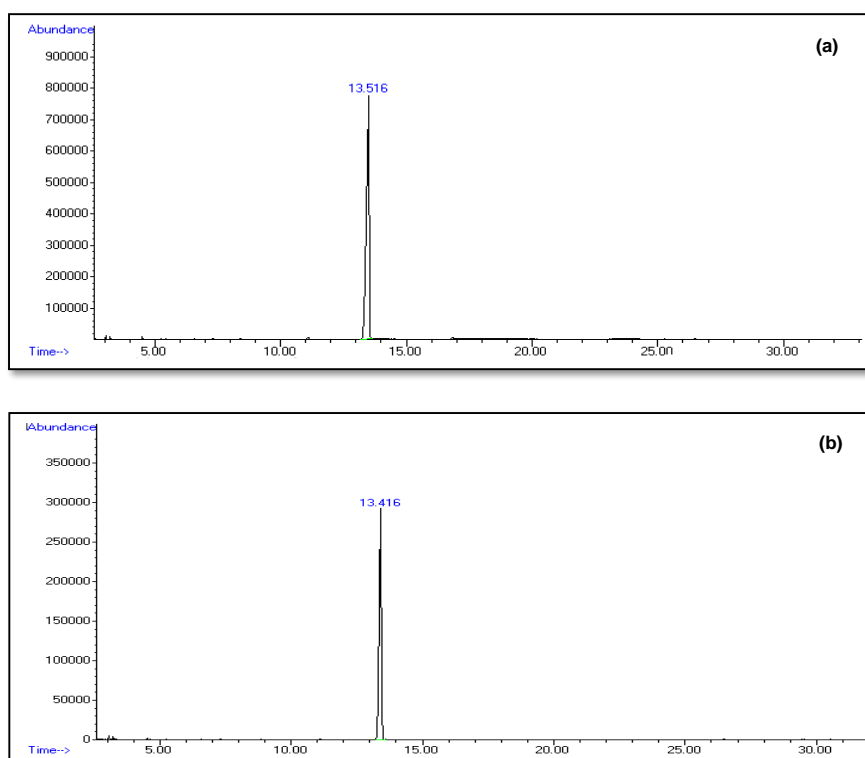
Figure 3-18: GC-chromatograms for sophorolipids after acid hydrolysis: (a) lactone, (2) and (b) acid, (3).
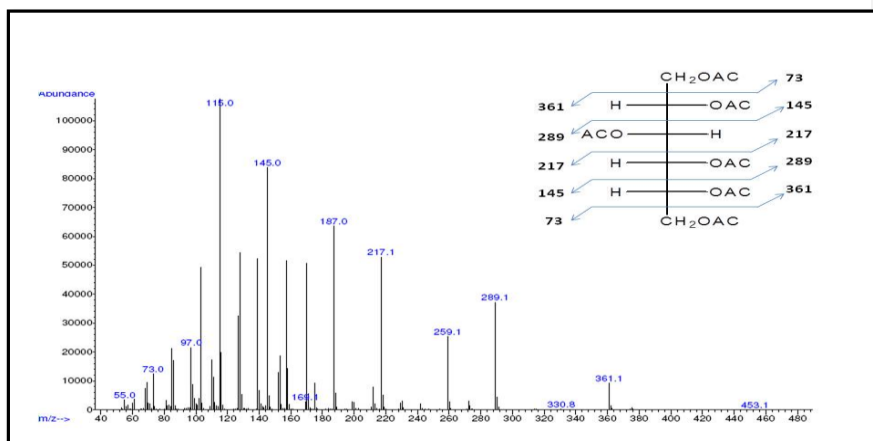
Figure 3-19: EI-mass spectrum of glucitol hexaacetate generated from sophorolipids and their mass fragmentation interpretation pattern (inset MS adapted from analysis of carbohydrates by GLC-MS)[169]

The monomer analysis results conducted by HPAEC-PAD and GC-MS both confirmed that the sugar monomer involved in the lactone and acid sophorolipid carbohydrate component is glucose with no other impurities or different sugar type incorporated in the sophorolipid structure. These results are also consistent with the monomer analysis results obtained for the initial sophorolipid sample.

3.8.5 Linkage analysis of lactone, (2) and acid, (3) sophorolipids

GC-MS analysis was also used to determine the type of linkage in the lactone and acid samples. The lactone and acid samples were converted to their permethylated alditol acetates (PMAAs). The permethylation analysis is utilized to establish the position of glycosidic linkages between monomer residues. The analysis can be used to determine the degree of acetylation at the C-6 positions on sophorolipid samples. The PMAA derivatisation of the lactone sample (Figure 3-20) produced peaks in the GC-MS chromatogram observed at 12.35, 15.25, 15.41, 16.31 and 19.54 min with a peak area ratio of 49.41, 100.00, 26.33, 20.60, and 44.69 % respectively.

94

In addition to other minor peak at 23.82 min with a ratio of 2.94 %. For interpretation of the mass spectrometry data for the PMAAs fragmentation patterns to these peaks were (Figure 3-21 & 22) compared to literature MS, [169] it was found that the first peak was for the 1,5-di-*O*-acetyl-(1-deuterio)-2,3,4,6-tetra-*O*-methyl glucitol, derived from terminally linked glucose moiety (T-glucose), whereas the second peak at 15.25 min was identified as a 1,2,5-tri-*O*-acetyl-(1-deuterio)-3,4,6-tri-*O*-methyl glucitol, which is derived from a 1→2 linked glucose moiety (1-2-glucose). These are the linkage expected to find in deacetylated sophorolipid samples, which is composed of two glucose molecules linked by 1→2 type linkage. The other peaks in the GC chromatogram 15.41 and 16.31 min were determined for 1,4,5-tri-*O*-acetyl-(1-deuterio)-2,3,6-tri-*O*-methyl glucitol and alternatively denoted as a 1→4 linked glucose moiety (1-4-glucose), which is also expected for the deacetylated lactone form and the 1,5,6-tri-*O*-acetyl-(1-deuterio)-2,3,4-tri-*O*-methyl glucitol, alternatively denoted as a 1-6 linked glucose moiety (1-6-glucose) (Figure 3-23 & 24) which is expected for the acetylated lactone sophorolipid form. The other peak in GC chromatogram 19.54 was determined for 1,2,5,6-tetra-*O*-acetyl-(1-deuterio)-,3,4-di-*O*-methyl glucitol (2→6 Linked glucose) (Figure 3-25). This is also expected for the acetylated lactone sophorolipid.
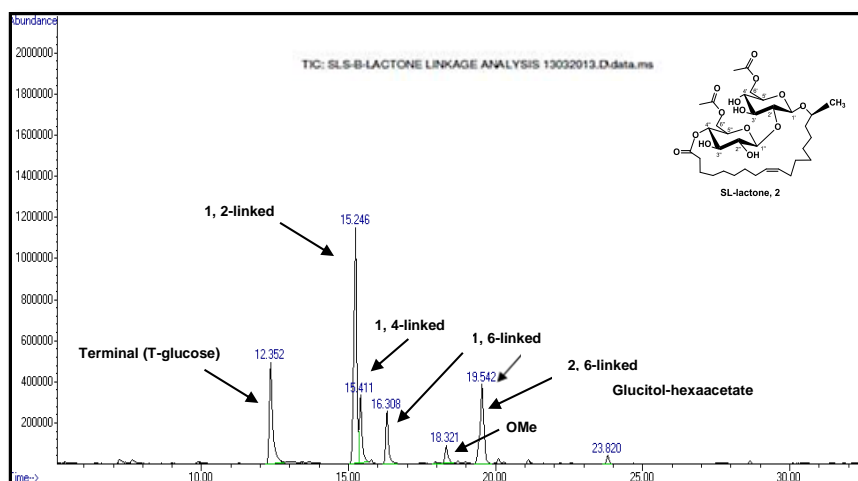
Figure 3-20: GC-chromatogram represents the linkage pattern for lactone sophorolipid, (2)

95
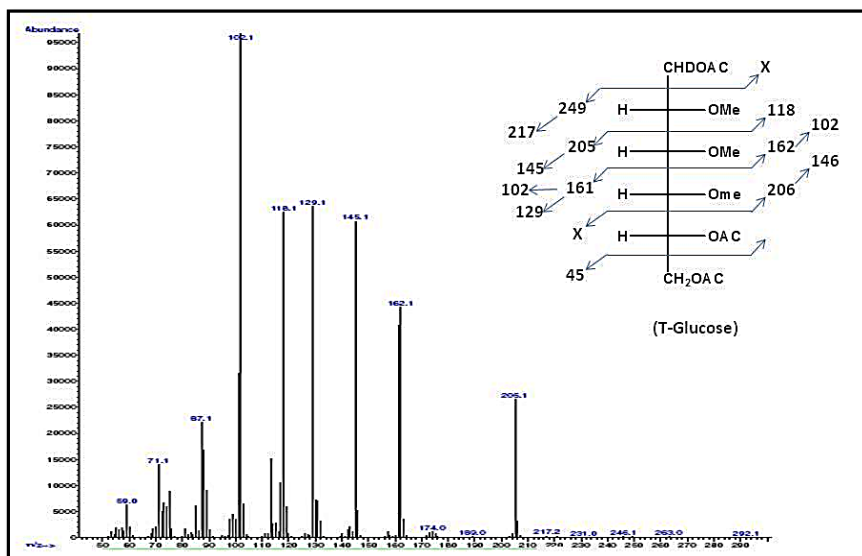
Figure 3-21: EI-mass spectrum for derivative 1, 5-di-*O*-acetyl-(1-deuterio)-2, 3, 4, 6-tetra-*O*-methyl glucitol (T-Glucose) derived from the 12.35 min GC-peak (inset MS adapted from analysis of carbohydrates by GLC-MS) [169]
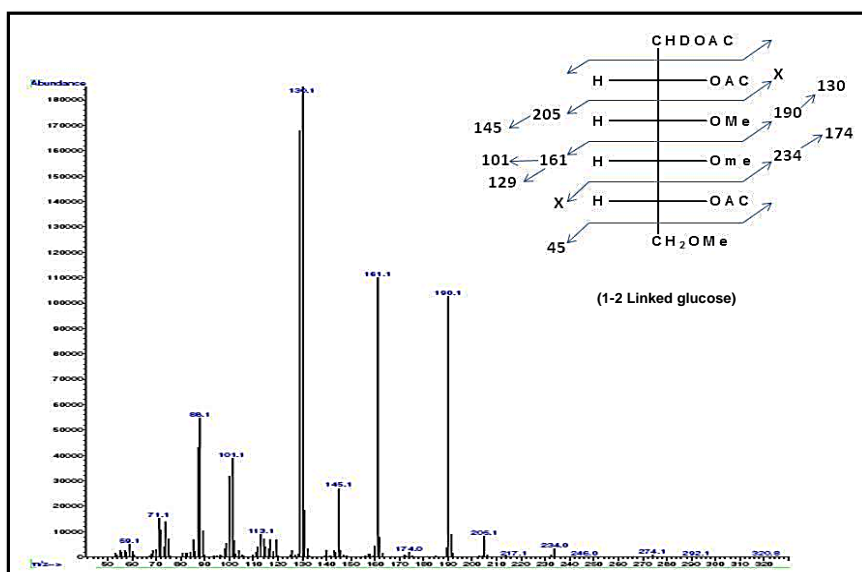
Figure 3-22: EI-mass spectrum for derivative of 1,2,5-tri-*O*-acetyl-(1-deuterio)-3,4,6-tri-*O*-methy glucitol (1→2 Linked glucose) derived from the 15.25 min GC-peak (inset MS adapted from analysis of carbohydrates by GLC-MS) [169]
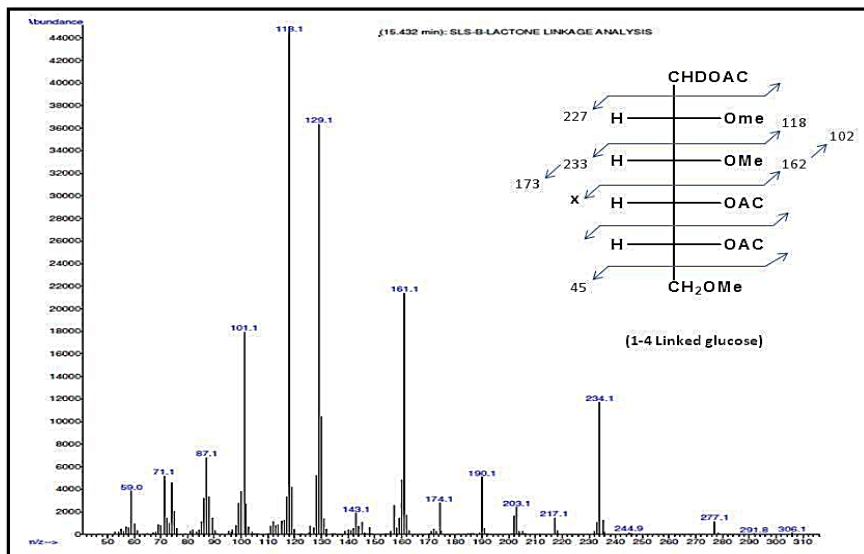
Figure 3-23: EI-mass spectrum for derivative of 1,4,5-tri-*O*-acetyl-(1-deuterio)-2,3,6-tri-*O*-methyl glucitol (1→4 Linked glucose) derived from the 15.41 min GC-peak. (inset MS adapted from analysis of carbohydrates by GLC-MS) [169]
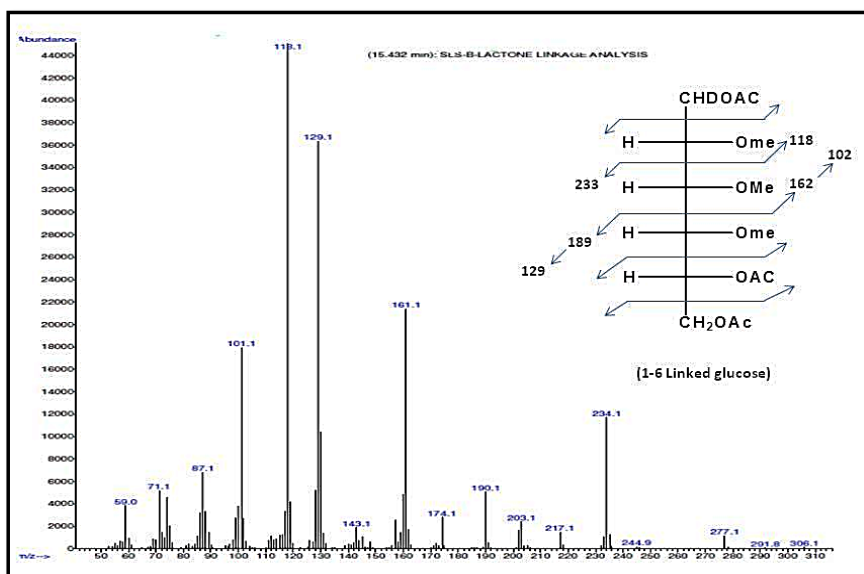
Figure 3-24: EI-mass spectrum for derivative of 1,5,6-tri-*O*-acetyl-(1-deuterio)-2,3,4-tri-*O*-methyl glucitol, alternatively denoted as a 1→6 linked glucose moiety (1→6 glucose) derived from the 16.31 min GC-peak. (inset MS adapted from analysis of carbohydrates by GLC-MS) [169]
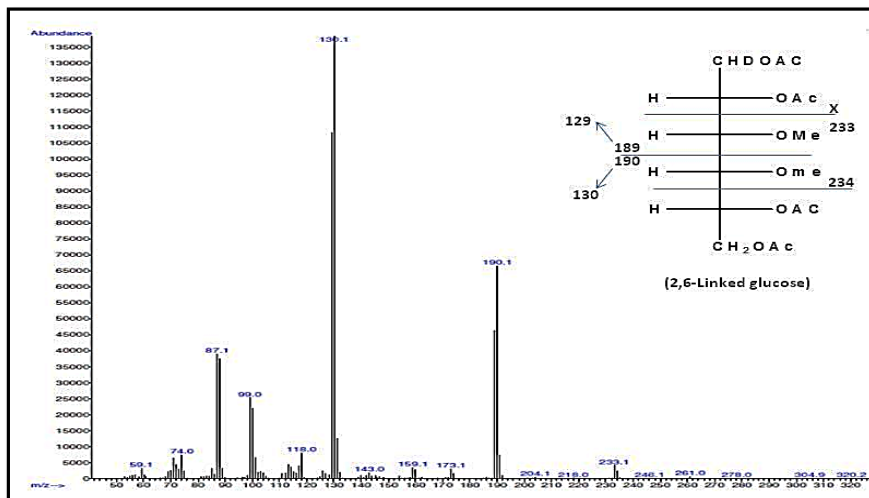
Figure 3-25: Mass spectrum for derivative of 1,2,5,6-tetra-*O*-acetyl-(1-deuterio)-,3,4-di-*O*-methyl glucitol, denoted as a 2-6 linked glucose moiety (2→6 glucose) derived from the 19.54 min GC-peak. (inset MS adapted from analysis of carbohydrates by GLC-MS) [169]

The PMAA derivatisation of the acid sophorolipid (Figure 3-26) produced the same peaks as those observed in the lactone form sample, but with different ratios. The peaks observed in the GC chromatogram are at 12.41, 15.26, 15.41, 16.31 and 19.51 min with a ratio of 50.74, 63.61, 6.23, 4.21, 3.44 respectively, in addition to other minor peak at 23.82 min with a ratio of 2.79 %.
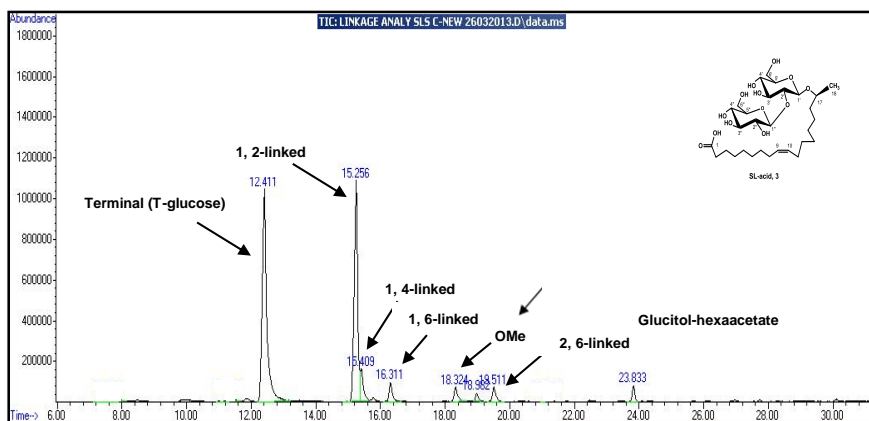
Figure 3-26: GC-chromatogram represents the linkage pattern for the acid sophorolipid (3

98

The interpretation of mass spectrometry data for the PMAA fragmentation patterns to these peaks were (Figure 3-21 & 22) also compared to literature MS, [169] it was found that the first major peak was for the 1,5-di-*O*-acetyl-(1-deuterio)-2,3,4,6-tetra-*O*-methyl glucitol, derived from the terminally linked glucose moiety (T-glucose), whereas the second major peak at 15.25 min was identified as 1,2,5-tri-*O*-acetyl-(1-deuterio)-3,4,6-tri-*O*-methyl glucitol, derived from a 1→2 linked glucose moiety (1-2-glucose). These are the linkage expected to find in deacetylated acid sophorolipid sample, which is composed of two glucose molecules linked by 1→2 type linkage.

The other minor peaks in the GC chromatogram at 15.41 and 16.31 min were of lower ratios (Table 3-2) compared to the peak ratios of the lactone sophorolipid and determined for 1,4,5-tri-*O*-acetyl-(1-deuterio)-2,3,6-tri-*O*-methyl glucitol, alternatively denoted as a 1→4 linked glucose moiety (1-4-glucose), which is also expected for the deacetylated acid form and 1,5,6-tri-*O*-acetyl-(1-deuterio)-2,3,4-tri-*O*-methyl glucitol, alternatively denoted as a 1-6 linked glucose moiety (1-6-glucose) (Figure 3-23 & 24) which is expected for the acetylated acid sophorolipid form, but in small amount. The other minor peak in GC chromatogram 19.54 was determined for 1,2,5,6-tetra-*O*-acetyl-(1-deuterio)-,3,4-di-*O*-methyl glucitol (2→6 Linked glucose) (Figure 3-25). This is also expected for the acetylated acidic sophorolipid but in very small amount. Overall, the results confirm that the structure of the acid sophorolipid is free of acetate groups at the C-6s position on the sophorose moiety (Table 3-2) and these results are concise with NMR data for the acid sophorolipid. The degree of acetylation on the C-6s of sophorose moiety in both sophorolipid forms are explained in terms of % peak ratios in table 3-2 below:

Table 3-2: GC-MS linkage analysis peak ratios for lactone and acid sophorolipids.

Linkage Type	% Peak ratio in lactone form	% Peak ratio in acid from
Terminal glucose	20	39
1→2	41	49
1→4	10	5
1→6	8	3
2→6	18	3
Glucitol-hexaacetate	1	2

3.9 Conclusion

The lactone and acid sophorolipids standards were successfully produced and isolated from the crude sophorolipid after the fermentation process by Croda Biotechnology, UK. Their structures were fully elucidated and characterized. The main form was found as the natural lactone, (2) with a hydroxyl fatty acid (C18:1) unit linked to the C-1′ position of the sophorose moiety and esterified at the C-4″ position of sophorose. Whereas the acid form, (3) produced successfully by the alkaline treatment of the lactone form and the NMR data confirmed the opening of the lactone ring and the deacetylation occurred on both of the C-6s positions. The NMR data confirmed sophorolipids are pure and there is no evidence of other impurities associated with the production of sophorolipids.

The monosaccharide composition of sophorolipids was investigated by HPAEC-PAD and GC-MS, the results showed that glucose was found as the only monosaccharide unit present in sophorolipids. These results were further confirmed and correlated with the GC-MS results, which also showed the glucose as the only monomer present in the sophorolipids. The linkage analysis results confirmed that the linkage in sophorolipids is a β (1-2)-glucose link.

4. Isolation of sophorose from the lactone waste and the conversion of sophorose to the isomeric 2-O-β-D-glucopyranosyl-D-mannose

4. Isolation of sophorose & isomaltose from the lactone waste and the conversion of sophorose to the isomeric 2-*O*-β-D-glucopyranosyl-D-mannose

4.1 Introduction

Sophorose, β-1,2-glucopyranosyl-D-glucose is considered to be a valuable disaccharide. This disaccharide possesses important biological activity and is a strong natural inducer of cellulases *e.g.* in *Hypocrea. jecorina* [175] and plays a vital role in activating the production of the different cellulase enzymes needed for the production of glucose which is used in the bioethanol production process. The structural carbohydrate constituent of the biologically active glycosides, saponins and ginsenoside are composed of sophorose. [176,177] Sophorose is also the carbohydrate portion of sophorolipids, [2,37,66] that are progressively being produced for the use as commercial surface-active agents.

In the early 1920s, the chemical synthesis of sophorose was first reported, by Freudenberg *et al.*, [178] . Interest in sophorose grew in the 1950s, when it was accidentally found to be existing in trace quantities in the supplies of D-glucose which had been produced by the inorganic acid catalysed the hydrolysis of starch [179] and these attracted researchers to find a more convenient method to sophorose synthesis. An improved method for the chemical synthesis of sophorose was reported by Coxon and Fletcher [180] in the 1960s. The isolation of sophorose from natural sources was first reported in the 1960s by several authors who extracted sophorose from natural sophoryl-glycosides, including kaempferol sophoroside isolated from pods of *Sophora japonica* [181] and from the sweet glycoside stevioside from *Stevia rebaudiana*. [182]

More recently, in 2012, sophorose and activated sophorose donors have been produced from sophorolipids by Pietruska *et al.* [183] who reported the isolation of per-*O*-acetyl-sophorosyl bromide from the reaction of acetylated sophorolipids with acetic acid and hydrogen bromide. Later on in 2015, Jourdier *et al.* [144] reported that the acid catalysed hydrolysis of

sophorolipids generating a mixture of glucolipids, glucose, and sophorose, these components were then isolated after treatment of the mixture with an enzyme to remove the contaminating glucose.

4.2 Chemical hydrolysis of natural sophorolipids

The diacetylated lactone sophorolipid contains both ester and glycosidic bonds, which are susceptible to either acid or alkaline catalysed hydrolysis. The process of the hydrolysis in aqueous solution will start with the cleavage of the ester bonds on the C-6s position which will be followed by the much slower subsequent hydrolysis of the glycosidic bond, which results in the removal of the disaccharide moiety to yield the hydroxyl-fatty acid. Sophorose is usually only observed during alkaline hydrolysis of sophorolipids when the reaction is conducted under harsher alkaline reaction conditions or via acid hydrolysis which involves heating at 50-70 ^{0}C. [144] In the isolation of the acid sophorolipid, during the alkaline hydrolysis of the lactone sophorolipid the gradual removal of the esters transforms the solid and insoluble diacetyl lactone sophorolipid into a liquid phase which is heavier than water and a mixture of acid and lactone sophorolipids with a varying degree of acetylation. Ultimately, the process generates the deacetylated acidic sophorolipid in the solution (Figure 4-1). [184]
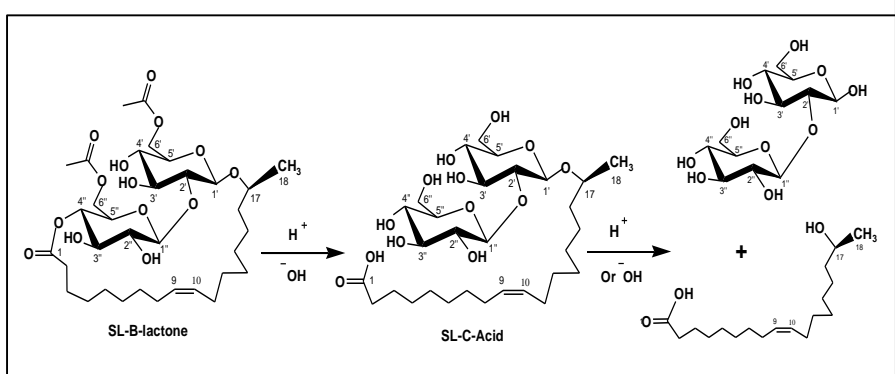
Figure 4-1: Schematic for alkaline / acid hydrolysis of the lactone sophorolipid

102

4.3 Extraction of sophorose from sophorolipids process waste streams

As was stated earlier, there are a number of processing steps involved in isolating the different sophorolipid solids (described in chapter 3) and in each of these processes a waste is generated: during a typical fermentation, sophorolipid production is allowed to proceed until the pH of the fermentation mixture falls to 3.5 at which point the mixture settles into two phases, a lipid rich bottom layer containing the sophorolipids [185] and an upper aqueous phase (spent liquors); in isolation of the lactone, there is a pH adjustment of the lipid phase which generates solid lactone and a waste aqueous phase. The lactone is recovered from the lipid-rich layer by extraction of acidic impurities with cold aqueous alkali; the lactone is converted into the acid form in a hydrolysis step involving the treatment and heating with aqueous alkali [87] (Figure 3-13). The hot alkali treatment gives two phases, an upper aqueous phase from which the acid form is precipitated on re-acidification and a brown lipid-phase (lactone waste). In an attempt to fully understand all of the products generated during the fermentation NMR and HPAEC-PAD were used to determine what products were present in the waste streams. HPAEC-PAD analysis of the lactone waste identified the presence of free sugars; the HPAEC chromatograph (Figure 4-1) contained peaks corresponding to both glucose and sophorose with a (ratio 1:10 w/w) the ratio being calculated using glucose and sophorose standard calibration curves.

As the commercial process generates large volumes of lactone waste (1000s of litres) it is a cheap source from which sophorose could be recovered and an attempt was made to isolate sophorose from the liquid phase. The extraction of sugar was based on the method described in section 2.10. The sugars were extracted into an aqueous phase leaving the lipid components as a separate organic phase. After separation of the two layers, the aqueous phase was evaporated to leave a brown solid residue which contained a range of salts as well as the desired sugars (5.5 g, 5.6 % w/w of the original waste 98 g, 100 ml).

Figure 4-1: HPAEC chromatograms for: (a) D-glucose standard, (b) sophorose standard and (c) extracted sugar mixture from the lactone waste.

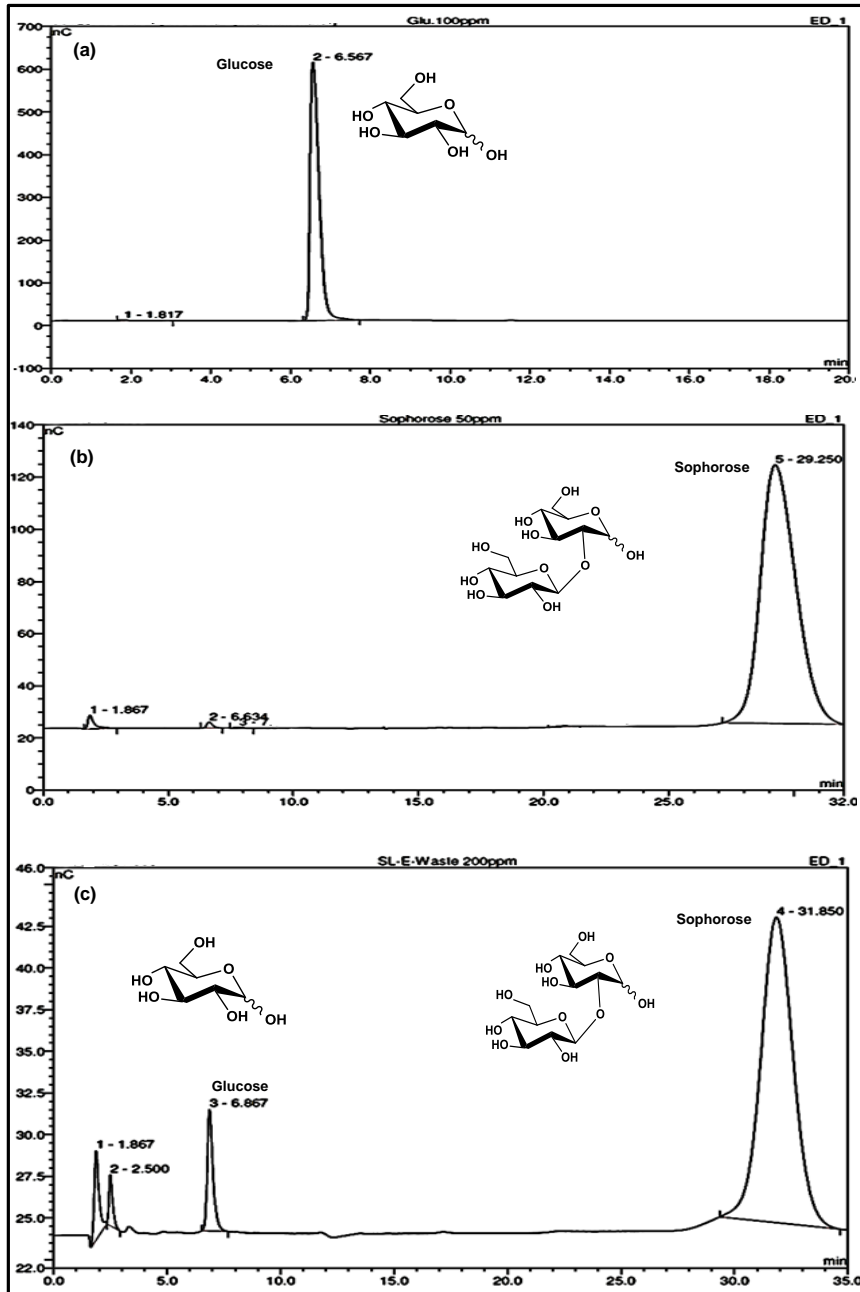**4.4 Use of Carbon: celite 535 column chromatography technique for the isolation of carbohydrates**

A number of researchers have used columns composed of mixtures of carbon and celite (filter aid, flux calcined) and elution with aqueous ethanol for the effective separation as well as high resolution of sugar mixtures into monosaccharides, and disaccharides. [186-188] Celite aids in maintaining a uniform flow-rate. The age of this technique is old, however, it is still valuable and is considered as a useful method for preparative-gram scale purifications, because of its ability to handle much greater quantities of material than most HPLC methods as a result of the high capacity of the carbon columns, thus permitting the quantitative isolation of minor components of a sugar mixture in reasonable amounts. This desirable technique was used recently for the isolation of four oligosaccharides from sugar beet molasses. [189,190]

4.5 Isolation and separation of glucose, isomaltose, (9) and sophorose, (10) using carbon: celite 535 column chromatography

The extracted sugar mix from the lactone waste was subjected to preparative column chromatography carbon: celite 535 according to the procedure described in section 2.10.1.1. The carbon was added to provide a mechanical support and to prevent compression of the column, which would be detrimental to eluent flow; the carbon also helps to absorb coloured materials. The carbon: celite chromatography results show that the column used of (5 cm x 50 cm) dimensions was suitable for the separation of between (5 to 8 g) of the sugar mix sample. The sugar mix (5.51 g) was dissolved in UPW and applied to a carbon-celite column and the column was eluted initially with water to remove impurities (salts) in the sample then with an aqueous mobile phase containing increasing amounts of ethanol (5-20 %). Most of the glucose was eluted using 5% ethanol (2 L), next a disaccharide which was later determined to be isomaltose was eluted from the column using 10% ethanol (2 L). Finally, a fraction containing sophorose was eluted using a more hydrophobic eluent 20% ethanol in water (2 L). The different fractions were collected (Table 4-1) and their reducing sugar content was assayed by HPAEC-PAD.

Table 4-1: Carbon: celite 535 column chromatography fraction elution process

Fraction tube number (45 ml / fraction)	Eluent concentration	Sugar assay (HPAEC) results
T (1-24)	UPW, 1 L	impurities
T (25-47) T (48-85)	5% Ethanol, 2 L	glucose
T (90-105) T (106-135)	10% Ethanol, 2 L	isomaltose
T (136-175)	20% Ethanol, 2 L	sophorose

According to the HPAEC data analysis, the fractions of interest for glucose, isomaltose and sophorose were determined and plotted as line graphs (Figure 4-2, a, b & c), which clearly show the sugar concentrations (area: nC*min) present in each sample fraction.
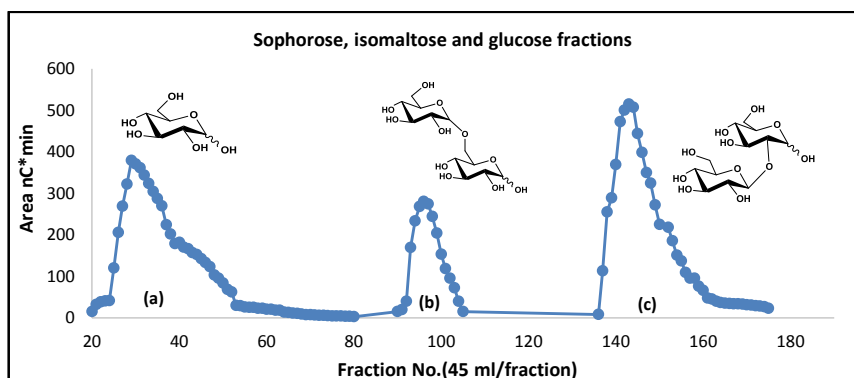
Figure 4-2: Graph represents the concentration of isolated sugars in the fractions of interest: (a) glucose, (b) isomaltose and (c) sophorose.

The HPAEC chromatographs (Figure 4-3) for the fractions of interest, and for glucose, an isomaltose and for sophorose standards; confirmed the fractions of interest. The signal peak for fraction T-48 (Figure 4-3, b) was observed at a retention time of 6.68 min, which was assigned to D-glucose, the signal peak for fraction T-95 (Figure 4-3, d) was observed at 11.55 min and represents isomaltose, (9).

106
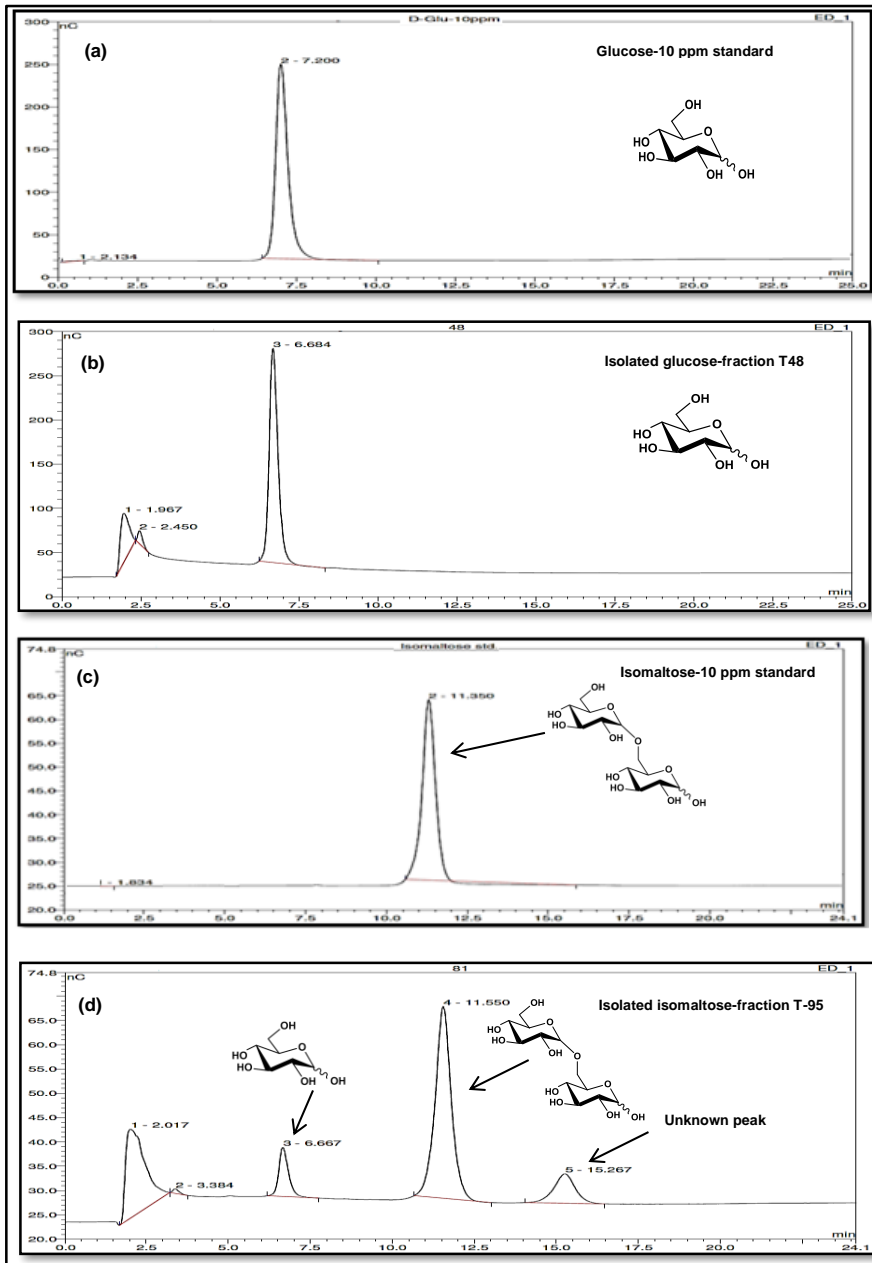
Figure 4-3: HPAEC chromatograms for (a) D-Glucose standard, (b) isolated D-Glucose, (c) Isomaltose standard and (d) Isomaltose isolated from the column.

The HPAEC analysis for the fraction T-138 (Figure 4-4) gave a peak at 28.15 min and this retention time was close to that of the sophorose standard (50 ppm), which had a retention time at 28.00 min. The HPAEC analysis (Figure 4-4) indicated that sophorose with a purity of greater than 95% had been recovered and this corresponds to approximately one percent of the mass of the original waste. Given the large volume of lactone waste available, this represents a potentially large source of the valuable disaccharide sophorose. As the biosynthetic pathway involves sequential addition of glucose residues to the lipid chain, [191] free sophorose was not expected to be a product of the fermentation process.
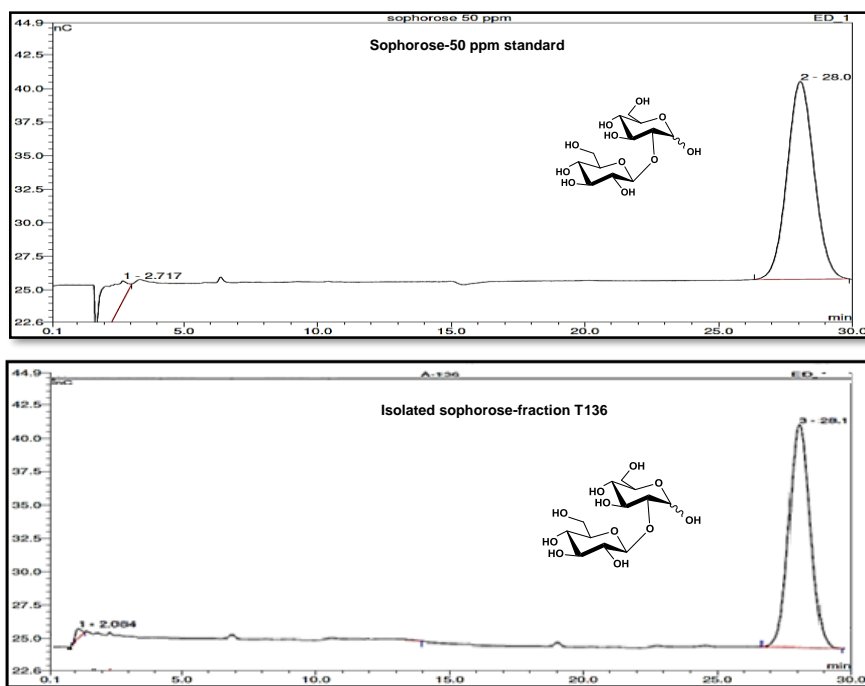
Figure 4-4: HPAEC chromatograms for: (a) sophorose standard and (b) isolated sophorose (T-138) from the column.

The fractions of interested were pooled and the solvent evaporated at 35-40 °C giving the product as a crystalline white solid. The total recovered sugars from the carbon: celite column separation method were as follows:

glucose (2.53 g, 46%), isomaltose (0.43 g, 8%) sophorose (0.95 g, 17%) and (1.60 g, 29%) of impurities. These have been isolated from 5.51 g of sugar mix. To confirm the identity of the products the recovered sugars were subjected to NMR analysis.

4.6 Structure elucidation of the isolated sugars using NMR technique

The ^{1}H-NMR analysis of the sugar mix extracted from the lactone waste (Figure 4-5) confirmed that the organic component of the material was mostly a mixture of glucose and sophorose and that no lipids were present; the ^{1}H-NMR spectrum was compared with the spectra of D-glucose and sophorose standards. Comparison of the integrals for the anomeric protons (α plus β-anomers) for the two sugars indicated that the extracted mixture contained a 1:2.3 (w/w) ratio of glucose to sophorose whereas HPAEC analysis suggested a slightly higher ratio of 1:2.7 (w/w).
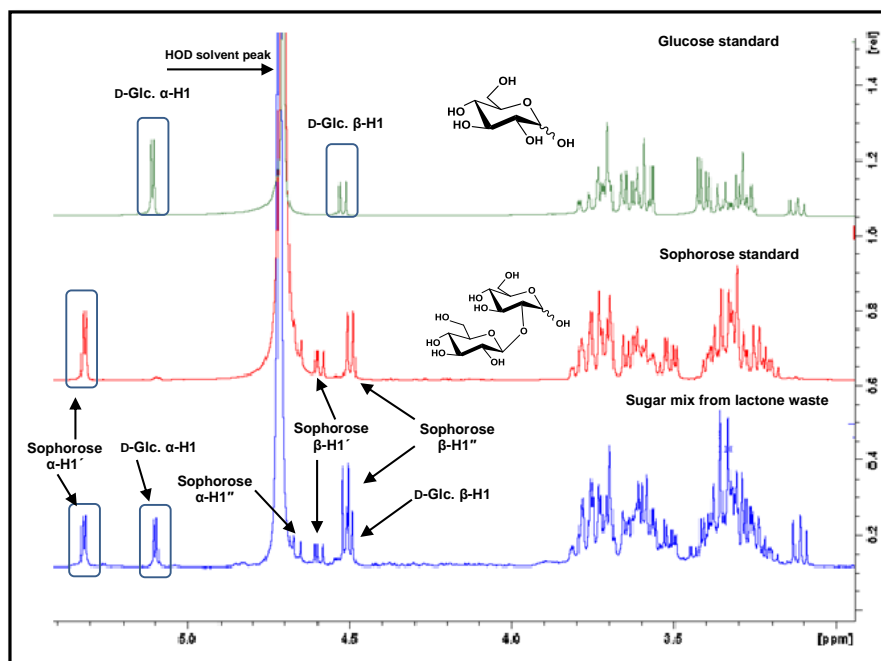
Figure 4-5: ¹H-NMR Spectra for standard D-glucose (top), sophorose (middle) and the sugar mix extracted from the lactone waste (bottom) recorded at 30 ºC in D₂O using 400 MHz NMR spectrometer.

The isolated sophorose, isomaltose and glucose chemical structures (Figure 4-6, 7 & 8) gave identical spectra to those of their standards and were of a high purity as the ^{1}H-NMR spectra indicated:
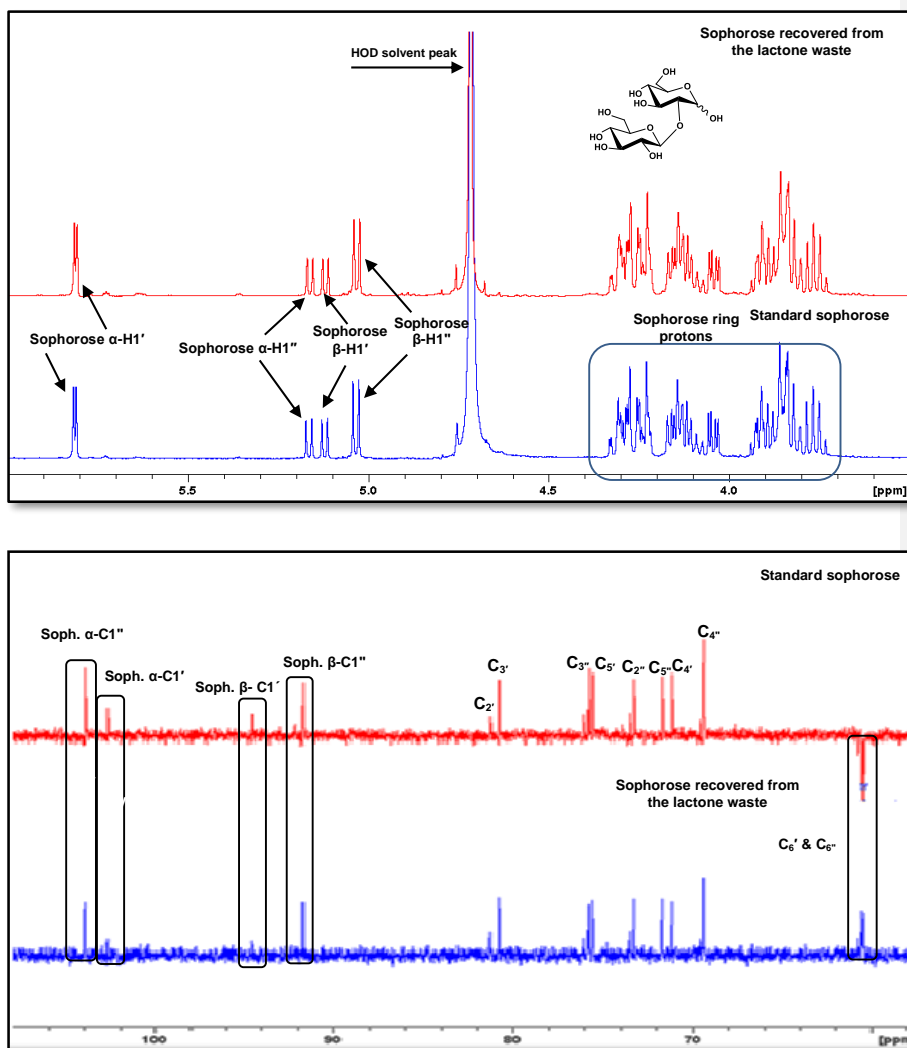
Figure 4-6: Top spectrum is the ^{1}H-NMR spectra for the recovered sophorose, (10) and the standard, while the bottom spectrum is the DEPT-135 for both the recovered and standard sophorose recorded at 70 °C in D$_2$O using 500 MHz NMR spectrometer.

The ^{1}H-NMR spectrum (Figure 4-6) for the isolated sophorose is identical to the standard sophorose spectrum, which confirms that the isolated sugar is sophorose with a purity of more than 95 %.

The ^{1}H-NMR spectrum (Figure 4-7) of the isomaltose isolated from the column was identical to that recorded for an isomaltose standard. The isolated sugar is isomaltose with a purity of more than 92 %.
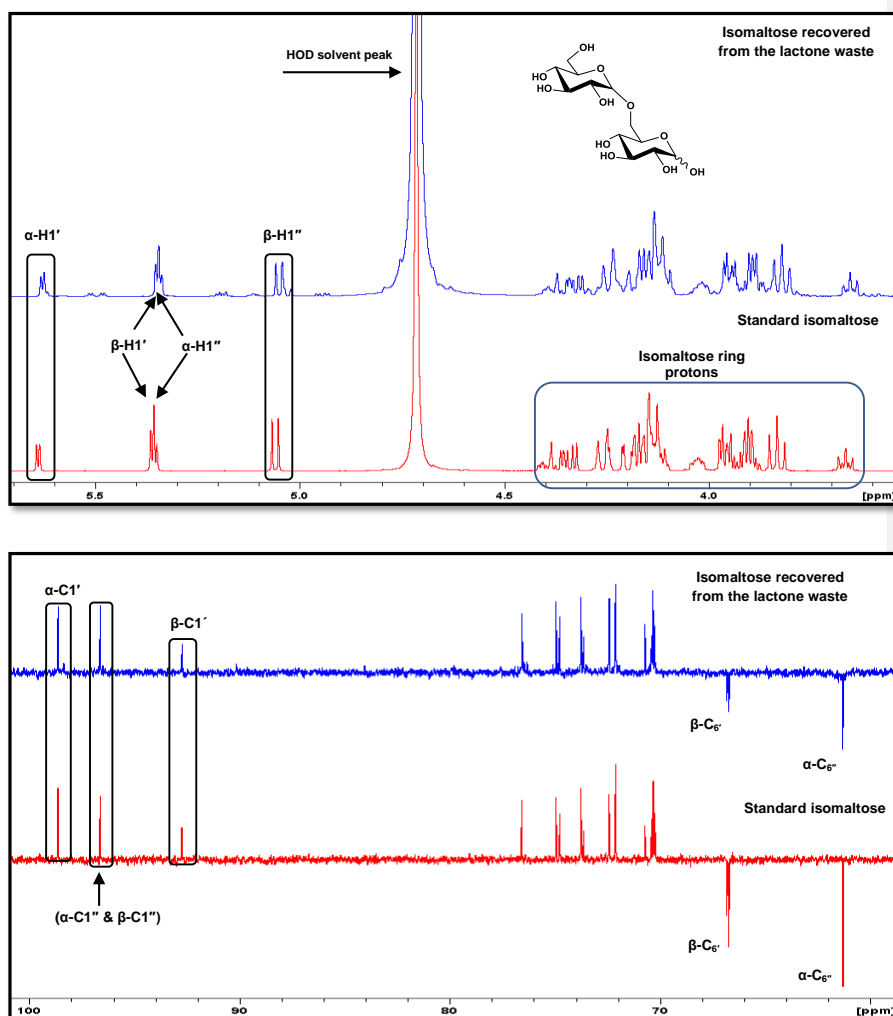
Figure 4-7: Top spectrum is the ^{1}H-NMR spectra for the recovered isomaltose, (9) and the standard, while the bottom spectrum is the DEPT-135 for both the recovered and standard isomaltose recorded at 70 °C in D$_2$O using 500 MHz NMR spectrometer.

111

Finally, the ^{1}H-NMR for the isolated sugar glucose was also identical to the standard glucose NMR as indicated in (Figure 4-8) below:
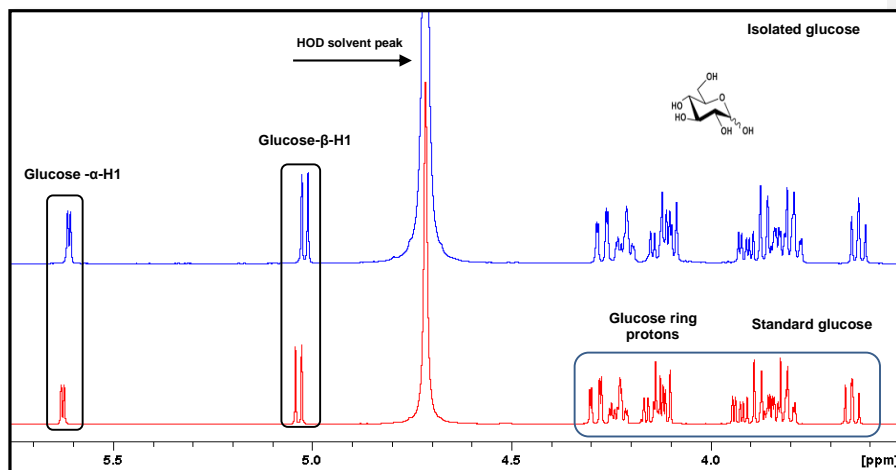
Figure 4-8: ^{1}H-NMR spectrum for the isolated glucose and the standard recorded at 70 °C in D$_2$O using 500 MHz NMR spectrometer.

4.7 Linkage analysis of isomaltose

The type of linkage present in the material suspected to be isomaltose was confirmed using linkage analysis and employing GC-MS. The isolated isomaltose was permethylated and then analysed using the methods described in sections 2.9.1 & 2.9.2. Isomaltose was derivatised to form acid stable methyl ethers, hydrolysed, reduced and then peracetylated before being analysed by GC-MS.

The GC-MS trace for the PMAA derivatisation of the isomaltose sample produced two major peaks observed in the GC-MS chromatogram (Figure 4-9) at 12.22 and 16.23 mins. Interpretation of the mass spectrometry data for the PMAA fragmentation linkage (Figure 2-10 & 2-11), it was found that the first peak was for 1,5-di-*O*-acetyl-(1-deuterio)-2,3,4,6-tetra-*O*-methyl glucitol, derived from a terminally linked hexose moiety (T-glucose), whereas the second peak at 16.23 min was identified as 1,5,6-tri-*O*-acetyl-(1-deuterio)-

112

2,3,4-tri-*O*-methyl glucitol, derived from a 1→6 linked hexose moiety (1-6-glucose). These are the linkage expected in isomlatose.
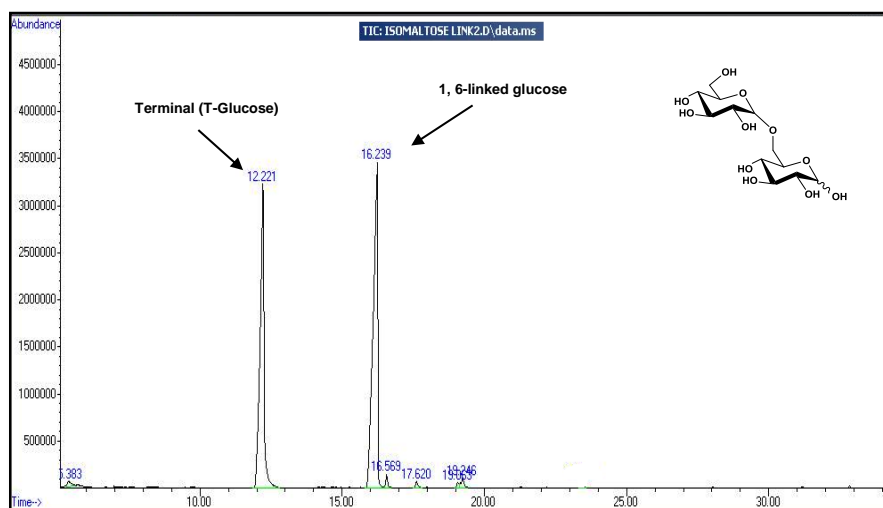
Figure 4-9: GC-chromatogram represents the linkage pattern for the isomaltose.
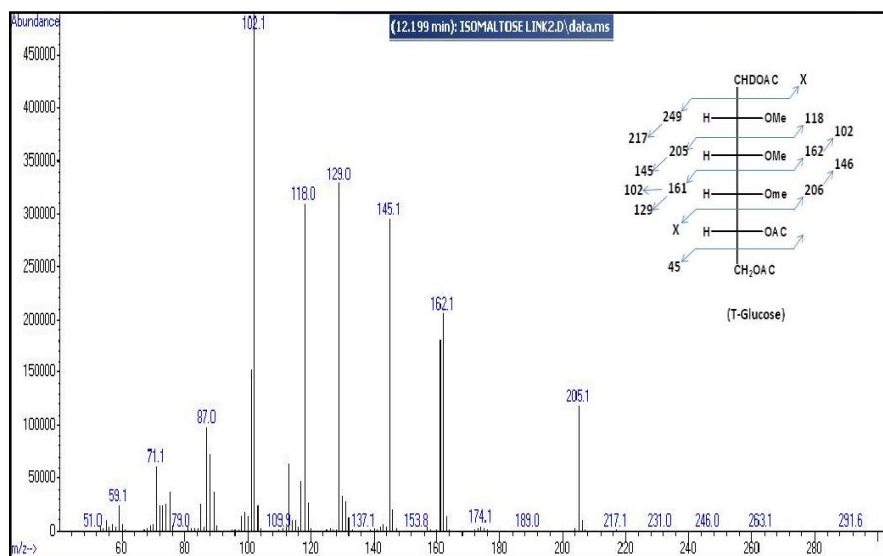
Figure 4-10: Mass spectrum for 1, 5-di-*O*-acetyl-(1-deuterio)-2, 3, 4, 6-tetra-*O*-methyl glucitol (T-Glucose) derived from the 12.20 min GC-peak (inset MS adapted from analysis of carbohydrates by GLC-MS)[169]
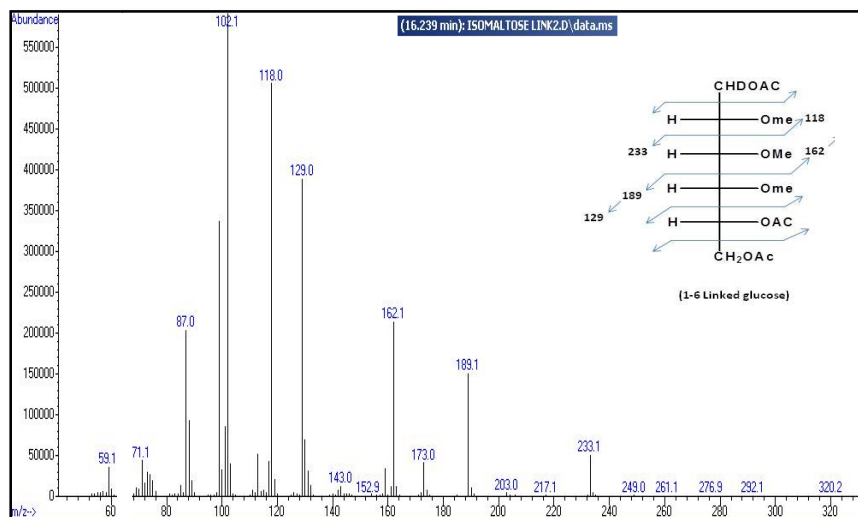
Figure 4-11: Mass spectrum for 1,5,6-tri-*O*-acetyl-(1-deuterio)-2,3,4-tri-*O*-methyl glucitol, alternatively denoted as a 1→6 linked glucose moiety (1→6 Glucose) derived from the 16.23 min GC-peak. (inset MS adapted from analysis of carbohydrates by GLC-MS)[169]

4.8 HPLC-MS analysis of sophorose and isomaltose

The molecular weight of the isolated sophorose was also confirmed using HPLC-HRMS analysis. The LC-chromatography detected one main compound and the total ion chromatogram of the main peak with a retention time (0.35 min) generated the ion at m/z= 365.106, which corresponded to the sodium salt [M+Na] $^+$ of the disaccharide sophorose as shown in (Figure 4-12):

114
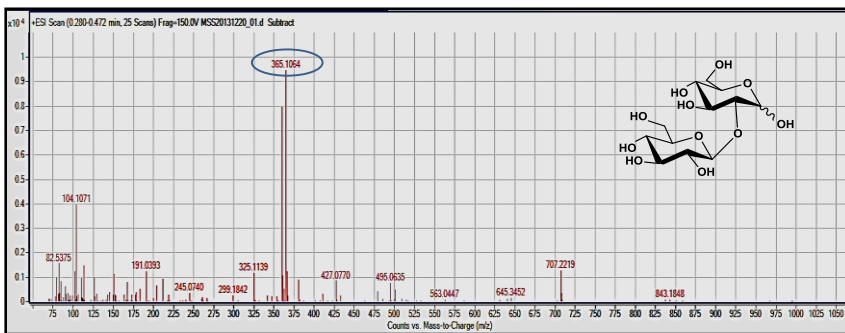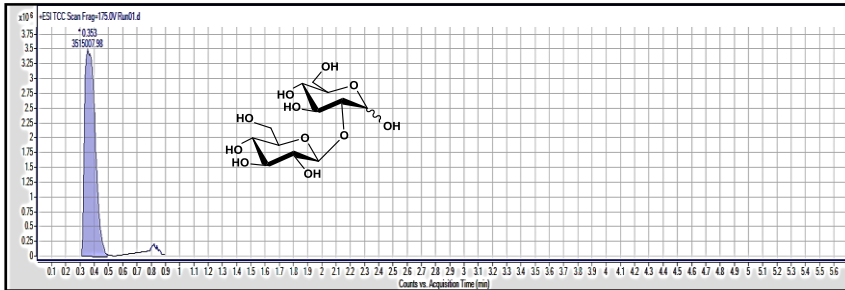
Best	Formula	Species	m/z	Mass	Mass (MFG)	Score	Diff (ppm)
●	C12 H22 O11	(M+Na)+	365.1064	342.1172	342.1162	96.94	-2.76

Figure 4-12: Total ion chromatogram, full mass spectrum and the correct formula matching for the isolated sophorose, (10).

The molecular weight of the isolated isomaltose was also determined using the HR-MS analysis method. The injection of isomaltose (100 ppm solution) into the ESI-MS source in +ve mode produced the mass spectra (Figure 4-13):

115
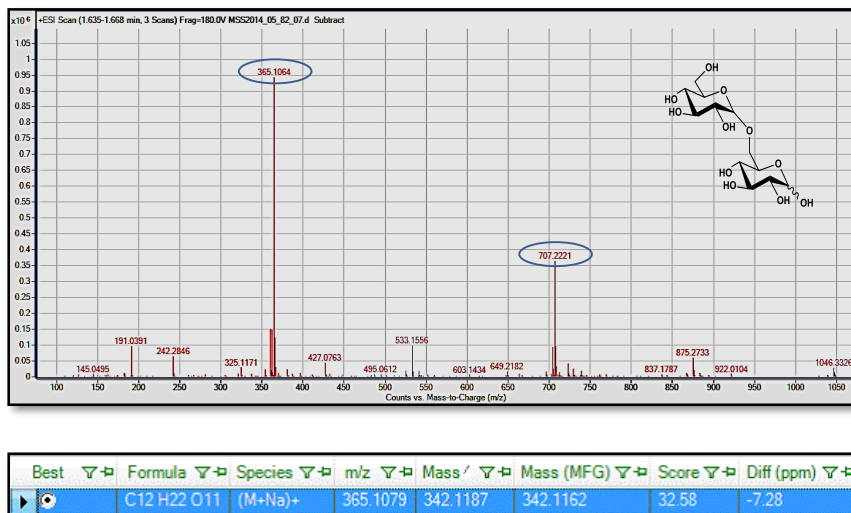
Figure 4-13: Full mass spectra and the correct formula matching for the isolated isomaltose, (9).

From the mass spectrum, the expected mass ion was observed as the [M+Na] + ion at 365.1064 m/z, in addition, the [2M+Na] + ion at 707.2221 m/z was also observed, this indicated the presence of isomaltose. The mass of the neutral compound was determined to be 342.1187 m/z, with the mass difference= -7.28 ppm. The theoretical mass of the neutral compound was calculated to be 342.1162 m/z.

4.9 Monitoring the base catalysed hydrolysis of sophorolipids

In an attempt to determine if sophorose was being produced by a base catalysed hydrolysis of the sophorolipid, an experiment was undertaken to see if sophorose was released from the acid form of the sophorolipid on heating with aqueous alkali. The acid form of the sophorolipid was chosen because of its solubility in aqueous alkali and because of the absence of acetyl-ester groups: the hydrolysis of which would consume base. The hydrolysis of the acid sophorolipids was conducted with aqueous alkali at a particularly mild hydroxide concentration to match the conditions used in the commercial

116

production of the acid sophorolipid (0.01 M, pH 12, 50 °C). The method is described in section 2.12. The reactions were monitored by HPAEC & NMR over a period of 24 h (Figure 4-14).

No reaction was observed by NMR, however, analysis of the HPAEC chromatographs (Figure 4-14, b) identified the rapid production of very small quantities of glucose, small quantities of sophorose and, a third peak which was identified as the C2-epimer of sophorose 2-*O*-β-D-glucopyranosyl-D-mannose-explained in section 4.11.1. These three sugars were produced in the first three hours after which time no further reaction was observed and their combined peak area suggested that less than 0.5% of the starting material had been converted to sophorose.
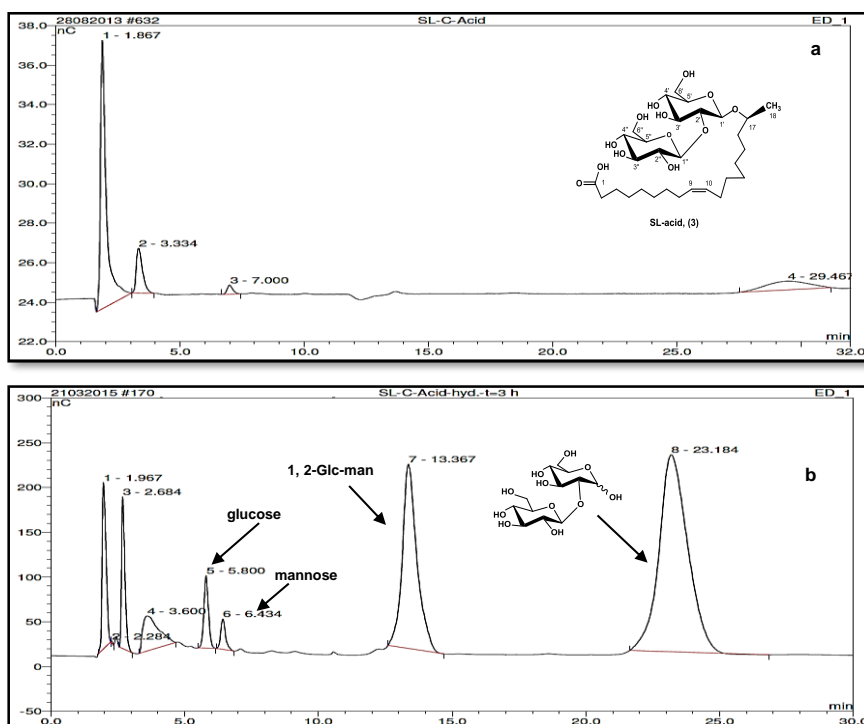
Figure 4-14: HPAEC chromatograms for (a) Acid and (b) sugar components form acid (3) hydrolysis after 90 mins.

Based on the HPAEC-PAD results, and from the chromatogram of sample taken at specific times, it was possible to determine the amount of the three sugars obtained (nC*min) as a function of the reaction time (hydrolysis time in hours) (Figure 4-15).
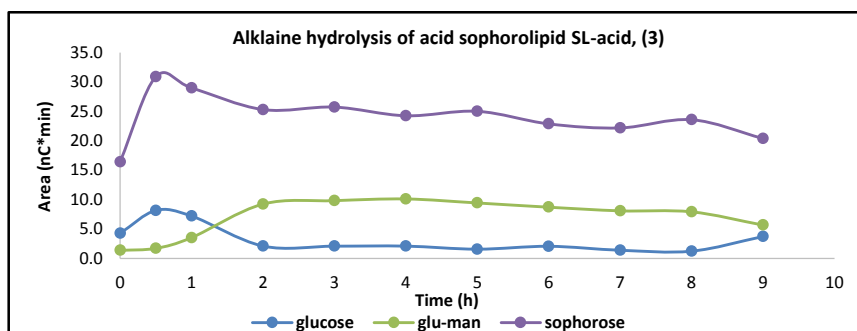
Figure 4-15: Graph represents the alkaline hydrolysis of the acid sophorolipid acid (3)

It is clear that the reaction system reaches a state of equilibrium after approximately two hours of hydrolysis. The sophorolipids were not expected to undergo glycosidic bond cleavage under the relatively mild alkaline conditions employed and it is more likely that the sophorose produced is generated through the rapid hydrolysis of small quantities of the corresponding acetylated-sugars that are present as minor impurities in the starting acid but which don't elute in the HPAEC experiment. The experimental result suggests that under moderately basic conditions hydrolysis of sophorolipids does not lead to the production of sophorose.

4.10 Monitoring the acid catalysed hydrolysis of sophorolipids

The acid catalysed hydrolysis method was conducted in an attempt to recover both the lipid and glucolipid in order to be able to characterise the reaction system by NMR. Jourdier and Ben[144] have reported that the acid catalysed the hydrolysis of sophorolipids generates a mixture of glucolipid, glucose and sophorose, however, they did not characterise either the glucolipid or the liberated lipid. The acid catalysed hydrolysis method was described in section 2.15.

118

The purpose of treating the acid sophorolipid with the acid catalyst was to release the (ω-1) fatty acid from sophorolipids by hydrolysis, which could then be recovered by extraction with an organic solvent which can be easily separated from the aqueous phase. In our experiments, the only sugar containing a molecule that was found in the aqueous phase was glucose. After extraction of the aqueous only the (ω-1) fatty acid was recovered and this was subsequently used in an attempt to synthesise the glucolipid using the glycosylation reaction involving the substrate (2,3,4,6-tetra-O-acetyl-alpha-D-glucopyranosyl bromide-see the next chapter).

Following the conditions employed in (section 2.15), the hydrolysis allows to preferentially break the glycosidic bond between sophorose and the lipid chain, which results in the release of sophorose. However, in a greater or lesser extent depending on the experimental conditions, the released sophorose may also be hydrolyzed to two glucose molecules. The use of high concentration of sulphuric acid (2 M) in this experiment, led to the fast hydrolysis of sophorose into glucose. The acid hydrolysis mechanism of the acid sophorolipid is explained in scheme (Figure 4-16) below:
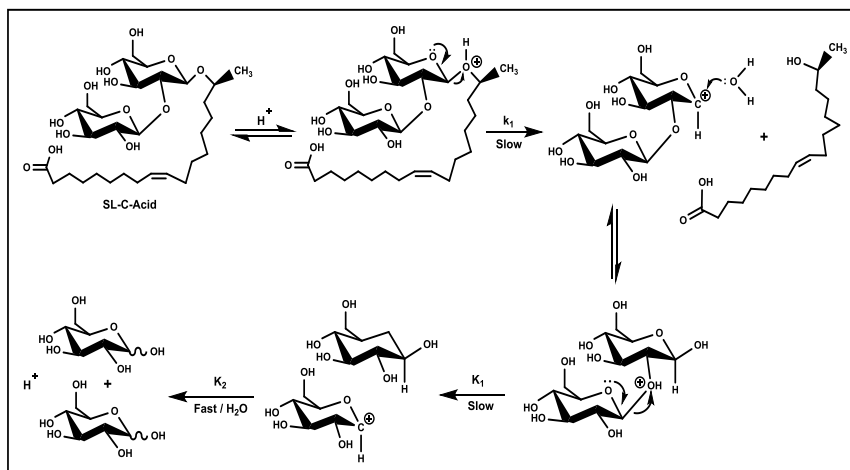
Figure 4-16: Schematic diagram represents the acid hydrolysis mechanism of the acid sophorolipid, (3)

119

The isolated (ω-1) fatty acid (lipid phase) was analysed using ^{1}H- & ^{13}C-NMR spectra and was characterised as 17-hydroxyoctadecenoic acid. The ^{1}H-NMR spectrum (Figure 4-17, a & b) indicated the presence of two forms of the lipid, the free open chain and the lactonated form with a ratio of 1:2 indicated by comparison of the integrals for the lipid H-17 protons. Thus, the NMR analysis of the hydrolysate obtained after the hydrolysis step confirmed that the isolated lipid is a 17-hydroxyoctadecenoic acid and no signs for any glucolipids were present in the hydrolyzate and this might be attributed to the high concentration of sulphuric acid (2 M) used in the experiment.
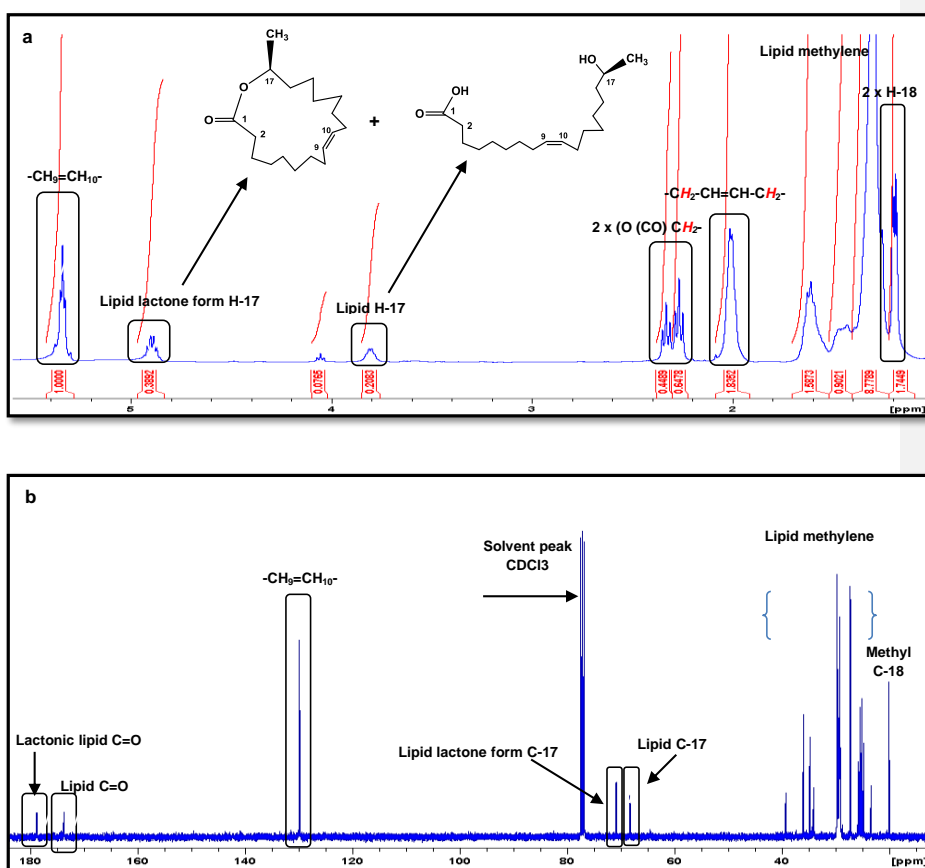
Figure 4-17: Full ^{1}H- and ^{13}C-NMR spectra for the lipid; 17-Hydroxyoctadecenoic acid isolated from the acid catalysed hydrolysis of the acid sophorolipid acid, (3)

4.11 Isolation of the 2-*O*-β-D-glucopyranosyl-D-mannose, (11)

In order to identify the unknown peak observed during the alkaline hydrolysis of the acid sophorolipid, sophorose was reacted with an aqueous alkaline solution at different temperatures and the reaction was monitored by both HPAEC and NMR.

4.11.1 Monitoring the stability of sophorose in aqueous alkaline solution (epimerization / hydrolysis) using the HPAEC-PAD

The disaccharide sophorose is also able to undergo an epimerisation reaction. The chemical reactivity of 1→2-linked glycosides such as sophorose is not very well understood. The treatment of the 1→3, 1→4 and 1→6-linked glycosides with aqueous alkali results in the observation of peeling reactions and small chain fatty acids including saccharinic acids.[192-194]

It was of interest to study the stability of sophorose in aqueous alkali as the process of peeling proceeds through enolisation and migration of the carbonyl carbon to C-2, this process is not possible in C-2-linked glycosides. Sophorose was treated with aqueous sodium hydroxide (100 mM, pH 13, 25 ⁰C) (section 2.13). In this study, sophorose was converted to glucose-mannose, *i.e.*, epimerized at carbon C-2 to produce the glucose-mannose form. Analysis by HPAEC-PAD was (Figure 4-18) used to follow this process.

The HPAEC chromatograms indicated the presence of two main carbohydrates at the start of the reaction: a late eluting peak corresponding to sophorose, small amount of an early eluting glucose peak and a third disaccharide peak, which was similar to that observed during the alkaline catalysed hydrolysis of the acid sophorolipid (Figure 4-14, b). These results were consistent with the epimerisation of the reducing sugar to form the corresponding 2-*O*-β-D-glucopyranosyl-D-mannose (11; Figure 4-18).

Figure 4-18: HPAEC chromatogram for the hydrolysis of sophorose, (10) in alkali solution (100 mM) after 5 h of reaction at 25 °C.
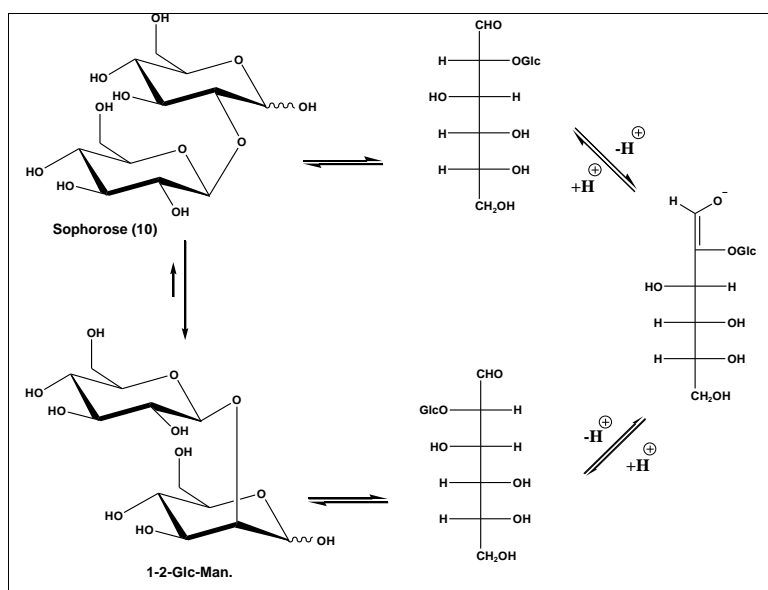
Figure 4-19: Schematic diagram representing the mechanism for the base catalysed interconversion of sophorose, (10) and 2-*O*-beta-D-glucopyranosyl-D-mannose, (11)

4.11.2 Monitoring the stability of sophorose in an aqueous sodium deuteroxide solution (epimerization / hydrolysis) using the ^{1}H-NMR

The same hydrolysis process was also carried out, but using sodium deuteroxide, NaOD (100 mM) and NMR was used to study the conversion (epimerization) of sophorose into the 1→2-glucose-mannose form. It was possible to follow the epimerization/hydrolysis reaction using NMR spectroscopy. ^{1}H-NMR spectra were recorded at different times and the reaction was allowed to proceed at 25 ºC (Figure 4-20) and deuterium was incorporated into the C-2 position during the course of the reaction. The production of 1→2-glucose-mannose was evident after 1h and then became obvious after 12 h of reaction as a new doublet peaks appeared at 4.3 ppm and 5.2 ppm, which confirms the conversion of sophorose into 1→2-glucose-mannose. Those peaks became more intense after 24 h of reaction indicating that a significant proportion of the sophorose has been converted.

The mechanism for this epimerisation reaction (Figure 4-19) was first proposed by Lobry de Bruyn and Alberda van Ekenstein [194] and involves ring-opening of the reducing glucose and base catalysed reversible enolate formation between C-2 and C-1. Reprotonation of the enolate anion on C-2 can take place on either the top Re-face to regenerate glucose or from the bottom Si-face to generate mannose. At equilibrium and under the conditions employed in these experiments, the thermodynamically more favourable mannose epimer dominates. The NMR analysis of the reaction mixture indicated that deuterium exchange was occurring at the C-2 position of the starting material and that a second disaccharide was present in which the configuration of C-2 had inverted. These results were consistent with the epimerisation of the reducing sugar to form the corresponding 2-*O*-β-D-glucopyranosyl-D-mannose, (11).
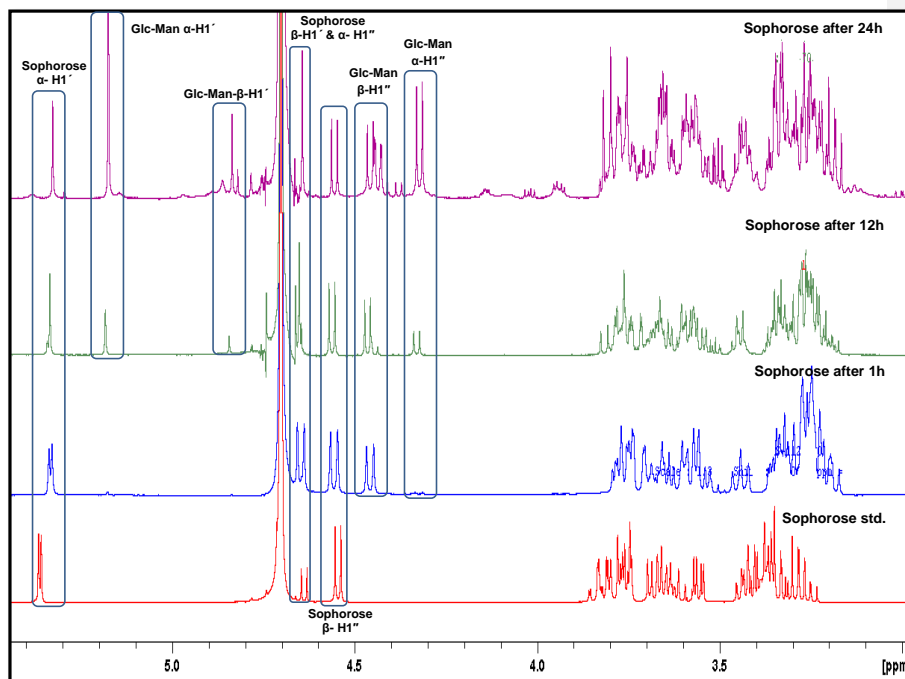
Figure 4-20: ¹H-NMR spectra for sophorose in alkaline solution (NaOD 0.1M) at different processing time recorded at 30 °C.

The partial epimerisation of sophorose has already been reported but the product 2-*O*-β-D-glucopyranosyl-D-mannose was not isolated and was not fully characterised. [195] The recorded NMR spectra above suggested that, under the conditions of the current experiments, 75% of the starting sophorose was converted to 2-*O*-β-D-glucopyranosyl-D-mannose.

4.11.3 Epimerization of sophorose in hot aqueous alkaline solution in order to isolate the 2-*O*-β-D-glucopyranosyl-D-mannose using carbon: celite column

In an attempt to isolate the 2-*O*-β-D-glucopyranosyl-D-mannose, (11) from the sophorose epimerization reaction, a small quantity of sophorose (50 mg) was treated with aqueous alkali (100 mM, 60 ºC), (section 2.11).

The progress of the reaction was monitored by withdrawing samples analysing these using HPEAC.

The experiment was carried out at 60 °C to accelerate the conversion to the 1→2-glucose-mannose. The HPAEC analysis (Figure 4-21) confirmed that the majority of the starting material had been converted to 2-O-β-D-glucopyranosyl-D-mannose after 24 h, at which point the reaction was quenched by acidification with acetic acid.
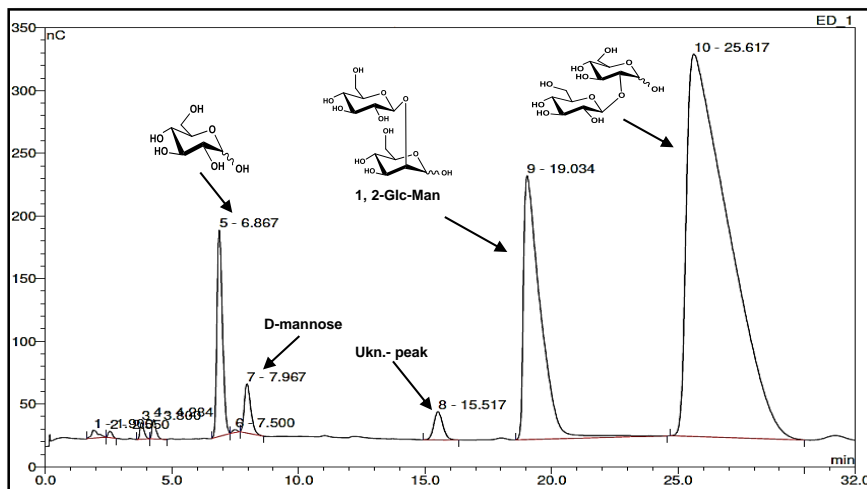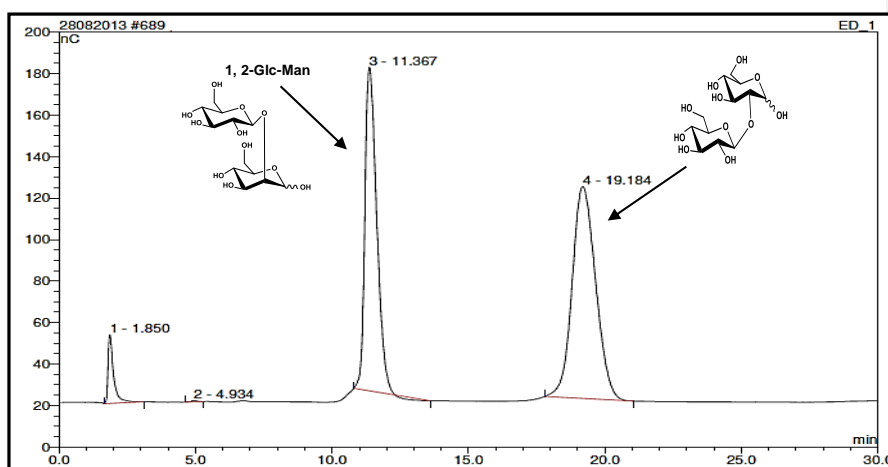

Figure 4-21: HPAEC chromatogram for the hydrolysis of sophorose in hot alkali solution (100 mM) after 8h of reaction at 60 ºC.

Using the HPAEC chromatograms, it was possible to study the time course of the epimerization reaction and to determine the relative amounts of the 2-O-β-D-glucopyranosyl-D-mannose and sophorose present at equilibrium.

The HPAEC results were plotted (peak area in nC*min versus time) (Figure 4-22) and the ratio of 2-O-β-D-glucopyranosyl-D-mannose to sophorose was determined to be 1.75:1.00.
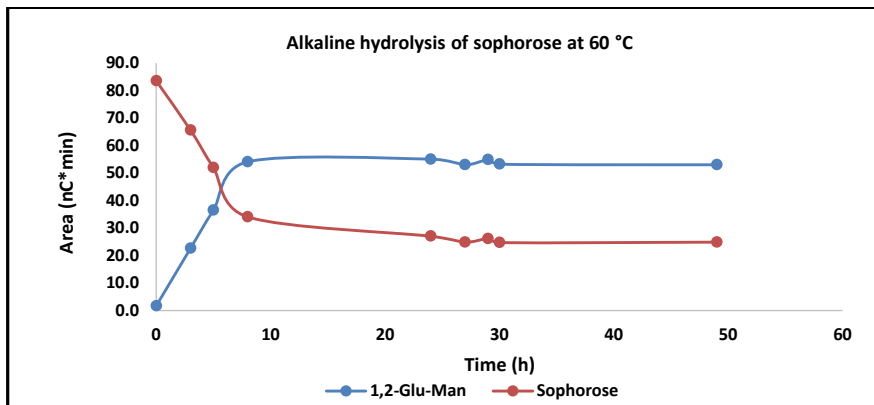
Figure 4-22: Graph represents the alkaline (0.01M) hydrolysis of the sophorose at 60 ºC.

The resulting crude product containing the 2-*O*-β-D-glucopyranosyl-D-mannose was then applied to a carbon: celite column and the new disaccharide was isolated by elution with aqueous ethanol (described in section 2.11). The product eluted as a single peak in 20% ethanol (Figure 4-23) and after evaporation of the solvent, 2-*O*-β-D-glucopyranosyl-D-mannose, (11) was recovered as a white powder (10 mg). The HPAEC chromatogram showed a single peak at 10.78 min corresponded to the 2-*O*-β-D-glucopyranosyl-D-mannose peak.
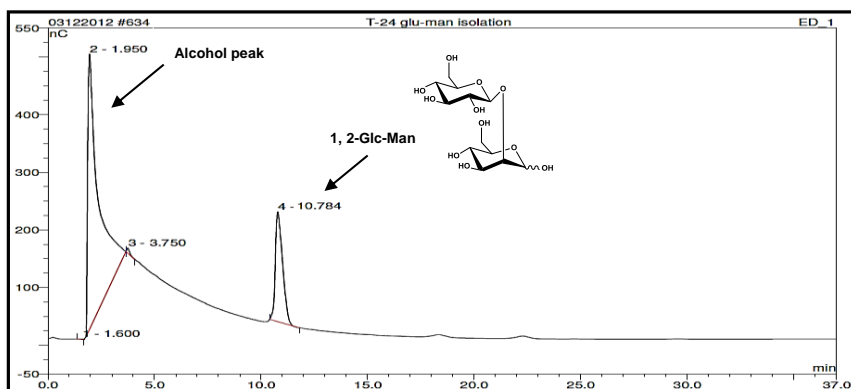
Figure 4-23: HPAEC chromatogram for the pure isolated 2-*O*-β-D-glucopyranosyl-D-mannose, (11).

126

A series of 1D- & 2 D-NMR experiments were conducted to characterize the disaccharide's structure. The ^{1}H-NMR of 2-*O*-β-D-glucopyranosyl-D-mannose indicated that the product was present as a pair of anomers (Figure 4-24). It was observed that at 30 °C in an aqueous D_2O solution that 2-*O*-β-D-glucopyranosyl-D-mannose, (11) exists as a mixture containing 77% of the alpha-anomer and 23% of the beta-anomer. The full assignment of the proton and carbons of the alpha anomer and for the protons of the beta-anomer (for the beta-anomer carbon signals were only visible for the anomeric signals) and the chemical shifts are listed in the (Table 4-2). It should be noted that the proton assignment for the anomeric glucose (H1′)-protons are different to those in the literature [183] (the values in the literature for the H1′-proton for alpha and beta may have been inverted).

In summary, when sophorose treated with aqueous alkali, it did not undergo either hydrolysis or a peeling reaction and instead underwent epimerisation at C-2 to generate 2-*O*-β-D-glucopyranosyl-D-mannose as the NMR and HPAEC results confirmed.
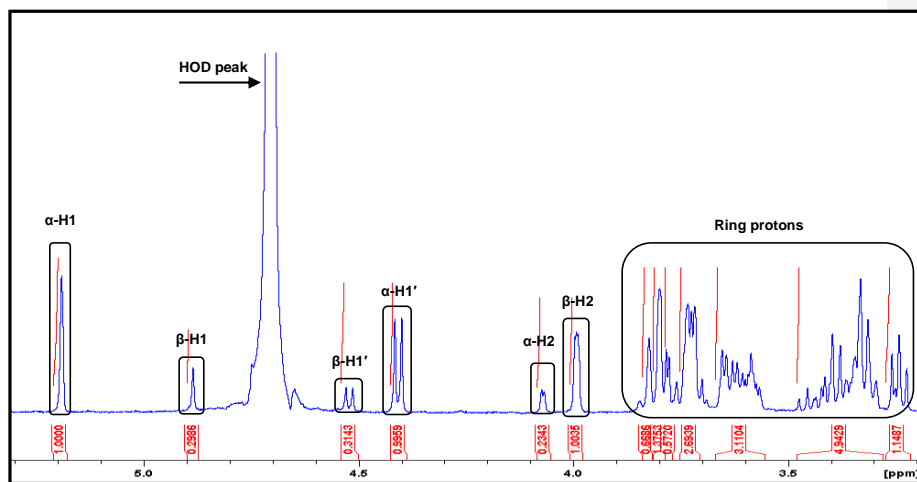
Figure 4-24: ^{1}H-NMR spectrum for the isolated 2-*O*-β-D-glucopyranosyl-D-mannose, (11) recorded at 30 °C.

Table 4-2: Individual chemical shifts for protons and carbon signals (chemical shift, ppm) for 2-*O*-β-D-glucopyranosyl-D-mannose, (11)

Sugar\Position for α-anomer	H-1	H-2	H-3	H-4	H-5	H-6s	C-1	C-2	C-3	C-4	C-5	C-6s
Reducing	5.19	4.07	3.88	3.81	3.69	3.93 & 3.72	92.3	78.6	69.6	72.4	67.2	60.7
Non-reducing	4.51	3.34	3.49	3.43	3.41	3.83	101.9	72.9	75.6	76.0	69.6	60.4

Sugar\Position for β-anomer	H-1	H-2	H-3	H-4	H-5	H-6s	C-1
Reducing	4.88	3.99	3.68	3.55	3.41	ND	93.9
Non-reducing	4.52	3.41	3.48	ND	ND	ND	104.1

The ^{1}H-^{13}C-HSQC-NMR spectrum confirms the identity of the isolated 2-*O*-β-D-glucopyranosyl-D-mannose, (11), which shows the correlation between the protons and carbons signals.
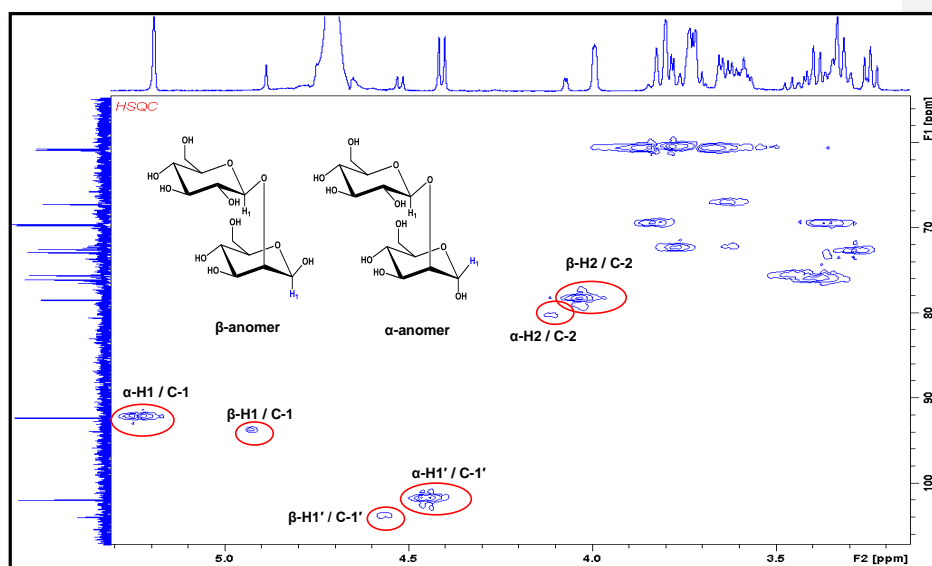
Figure 4-25: Selected region of the HSQC-NMR spectrum of 2-*O*-β-D-glucopyranosyl-D-mannose, (11).

4.12 Observation of an enzyme catalyzed hydrolysis of sophorolipids by spent fermentation broth

In order to study the possibility that the yeast *C.bombicola* releases an enzyme which has the ability to catalyse the hydrolysis of the gluco-lipid bond of sophorolipids, a sample of a fermentation broth (100 ml) recovered at the end of the fermentation process was supplied by Croda Biotechnology and was kept in a cold-room for 24 h before being used to test for the presence of enzyme activity that may hydrolyse sophorolipids (pH 3.5). The procedure for this experiment is described in section 2.14. It has previously been suggested that sophorolipids are metabolized by *C.bombicola* upon carbon starvation. [196]

The activity was investigated using the lactone and acid sophorolipids. In separate experiments, both lactone and acid sophorolipid were added to the spent fermentation liquors recovered at the end of a large-scale fermentation, which had been filtered to remove any biomass.

The HPAEC results for the samples assayed after 24 h of incubation showed a number of different peaks each of which represented a sugar component, the use of the acid sophorolipid as a feedstock gave a chromatogram (Figure 4-26, b), which shows four components peak, at 8.50, 10.99, 17.11 and the last peak at 22.03 min, which has the higher concentration in comparison to other components. Three of peaks had retention times which were close to the retention times of the glucose (8.10 min), isomaltose (16.83) and sophorose (21.92 min) standards, except the peak at the retention time 10.99 min, which might be attributed to the presence of an unknown component (potentially glucolipid).

The lactone sophorolipid feedstock chromatogram (figure 2-26, d) also shows four main component peaks at 8.17, 10.35, 16.04 and the last peak was at 20.55 min, which is again similar to the retention time of the standards. These resulting chromatograms were compared with the lactone and acid sophorolipids HPAEC chromatograms (Figure 4-26, a & c). The amount of sophorose was higher when the acid sophorolipid was used as a substrate.

129

The results are consistent with the presence of an enzyme that is able to catalyse the hydrolysis of the acid form and which is able to release sophorose, in contrast, the product formed from the lactone form would be expected to be diacetylated-sophorose. The later result is consistent with the presence of an enzyme (s) which is capable of cleaving both of the 1→2-glycosidic bond and the lipid-glycosidic bond. This enzyme catalysed the hydrolysis of the 1→2-glycosidic link would firstly, generate a gluco-lipid and a glucosyl-enzyme intermediate. If the glucosyl-enzyme intermediate is attacked by a water molecule this would generate glucose and release the enzyme. Attack by a second glucose molecule or a primary hydroxyl on the glucosyl-enzyme intermediate would lead to the production of isomaltose and release the enzyme. Production of isomaltose requires the transferase activity of an inverting enzyme.

The observation of the hydrolysis of sophorolipids provided evidence for the possibility of the presence of an enzyme, which is responsible for the generation of sophorose and isomaltose during the production of sophorolipids. From these result, it can be concluded that there is an enzyme, which is capable of hydrolysing sophorolipids present in the fermentation broth at the end of sophorolipids production.
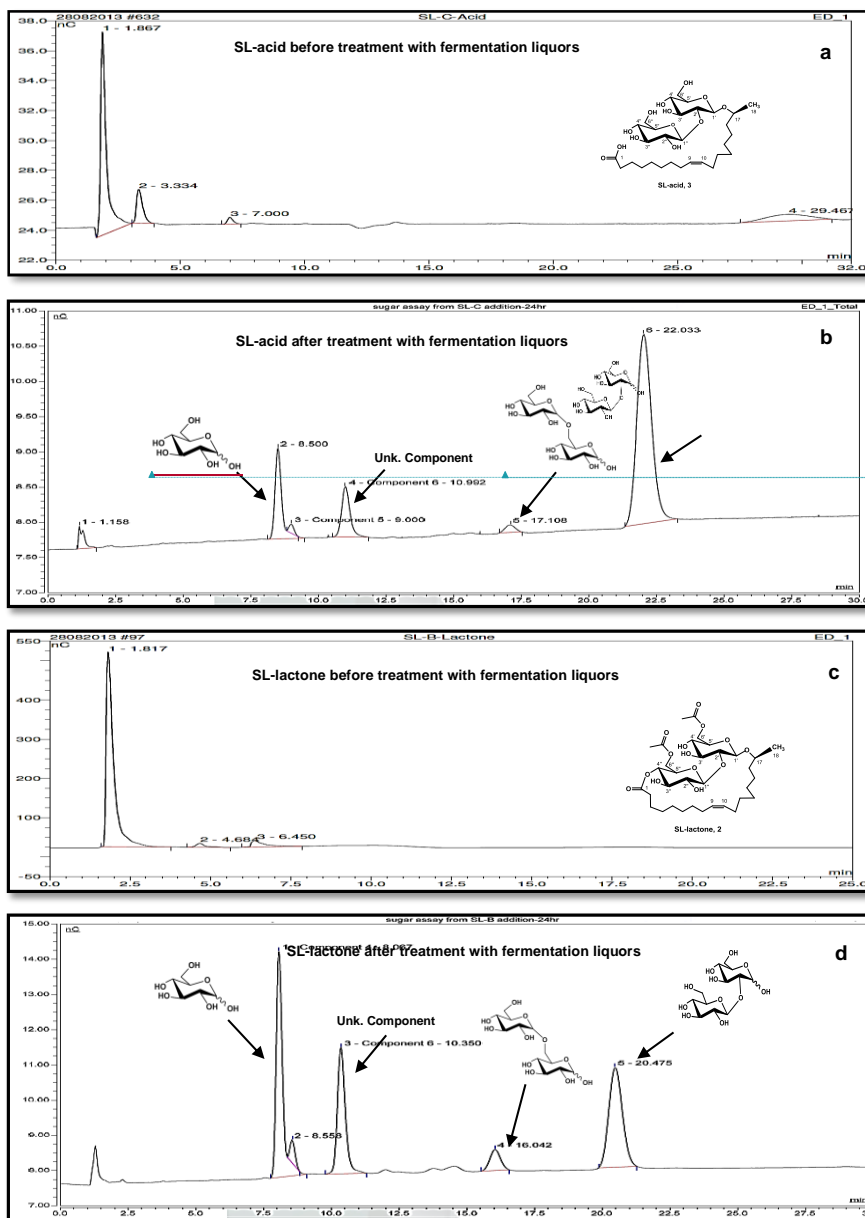
Figure 4-26: Use of HPAEC chromatography to monitor the enzyme catalysed hydrolysis of (a) SL-acid before treatment (b) SL-acid after treatment with spent fermentation liquors (c) SL-lactone before treatment (d) SL-lactone after treatment with spent fermentation liquors.

4.13 Conclusion

The valuable sugar β-1→2-linked disaccharide sophorose was isolated from the waste streams generated during the commercial manufacture of sophorolipids and characterized successfully as a pure white crystalline sugar in gram scale quantities and the chemical structure of sophorose and isomaltose was also fully elucidated using the combination of the NMR and HPAEC-PAD, which all confirmed the identity of these two disaccharides.

The base catalysed-hydrolysis of the acid sophorolipid was explored in an attempt to investigate the origin of the sophorose in the lactone waste streams. The treatment of sophorose with an aqueous alkaline solution led to the formation of the disaccharide 2-*O*-β-D-glucopyranosyl-D-mannose, (11) via the epimerisation, at C-2; however, sophorose did not undergo either hydrolysis or a peeling reaction. The disaccharide 2-*O*-β-D-glucopyranosyl-D-mannose, (11) was clearly observed in the HPAEC and NMR results. Thereafter, the product was successfully isolated and its structure fully elucidated by NMR and HPAEC.

The results of adding sophorolipids to spent fermentation media during the starvation period of sophorolipid fermentation point towards the presence of an enzyme, which is able to hydrolyse sophorolipids. HPAEC analysis after 24 h confirmed the presence of sophorose, isomaltose and glucose. The results were similar to those of the chemical hydrolysis when using the aqueous alkaline solution.

5. Synthesis of novel sophorolipids using the lipase-catalysed trans-esterification and using chemical glycosylation coupling reactions

5. Synthesis of novel sophorolipids

5.1 Enzyme-catalysed esterification reaction

The structural modification of natural sophorolipids facilitates the production of derivatives which have novel properties, including new biological activities and enhanced surface tension properties. In previous work, [91,93,168] short to medium chain fatty acids/fatty acid esters have been attached to the C-6′ and C-6″ position on the sophorose moiety via a specific enzyme-catalysed esterification reaction utilizing the Novozyme 435 lipase. The lipase can specifically re-acetylate the C-6′ and C-6″ positions on sophorose moiety. [69,197] Sugar ester synthesis utilizing the Novozyme 435 lipase is based on esterification reactions catalysed by reversing their hydrolase activity. Esterification is a reversible reaction, hence the reaction by-product (water), which is generated in the media should be removed to shift the reaction equilibrium away from hydrolysis to obtain a maximum yield of the esterified sugar. [88]

5.2 Introduction to glycosylation

In 1901 Koenigs and Knorr [198] developed the chemical glycosylation reaction by reacting glycosyl halides as donors with normal acceptors (alcohol) in the presence of silver salts as catalytic activators (Ag_2CO_3 or Ag_2O) (Scheme 22). These silver salts were used as catalysts (mild bases) for the purpose to scavenge the hydrogen halide side product, it was not clear until the early 1930s when it was realized that the catalytic activator plays an active role in facilitating the leaving group departure and therefore they are commonly used with *O*-glycosyl halides or *O*-glycosyl trichloroacetimidates. The activating agent is used in catalytic amount here is usually a Lewis acid. [199] Some activators are soluble or insoluble in reaction solvents, which make a difference in whether the reaction system is homogenous or heterogeneous. Some widely used activators in *O*-glycosylation reaction are TMSOTf, $BF_3.OEt_2$, and NBS. [151,200-202]

The use of acid scavengers during the glycosylation reaction is important and necessary, especially when there is a risk of acid accumulation as the reaction progresses because the glycosidic bond is susceptible to acidic condition and might cleave/hydrolyse during the synthesis. Some of commonly used acid scavengers in glycosylation reactions include molecular sieves, tetramethylurea [151] and 2,6-tert-butyl-4-methylpyridine (TBMP). [203]

Scheme 22
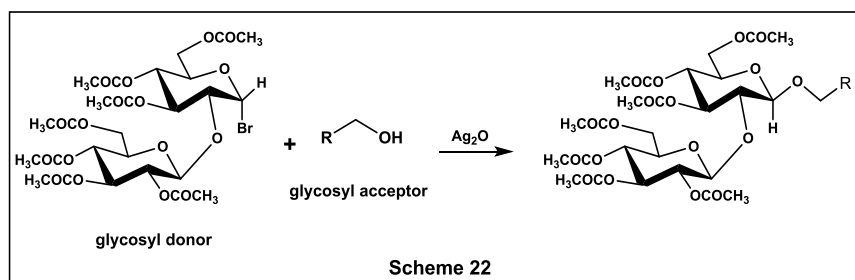
Glycosides are considered as valuable compounds in biological systems, as a result, there is a huge amount of literature focused on their synthesis. *O*-glycosides are synthesised via the activation of a glycosyl donor to assist in the formation of an oxocarbenium ion by assisted displacement of the anomeric leaving group. Various leaving groups have been developed and used in *O*-glycoside formation, consisting of halides, orthoesters, thioethers, carbonates, trichloroimidates, sulfones, phosphates and trichoroacetimidates. [204,205] Upon activation of the glycosyl donor, a glycosyl acceptor hydroxy group adds to the electrophilic oxocarbenium ion to form the desired glycosidic bond. In order to form the required glycosidic bond with a desirable yield, all reactive nucleophilic groups (-OH) must be selectively protected on the glycosyl donor. Formation of the *O*-glycosidic bond may occur from either of the two faces of the oxocarbenium ion, resulting in two different anomers of the same product. In 1968, Koeppen [205] described the condensation of the tetra-*O*-acetyl-α-D-glucopyranosyl bromide with 1,3,4,6-tetra-*O*-acetyl-α-D-glucopyranose in the presence of mercuric bromide / mercuric cyanide to obtain sophorose-octa-acetates (2-*O*-β-D-glucopyranosyl-D-glucose) and the product was isolated in low yield approximately 28% according to the method used.

135

Later on in 1980, Takeo demonstrated the synthesis of the benzyl α and β-sophorosides (benzyl-2-*O*-β-D-glucopyranosyl-α/β-D-glucopyranosides) via the condensation of the methyl 4,6-*O*-benzylidene-α-D-glucopyranosides with 2,3,4,6-tetra-*O*-acetyl-α-D-glucopyranosyl bromide using silver carbonate as an activator, this condensation reaction resulted in the formation of a β-(1-2-linked) disaccharide derivatives. [206,207]

There are some natural active glycosides and medical products, in which sophorose moiety is present. A number of natural products were isolated from semi-mangrove plants of the genus *Acanthus.* Examples of such products are the sophorose-containing glycosides; Ebracteatoside C, phenethyl glycoside and Zizybeoside I. These glycosides are utilized as anti-inflammatory and anti-hepatitis agents in traditional Chinese medicine. These were first isolated from *A. ebracteatus* [183] and *A. ilicifolius* [208] from Thailand and China in 2001. These natural products were chemically synthesised in 2012 by Hoffmann *et al.*, [183] starting from the standard sophorolipids as a route to obtain sophorose as disaccharide and the synthesis involved converting the natural sophorolipids to the 2″,3′,3″,4′,4″,6′,6″-hepta-*O*-acetyl-α-D-sophoryl bromide through a series of chemical reactions. The later was reacted with benzyl alcohol or phenyl ethanol in the presence of silver carbonate and peracetylated glycosides were deprotected using sodium methoxide in methanol to furnish the Zizybeoside I and phenethyl glycoside.
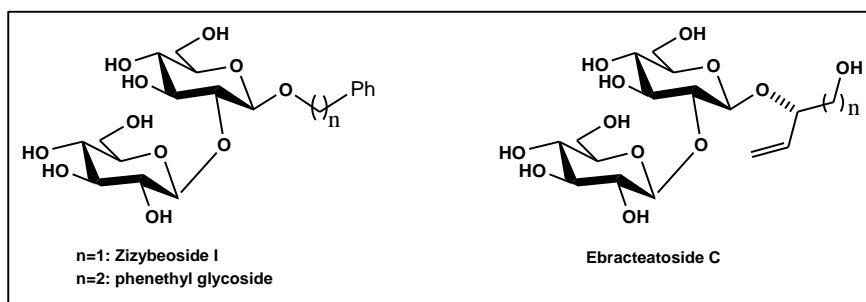
Figure 5-1: Sophorose-containing natural products

5.3 Synthesis and analysis of novel sophorolipids

This section discusses the analysis and structural characterization of a range of novel sophorolipids, which were synthesised using the enzyme-catalysed trans-esterification reaction starting from the methyl ester sophorolipid as a substrate either with or without an acetylation reagent such as, vinyl acetate or vinyl butyrate.

5.3.1 Structural analysis of the methyl ester, (4) and ethyl ester, (5) sophorolipids using NMR spectroscopy

Initially, the sophorolipid lactone, (2) was reacted with either sodium methoxide or sodium ethoxide in order to prepare the deacetylated and esterified acidic sophorolipids methyl ester (4) and ethyl ester, (5) both reactions proceeded smoothly and afforded the desired products in high yield. The products were soluble in anhydrous THF. The NMR spectra for the methyl ester sophorolipid, (4) were recorded at 500MHz. The sample was dissolved directly in CD$_3$OD (600μl), whereas the spectra for the ethyl ester sophorolipid, (5) was recorded using DMSO-d$_6$ as a solvent.

5.3.1.1 Analysis of NMR-Spectra of the methyl ester derivative SL-Me, (4)
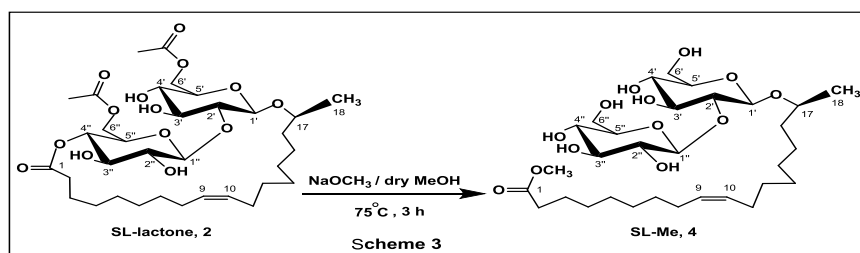
The NMR spectra can be compared with the ^{1}H-NMR of the lactone sample in order to confirm that ring opening has occurred (esterification). From the SL-Me, (4) spectra (Figure 5-1), it is clear that the triplet peak at

137

(4.95-4.85 ppm, 1H) which was for the H-4" has shifted from its location in the lactone.

This confirms the lactone has ring opened and the formation of the methyl ester has occurred; the methyl ester peak is observed as a singlet at 3.65 ppm, 3H, the spectra are confirming the removal of the acetyl groups which are usually observed around 2.1 ppm and this is accompanied by the movement of the H-6' & H-6" protons upfield.

In addition to the proton NMR spectra, the DEPT-135 NMR spectra were also used to assign resonances for the carbons and they further confirmed the formation of the desired product. The spectra (Figure 5-2, (a): SL-Lactone and (b): SL-Me) show a downfield shift of about 2.0 ppm in the resonance positions of both the C-6' and C-6" compared to the corresponding diacetylated lactone sophorolipid (a). In addition to the presence of the methyl ester group $C(O)OCH_3$, which resonated at 51.4 ppm in the methyl ester spectrum.
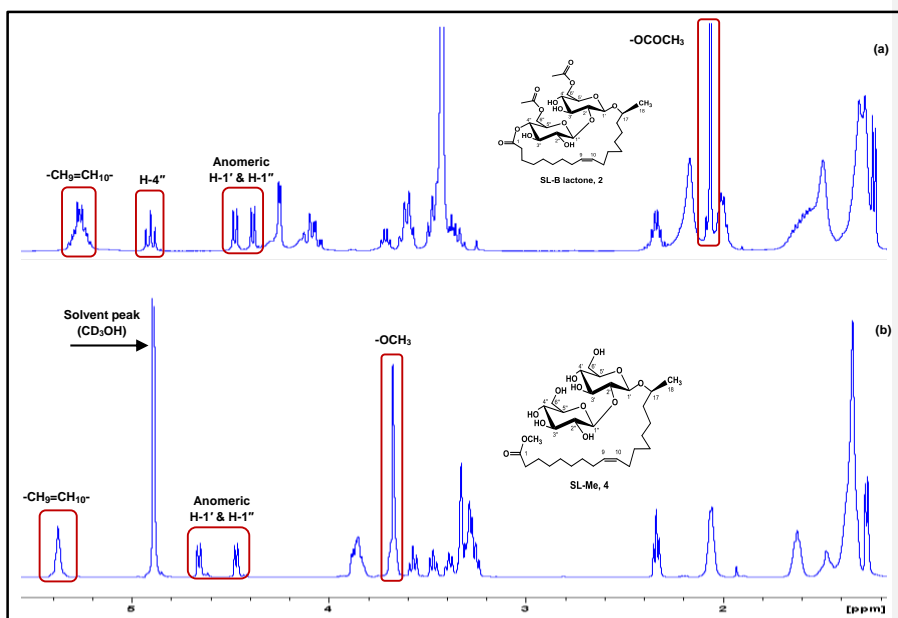
Figure 5-1: Comparison of the full ^{1}H-NMR-spectra for (a) lactone, (2) and (b) the methyl ester, (4) sophorolipids.
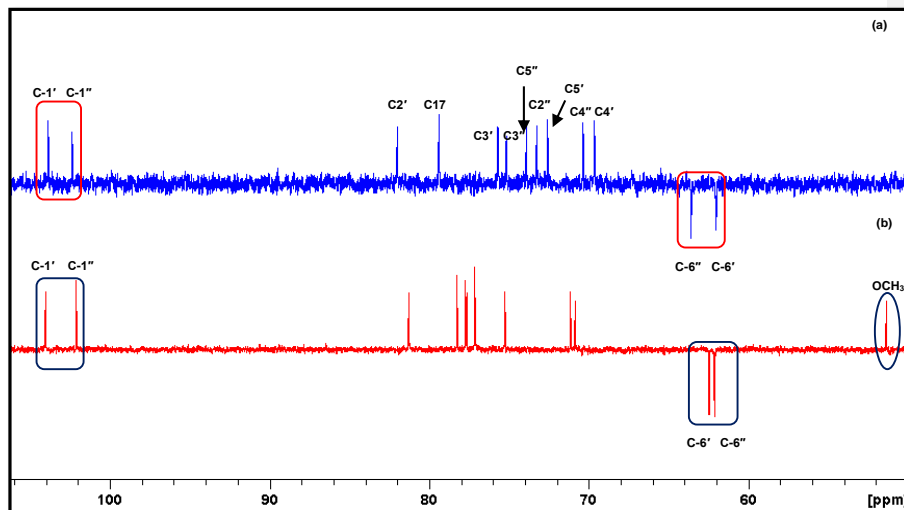
Figure 5-2: DEPT-135 NMR spectra for (a) lactone, (2) and (b) the methyl ester, (4) sophorolipids.

5.3.1.2 Analysis of NMR-spectra of the ethyl ester derivative, (5)
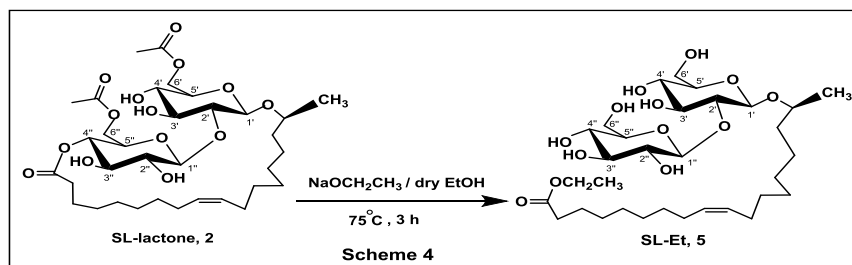
The ^{1}H-, and ^{13}C-NMR data for the ethyl ester derivative, (5) is fully explained in section 2.5.2. The ^{1}H-NMR spectrum of the ethyl ester SL-Et, (5) (Figure 5-3) is very similar to that of the methyl ester; the only significant difference is that the appearance of the quartet peak at (4.18-4.05 ppm, 2H), which is assigned to the methylene group of the ethyl ester C(O)OCH_2CH$_3$. The absence of the H-4" triplet peak at (5.12-5.0 ppm, 1H), confirms the opening of the lactone ring. Another indication, which confirmed the esterification, is the presence of the methyl group C(O)OCH$_2$CH_3 as a triplet

139

peak at (1.18-1.22 ppm, 3H) as well as the absence of acetyl groups usually observed around 2.1 ppm in the lactone sophorolipid.
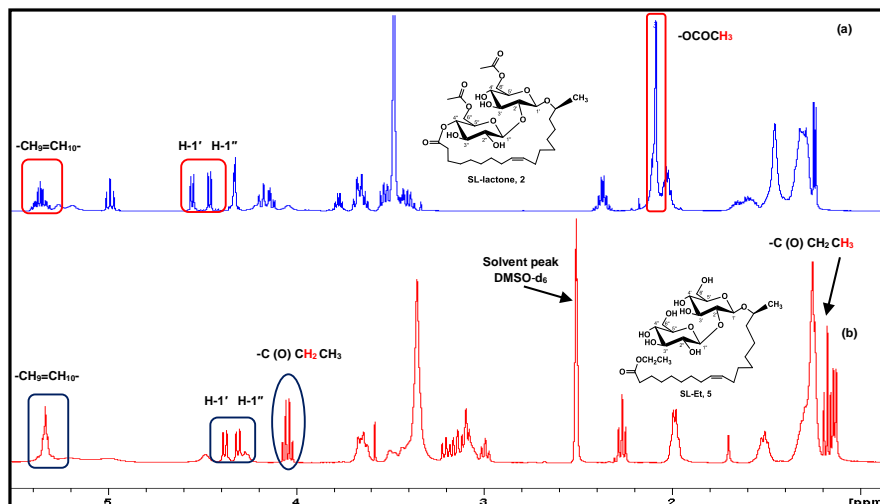
Figure 5-3: Comparison of the ^{1}H-NMR-spectra for (a) lactone, (2) and (b) the ethyl ester (5) sophorolipids.

5.3.1.3 Analysis of NMR-Spectra of the 1′,6″-sophorolactone, (6), 1′,6"-sophorolactone-6′-acetate, (7) and methyl ester-6′,6″-sophorose dibutyrate, (8) derivatives
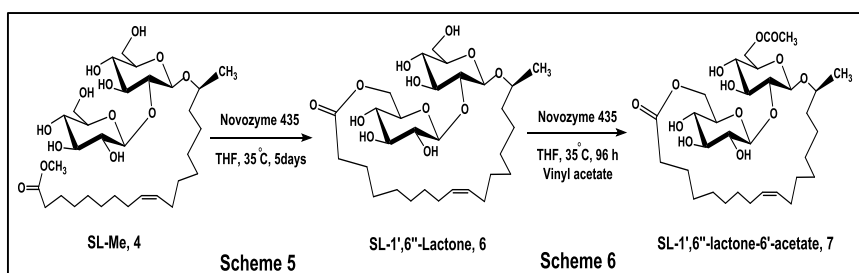
The next molecule that was prepared as an intermediate in the trans-esterification reactions was the 1,6-cyclic lactones. The methyl ester was subjected to Lipase Novozyme 435 catalysed acylation in dry tetrahydrofuran (THF) to produce either the 1′,6″-sophorolactone in the absence of an acylating agent or, in the presence of vinyl acetate, to produce the monoacetylated 1′,6″-sophorolactone-6′-acetatem derivatives (6).

The ^{1}H- & ^{13}C-NMR data for sophorolipid derivative 1′,6″-lactone, (6), 1′,6″-sophorolactone-6′-acetate,(7) and the methyl ester-6′,6″-sophorose dibutyrate, (8) are explained in sections 2.6.1-2.6.3. The esterification reaction was highly regioselective, and exclusive acylation of the hydroxyl groups on C-6' and C-6" took place. In the 1′,6″-sophorolactone, unlike the natural sophorolipids, the fatty acid carboxyl carbon is linked to the C-6″ hydroxyl, not the C-4″ hydroxyl. The subsequent acylation of this sophorolactone catalysed by Novozyme 435 led to the formation of the C-6′ monoacetyl derivative *i.e.*, esterification at the primary hydroxy. Comparison of the ^{13}C-NMR assignment and the DEPT-135 spectra for both 1′,6"-sophorolactone and the methyl ester sophorolipids (Figure 5-4) confirm the transformation was successful. The significant difference, which is noted from the sophorolactone spectrum (b), is the resonances of the C-6′ and C-6″ at (61.5 and 63.9 ppm) respectively, *i.e.*, they are shifted downfield shift 2.0 ppm compared to the C-6″ in the corresponding methyl ester (a, spectrum). This showed clear evidence for the formation of the 1′,6″-lactone ring. Another difference is the disappearance of the methyl ester at (50.8 ppm) in the sophorolactone spectrum.
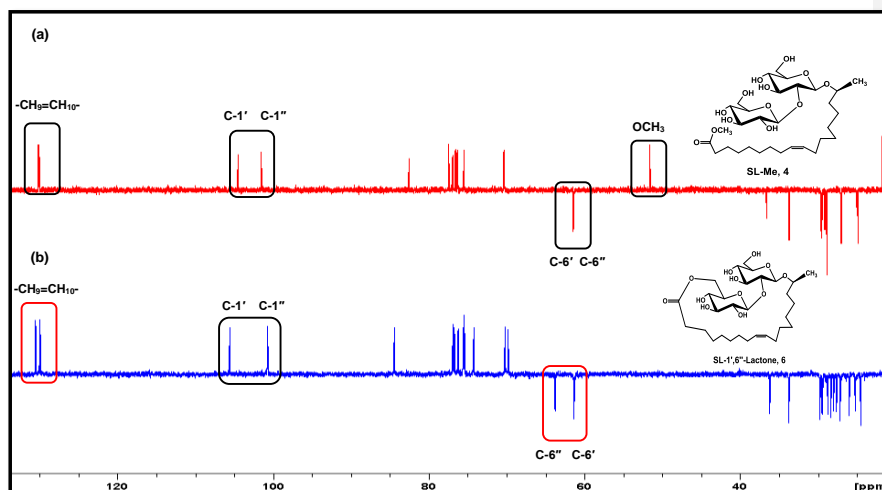
Figure 5-4: Comparison of the DEPT-135 Spectra for (a) methyl ester in CD$_3$OD solvent, (4) and (b) 1′,6″-sophorolactone, (6) in CDCl$_3$ solvent.

Confirmation of the structure of the 1′,6″-sophorolactone-6′-acetate, (7) derivative was determined using ^{13}C-NMR assignments (Figure 5-5). This derivative was synthesised via the lipase-catalysed esterification of the 1′,6"-sophorolactone using Novozyme 435 and employing vinyl acetate as an acylating agent. The ^{13}C-NMR-spectrum showed the presence of an additional carbonyl group resonating at 171.8 ppm, which was assigned to the acetate group on position C-6' on the sophorose moiety. The appearance of this peak confirms the acetylation on the C-6' position; this peak was absent in the 1′,6"-sophorolactone spectrum. In addition to the presence of the lactone carbonyl signal resonated at (173.2 ppm).
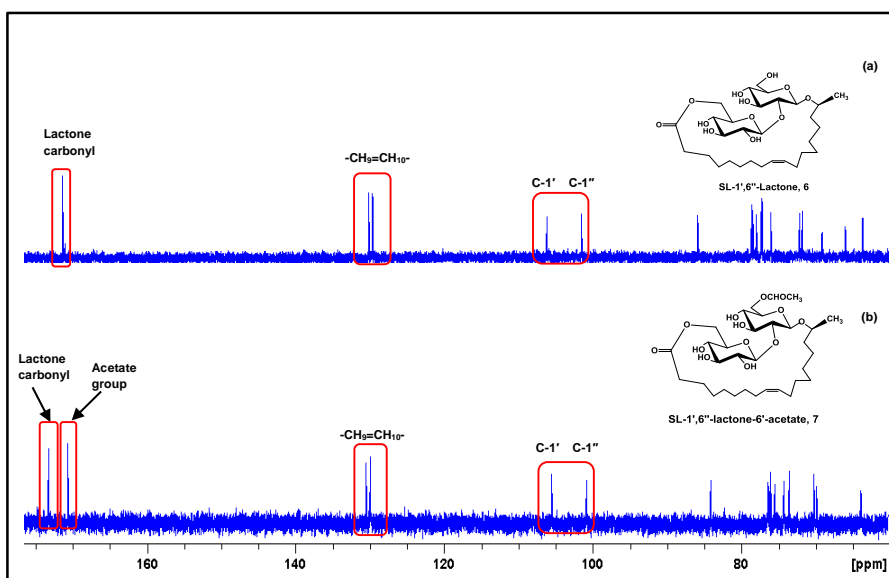
Figure 5-5: Comparison of the ^{13}C-NMR spectra for (a) 1′,6″-sophorolactone, (6) and (b) 1′,6"-sophorolactone-6'-acetate, (7).

Furthermore, the DEPT-135 spectra (Figure 5-6) provides clear evidence that acetylation has occurred at C-6' of the sophorose: The C-6' signal (64.2 ppm) has shifted about 2-3 ppm downfield in comparison with the position of both C6s in the corresponding 1′,6"-sophorolactone (61.5 and 63.9 ppm). The NMR data for the sophorolipid derivatives are consistent with the data reported for these derivatives by Bisht *et al*. [91-93] and this confirms the correct chemical synthesis of these derivatives.
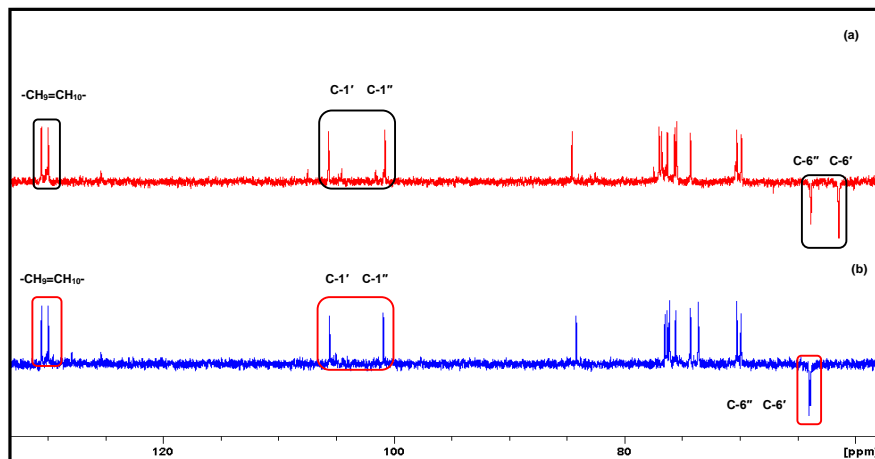
Figure 5-6: Comparison of the DEPT-135 spectral region for (a) 1,6″-sophorolactone, (6) and (b) 1′,6″-sophorolactone-6'-acetate, (7).
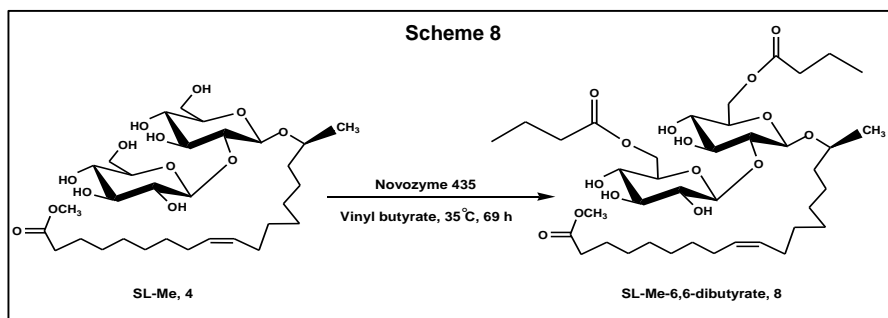
Finally, the analysis of the structure of the methyl ester of the 6′,6″-sophorose dibutyrate, (8) was also investigated using ^{13}C-NMR assignments. This derivative was synthesised through the lipase-catalysed esterification of the methyl ester using Novozyme 435 and employing vinyl butyrate as the acylating agent. Again, the esterification reaction was highly regioselective, and exclusive acylation of the hydroxyl groups on C-6' and C-6" took place. Furthermore, the DEPT-135 spectra (Figure 5-7) shows clear evidence that the acetylation occurred on both C-6 positions of the sophorose moiety: The C-6s signal have shifted about 2.5 ppm downfield in comparison with their positions in the corresponding methyl ester (61.64 and 62.13 ppm).
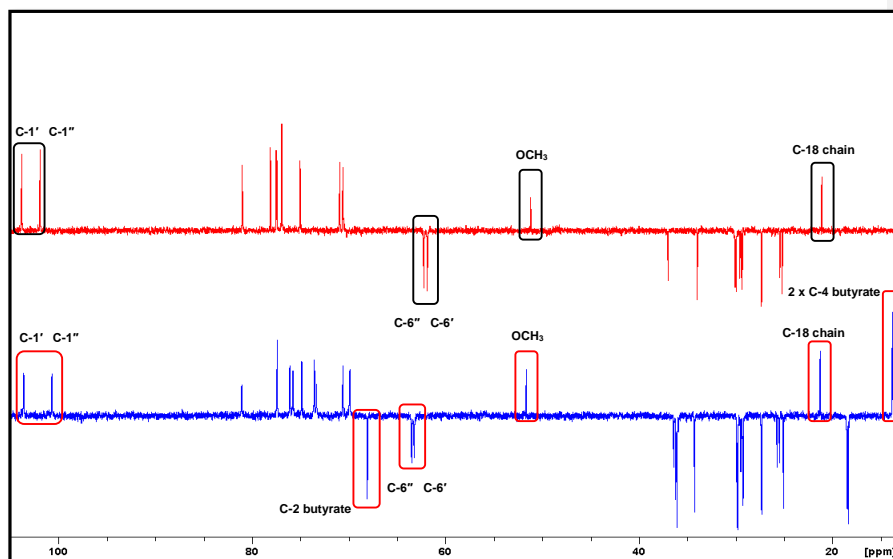
Figure 5-7: Comparison of the DEPT-135 spectral region for (a) methyl ester, (4) and (b) methyl ester-6′,6"-sophorose dibutyrate, (8).

The HMBC–spectrum for methyl ester of the 6′,6″-sophorose dibutyrate, (8) (Figure 5-8) shows long-range coupling and the correlation between the protons H-6$_S$ (4.35-4.40 ppm) with the methylene group -CH$_2$- (2.24 ppm) close to the carbonyl in the vinyl butyrate (174.08-174.36 ppm). In addition, the two new carbonyl groups, which resonate at 174.08-174.36 ppm show a long-range coupling to the sophorose C6s-H-2 butyrate.
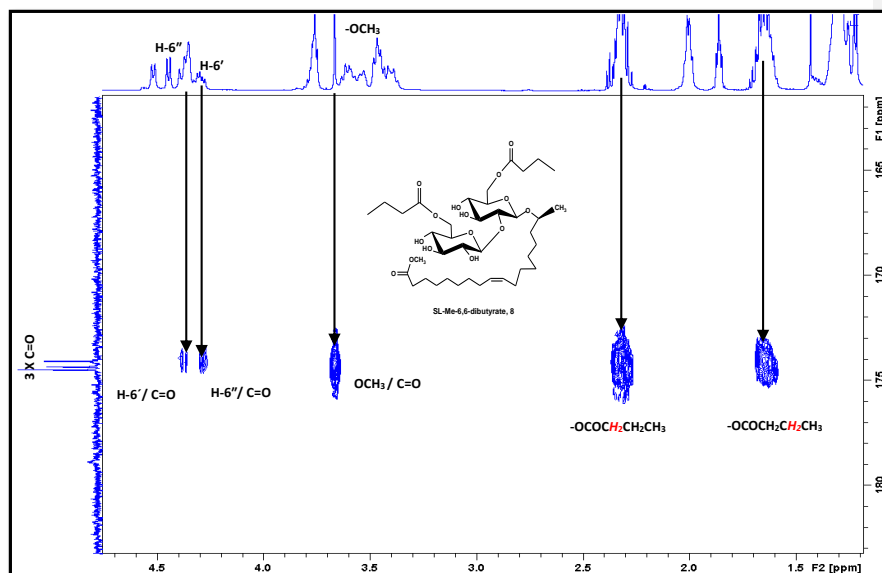
Figure 5-8: ^{1}H-^{13}C–HMBC-spectrum for methyl ester-6′,6″-dibutyrate, (8)

5.4 Analysis of FT-IR spectra of sophorolipid derivatives

The chemical structures of sophorolipid derivatives were also investigated using FT-IR. The procedure used was as discussed in the experimental section 2.3.2. The FT-IR spectra for the methyl ester, (4) and ethyl ester, (5) sophorolipids were compared with that for the lactone form (Figure 5-9, a, b & c). The stretching absorption of the hydroxyl groups was observed at 3324 cm^{-1} as a broad band, whereas the asymmetrical and symmetrical stretching of methylene (-CH$_2$-) occurred at 2924-2854 cm^{-1} as medium bands. The C=O stretching absorption band for the lactone (Figure 5-9, c) appeared as a strong band at 1744 cm^{-1} with a small shoulder assigned for the acetate groups on the C6s; this band was less intense and the small shoulder was absent for the methyl (Figure 5-9, b) and ethyl (Figure 5-9, a) ester forms confirming the deacetylation (alcoholysis). The 1651 cm^{-1} weak stretching absorption band for the alkene (-CH=CH-) in the lactone form was shifted to 1591&1573 cm^{-1} for the ethyl and methyl ester forms and this shift in the absorption minima was found to be indicative of lactone ring opening. It is also clear that the broad band at 1234 cm^{-1} for the acetyl (-C-O-) stretching in the lactone, is assigned for the acetate groups on the (C6' & C6") positions; this

145

band was weaker or had disappeared in the methyl and ethyl ester forms, confirming the de-acetylation on the C6 positions.
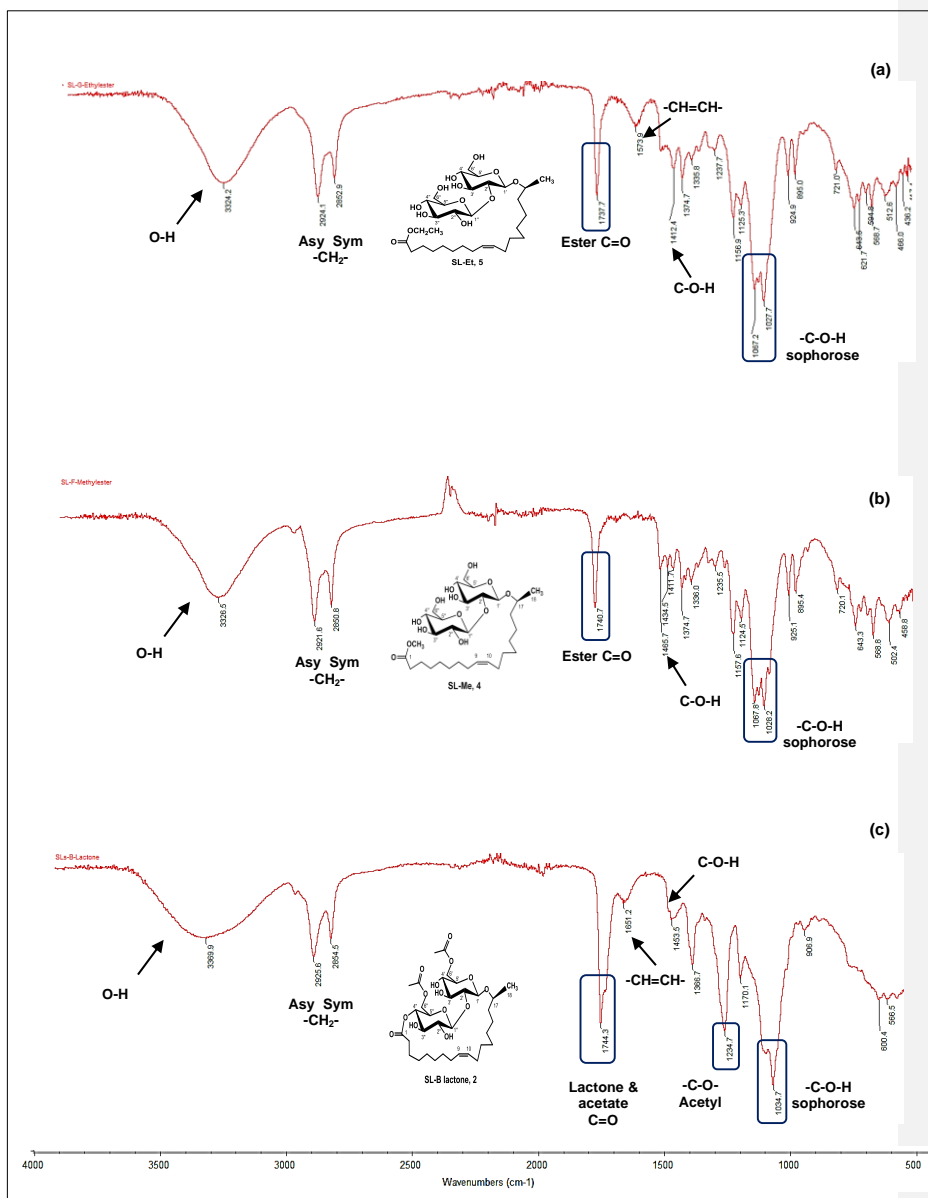
Figure 5-9: Comparison of FT-IR spectra for sophorolipids: (a) ethyl ester, (b) methyl ester and (c) lactone.

146

The FT-IR spectra for derivatives methyl ester of the 6′,6″-sophorose dibutyrate, (8), 1′,6″-sophorolactone-6′-acetate, (7) and 1′,6″-sophorolactone, (6) were also compared with that of the starting methyl ester derivative (Figure 5-10, a, b & c). The (C=O) absorption band for both methyl ester-6′,6″-sophorose dibutyrate and 1′,6″-sophorolactone-6′-acetate (spectra, a & b) appeared as a sharp band at 1736 & 1731 cm^{-1} with an obvious small shoulder, at 1722 & 1698 cm^{-1} for the dibutyrate and acetate groups on position C6′ & C6″, this band was less intense for the methyl ester sophorolipid at 1740 cm^{-1} and 1727 cm^{-1} for the 1′,6″-sophorolactone (spectrum, c) and the shoulder has disappeared confirming the absence of the acetate groups on the C6 positions, further evidence supporting the deacetylation is the absence of the broad band at 1238 cm^{-1} for the acetate (-C-O-) stretching, which is clearly seen in the 1′,6″-sophorolipid-6′-acetate spectrum, this band is for the acetate group (O)COCH$_3$ on the C6′ position and it confirms the esterification on this position and the formation of the 1′,6″-sophorolactone-6′-acetate.

It is clear (spectrum, a) for methyl ester-6′,6″-sophorose dibutyrate that the broad band at 1255 cm^{-1} for the (-C-O-) stretching in this derivative, is assigned for the dibutyrate groups on the (C6′ & C6″) positions; this band was weaker or had disappeared in the methyl ester form.

147
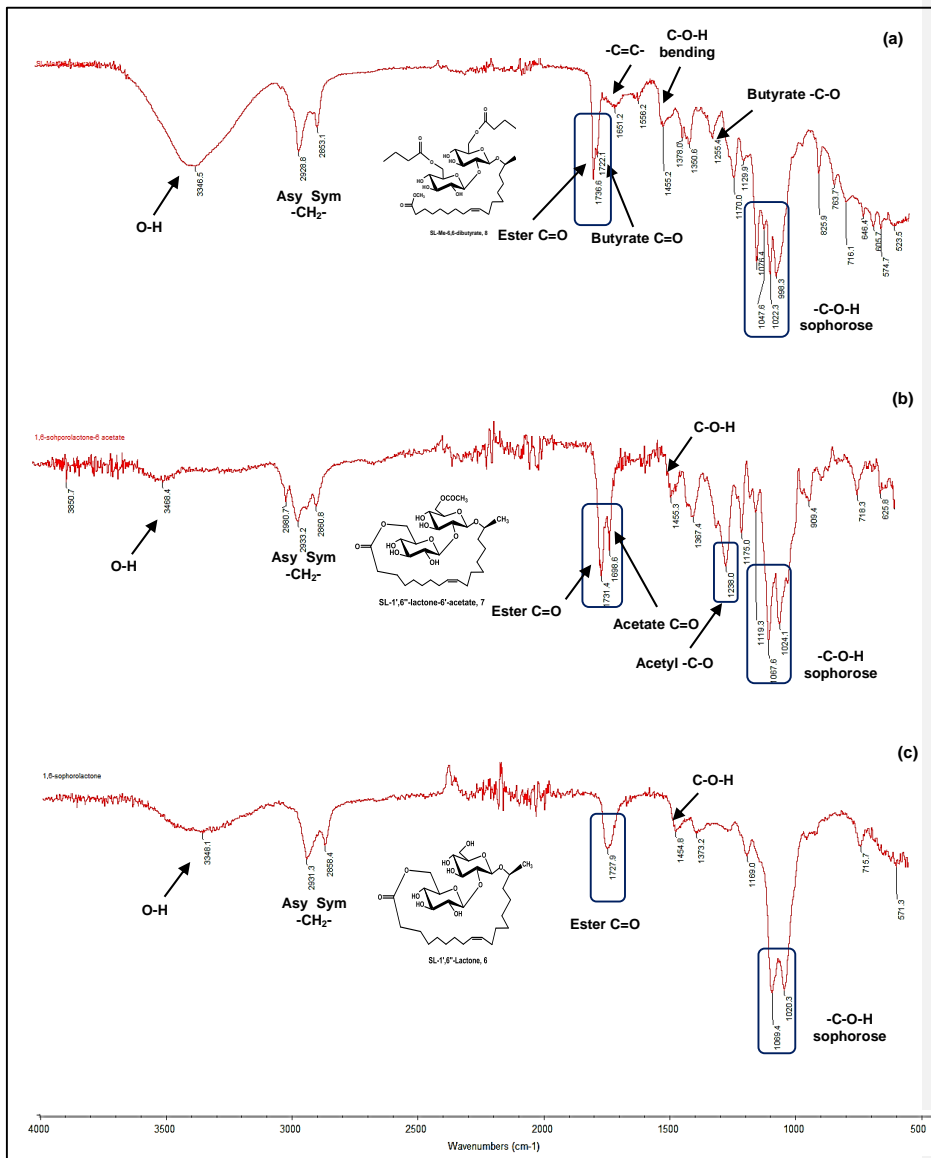
Figure 5-10: Comparison of FT-IR spectra for sophorolipids: (a) methyl ester-6',6"-sophorose dibutyrate, (b) 1′,6″-sophorolactone-6′-acetate, and (c) 1′,6″-sophorolactone.

148

5.5 NMR spectral analysis of novel sophorolipids

This section focuses on the NMR, FT-IR and HPLC-MS analysis of novel sophorolipids, which were synthesised starting from sophorose as a substrate via the chemical synthesis pathway utilizing the glycosylation coupling reaction of Koenigs and Knorr. The coupling reaction is between the 2″,3′,3″,4′,4″,6′,6″-hepta-*O*-acetyl-α-D-sophoryl bromide (glycosyl donor) and using different fatty alcohols as the aglycon (glycosyl acceptors).

5.5.1 NMR analysis of 1′, 2″, 3′, 3″, 4′, 4″, 6′, 6″-octa-*O*-acetyl-β-D-sophorose, (12)
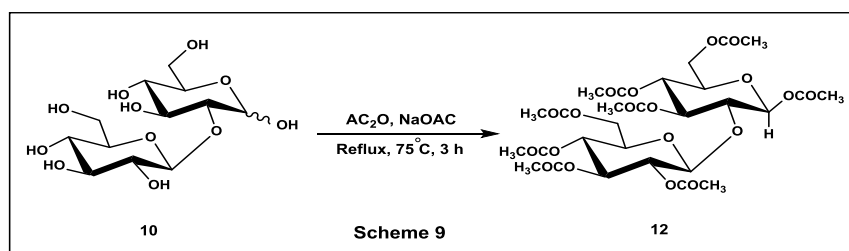
Scheme 9

The first step in the synthesis of novel sophorolipids required the peracetylation of sophorose and this was performed using a mixture of acetic anhydride and sodium acetate (scheme 9). The ^{1}H-NMR spectrum of the product β-D-sophorose octaacetate (Figure 5-11) confirmed the presence of the eight acetate groups and the synthesis of the β-anomer ($J_{1,2}$ = 8.08 Hz). [145,146] The reaction conditions afforded the product as a single β-anomer with a good yield (78.7%). All protons are labelled on the spectrum. The anomeric protons H-1′ resonated at 5.65 and H-1″ at 4.55 ppm respectively; there was no evidence for any contaminating α-anomer. The FT-IR data further confirmed the chemical structure of the product: the absence of the broad band of the hydroxyl groups at 3332-3377 cm^{-1} and the presence of a strong band observed at 1740 cm^{-1} which is assigned for the acetyl ester groups. The HPLC-MS (TIC) chromatogram showed a single peak, derived from the ammonium adduct [M+NH$_4$]$^+$, which had the mass ion m/z= 696.2345.

This is the expected mass for the product, which was calculated to be m/z= 678.2345, (Literature value, m/z=678.5892). [209]
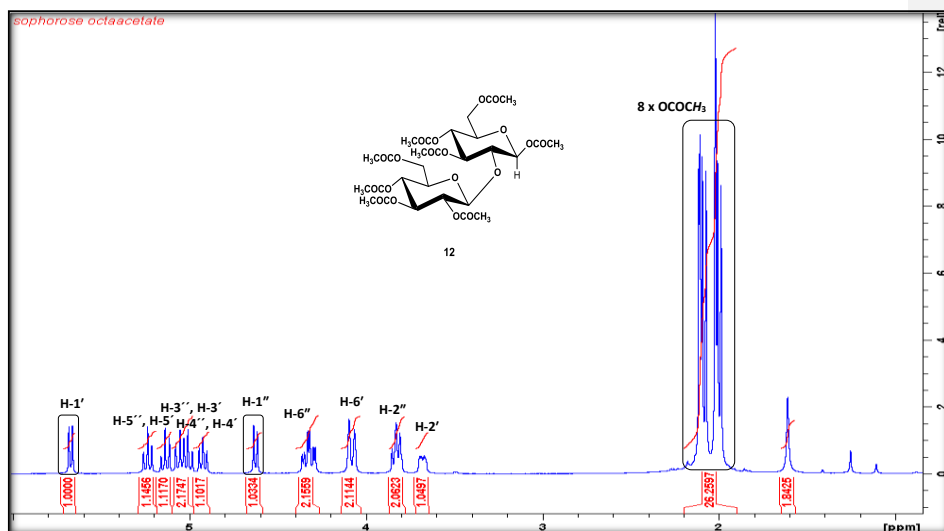
Figure 5-11: Full ^{1}H-NMR spectrum for β-D-sophorose octaacetate, (12)

5.5.2 NMR analysis of 2″,3′,3″,4′,4″,6′,6″-hepta-*O*-acetyl-α-D-sophoryl bromide, (13)
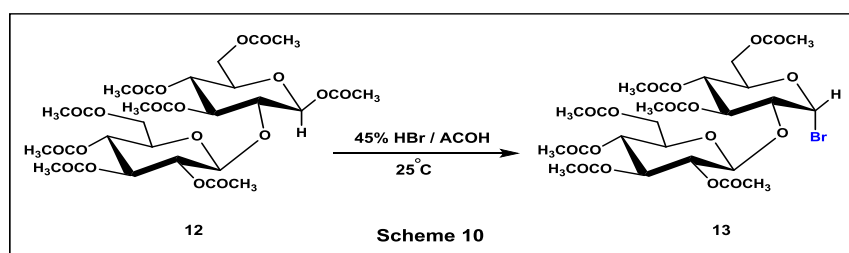
In activating the substrate for coupling, the β-D-sophorose octa-acetate, (12) was treated with HBr in acetic acid. The aim was to substitutes a bromine as a good leaving group (glycosyl donor) on the anomeric carbon C-1′, which could then be reacted with a fatty alcohol chain in a glycosylation coupling reaction.

150

The ^{1}H-NMR spectrum for hepta-*O*-acetyl-α-bromo-D-sophorose (Figure 5-12) is very different to that for the starting material. From the ^{1}H-NMR spectrum, it is clear that the bromination reaction has occurred on the reducing end: the anomeric proton (α-H-1′, $J_{1,2}$ = 4.0 Hz) peak has shifted from 5.65 ppm to 6.42 ppm in the hepta-*O*-acetyl-β-bromo-D-sophorose spectrum. This shift and the reduction in the coupling constant confirmed the substitution of bromine and the formation of the α- anomeric. [149,150] The seven acetate groups resonated at 1.9-2.3 ppm, which has an integration of 20.99 indicating the absence of the eighth acetate group.

The ^{13}C-NMR spectrum for hepta-*O*-acetyl-α-bromo-D-sophorose (Figure 5-13) also shows a downfield shift of 6 ppm in the position of the reducing sugars anomeric C-1', which resonates at 86 ppm compared to the anomeric C-1′ for the sophorose octaacetate that was found to resonate at 92 ppm. The NMR data obtained is consistent with the data reported by Hoffmann [183]. Using the reaction conditions employed, the product afforded mostly a single α-anomer having an 82% anomeric purity and a 77.2% yield. The FT-IR spectrum of the product is similar to that of the starting material, except the presence of the band for C-Br bending which appeared as a sharp small band at 551.7 cm^{-1}, this band was absent in the spectrum of the starting material. This band is consistent with the bromination of β-D-sophorose. [210]

The mass spectrum of the bromide provided a molecular ion as both a sodium adduct [M+Na]$^+$ at m/z= 721.0936 and as an ammonium adduct [M+NH$_4$]$^+$ at m/z= 716.1385. The mass for the neutral compound was determined to be 698.1045 m/z, whereas the theoretical mass was calculated to be 698.1058 m/z with a mass difference 1.3 ppm. This was the correct mass, which matches the expected chemical formula ($C_{26}H_{35}O_{17}Br$) for the product.
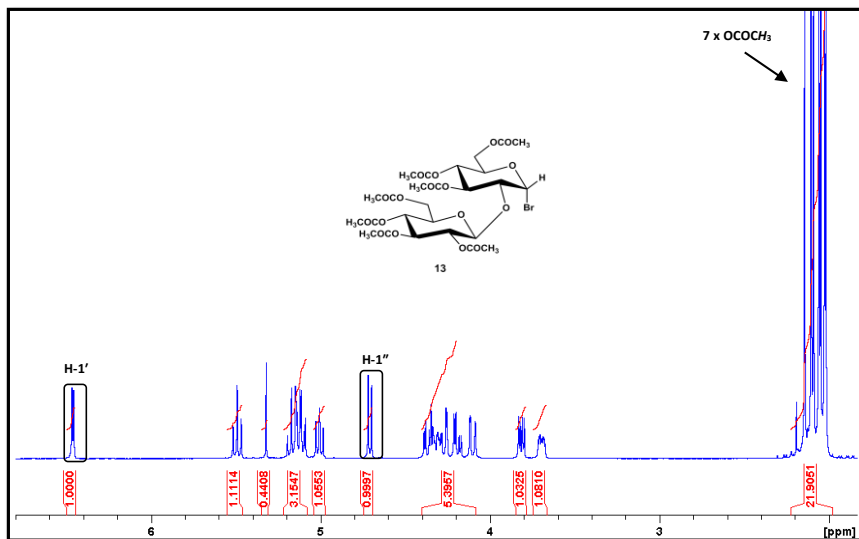
Figure 5-12: Full ^{1}H-NMR spectrum of 2″,3′,3″,4′,4″,6′,6″-hepta-*O*-acetyl-α-D-sophoryl bromide, (13)
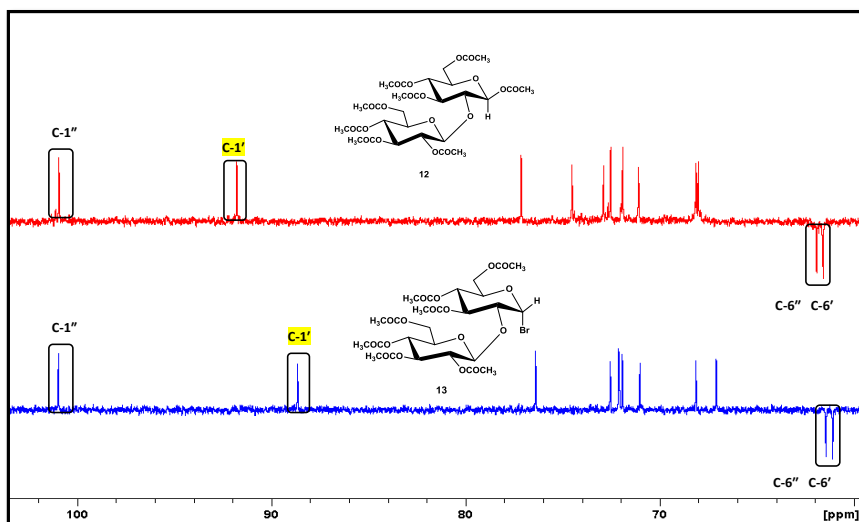
Figure 5-13: Comparison between the DEPT-135 spectra of β-D-sophorose octaacetate, (12) and 2″, 3′, 3″, 4′, 4″, 6′, 6″-hepta-*O*-acetyl-α-D-sophoryl bromide, (13)

5.5.3 NMR analysis of oleyl 2″, 3′, 3″, 4′, 4″, 6′, 6″-hepta-*O*-acetyl-β-D-sophoroside, (14)

Scheme 11
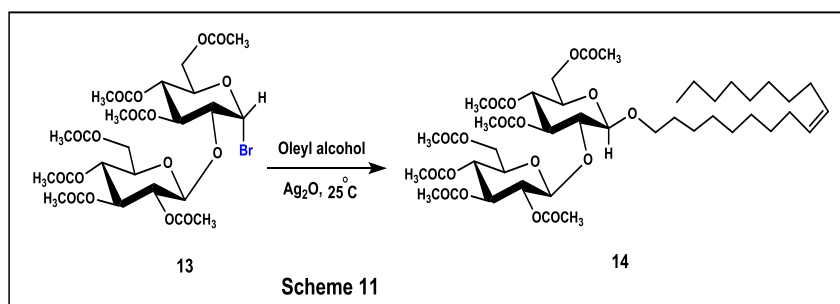
Attempt to synthesize sophorolipids following the chemical pathway was conducted successfully. The Koeings-Knorr reaction was followed to prepare a variety of *O*-glycosides. The heptaacetylated β-oleyl-D-sophoroside, (14) was prepared following the coupling of hepta-*O*-acetyl-β-bromo-D-sophorose, (13) as the glycosyl donor and with the fatty alcohol as a glycosyl acceptor; utilizing silver oxide as an activator (promoter) to form the new glycoside.

The stereochemistry of the coupling generates a 1,2-trans product as a consequence of neighbouring group participation. After recrystallization from methanol, the ^{1}H-NMR spectrum (Figure 5-14) shows that the anomeric proton H-1′ ($J_{1,2}$ = 7.7 Hz) has shifted downfield to resonate at 4.85 ppm and it is close to the anomeric proton H-1″ ($J_{1,2}$ = 7.9 Hz) at 4.90 ppm. The alkene protons H-C=C-H resonate at 5.42 ppm and the integration confirms 2 protons. The methylene group immediately adjacent to the newly formed glycosidic linkage resonates at 3.75 ppm and the seven strong acetyl signals resonate at 1.95-2.2 ppm. The area below 1.8 ppm contains resonances that can be assigned for the octadecene lipid methylene protons and the C-18 methyl group. The DEPT-135 NMR (Figure 5-15) show that both the anomeric C-1′ & C-1″ resonate between 102-103 ppm and it is clear that the anomeric C-1′ has a downfield shift of about 16 ppm compared to its position in the bromide, which resonated at 86 ppm. This is clear evidence that the coupling has occurred. In addition, the lipid metheylene-CH_2- attached to the glycosidic oxygen has also shifted and resonates at 69 ppm as shown in the DEPT-135 spectrum. The product yield was 64.4 %.

153
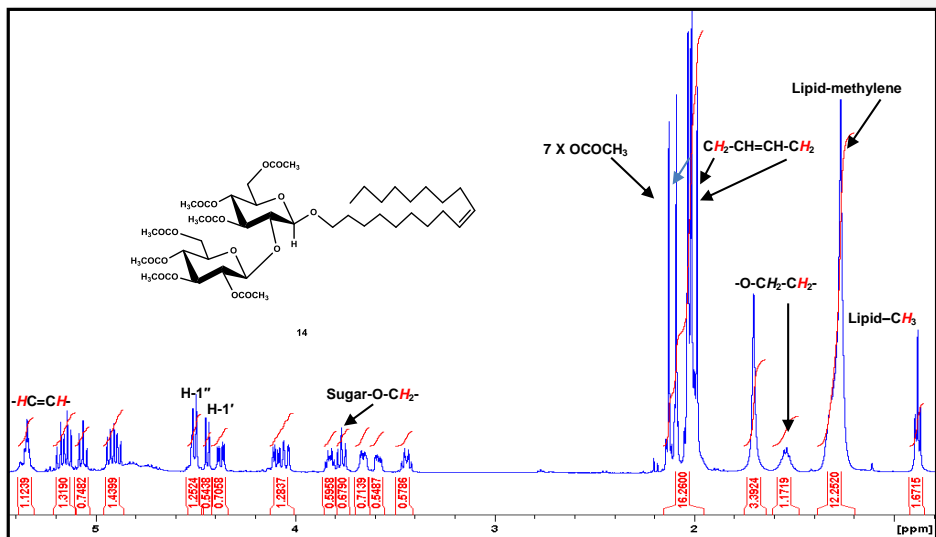
Figure 5-14: Full ¹H-NMR spectrum of oleyl 2″, 3′, 3″, 4′, 4″, 6′, 6″-hepta-*O*-acetyl-β-D-sophoroside, (14)
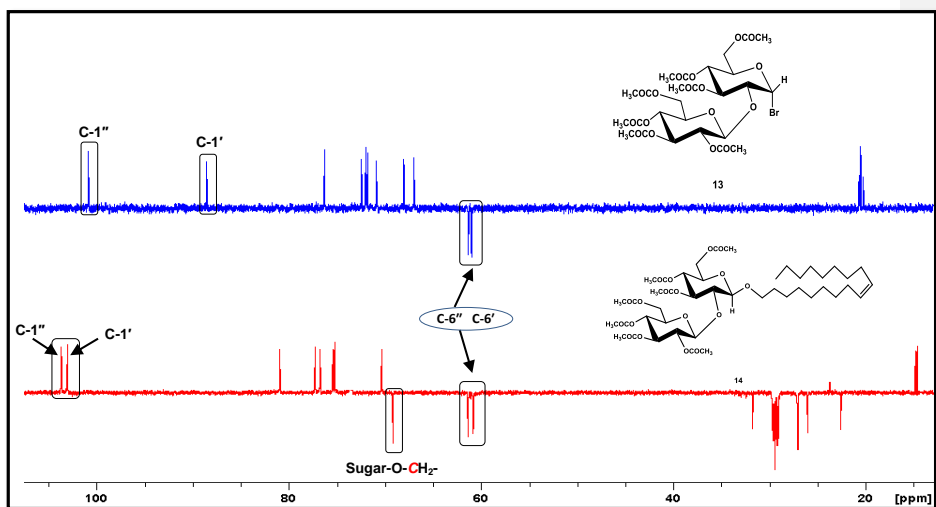
Figure 5-15: Comparison between the DEPT-135 NMR spectra of hepta-*O*-acetyl-α-D-sophoryl bromide, (13) and oleyl 2″, 3′, 3″, 4′, 4″, 6′, 6″-hepta-*O*-acetyl-β-D-sophoroside, (14)

The FT-IR spectrum of the product confirmed the presence of the fatty alcohol. The asymmetrical and symmetrical stretching of methylene (-CH2-) for the oleyl alcohol chain occurred at 2924-2854 cm-1 as strong bands,

154

another significant evidence for successful coupling is that the C-Br band was absent from the oleyl 2″, 3′, 3″, 4′, 4″, 6′, 6″-hepta-O-acetyl-β-D-sophoroside. The accurate mass of the product was determined using a direct injection method. The mass spectrum obtained shows the expected molecular ion as its ammonium adducts [M + NH$_4$] $^+$ ion at 904.4894 m/z. The mass of the neutral compound was determined to be 886.4553 m/z and the theoretical mass of the neutral compound was calculated to be 886.4562 m/z. The mass difference was = 1.07 ppm. This was the correct mass, which matches the expected formula (C$_{44}$H$_{70}$O$_{18}$) for the compound. To our best knowledge, this is the first time the synthesis of this molecule has been reported and no literature data is available.

5.5.4 NMR analysis of oleyl-β-D-sophoroside, (15)

Scheme 12
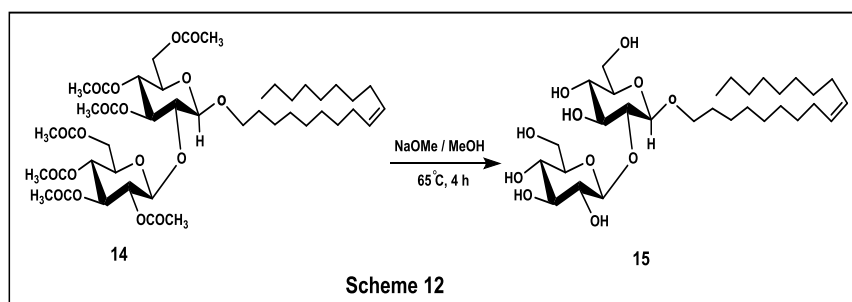
In order to isolate the parent sophorolipid, the product hepta-*O*-acetyl-β-oleyl-D-sophorose (14) was subjected to de-esterification by treating with sodium methoxide in methanol. The aim was to hydrolyse the acetate groups and to prepare the free sophorolipid. Comparing the ^{1}H-NMR spectra (Figure 5-16) of the starting material oleyl 2″, 3′, 3″, 4′, 4″, 6′, 6″-hepta-O-acetyl-β-D-sophoroside and that of the deacetylated product oleyl-β-D-sophoroside confirms that deacetylation has taken place and the formation of the product as a single β-anomer. The spectra are similar, except within the area 1.95-2.22 ppm where the seven acetyl signals were originally observed. It can be clearly seen that these signals were absent in the oleyl-β-D-sophoroside spectrum.
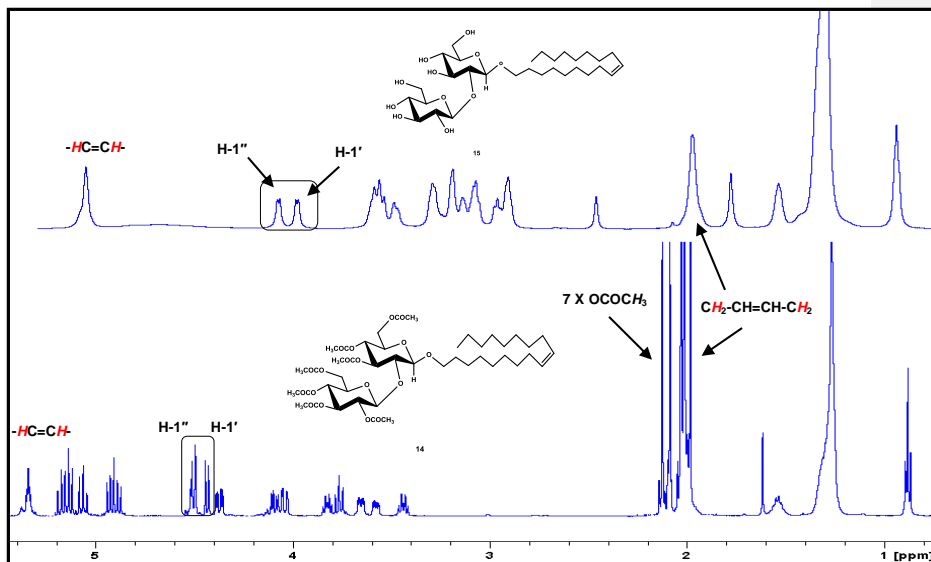
Figure 5-16: Comparison between ¹H-NMR spectra for oleyl-β-D-sophoroside (15) oleyl 2″, 3′, 3″, 4′, 4″, 6′, 6″-hepta-*O*-acetyl-β-D-sophoroside, (14)

The ¹³C-NMR spectra (figure 5-17) further confirms the success of the alcoholysis reaction as the acetate groups, which previously resonated at 170-174.5 ppm have disappeared from the carbon spectrum of the β-D-oleyl sophorose. The product yield was 70.10 %.
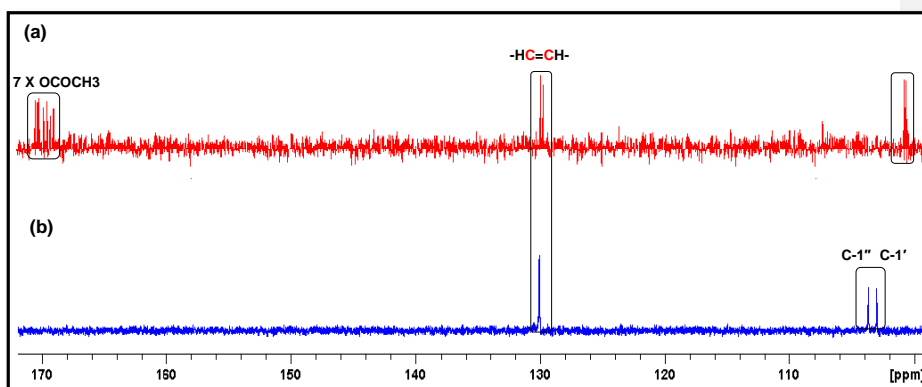
Figure 5-17: Comparison between ¹³C-NMR spectra for (a) oleyl 2″, 3′, 3″, 4′, 4″, 6′, 6″-hepta-*O*-acetyl-β-D-sophoroside and (b) (14) oleyl-β-D-sophoroside (15)

A comparison of FT-IR spectra (figure 5-18) for oleyl 2″, 3′, 3″, 4′, 4″, 6′, 6″-hepta-O-acetyl-β-D-sophoroside, (14) and oleyl-β-D-sophoroside,(15) suggests that the product was produced during the alcoholysis, the spectrum (Figure 5-18, b) clearly shows a broad band around 3433-3377 cm^{-1} corresponding to the O-H stretching for the hydroxyl O-H groups after the de-esterification as well as the disappearance of the C=O stretching band at 1740 cm^{-1}, which is assigned for the acetyl groups (Figure 5-18, a).
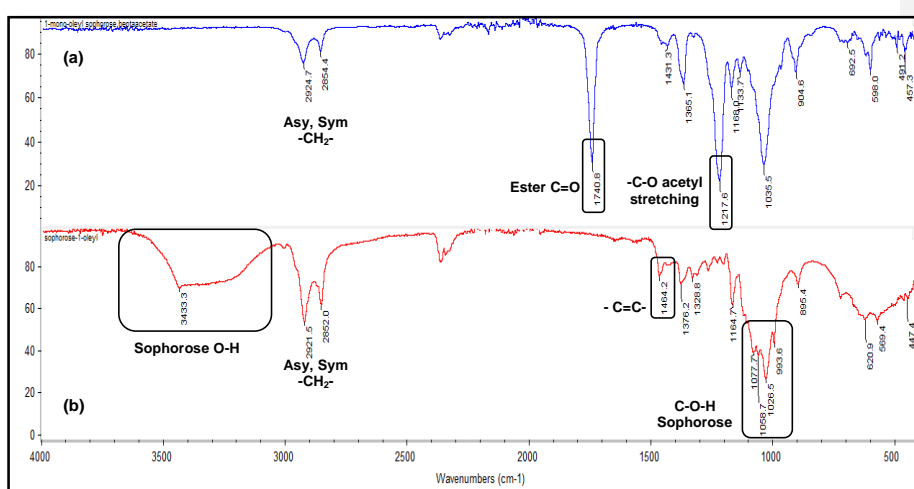
Figure (5-18): Comparison of FT-IR spectra for (a) oleyl 2″, 3′, 3″, 4′, 4″, 6′, 6″-hepta-O-acetyl-β-D-sophoroside, (14) and (b) oleyl-β-D-sophoroside, (15).

The molecular weight of oleyl-β-D-sophoroside was determined using the direct injection method. The mass spectrum contained the expected molecular ion as the ammonium adduct [M+NH$_4$]$^+$ at m/z = 610.4153. The mass of the neutral compound was determined to be 592.3816 and the theoretical mass of the neutral compound was calculated to be 592.3823. The mass difference was 1.08 ppm. This was the correct mass, which matches the expected formula (C$_{30}$H$_{56}$O$_{11}$) for oleyl-β-D-sophoroside. To our best knowledge, this is the first time the synthesis of this product has been reported and no literature data is available.

5.5.5 NMR analysis of stearyl 2″, 3′, 3″, 4′, 4″, 6′, 6″-hepta-*O*-acetyl-β-D-sophoroside, (16)

Scheme 13
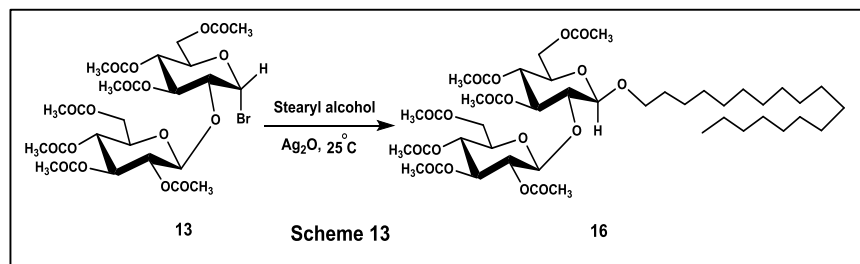
The product was prepared by coupling the hepta-*O*-acetyl-β-bromo-D-sophorose (13) with stearyl alcohol utilizing silver oxide as a promoter to form the new sophorolipid. After recrystallization from methanol, the ^{1}H-NMR spectrum (Figure 5-19) shows that the anomeric proton H-1′ ($J_{1,2}$= 7.9 Hz) has shifted downfield to resonate at 4.45 ppm and its close to the other anomeric proton H-1″ ($J_{1,2}$= 8.0 Hz) at 4.35 ppm. The methylene group immediately adjacent to the glycosidic linkage resonates at 3.65 ppm, the seven acetyl signals resonate between 1.95-2.2 ppm. Signals resonating in the area below 1.8 ppm are assigned to the lipid C-18 methylene protons and the methyl group.
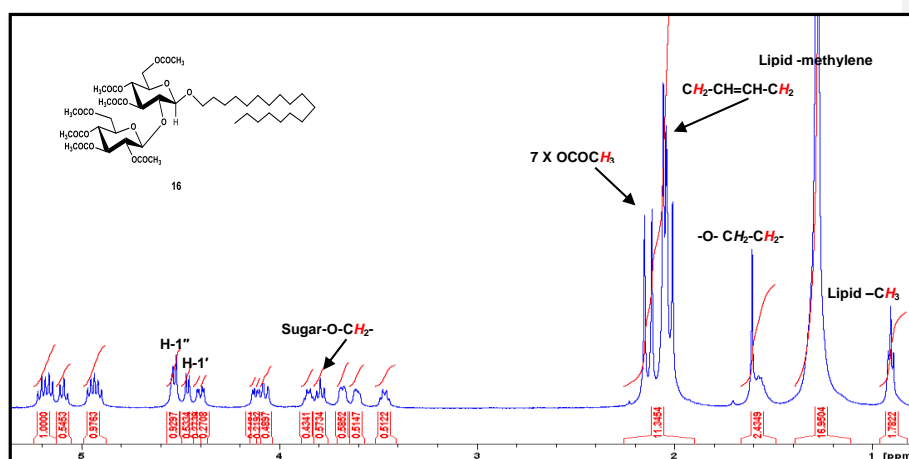
Figure 5-19: Full ^{1}H-NMR spectra for stearyl 2″, 3′, 3″, 4′, 4″, 6′, 6″-hepta-*O*-acetyl-β-D-sophoroside, (16).

The DEPT-135 NMR-spectra (Figure 5-19) show that both the anomeric C-1′ & C-1″ resonate between 100-101 ppm and it is clear that the anomeric C-1′ has shifted about 12 ppm compared to its position in the bromide, where it resonated at 87 ppm. In addition, the lipid metheylene-CH_2-attached to the glycosidic oxygen has also shifted and resonates at 64 ppm as indicated in the DEPT-135 spectrum. According to the reaction conditions used, the product has been generated as a mixture of anomers and the α/β-anomeric ratio is 36.5 / 63.5% and the overall yield is 76.5%. To our best knowledge, this is the first time the synthesis of this molecule has been reported.
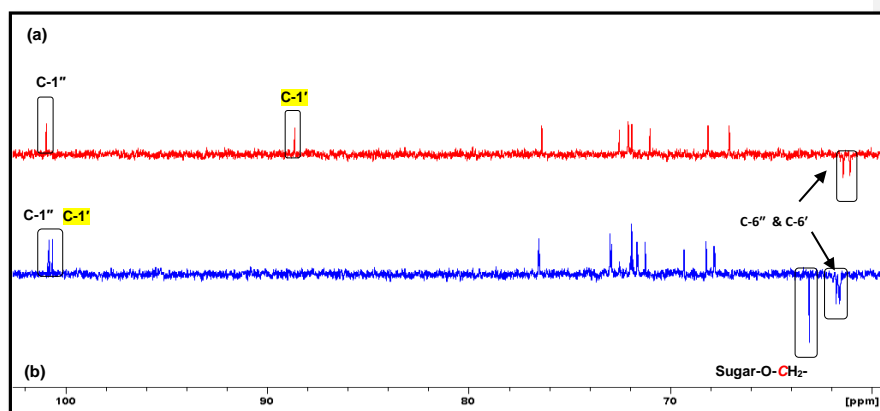
 Figure 5-19: Comparison between the DEPT-13 NMR spectra for (a) hepta-*O*-acetyl-α-D-sophoryl bromide and (b) stearyl 2″, 3′, 3″, 4′, 4″, 6′, 6″-hepta-*O*-acetyl-β-D-sophoroside, (16).

The FT-IR spectrum of the product was compared with that of the starting material. The spectrum is very similar to that observed for oleyl-hepta-*O*-acetyl-β-D-sophoroside spectrum; the C-Br absorption band was absent which confirms the coupling between the sophorose bromide and the stearyl alcohol. The molecular weight was also determined and the mass spectrum shows the expected molecular ion was observed as the ammonium adduct [M+NH4] $^{+}$ ion at m/z= 906.5047. The mass of the neutral compound was determined to be 888.4703 m/z and the theoretical mass of the neutral compound was calculated to be 888.4719 m/z. The mass difference was 1.71 ppm. This was the correct mass, which matches the expected formula ($C_{44}H_{72}O_{18}$) for the stearyl 2″,3′,3″,4′,4″,6′,6″-hepta-*O*-acetyl-β-D-sophoroside.

5.5.6 NMR analysis of 2″, 3′, 3″, 4′, 4″, 6′, 6″-hepta-*O*-acetyl-α/β-D-sophorose
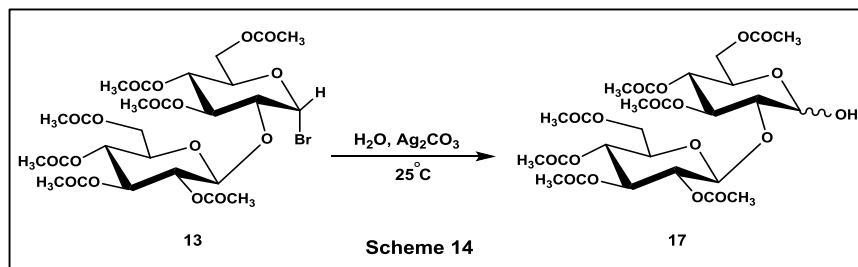
The product hepta-*O*-acetyl-α-bromo-D-sophorose was reacted with UPW to convert the bromide group on the anomeric C-1′ position to a hydroxyl group, which was required for further reaction with palmitoyl chloride to produce new sophorolipids. Again, the chemical structure of the product was characterized using 1-D and 2-D-NMR. The ^{1}H-NMR spectra (Figure 5-20) show that the anomeric H-1′ signal has shifted from 6.42 ppm in the hepta-*O*-acetyl-β-bromo-D-sophorose spectrum (Figure 5-20, a) to 5.37 ppm in the ^{1}H-NMR spectrum (Figure 5-20, b) of the product. This shift confirmed the substitution of OH group on the anomeric H-1′ position.
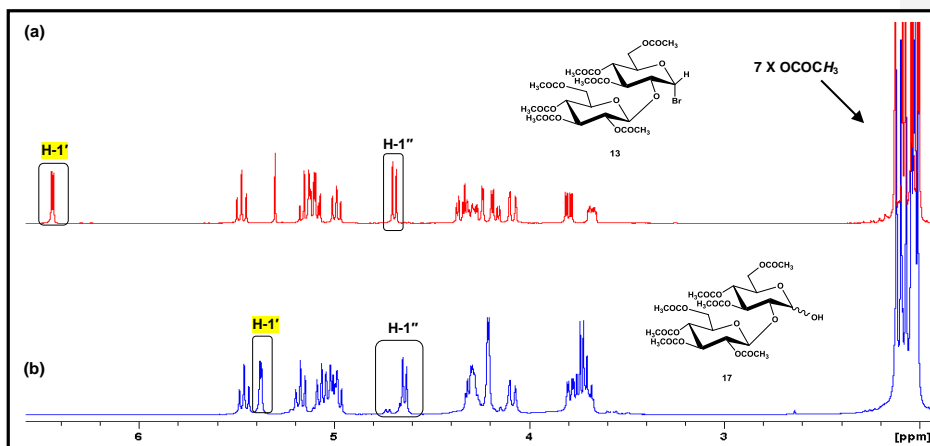
Figure 5-20: Comparison between ^{1}H-NMR spectra of hepta-*O*-acetyl-α-D-sophoryl bromide, (13) and hepta-*O*-acetyl-α/β-D-sophorose, (17)

Analysis of the ^{1}H-^{13}C-HSQC-NMR spectrum (Figure 5-21) confirmed the that the product contains mostly the α-anomer and only a very small amount of the β-anomer: the α-anomeric H-1′ resonates at 5.37 ppm ($J_{1,2}$ = 3.3 Hz) and a very small amount of the β-anomeric H-1′ resonates at 4.96 ppm, whereas the β-anomeric H-1″ resonates at 4.72 ($J_{1,2}$ = 7.06 Hz) and α-anomers H-1″ which is beta-linked resonates at 4.64 ($J_{1,2}$ = 7.9 Hz). The carbon spectrum also identified that there is around 95% of the alpha isomer. The β-signals are very small peaks which are visible in the ^{1}H-NMR spectra, but are not visible in the ^{13}C-NMR-spectrum. It should also be expected that mutarotation would provide both anomers in solution. The product yield is approximately 83.6 %.
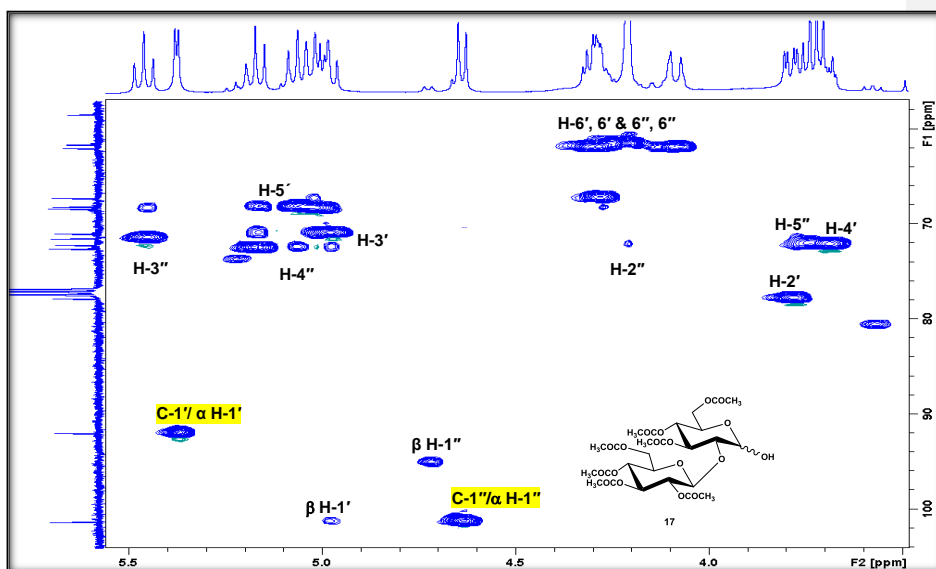
 Figure 5-21: ^{1}H-^{13}C-HSQC-NMR for **2″, 3′, 3″, 4′, 4″, 6′, 6″-hepta-*O*-acetyl-α/β-D-sophorose, (17)**

The FT-IR spectrum for hepta-*O*-acetyl-α/β-D-sophorose confirms the presence of a new stretching band for the hydroxy group O-H occurred at 3239.9 cm^{-1}, whereas this peak is absent in the starting material's spectrum indicating the addition of the OH group on the anomeric C-1′ position on the sophorose moiety.

The stretching absorption band for C=O appeared at 1742 cm^{-1}. Also, the C-Br band was absent from the product, which confirms the substitution of bromide with a hydroxyl group.

Finally, HPLC-MS was also used for the analysis of the hepta-O-acetyl-α/β-D-sophorose and the major peak in the HPLC chromatogram at (2.589-2.817min) is that for the desired compound. The total ion chromatogram for the main peak was for the sodium adduct of the product [M+Na] $^{+}$ ion at m/z = 659.1794. The mass of the neutral compound was determined to be m/z= 636.1885 and the theoretical mass of the neutral compound was calculated to be m/z = 636.1902 with the measured mass difference of 2.57 ppm. This was the correct mass for the compound 2″, 3′, 3″, 4′, 4″, 6′, 6″-hepta-O-acetyl-α/β-D-sophorose. To the best of our knowledge, this is the first time the synthesis of this compound has been reported.

5.5.7 NMR analysis of 2″, 3′, 3″, 4′, 4″, 6′, 6″-hepta-O-acetyl-1'-O-palmitoyl- β-D-sophoroside

Scheme 15
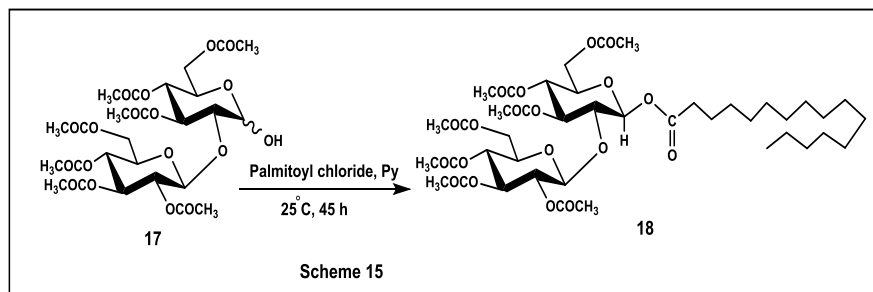
The 2″, 3′, 3″, 4′, 4″, 6′, 6″-hepta-O-acetyl-1'-O-palmitoyl-β-D-sophoroside was prepared following the reaction of the hepta-O-acetyl-α/β-D-sophorose with palmitoyl chloride in the presence of pyridine to form a new sophorose glycoside. The chemical structure of the product was also characterized using 1-D and 2-D-NMR.

162

The ^{1}H-NMR spectrum (Figure 5-22) shows that the anomeric H-1′ signal has shifted from 5.35 ppm in the starting material to 5.68 ppm in the new product: the shift confirmed the addition of the palmitoyl group on the anomeric C-1′ position.

The H-1′ resonates at 5.68 ppm and the $J_{1,2}$ coupling constant (8.2 Hz) indicates that the β-anomer has been preferentially formed, the β-H-1″ ($J_{1,2}$= 7.8 Hz) resonates at 4.52 ppm. The product was obtained as a β-anomer in 70.3 % yield.
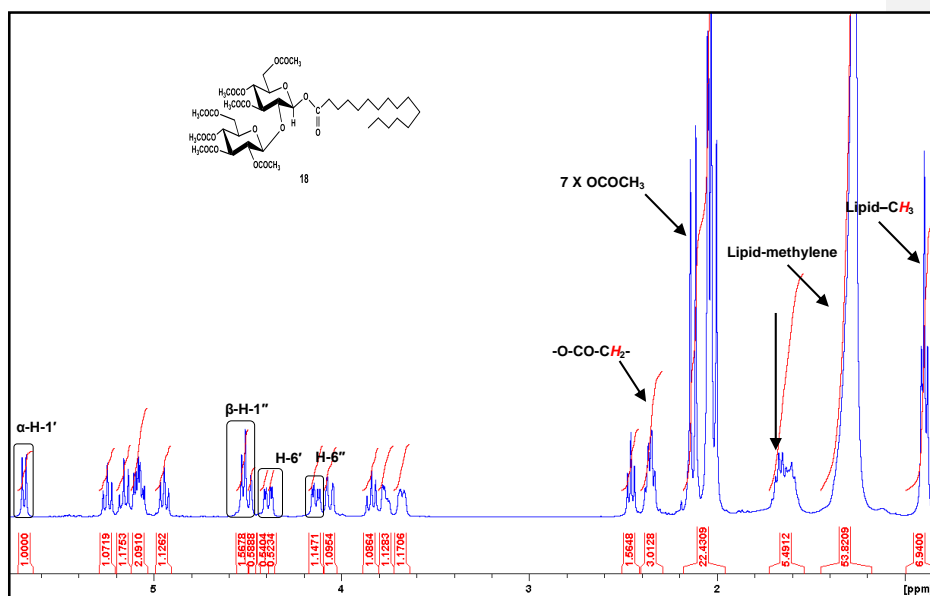
Figure 5-22: Full ^{1}H-NMR spectrum for 2″, 3′, 3″, 4′, 4″, 6′, 6″-hepta-*O*-acetyl-1'-*O*-palmitoyl-β-D-sophoroside, (18)

Inspection of the ^{1}H-^{13}C-HMBC-NMR spectrum (Figure 5-23) confirmed the formation of the new glycoside as there is a correlation between the methylene -CH₂- in the lipid chain (Sugar-O-CO-*C*H₂-) and the anomeric C-1′ through the carbonyl of the palmitoyl chain.
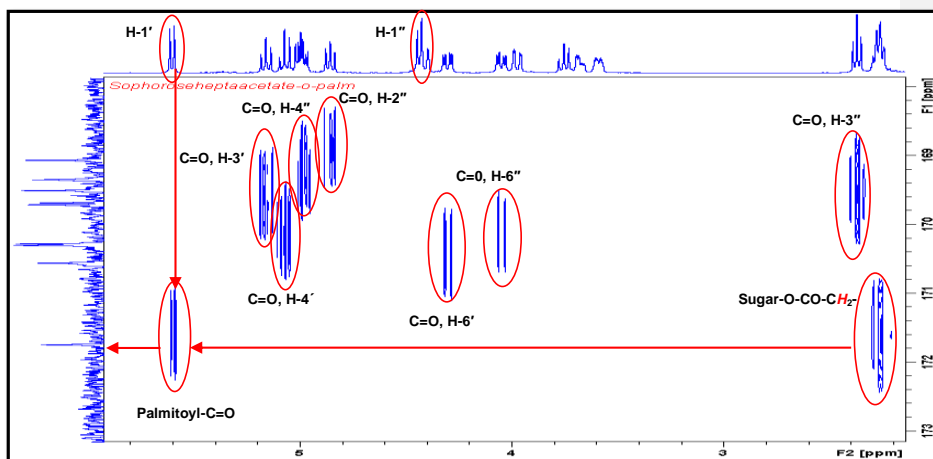
Figure 5-23: ^{1}H-^{13}C-HMBC-NMR for 2″, 3′, 3″, 4′, 4″, 6′, 6″-hepta-*O*-acetyl-1'-*O*-palmitoyl-β-D-sophoroside, (18)

Furthermore, the FT-IR spectrum for the product contains a sharp stretching absorption band for the acetyl C=O groups at 1740 cm^{-1} in addition to the shoulder at 1703 cm^{-1}, which is assigned for the palmitoyl C=O. The absence of the hydroxy group O-H band at 3239.9 cm^{-1} which was present in the starting material suggests the reaction was successful.

The molecular weight of the product was determined and the mass spectrum shows the expected molecular ion as the ammonium adduct [M+NH$_4$]$^+$ at 892.4545 m/z as the major signal. The mass of the neutral compound was determined to be 874.4208 m/z and the theoretical mass of the neutral compound was calculated to be 874.4198 m/z. The mass difference was equal to 1.09 ppm and, therefore, this matches the expected formula ($C_{44}H_{72}O_{18}$) for the 2″,3′,3″,4′,4″,6′,6″-hepta-*O*-acetyl-α/β-D-sophorose. To the best of our knowledge, this is a new compound, which has not previously been reported.

5.5.8 NMR analysis of 2″, 3′, 3″, 4′, 4″, 6′, 6″-hepta-O-acetyl-α-(4-nitrophenyl)-D-sophorose

Scheme 16
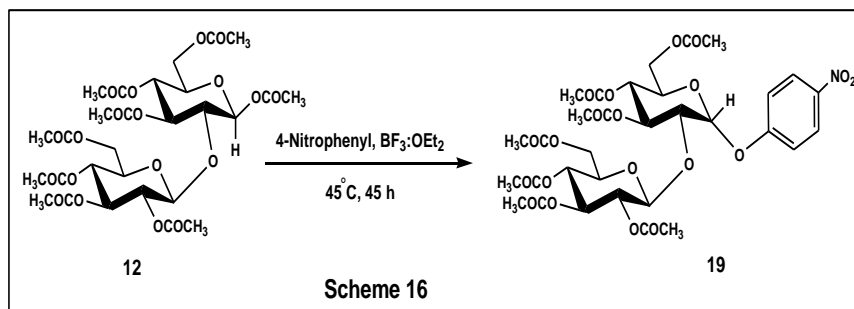
In the next experiment, an attempt was made to add an activated chromophore to sophorose via a glycosidic bond, to generate a molecule which could be used to identify enzymes capable of hydrolysing sophorolipids. The β-D-sophorose octaacetate, (12) was reacted as a glycosyl donor, employing 4-nitrophenol as the acceptor and using boron trifluoride etherate as a catalyst. The aim was to prepare an enzyme substrate via substituting a nitrophenol ring as a good leaving group and as a chromophore on the anomeric carbon C-1′, specifically for use in the detection of enzyme activity in the fermentation liquors as described in section 2.18. The BF_3: OEt_2 used in the synthesis is a Lewis-acid catalyst, which potentially is capable of promoting the stereoselective formation of the α-anomer. [154-156]

The chemical structure of the product was elucidated using 1D- & 2-D-NMR. The DEPT-135 NMR spectra (Figure 5-24) for the starting material and the product show that the anomeric C-1′ signal has shifted from 91.51 ppm in the starting material β-D-sophorose octaacetate, to 97.20 ppm in the new product, this is a downfield shift of 6 ppm. This shift confirmed the coupling of the 4-nitrophenol on the anomeric C-1′ position.
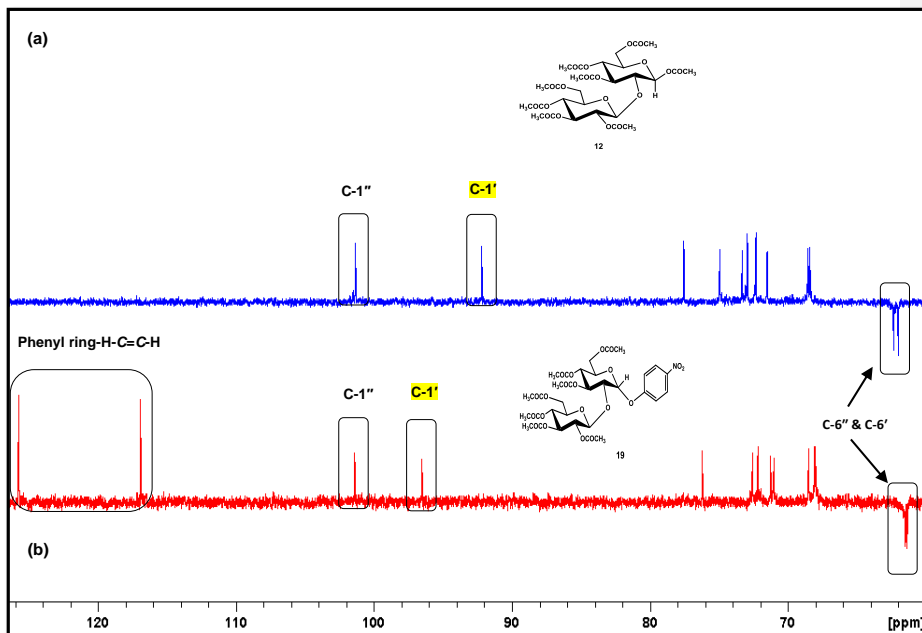
Figure 5-24: Comparison between the DEPT-135 NMR spectra of (a) β-D-sophorose octaacetate, (12) and (b) hepta-*O*-acetyl-α-(4-nitrophenyl)-D-sophorose, (19)

The ^{1}H-^{13}C-HSQC-spectrum of the product (Figure 5-25) confirmed the formation of the alpha isomer. The anomeric signals α H-1′ & β H-1″ resonate at 5.73 ppm ($J_{1,2}$ = 4.01 Hz, α-H-1′) and 4.68 ppm ($J_{1,2}$ = 8.0 Hz, β-H-1″) respectively and show correlations with the anomeric carbon signals C-1″ & C-1′ at 101.40 and 97.00 ppm respectively. Crystallisation from ethanol afforded the α-anomeric product in 70 % yield.
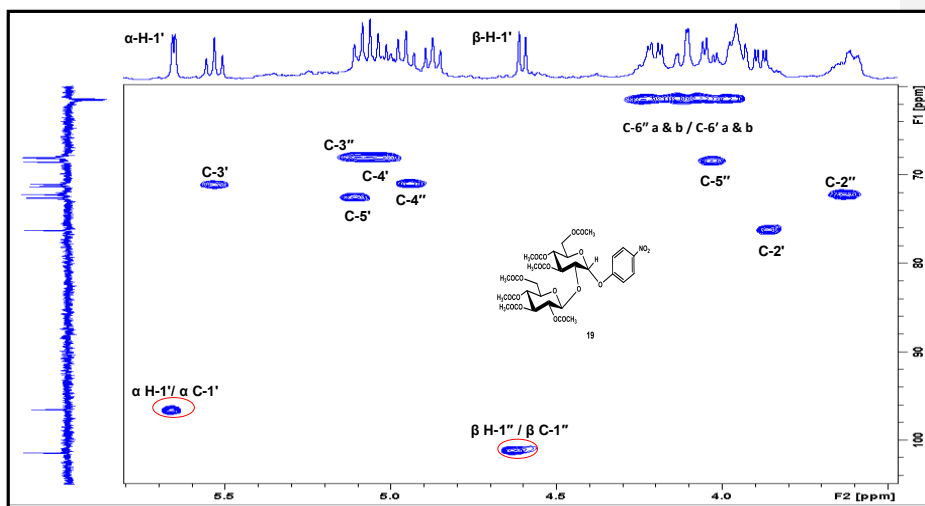
Figure 5-25: ^{1}H-^{13}C-HSQC-NMR for 2″,3′,3″,4′, 4″, 6′, 6″-hepta-*O*-acetyl-α-(4-nitrophenyl)-D-sophorose

The FT-IR spectrum of the product confirmed the presence of the aromatic C-H stretching band for the nitrophenol ring at 3119-3084 cm^{-1} as sharp bands, at the same time the strong absorption band occurred at 1738 cm^{-1} is from the C=O stretching vibration of the acetyl ester groups. The medium absorption bands visible at 1593 & 1519 cm^{-1} were for the stretching of the aromatic -CH=CH- group. The strong C-O absorption band for acetyl esters was observed at 1240 cm^{-1}.

Finally, the molecular weight of the hepta-*O*-acetyl-α-(4-nitrophenyl)-D-sophorose was determined. The mass spectrum shows the expected molecular ion as the ammoniums adduct [M+NH$_4$] $^{+}$ ion at 775.2397 m/z as the major ion. The mass of the neutral compound was determined to be 757.2061 m/z and the theoretical mass of the neutral compound was calculated to be 757.2065 m/z. The mass difference is equal to -0.59 ppm. This was the correct mass, which matches the expected formula ($C_{32}H_{39}O_{20}$) for the product. To the best of our knowledge, this is a new compound, which has not reported in the literature.

167

5.5.9 Removal of protecting groups and production of 4-nitrophenyl-α-D-sophoroside, (20)

Scheme 17
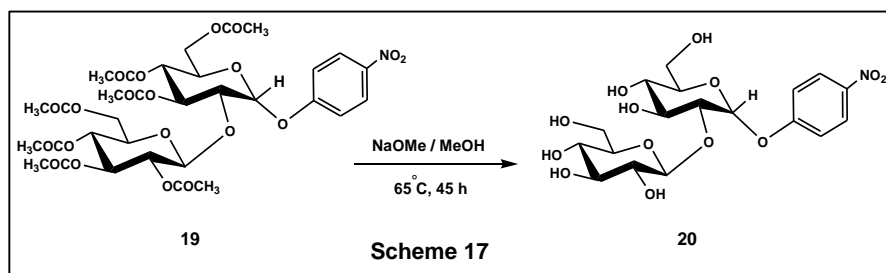
The final step in the synthesis required the removal of the protecting groups and the preparation of α-(4-nitrophenyl)-D-sophorose which was synthesised in an attempt to prepare a substrate for the enzyme. The procedure involved simple deacetylation using a catalytic amount of sodium methoxide in methanol. The ^{13}C-NMR spectra de-acetylated product (20) was recorded and compared with that of the starting material (19), the spectrum of the product (Figure 5-26) show the absence of the acetyl groups (resonating around 170-173 ppm in the starting material). The product as produced as a single α-anomer in 70.0 % yield.

Figure 5-26: Comparison between ^{13}C-NMR spectra of (a) hepta-*O*-acetyl-α-(4-nitrophenyl)-D-sophorose, (19) and (b) 4-nitrophenyl-α-D-sophoroside, (20).

A comparison of the FT-IR spectra (figure 5-27) for the hepta-*O*-acetyl-α-(4-nitrophenyl)-D-sophorose and for 4-nitrophenyl-α-D-sophoroside, suggests that the α-anomer was produced during the alcoholysis, the spectrum (Figure 5-27, b) clearly shows a broad absorption band around 3433-3307 cm^{-1} corresponding to the O-H stretching for the hydroxyl O-H groups on sophorose and the absence of the C=O stretching band at 1738 cm^{-1}, which is assigned for the acetyl groups in case of hepta-*O*-acetyl-α-(4-nitrophenyl)-D-sophorose FTIR spectrum (Figure 5-27, a). In addition to the presence of the C-O stretch band for C-O-H groups of sugar (sophorose moiety) is observed at 1052-1029 cm^{-1}.
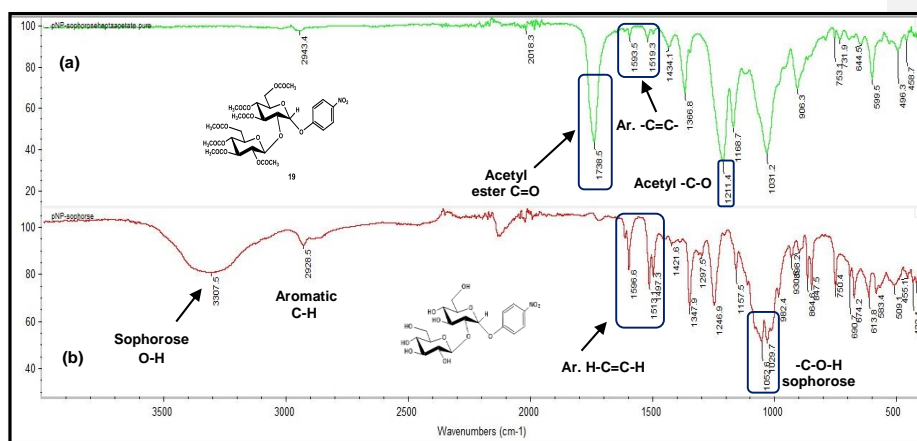
Figure (5-27): Comparison of FT-IR spectra for (a) hepta-*O*-acetyl-α-(4-nitrophenyl)-D-sophorose, (19) and (b) 4-nitrophenyl-α-D-sophoroside, (20)

The molecular weight of the de-acetylated 4-nitrophenyl-α-D-sophoroside was determined by direct insertion MS. The mass spectrum shows the expected molecular ion as the sodium adduct [M+Na]$^{+}$ at 486.1225 m/z. The mass of the neutral compound was determined to be 463.1332 m/z and the theoretical mass of the neutral compound was calculated to be 463.1326 m/z. The mass difference is equal to -1.42 ppm. This was the correct mass, which matches the expected formula ($C_{18}H_{25}NO_{13}$) for the 4-nitrophenyl-α-D-sophoroside, (20). To the best of our knowledge, this is the first time the synthesis of this molecule has been reported.

169

5.5.10 NMR analysis of 2″, 3′, 3″, 4′, 4″, 6′, 6″-hepta-*O*-acetyl-β-(4-nitrophenyl)-D-sophorose

Scheme 18
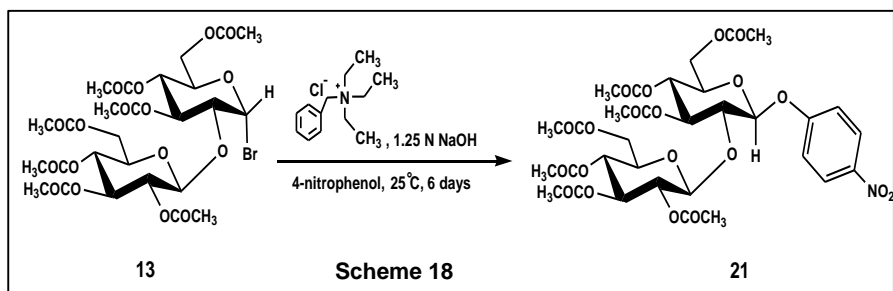
The next molecule whose synthesis was attempted was the 4-nitrophenyl-β-D-sophoroside; the synthesis of this product, (21) was performed using a phase-transfer catalyst, [157-159] triethylbenzylammonium chloride under neutral and mild conditions which generate the sophoryl-chloride as an intermediate. The β-anomer product, hepta-*O*-acetyl-β-(4-nitrophenyl)-D-sophorose was produced via the treatment of hepta-*O*-acetyl-α-bromo-D-sophorose with 4-nitrophenol in the presence of the phase-transfer catalyst in aqueous sodium hydroxide (base) to give the corresponding hepta-*O*-acetyl-β-(4-nitrophenyl)-D-sophorose with inversion of configuration at the anomeric centre that resulted in the stereoselective substitution of the nitrophenol ring on the β-anomeric C-1′ position.

Again, the chemical structure of the product was elucidated using 1- & 2-D-NMR. The ^{13}C-NMR spectrum (Figure 5-28) shows that the anomeric β-C-1′ signal has shifted from 86.43 ppm in the starting material hepta-*O*-acetyl-α-bromo-D-sophorose to 98.28 ppm in the new product; this is a downfield shift of 11.85 ppm. This shift confirms the coupling of the 4-nitrophenol on the anomeric C-1′ position.

170
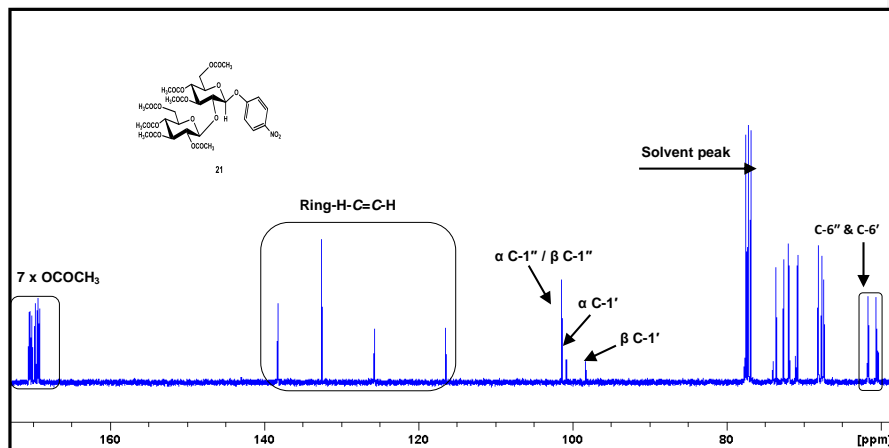
Figure 5-28: Full ¹³C-NMR spectrum for the 2″,3′,3″,4′,4″,6′,6″-hepta-*O*-acetyl-β-(4-nitrophenyl)-D-sophorose, (21)

The product's ¹H-¹³C-HSQC-spectrum (Figure 5-29) confirms that there is a trace of around 20% of the α-anomer produced during the synthesis as the spectrum shows another set of contours for a second anomeric signal α-H-1′ resonated at 4.68 (H) & 100.79 (C) ppm as well as β-H-1″ which resonates at 4.99 & 101.35 ppm. Those signals are small peaks which are visible in both the ¹H- and ¹³C-NMR-spectra.
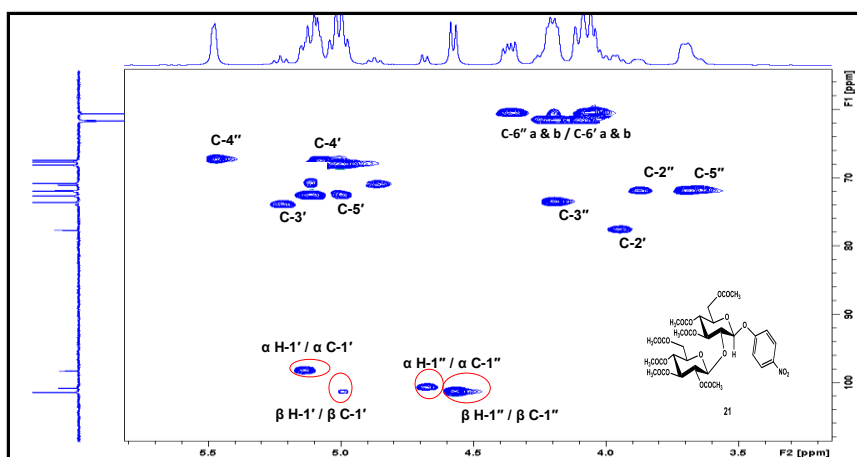
Figure 5-29: ¹H-¹³C-HSQC-NMR for 2″,3′,3″,4′,4″,6′,6″-hepta-*O*-acetyl-β-(4-nitrophenyl)-D-sophorose, (21)

171

The structure of the product was also investigated using FT-IR. The spectrum confirms the presence of the aromatic C-H stretching band for the nitrophenol ring occurred at 3115-3080 cm^{-1} as sharp bands, whereas the strong absorption band at 1741cm^{-1} is from the C=O stretching vibration of the acetyl ester groups on the sophorose moiety. The medium absorption bands visible at 1590 & 1515 cm^{-1} were for the stretching of the aromatic -CH=CH- group. The strong C-O absorption band for the acetyl esters was observed at 1241 cm^{-1}. The HPLC-MS was used to detect the molecular weight of the β-anomer of product (21). The major peak visible at a retention time of 11.337-12.065 min is for the main compound and in the total ion chromatogram, the main peak generated the molecular ion as its sodium adduct [M+Na] $^{+}$ at m/z= 780.1943, which is the expected mass. The mass of the neutral compound was determined to be m/z= 757.2034 and the theoretical mass of the neutral compound was calculated to be m/z= 757.2065 with a mass difference equal to - 4.09 ppm. This was the correct mass, which matches the expected formula ($C_{32}H_{39}O_{20}$) for the 2″, 3′, 3″, 4′, 4″, 6′, 6″-hepta-*O*-acetyl-α-(4-nitrophenyl)-D-sophorose. To the best of our knowledge, this is the first time synthesis of this compound has been reported.

5.5.11 NMR analysis of 4-nitrophenyl-β-D-sophoroside

Scheme 19
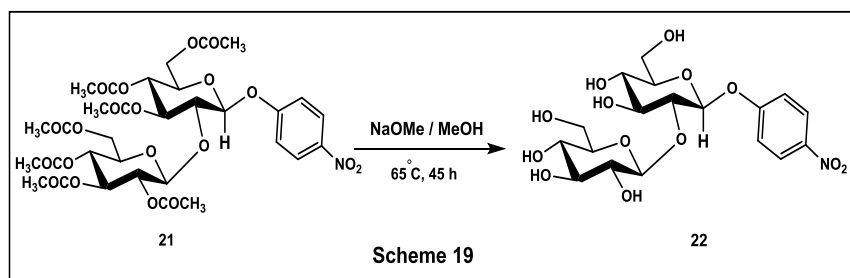
The acetylated β-anomeric product (21) was subjected to alcoholysis to recover the de-acetylated product (22). The ^{13}C-NMR spectra for the acetylated product hepta-*O*-acetyl-β-(4-nitrophenyl)-D-sophorose (21) and the de-acetylated product (22) were recorded, the spectra (Figure 5-30) confirm

the complete removal of the acetyl groups (observed in the starting material spectrum around 170-173 ppm).
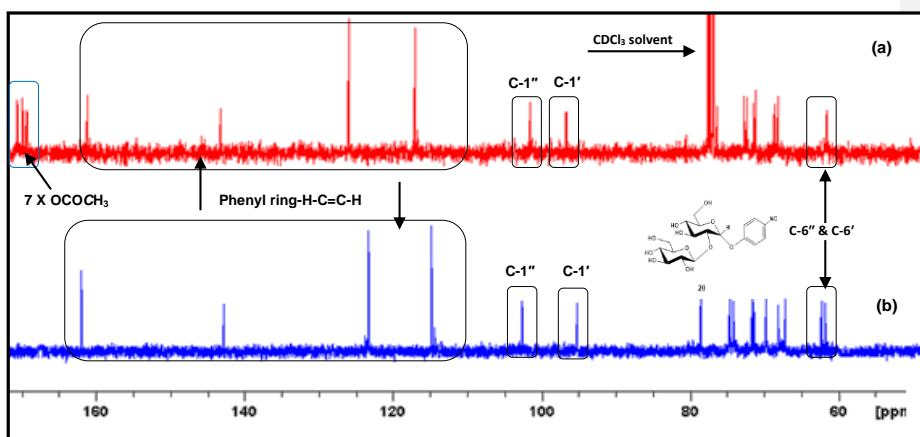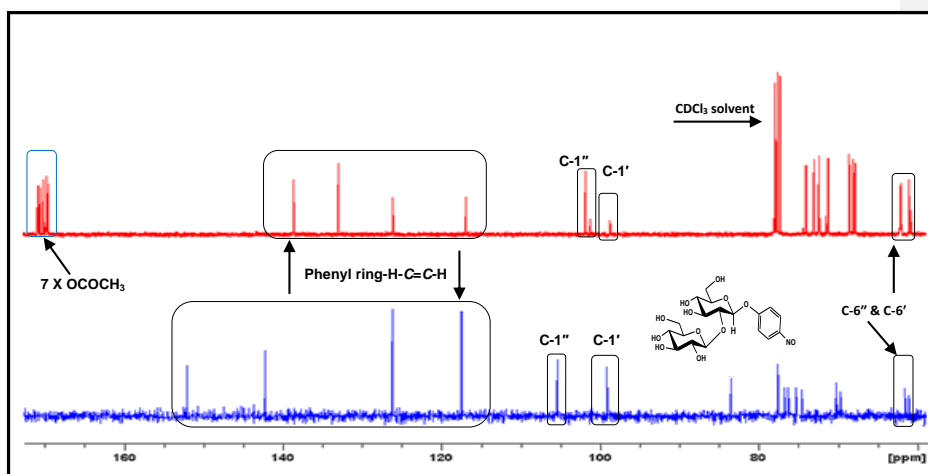

Figure 5-30: Comparison between ^{13}C-NMR spectra of (a) hepta-*O*-acetyl-β-(4-nitrophenyl)-D-sophorose, (21) and (b) 4-nitrophenyl-β-D-sophoroside, (22)

The FT-IR spectrum for the hepta-*O*-acetyl-β-(4-nitrophenyl)-D-sophorose, suggests that the desired product was produced during the alcoholysis, the spectrum shows a broad band around 3430-3302 cm^{-1} corresponding to the O-H stretching for the hydroxyl O-H groups on sophorose and the absence of the C=O stretching band at 1741 cm^{-1}, which is assigned for the acetyl groups in case of hepta-*O*-acetyl-β-(4-nitrophenyl)-D-sophorose spectrum. The molecular weight of the de-acetylated β-anomer compound (22) was determined using a direct injection MS method. The mass spectrum gave the expected molecular ion as the sodium adduct [M+ Na] $^{+}$ at m/z = 486.1235. The mass of the neutral compound was determined to be 463.1339 and the theoretical mass of the neutral compound was calculated to be 463.1326. The mass difference is equal to -2.81 ppm. This was the correct mass, which matches the expected formula ($C_{18}H_{25}NO_{13}$) for the 4-nitrophenyl-β-D-sophoroside.

173

5.6 Structural analysis of novel sophorolipids using HPLC-MS or MS analysis

After the confirmation of the sophorolipids by structural elucidation through the NMR, monomer and linkage analysis, HPLC-MS and MS direct injection method were used to further confirm and characterise the molecular weight of sophorolipids and their derivatives.

5.6.1 HPLC-MS analysis of lactone sophorolipid, (2)

In the HPLC-MS detected one main compound and four minor impurities from the SL-lactone, (2) were obtained as shown in (Figure 5-31). According to the total ion chromatogram, the main peak of retention time (3.86 min) was generated by an ion with m/z= 688.369, which only matches the formula ($C_{34}H_{56}O_{14}$). This was the correct formula corresponded to the sodium salt of the 6', 6"-diacetylated lactone sophorolipid. The four minor impurities were not matching the correct formula assigned for the lactone sophorolipid.
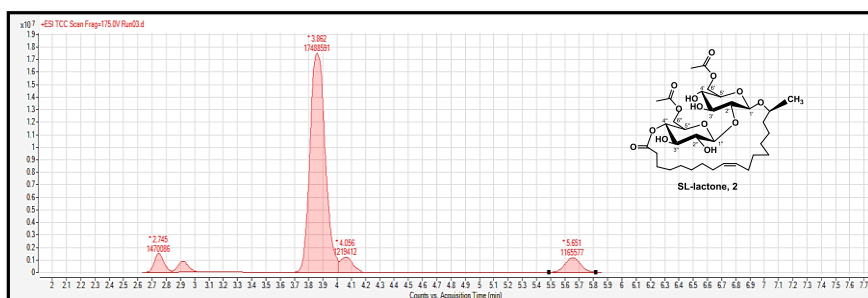
The following formula for the peak at 3.86 mins was generated:

Best	▽	ID Source	▽	Formula	▽	Score	▽▽	Diff (ppm)	▽	Diff (abs. ppm)	▽	Diff (mDa)	▽	Score (Tgt)	▽	Score (MFG)	▽	RT	▽	Mass	▽
6			MFG	C34 H56 O14		89.94		-3.93		3.93		-2.71				89.94		3.861		688.3697	

Figure 5-31: Total ion chromatogram, peak retention times and the correct matching formula along with the mass (m/z) obtained for the lactone sophorolipid, (2)

174

5.6.2 HPLC-MS analysis of sophorolipid derivatives

The molecular weight of the modified sophorolipids was also determined using HPLC-MS. The same method was used as described in section 2.3.3. The total ion chromatograms (Figure 5-32) for the modified sophorolipids, methyl ester SL-Me, (4) and ethyl ester SL-Et, (5) each show one distinct peak at 1.75 and 2.14 min, respectively and the masses obtained from these peaks were m/z 636.37 and 650.39 and both represent the corrected formula ($C_{31}H_{56}O_{13}$ and $C_{32}H_{58}O_{13}$) for the methyl and ethyl ester sophorolipids.
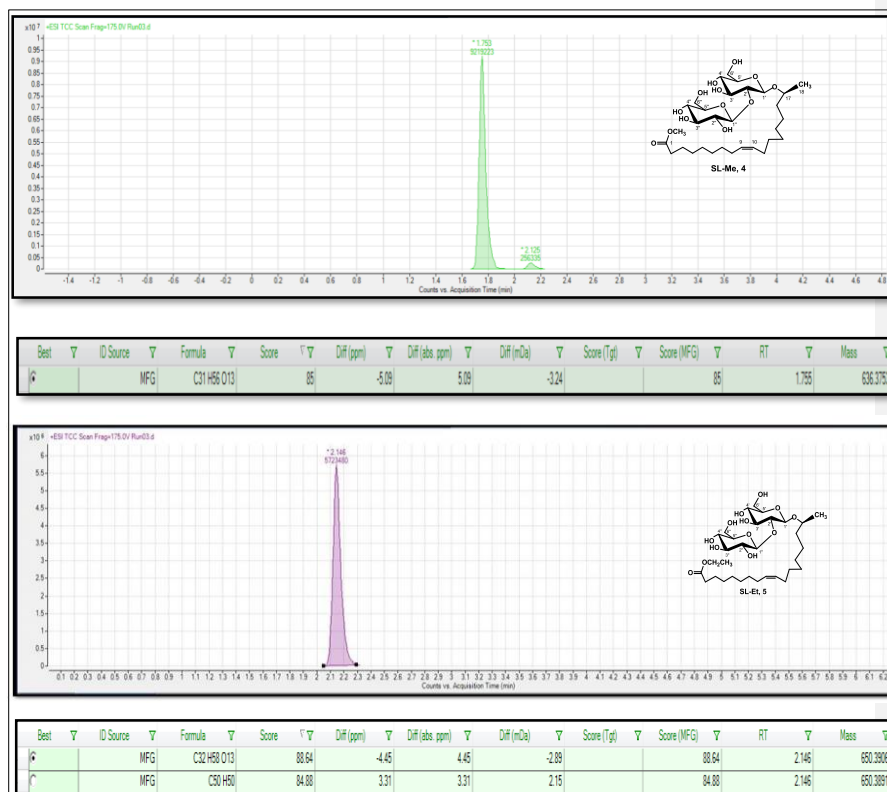
Figure 5-32: Total ion chromatogram, and the correct matching formula along with the mass (m/z) obtained for methyl and ethyl ester sophorolipids SL-Me & SL-Et

Moreover, the mass spectra for the modified sophorolipids, SL-1',6"-lactone, (6) and 1',6"-lactone-6'-acetate, (7) were also investigated and their molecular weights were determined. The total ion chromatograms (Figure 5-33) for the 1',6"-lactone shows one main peak at 2.15 min and a minor impurity peak, whereas for the 1',6"-lactone-6'-acetate, there was one main peak (2.99 min) for the main compound and six minor impurities from the sample. The mass spectra obtained from these major peaks (m/z 604.34 and 646.35) were both for the corrected formula ($C_{30}H_{52}O_{12}$ and $C_{32}H_{54}O_{13}$) respectively for the synthesised the derivatives, (6 and 7).
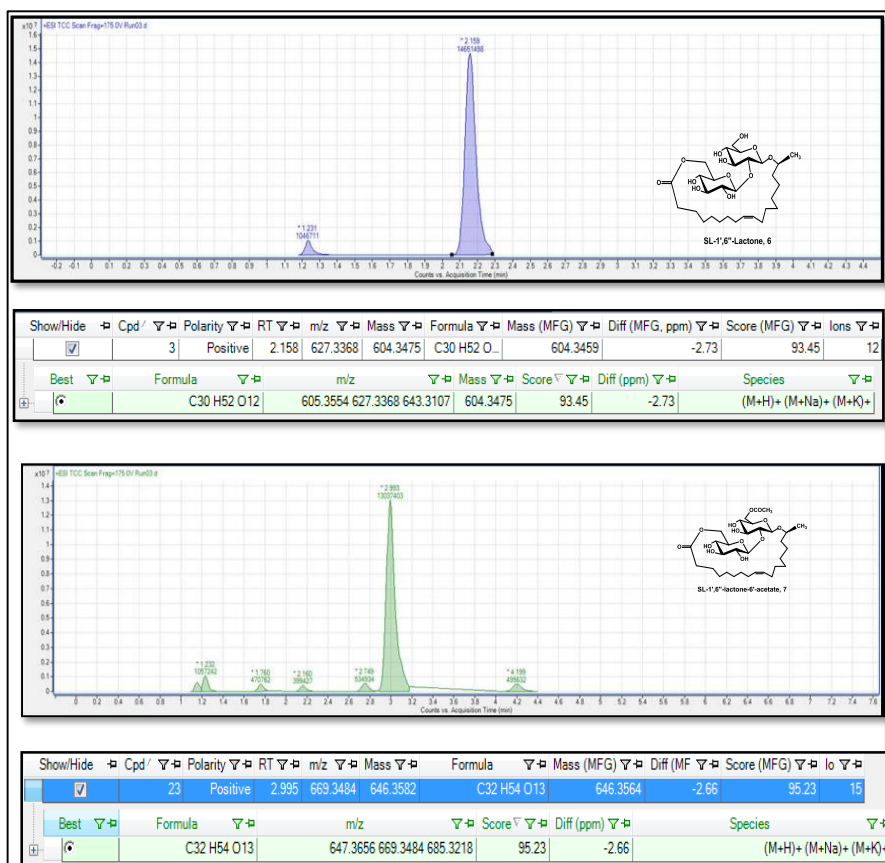
Figure 5-33: Total ion chromatograms, and the correct matching formulas along with the mass (m/z) obtained for 1', 6"-sophorolactone and 1', 6"-sophorolactone-6'-acetate derivatives

Finally, HPLC-MS analysis was used to investigate the SL-Me-6′,6″-dibutyrate, (8). The total ion chromatogram contained two peaks; the major peak at 3.644 min was for the main compound (Figure 5-34). The second peak with a retention time (2.109 min) generated the ion at m/z = 785.4362, which is the [M+ Na] + adduct and the ion at m/z= 801, which is corresponding to the mass of m/z the potassium adducts [M + K] + these are the correct masses for the sodium & potassium salts of the compound, which match the formula ($C_{38}H_{66}O_{15}$). Hence, this was the correct formula corresponded to the sodium salt of the methyl ester-6′,6″-sophorose dibutyrate, (8). The mass spectra show the presence of two molecules as the formic acid was used; therefore, it charges the molecule and hence generated the carboxylic sodium salt of the compound, which is the first peak in the HPLC-TIC. Whereas the main peak of retention time 3.644 min generated the ion at m/z= 799.4531, which is corresponding to the [M + Na] + adduct (Figure 5-35) and this is the correct mass for this derivative, that only matches the formula ($C_{39}H_{68}O_{15}$).
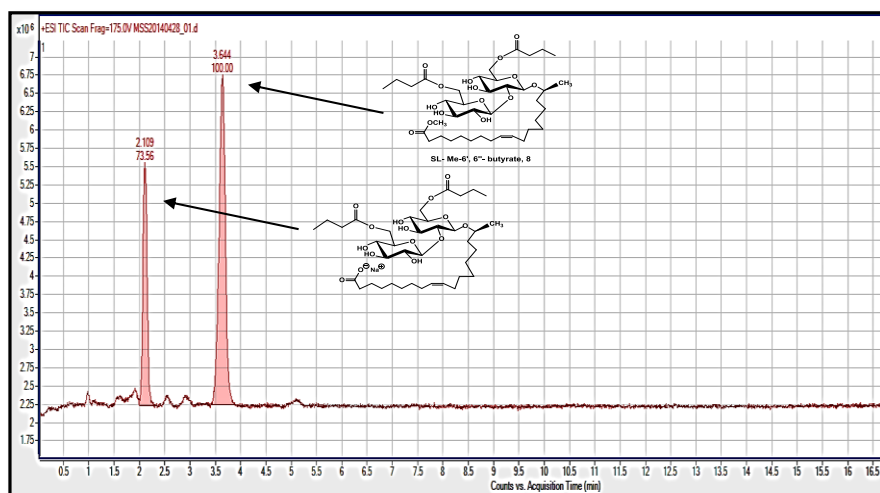
Figure 5-34: TIC-chromatogram for the derivative methyl ester-6′,6″-sophorose dibutyrate, (8).
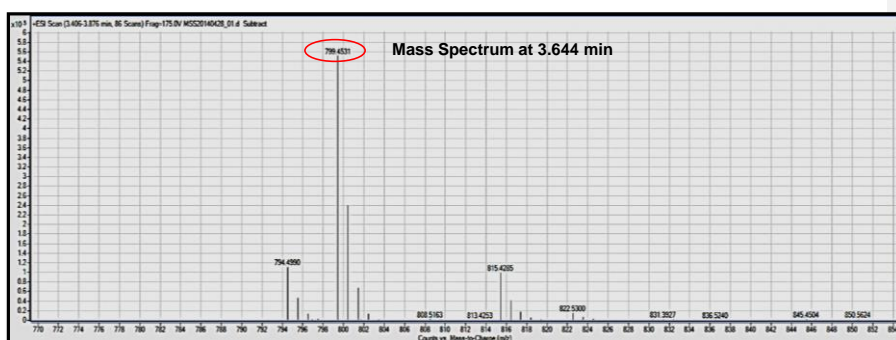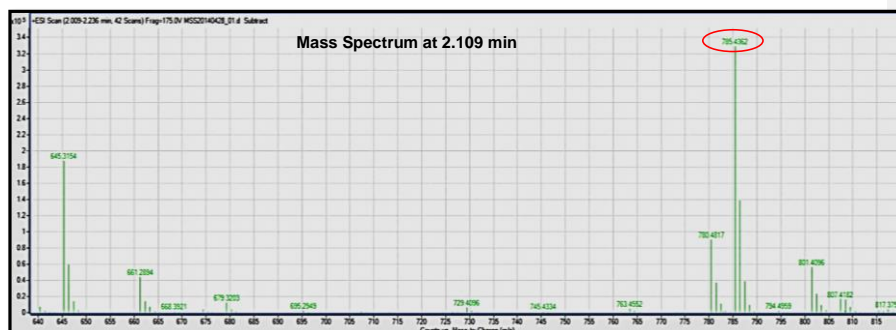
Figure 5-35: Expected mass region and the correct formula matching for the compound methyl ester-6′, 6″-sophorose dibutyrate, (8)

5.6.3 Mass spectra analysis of 1′, 2″, 3′, 3″, 4′, 4″, 6′, 6″-octa-*O*-acetyl-β-D-sophorose, (12)

The molecular weight of the newly synthesised sophorolipids was determined using either HPLC-MS or through a direct injection MS method. The following HPLC-MS result is a good example for the analysis of 1′, 2″, 3′, 3″, 4′, 4″,6′,6″-octa-*O*-acetyl-β-D-sophorose, (12) derivative.

The total ion chromatogram (TIC) chromatogram confirms the presence of a single peak at 3.544 min, which is for the compound as shown (Figure 5-36). The main peak has generated the $[M + NH_4]^+$ ion at m/z = 696.2345, which is the expected mass ion.

178

The mass of the neutral compound was determined to be m/z= 678.2006 and the theoretical mass was calculated to be m/z= 678.2007; with mass difference equal to -0.15 ppm.

This is the correct mass, which matches the expected formula ($C_{28}H_{38}O_{19}$) for the product.
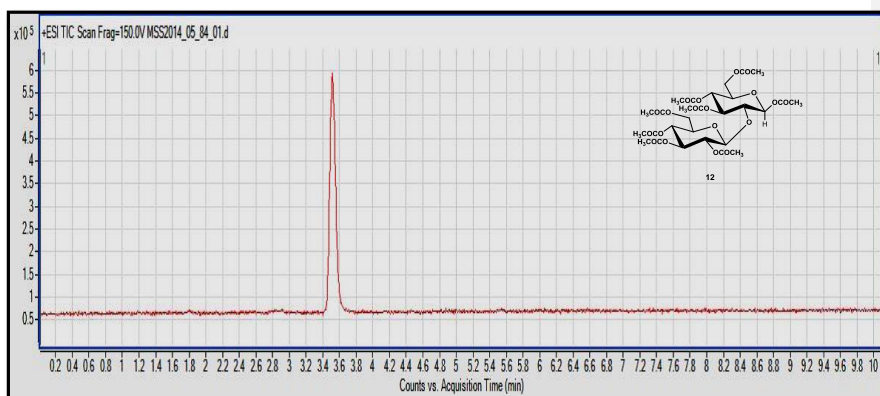
Mass Spectrum at (3.548-3.695 min):
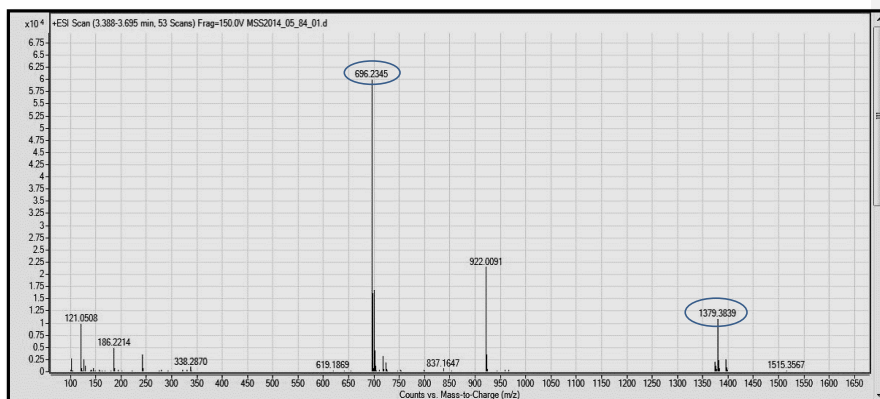
Figure 5-36: HPLC-TIC chromatogram and the expected mass region for the compound 1′, 2″, 3′, 3″, 4′, 4″, 6′, 6″-octa-*O*-acetyl-β-D-sophorose, (12)

5.7 Conclusion

Simple alcoholysis of the lactone form of the sophorolipid was successfully employed to produce the ethyl and methyl ester sophorolipids as derivatives with a good yield, these were then used in the preparation of a range of 1,6″-lactone derivatives including: 1,6″-sophorolactone, 1,6″-sophorolactone-6′-acetate and methyl ester-6′,6″-sophorose dibutyrate. The NMR, MS and FT-IR data all confirmed the formation of these derivatives and the substitution of the acetate / butyrate groups on the C-6′/C-6″ position (s).

Sophorose was successfully used in a sequence of chemical steps to produce a range of new sophorolipids utilizing a classical glycosylation reaction between 2″,3′,3″,4′,4″,6′,6″-hepta-O-acetyl-α-D-sophoryl bromide and a range of fatty alcohols. The chemical structures of the newly synthesised sophorolipids were investigated using 1- & 2-D-NMR, FT-IR and HPLC-MS.

The main driving force for the synthesis of these novel sophorolipids has been the design of new SLs for generation of compounds with novel effect on the surface tension properties and with a view to the determination of their biological activity and this will be described in the next chapter. The α and β-p-nitrophenyl sophorylsides were designed as activated colourimetric substrates for use in the search for glycosyl-hydrolase enzymes that have been reported to be present in the fermentation liquor and which potentially can cleave the sophorose-lipid bond. The results of this investigation are also described in the next chapter.

6. Applications of novel sophorolipids

6. Applications of novel sophorolipids

6.1 Introduction

6.1.1 Surface tension properties of sophorolipids

Sophorolipids and their derivatives have been reported to display different physicochemical properties and they have found multiple applications in a range of different fields. [203,211] These characteristics are mainly due to the presence of both hydrophilic and hydrophobic components in their chemical structures, the balance of these characters plays vital role in the surface properties of sophorolipids. Generally, sophorolipids are found to reduce the surface tension of water from 72.80 mN/m to 40-30 mN/m with typical critical micelle concentrations (CMC) of 100-250 mg/L. [212,213] According to previous studies, solutions of the diacetylated lactone sophorolipid have a lower surface tension and CMC values compared to the nonacetylated acidic sophorolipid form. [56,66] The degree of acetylation of the sophorose moiety has a great effect on the surface tension and biological properties of sophorolipids. [43,140] The monoacetylated lactone form C18:1 possesses a similar CMC to the diacetylated sophorolipid C18:1. However, the surface tension reduction value at CMC (γ_{CMC}= 40 mN/m) measured for the monoacetylated was marginally greater than that of the diacetylated form (γ_{CMC}= 36 mN/m).[86,214] A glucolipid, generated through the enzymatic modification reaction of an acid sophorolipid using hesperidianse glycosidase, displayed very similar surface tension properties as for the acidic sophorolipid but was less soluble in water compared to the acidic form. [87] Another study confirmed that sophorolipids with fatty acid of longer carbon chain such as, the alkyl (*i.e.*, methyl, propyl and butyl) esters had lower CMC and γ_{CMC} values than those with shorter carbon chain. [90,104]

In summary, the degree of acetylation, the chain length of the lipid component of sophorolipids and their carbohydrate structure all influence their CMC values and the corresponding surface tension value at the γ_{CMC}. [86]

The surface tension properties of sophorolipids are about two fold lower in magnitude than that for the chemical-based surfactants. In general, it has been reported that the lactone form of sophorolipids showed enhanced surface tension reducing properties. In contrast, the acid form of sophorolipids displayed better foam formation and better solubility. [191] Sophorolipids possess properties that render them attractive 'natural' surfactants and as a consequence, they are used in applications in the field of cosmetics, detergents, soil remediation and oil recovery. [90]

6.1.2 Sophorolipids as activators or inhibitors of enzyme activities

Sophorolipids are able to modulate enzyme activity either by inhibiting the activity of enzymes or alternatively, by altering the structure of cell-membranes, sophorolipids can promote enzyme activity by facilitating their release. Glycolipids can also modulate enzyme activity by influencing an enzyme's stability, preventing their denaturation during their activity. [196,215] In 1993, Helle *et al*. [216] confirmed the enhancement of cellulase stability during cellulose hydrolysis by desorbing it from the cellulose substrate through the addition of sophorolipids. This desorbing and stabilizing effect were attributed to the molecular structure of the enzymes and surfactants as well as the interface between the enzymes and surfactants. [160] Sophorolipids allow for the disruption of the structure of cellulose, making the cellulose more accessible to the enzymes.

It has previously been suggested that sophorolipids are metabolized by *C.bombicola* upon carbon starvation. [196] The metabolism of sophorose would require the presence of an enzyme with hydrolase activity in the fermentation liquors *i.e.*, an enzyme which has the ability to either cleave the glycosyl-lipid bond to give sophorose and free lipid or to hydrolyse the glycosyl-glucopyranose bond to give glucose and glucolipid. One way of searching for the presence of an enzyme that could cleave the sophorose-lipid bond is to generate an activated colourimetric substrate for monitoring this activity.

In the previous chapter, the synthesis of both α- and β-*p*-nitrophenyl sophorylsides was described and these were synthesised in an attempt to

generate colourimetric substrates for enzymes capable of hydrolysing sophorolipids. These were tested to determine if they would act as substrates for simple glycosyl-hydrolases.

6.1.3 Biological activity of sophorolipids

Another reason why researchers are interested in sophorolipids is related to their biological activity including anticancer, antiviral (anti-HIV) and antibacterial activity. These activities have resulted in sophorolipids being used in an application in the pharmacological, pharmaceuticals and clinical fields. [18,79,217,218] Recently, in 2015, De Rienzo and co-workers studied the antimicrobial activity and biofilm disruption properties of a range of different concentrations of sophorolipids. The study confirmed the inhibition of the growth of Gram-positive *Bacillus subtilis* BBK006 and Gram-negative *Cupriavidus necator* ATCC 17699 by sophorolipids at a concentration 5% v/v. [219]

Generally, the chemical structures of sophorolipids greatly influence their biological activity: the diacetylated lactone form displayed higher antimicrobial activity against bacteria, fungi, and virus compared to the deacetylated acidic form. Moreover, the lactone form was also shown to have higher cytotoxic activity than the monoacetylated and deacetylated acid form towards cancer cells and viruses. [79,105,220]

It has also been shown that both chemical and enzyme modification of natural sophorolipids has led to the production of sophorolipid derivatives with increased biological activity. For example, the substitution of acetyl groups can lower the hydrophilicity of the sophorolipid molecule and improve their antimicrobial activity and their ability to influence to change the production of a cytokine. [73,217,218] The diacetylated ethyl ester of sophorolipids exhibited good spermicidal activity and was more effective against HIV than the standard lactone sophorolipid. [79,217] The deacetylated ethyl ester form of sophorolipids can be used for the treatment of sepsis, acting primarily through decreasing

inflammatory cytokines by blocking TLR4-CD14 upstream of the inflammatory signalling cascade. [170]

Recently, a quaternary ammonium sophorolipid derivative that was synthesised by Delbeke and co-workers was assessed for its antibacterial activity against the Gram-positive and negative bacteria. [221]

Natural sophorolipids have displayed cytotoxic activity against pancreatic carcinoma cells, while sophorolipids from *W. domercquiae* exhibited a considerable effect on esophageal cancer KYSE109 and KYSE450, [73] human lung cancer A549, human liver cancer H7402, and human leukemia HL60 and K562 cell lines. [37] The biological activity of sophorolipids on human liver cancer cells H7402 was linked to their ability to trigger apoptosis.

Whilst the initial aim of this work was the chemical synthesis of novel sophorolipids, their purification and their characterisation. The secondary aim was to investigate the effect of their structure on their chemical and biological activities. We were specifically interested in:

Determining the interfacial properties of the synthesised sophorolipids;

Determining if the products synthesised as part of this research displayed pharmacological activity against cancer cells;

Finally, we were interested to see if the activated substrates (SLs, 20 & 22) could be used to detect enzyme activity.

6.2 Determination of the interfacial properties of sophorolipids

The surface tension lowering and micellization ability in solution are the most vital properties of a surfactant. The surface active properties of the sophorolipids generated in this research programme were evaluated and measured at 25 °C according to the procedure described in section 2.17. The aim of this experiment was to understand the relationship between the alkyl ester chain length and their interfacial properties, also to investigate the effect of the acetate and butyrate groups attached to the C-6s position on sophorose moiety and how these influence interfacial properties.

The principal surface characteristics of surfactants are measured by studying the variation of the surface tension (γ) as a function of the substrates concentration [mM]. A series of experiments were performed to determine the variation of the surface tension (γ) of an aqueous phase as a function of the concentration of the novel sophorolipids whose synthesis was described in the previous chapter, at the same time the properties of the sophorolipid acid and lactone were measured as control experiments. Plots of the surface tension (γ) against substrate concentration are shown in (Figure 6-1 & 2) and the effects on a range of interfacial properties are summarized in Table 6-1. The interpretation of the plots is straightforward: near the CMC, surfactants begin to form micelles in the bulk aqueous phase and as a result, at or above the CMC, a further increase in surfactant monomers gives a very little decrease in surface tension. The chemical surfactant, sodium dodecyl sulphate (SDS) was used as a control in these experiments.
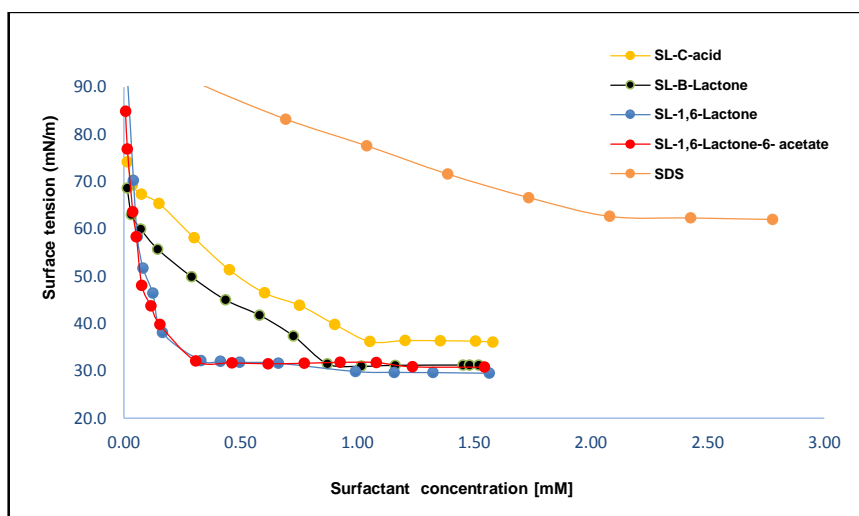
Figure 6-1: Surface tension vs. concentration plots for sophorolipids: acid, 1',4''-sophorolactone, 1',6''-sophorolactone, 1',6''-sophorolactone-6'-acetate and SDS with the ring method at 25 °C
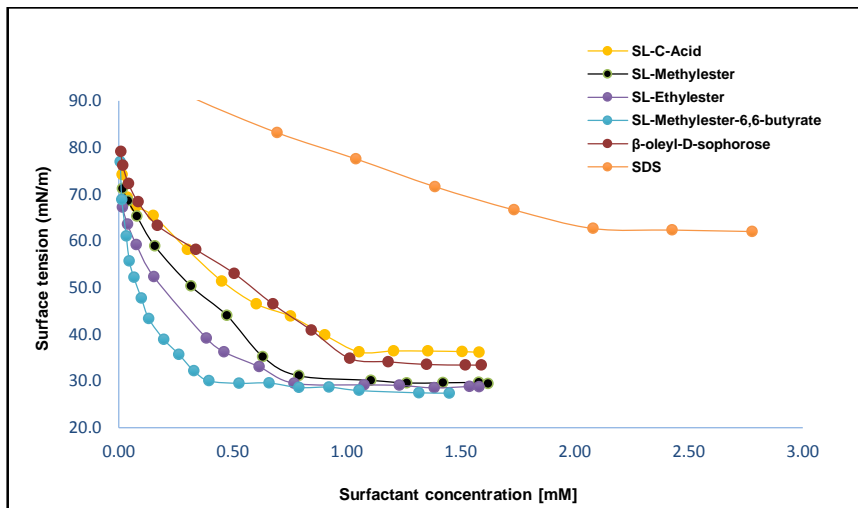
Figure 6-2: Surface tension vs. concentration plots for sophorolipids: acid, methyl ester, ethyl ester, methyl ester-6′,6″-sophorose dibutyrate, β-oleyl-D-sophorose and SDS with ring method at 25 °C

In both sets of results, sophorolipids reduced the surface tension of distilled water from 72.8 mN/m down to values within the range of 36.20-29.50 mN/m with the recorded CMC values being in the range of 1.05-0.31 mM. These values fall within the range of values reported by previous studies [212] where sophorolipids dissolved in water, lowered the surface tension from 72.8 down to 40-30 mN/m. The CMC (γ_{CMC}) for each sophorolipid were calculated from the graphical representation of surface tension (γ) versus logarithm of SL concentration as shown in (Figure 6-3) below:
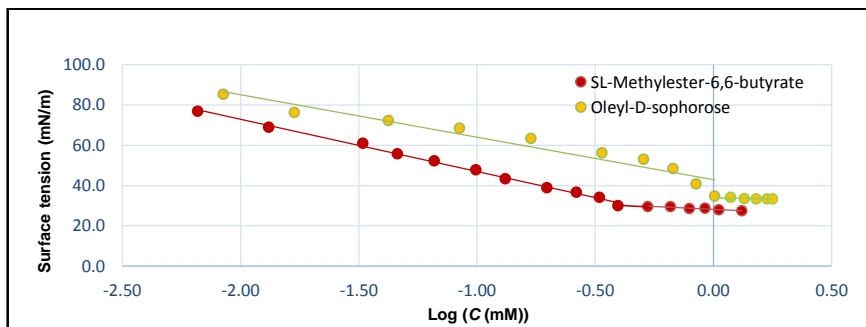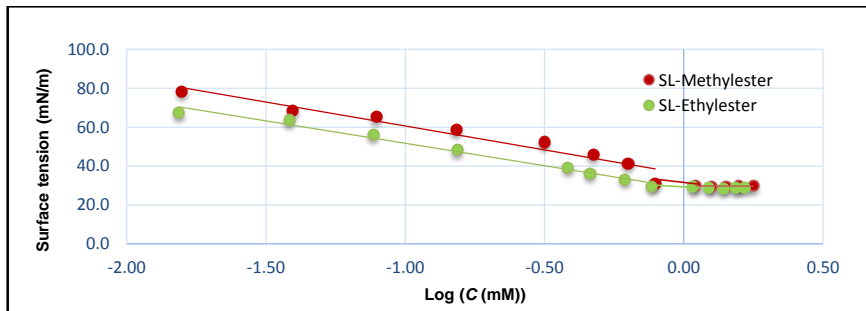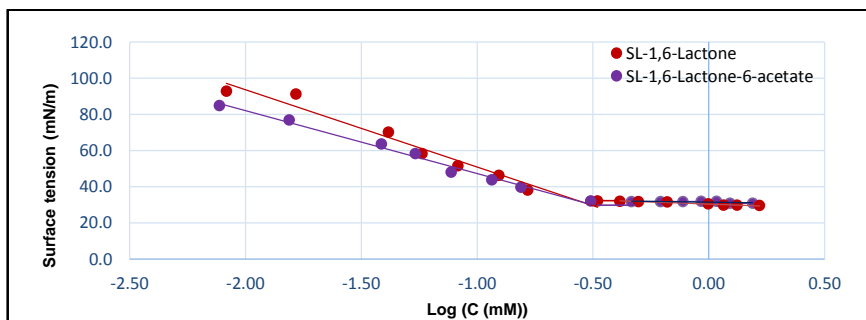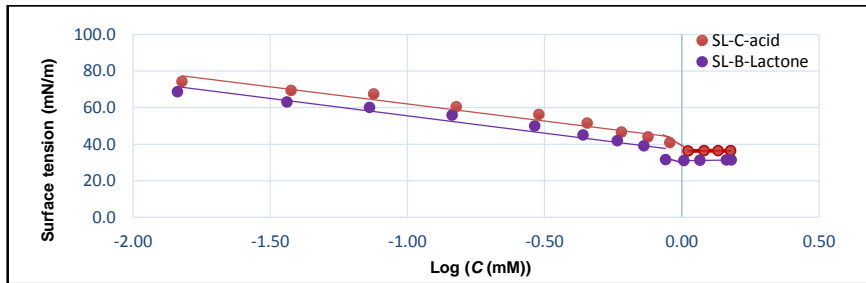
Figure 6-3: Plots of surface tension (mN/m) versus the logarithm of millimolar concentration (log *C*) of classical sophorolipids and their derivatives.

Table 6-1: Surface-active properties of sophorolipids and their derivatives

Sophorolipid	CMC [mM]	γ_{CMC} (mN/m)	Γ_{max} (mol/m^2)	A_{min} (Å^2)
SDS control	2.08	62.65	1.27×10^{-8}	138.36
SL-Acid	1.05	36.20	2.16×10^{-7}	102.35
1′,4″-sophorolactone	0.87	31.60	1.20×10^{-6}	96.85
1′,6″-sophorolactone	0.33	32.15	0.45×10^{-6}	94.34
1′,6″-sophorolactone-6′-acetate	0.31	32.08	0.62×10^{-6}	92.68
SL-Methyl ester	0.79	31.10	2.07×10^{-6}	82.92
SL-Ethyl ester	0.72	29.40	1.07×10^{-7}	85.79
Methyl ester-6′,6″-sophorose dibutyrate	0.40	30.00	3.04×10^{-6}	75.23
β-D-oleyl sophorose	1.01	34.82	4.87×10^{-7}	100.21

In each of the surface tension (γ) versus the logarithm of sophorolipids concentration plots, the curves showed a significant inflection at a particular surfactant concentration (Figure 6-3) corresponding to the substrates CMC. The sophorolipid lactone and sophorolipid acid showed a lower surface tension of (31.60 & 36.20 mN/m) at a CMC (0.87 & 1.05 mM) respectively. These values are slightly lower than the values reported in previous studies, [43,140,212,213] while the surface tensions of other lactone derivatives; 1′,6″-sophorolactone and 1′,6″-sophorolactone-6′-acetate were slightly higher than that for the natural lactone (Table 6-1). The lowest average adsorption density is for the ethyl ester sophorolipid 1.07×10^{-7} mol/m ^{2} and the lowest area per molecule value is 75.23 Å^2 for the methyl ester-6′,6″-sophorose dibutyrate. The areas per molecule values for these surfactants are higher than those of other surfactants with a similar structure such as, *n*-dodecyl-β-D-maltoside, which is ~50 Å^2. [222] From simple visual inspection, the surfactants solubilities were investigated and it was noted that the alkyl ester derivatives methyl, ethyl ester, and methyl ester-6′,6″-sophorose dibutyrate demonstrated high and rapid solubility in water with good foam formation compared to the natural

Commented [AL1]: Ammar-you must explain what the two additional terms/coumns that are located in table refer to.

A2 and Tmax

188

acid. While the lactones sophorolipids were sparingly soluble with less foam formation.

Concerning the group of sophorolipid derivatives, SL-Me, SL-Et and methyl ester-6′,6″-sophorose dibutyrate, it is clearly seen that, as the chain length of the *n*-alkyl ester moiety increases, the surface tensions of the surfactants decreases. The surface tension values for these derivatives are lower in comparison with the other sophorolipids that were tested and the values obtained are lower than the values reported by Zhang *et al.* [90] The surface tension for the β-D-oleyl sophorose derivative has a surface tension lower than that of the acid form of the sophorolipid and this might be attributed to the lack of the carboxyl group in the C18:1 chain of the β-D-oleyl sophoroside. Furthermore, Gibbs adsorption density Γ_{max} (mol/m^2) values for the methyl ester, ethyl ester and methyl ester-6′,6″-sophorose dibutyrate were measured and the results are tabulated in (Table 6-1). All values (maximum adsorption densities) are similar in size and within the range 3.04×10^{-6} to 1.07×10^{-7} mol/m^2 and the surface area per adsorbed molecule was 85.79-75.23 $^{\circ}$A^2. Whereas, the values for the maximum adsorption density of the lactones sophorolipids are slightly lower than these of its open chain alkyl ester analogues.

This study suggests that desirable surface-active sophorolipids can be synthesised by careful modification of the hydrophilic/lipophilic balance of the natural sophorolipid molecules.

6.3 Results of substrate studies: Are the sophorose derivative, α and β-*p*-nitrophenyl sophorylsides substrates for a α-glucosidase enzyme?

The results of the experiments reported in chapter 4 (see section 4.12) in which sophorolipids were added to the spent fermentation media during the starvation period of the sophorolipid fermentation pointed to the presence of an enzyme which is able to hydrolyse sophorolipids. This enzyme catalyses the hydrolysis of sophorolipids leading to the production of sophorose, isomaltose and glucose with the cleavage of both the 1→2-glycosidic bond and the lipid-glycosidic bond.

189

An attempt was made to provide additional evidence for the presence of this enzyme by preparing an activated colourimetric substrate for use in its detection.

Therefore, an attempt was made to develop a simple colorimetric assay for the enzyme and, in the first part of the development of the assay, a set of experiments were performed to test if the activated α and β-*p*-sophorylsides were substrates for a simple glycosyl hydrolase. Both α and β-*p*-nitrophenyl sophorylsides were tested as substrates for a commercial α-glucosidase (described in section 2.18.1.1). It was hoped that *p*-nitrophenol would be released and an intense yellow colour would be observed if the activated sophorolipids were substrates of the enzyme. Unfortunately, the initial tests were negative and no *p*-nitrophenol was released when either α or β-*p*-nitrophenyl sophorylsides were exposed to the enzyme. In contrast, a positive reaction was observed when α-*p*-nitrophenyl-D-glucopyranoside was used as a control. Failure to observe catalytic activity is likely to simply reflect that the 1→2-linked α or β-*p*-nitrophenyl sophorylsides were not able to bind productively to the active site of the enzyme whose natural substrate is the disaccharide maltose (an alpha-1,4-linked disaccharide).

In an attempt to see if the substrates were able to bind to the enzyme a second set of experiments was conducted (see section 6.4) in which the effect of the presence of α-*p*-nitrophenyl sophorylsides on the hydrolysis of α-*p*-nitrophenyl-D-glucopyranoside was determined.

6.4 Results of inhibition studies: Is the sophorose-derivative, α-*p*-nitrophenyl sophorylside an inhibitor of the α-glucosidase enzyme?

To test for potential inhibition of the enzyme, α or β-*p*-nitrophenyl sophorylsides were added to the enzyme α-glucosidase in the presence of the substrate *p*-nitrophenyl-α-D-glucopyranoside; the colourimetric assays were conducted based on the procedure described in sections 2.19.1.

6.4.1 Inhibition results

The modification of α-glycosidase activity via inhibitors in *vitro* is of an interest due to the involvement of glycosidases in a variety of anabolic and catabolic processes, such as lysosomal catabolism of glycoconjugates and associated degradation of glycoproteins. Glycosidase inhibitors have different beneficial effects as therapeutic agents, such as antifungal agents, insecticides and antivirals [223] in order to test the effect of the α-*p*-nitrophenyl-D-sophorylside, (soph-α-*p*NP) on the activity of α-glycosidase in the presence of the substrate α-*p*-nitrophenyl-D-glucopyranoside (glc-α-*p*NP), three separate experiments were carried out and plots of substrate concentration versus time were measured in the presence of varying amounts of the inhibitors (Figure 6-4). In the control experiment, (Figure 6-5, top curve) the release of *p*-nitrophenol was measured at different time intervals during the hydrolysis of the substrate glc-α-*p*NP, (5 mM) in the absence of soph-α-*p*NP.

In the second experiment, the same reaction was performed with the addition of soph-α-*p*NP, (5 mM), (Figure 6-4, middle curve). From inspection of the curves it is clear that soph-α-*p*NP acts as an inhibitor and there is a reduced release of *p*-nitrophenol at all-time points. In order to understand the type of inhibition being observed, a third experiment was conducted, the concentration of the standard substrate glc-α-*p*NP, 5 mM was kept constant while increasing the concentration of the derivative soph-α-*p*NP to 10 mM. The result (Figure 6-4, bottom curve) revealed that the rate of the catalytic-reaction was further reduced (decrease in the reaction rate). The concentrations of *p*-nitrophenol (Figure 6-5, bottom curve) were also reduced below those observed in the first two experiments. The experimental results confirm that the added derivative soph-α-*p*NP has an inhibitory effect on the hydrolysis of the substrate glc-α-*p*NP. The added soph-α-*p*NP altered the catalytic-activity of the α-glucosidase, through slowing down the rate of the hydrolysis reaction and the release of the *p*-nitrophenol.
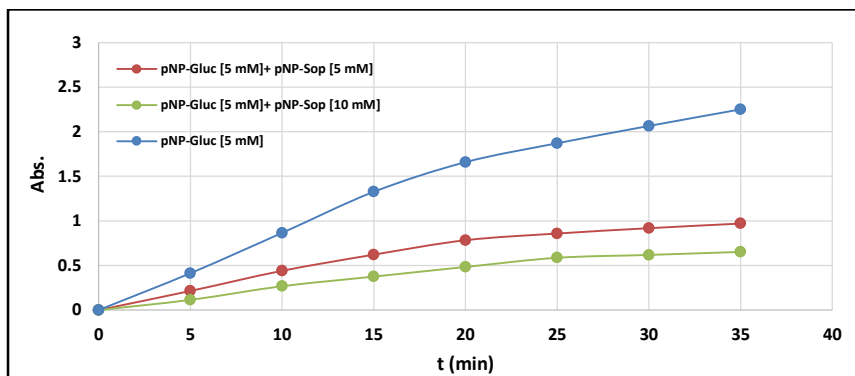
Figure 6-4: Plots of absorbance (Abs.) versus time (min) of the α-glycosidase assay using a constant concentration of substrate glc-α-*p*NP and various concentration of *s*oph-α-*p*NP inhibitor
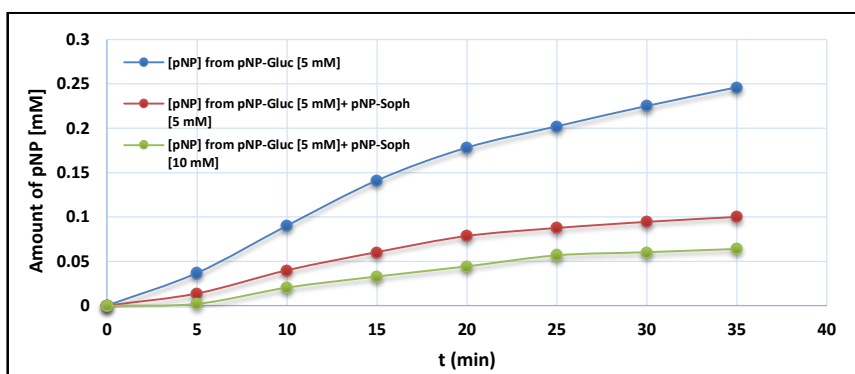
Figure 6-5: Plots of the amount of *p*NP [mM] versus time (min) produced form the three conducted experiments.

6.4.2 Checks to see if α or β-*p*-nitrophenyl sophorylsides could detect enzyme activity in the spent fermentation liquors.

In an attempt to check for the presence of enzymes in the fermentation liquors that were capable of hydrolysing the activated substrate soph-α-*p*NP, the two were incubated together and attempts were made to observe the release of *p*-nitrophenol. Unfortunately, no reaction was observed and as such this line of experimental work was abandoned in favour of studying the biological activity and specifically the anticancer activity of the new sophorolipids, as this area was providing a number of interesting results.

192

6.5 The cell viability and cytotoxicity assays of sophorolipids

The following work was undertaken at the University of Huddersfield and was conducted in the collaboration with the postgraduate researcher Glenn Robinson and with two undergraduate project students (Hanna White and Emily Roddy). The researchers studied the biological activity of a number of sophorolipids in a cell-viability assay using breast adenocarcinoma MCF7 and prostate PC3 cell lines and utilizing an MTT assay. A range of sophoroipid concentrations of (1nM -100 μM) were used and added to the cells for 24, 48, 72 and 96 h incubation.

6.5.1 Result of the cell viability (MTT assay) of sophorolipids derivatives

The results revealed that the selected purified sophorolipids compounds displayed cytotoxic effects against both human breast cancer MCF7 and prostate PC3 cell lines, except the methyl ester sophorolipid, which had an IC$_{50}$: > 100 μM. The cell viability (MTT) data is recorded in Table 6-2. The anti-proliferative activities are expressed as mean values of the growth inhibitory concentration (IC$_{50}$), which is the concentration of the drug required to reduce the cell viability by 50%.

The results revealed that after 96 h of incubation the tested sophorolipids influence cell viability in the following order: oleyl 2″,3',3″,4',4″,6',6″-hepta-*O*-acetyl-β-D-sophoroside > 1',6"-sophorolactone-6'-acetate > methyl ester-6',6"-sophorose dibutyrate > 1',6″-sophorolactone > methyl ester.

The cell lines were most sensitive to oleyl 2″,3',3″,4',4″,6',6″-hepta-*O*-acetyl-β-D-sophoroside; at this moment in time, further work is underway to determine the mechanism of cytotoxicity of the compound used and its deacetylated form.

193

The derivative 1',6"-sophorolactone-6'-acetate was also found to be a potent inhibitor of cell growth suggesting that the lactone ring also has an effect on the cell viability along with the acetate group on position C-6'.

It was also observed that the substitution of a longer chain fatty acid (butyrate) on to the C-6s position in the methyl ester sophorolipid reduced the cell viability. In the assay results, there is clear evidence that the degree of acetylation on the sophorose moiety has an effect on the cell viability. [224-226]

To the best of our knowledge, this is the first time that the biological activity of these sophorolipid derivatives has been studied and cytotoxic responses demonstrated in both MCF7 and PC3 cell lines. These anticancer effects were dose and derivative-dependent.

Table 6-2: IC$_{50}$ (μm) results for different sophorolipid derivatives on the MCF 7 & PC 3 cell lines after 96 h of incubation

Sophorolipid	Average IC$_{50}$ (μM) + S.E.M (μM) MCF7 cell line at 96 h	Average IC$_{50}$ (μM) + S.E.M (μM) PC3 cell line at 96 h
oleyl 2″,3',3″,4',4″,6',6″-hepta-O-acetyl-β-D-sophoroside	6.36 ± 1.13	5.62 ± 0.07
1',6"-sophorolactone-6'-acetate	10.00 ± 1.22	18.40 ± 7.37
Methyl ester-6',6"-sophorose dibutyrate	29.60 ± 5.55	57.80 ± 3.13
1',6″-sophorolactone	52.70 ± 8.59	40.53 ± 6.22
methyl ester	>100	>100

6.5.2 Detailed results of the MTT assay of oleyl 2″,3',3″,4',4″,6',6″-hepta-*O*-acetyl-β-D-sophoroside, oleyl β-D-sophoroside and 1′, 2″, 3′, 3″, 4′, 4″, 6′, 6″-octa-*O*-acetyl-β-D-sophorose

Researchers at Huddersfield also explored the cytotoxic effect of the purified oleyl 2″,3',3″,4',4″,6',6″-hepta-*O*-acetyl-β-D-sophoroside, oleyl-β-D-sophoroside and β-octaacetate-D-sophorose which was used as a control.

The cytotoxicity of these three substrates was examined on both MCF7 and PC3 cell lines after exposure for 24, 48, 72 and 96 h. Cells were treated with sophorolipids at a different concentration ranging from (1nM-100 µM). The IC_{50} values for these derivatives obtained from the MTT assay; the average of four experiments were performed for each time period that was studied.

The IC_{50} results for the first derivative oleyl 2″,3',3″,4',4″,6',6″-hepta-*O*-acetyl-β-D-sophoroside are tabulated (Table 6-3) below:

Table 6-3: IC_{50} (µm) results for the oleyl 2″,3',3″,4',4″,6',6″-hepta-*O*-acetyl-β-D-sophoroside on the MCF7 cell line after 24, 48, 72 & 96 h of incubation

Incubation period (h)	Average IC_{50} (µM) + S.E.M (µM) MCF7 cell line	Average IC_{50} (µM) + S.E.M (µM) PC3 cell line
24	29.82 ± 9.24	Cells more than 50 % viable
48	11.23 ± 3.77	11.88 ± 2.23
72	8.69 ± 1.04	9.00 ± 1.62
96	4.78 ± 0.85	5.82 ± 1.98

195

The IC_{50} results show a correlation between the concentrations of the sophorolipids used and cell viability. The results in (Table 6-3) show a decrease in the IC_{50} from 29.8 µM after 24 h to 4.8 µM after 96 h for the MCF7 cell line.

The IC_{50} values after 96 h period confirmed that oleyl 2″,3',3″,4',4″,6',6″-hepta-*O*-acetyl-β-D-sophoroside has a significant cytotoxic effect. Whereas, the IC_{50} results for the PC3 cell line assay were slightly different: cells were 50 % viable at 24h of incubation whilst between 48 and 96 h of incubation the compound demonstrated a large reduction in the IC_{50}.

To test the cytotoxic effect of the deacetylated oleyl β-D-sophorose and to study the effect of the substituted acetate groups on the sophorose moiety, the MTT assay was also conducted for this corresponding sophorolipid derivative.

The IC_{50} results for the oleyl β-D-sophorose on the PC3 and MCF7 cell lines after 24, 48, 72 & 96 h of incubation showed that the percentage cell viability does not reduce below 50% for all of the tested drug concentrations. The results revealed that the drug has no cytotoxic effect against those cell lines in stark comparison to that of the corresponding acetylated sophorolipid: oleyl 2″,3',3″,4',4″,6',6″-hepta-*O*-acetyl-β-D-sophoroside.

According to the Cancer Research UK, a lead compound in a cancer study must have an IC_{50} <10 µM. [227] A study was conducted by Shao and co-workers in 2012 [73] who demonstrated cytotoxicity of sophorolipids on esophageal cancer cells. They also demonstrated that the activity of the sophorolipids was dependent on the degree of acetylation present within the molecule. [225] For example, the diacylated sophorolipids were found to have much anti-tumour activity than monoacylated sophorolipids. This suggests that the number of acetate groups present in the compound correlates with an increase in cytotoxicity. They also reported that acidic sophorolipids were less cytotoxic compared to lactonic sophorolipids.

Finally, the cytotoxic effect of the control compound β-octaacetate-D-sophorose was also investigated using the MTT assay. Sophorose octaacetate was also chosen as a control when conducting the MTT assay of sophorolipids in order to study the effect of the substituted acetate group on the cell viability.

The MTT results on cell lines after 24, 48, 72 & 96 h of incubation showed that the percentage cell viability does not reduce below 50% for all of the tested concentrations. Therefore, the results revealed that there is no cytotoxicity against these cell lines which again is in sharp contrast to the results, which was observed for the corresponding acetylated sophorolipid, oleyl 2″,3',3″,4',4″,6',6″-hepta-O-acetyl-β-D-sophoroside

The lack of any cytotoxic activity for the β-octaacetate-D-sophorose might be attributing to the absence of the C18:1 fatty acid chain. It has previously been shown that cytotoxicity changes with different degrees of unsaturation present in the fatty acid section of sophorolipids. Sophorolipids with a fatty acid chain containing one double bond were shown to be the most effective, whereas no double bonds proved to be the least effective. [218,225]

6.5.3 Cell lysis microscopic results of MCF7 and PC3

Researchers at Huddersfield also studied cell lysis for MCF7 and PC3 cell lines before and after the treatment with the sophorolipid, oleyl 2″,3',3″,4',4″,6',6″-hepta-O-acetyl-β-D-sophoroside by analysis of microscopic images. The microscopic images obtained by the researchers showed the cultured cells before and after cell lysis. On exposure to oleyl 2″,3',3″,4',4″,6',6″-hepta-O-acetyl-β-D-sophoroside there is a significant difference in the number of cells when comparing cells in the media at 0h and 48 h for both MCF7 and PC3 as shown in (Figures 6-6 & 7).

197

MCF7-cells in media 0 h, 20 x magnification

MCF7-cells in media 48h, 20 x magnification

MCF7-cells in ethanol 48h, 20x magnification

MCF7-cells with drug 59. 6µM 48h, 20x mag
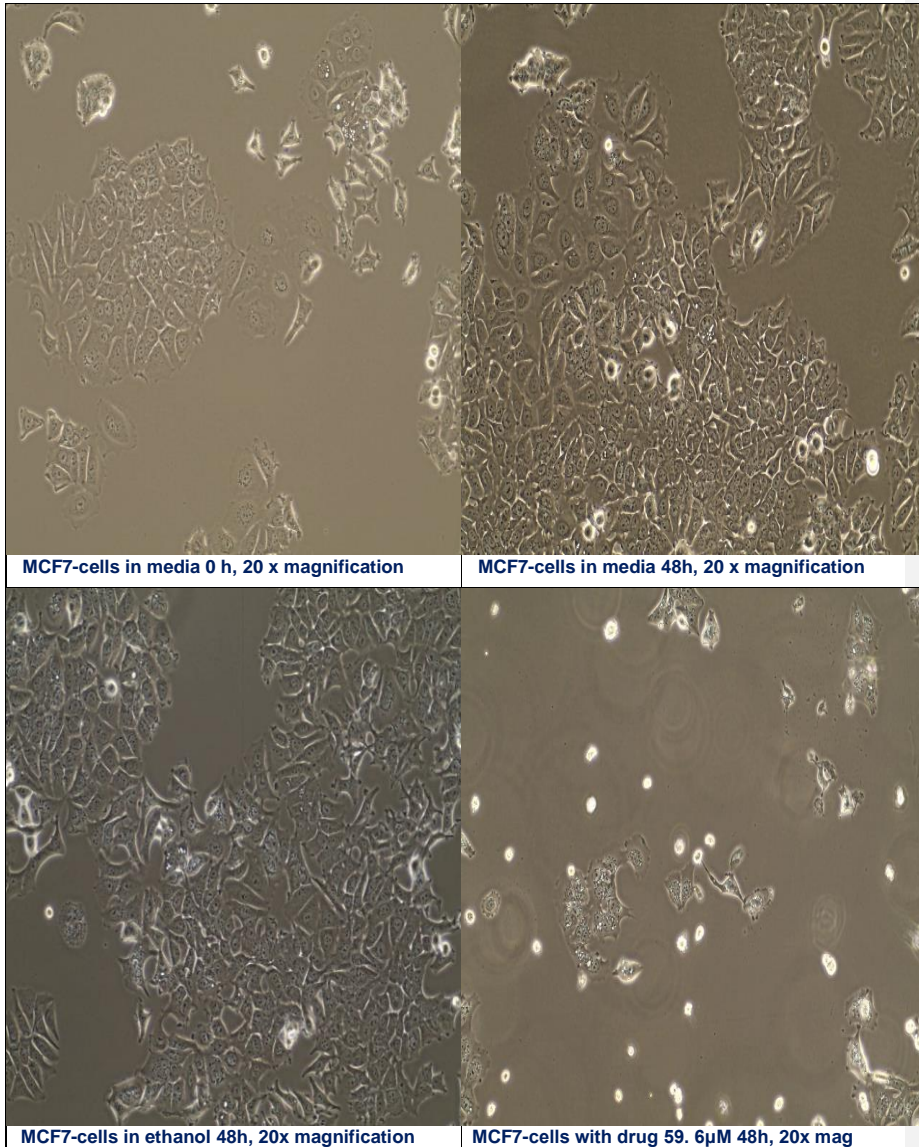
Figure 6-6 Microscopic images depicting MCF7-cells treated with media, ethanol, and sophorolipid oleyl 2″,3',3″,4',4″,6',6″-hepta-*O*-acetyl-β-D-sophoroside after 48 h.

PC3-cells in media 48 h, 20 x magnification

PC3-cells in ethanol 48 h, 20x magnification

PC3-cells with drug 14.21 µM, 48 h, 20 x magn.

PC3-cells with drug 28.42 µM, 48 h, 20x magn.
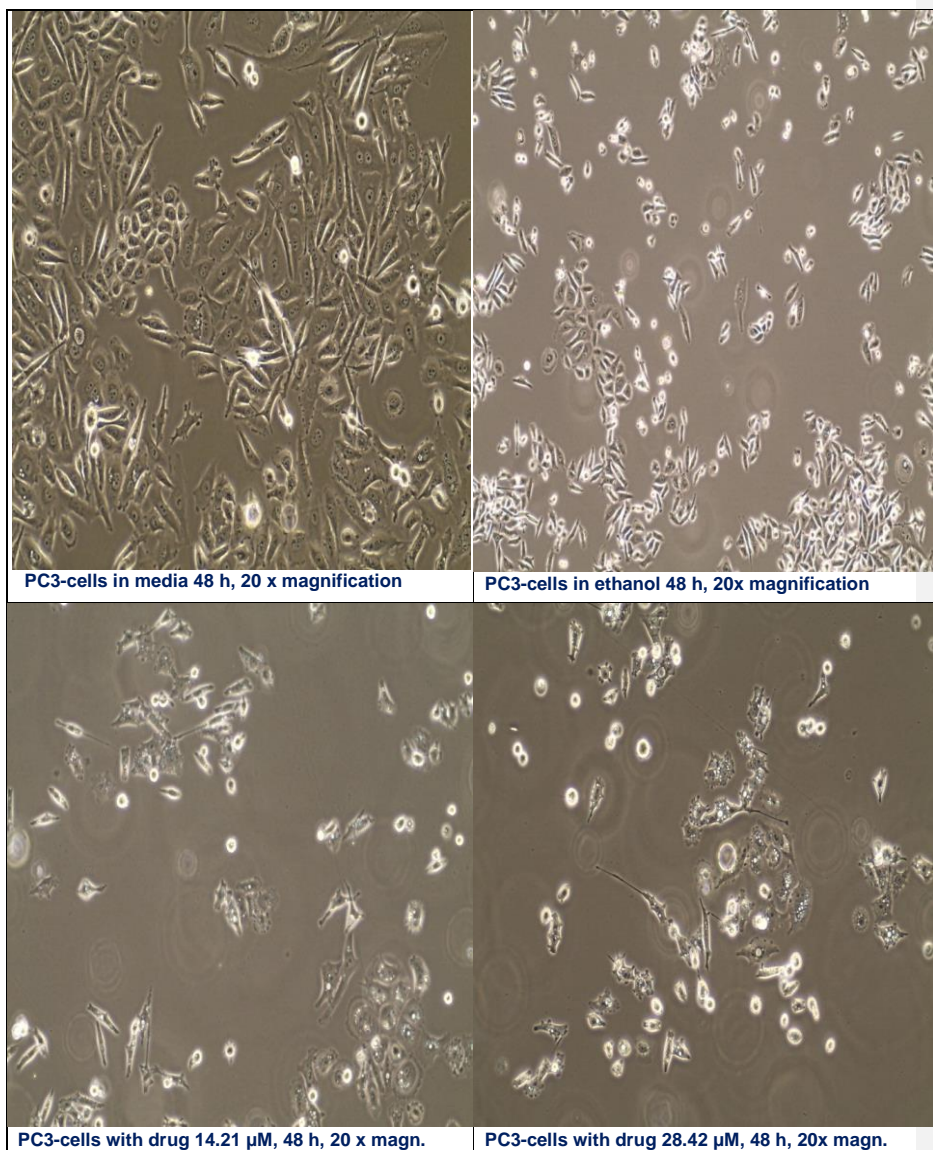
Figure 6-7: Microscopic images depicting PC3-cells treated with media, ethanol, and sophorolipid oleyl 2″,3',3″,4',4″,6',6″-hepta-*O*-acetyl-β-D-sophoroside after 48 h.

The microscopic images in (Figure 6-6) show that very few cells remaining viable after treatment with the sophorolipid (59.6 µM, 48 h), in comparison to cells in media and in ethanol, which show that MCF7 where cells were still intact. On close inspection of the images, the structure of the cells, show evidence of cell blebbing. Cell blebbing occurs in apoptotic cells when the plasma membrane protrudes from the cell due to the localised decoupling of the cytoskeleton from the plasma membrane. [228]

The shape of the MCF7 cells in media was well structured, whereas the cells treated with the drug after 48h are a more circular, disordered-like shape and the number of cells was reduced due to the blebbing effect.

A similar story was observed for the PC3 cell line (Figure 6-7); from the microscopic images obtained after exposure to oleyl 2″,3',3″,4',4″,6',6″-hepta-*O*-acetyl-β-D-sophoroside. It is clear that whilst there are many intact PC3 cells present in the media and in ethanol after 48 h treatment with 14.21 µM of the sophorolipid oleyl 2″,3',3″,4',4″,6',6″-hepta-*O*-acetyl-β-D-sophoroside, the number of cells has decreased dramatically with a high amount of bleb action occurring. Although there are still a small number of cells present, there doesn't seem to be any new cell growth. The addition of the 28.42 µM of the sophorolipid resulted in a distinct lack of cells present in the image. All cell shapes suggest that apoptosis is occurring due to the presence of swollen areas indicating blebbing.

6.6 Conclusion

The interfacial properties of classical sophorolipids and their derivatives were evaluated successfully. The results indicated that the lactone sophorolipid derivatives have lower surface tension and CMC values than the open chain acidic analogues and the oleyl β-D-sophoroside. The methyl ester, ethyl ester and methyl ester-6′,6″-sophorose dibutyrate showed the lowest surface tension values.

The enzyme-substrate studies for α-glucosidase utilizing the 4-nitrophenyl-α/β-sophorylsides didn't provide the expected results: they were inhibitors of the enzyme and not substrates. The use of the activated sophorose derivatives to check for glycosyl-hydrolase activity in spent fermentation media did not provide a positive result.

Finally, the biological activity of different sophorolipids derivatives on MCF7 and PC3 cell lines was investigated. Most of the sophorolipids displayed inhibitory activity, except the methyl ester sophorolipid, which has an IC_{50}: >100 µM. These anticancer responses were both dose and derivative dependent. The results showed that cell lines were most sensitive to the oleyl 2″,3',3″,4',4″,6',6″-hepta-O-acetyl-β-D-sophoroside, which was capable of causing the death of MCF7 & PC3 cells giving an IC_{50} value of 5.82 µM and 4.78 µM at 96 h, respectively. The study showed that increasing the contact time decreases the IC_{50}, meaning that a lower drug dose can be administered over an extended period of time.

7. Overall conclusions and future work

7. Overall conclusions

A variety of analytical techniques namely (NMR, FTIR, HPLC-MS, GC-MS, and HPAEC-PAD) were used for structure elucidation and characterisation of a number of natural sophorolipids, which were obtained from Croda Biotechnology. Two main forms were found as the natural diacetylated lactone which is esterified at the C-4" position of sophorose and the acid form, which was produced by the alkaline treatment of the lactone form.

In addition, a range of novel sophorose derivatives have been synthesised. These novel molecules have been prepared via the lipase Novozyme 435 catalysed acylation reaction of the sophorolipid methyl ester producing a range of lactone derivatives include, 1′,6″-sophorolactone and 1′,6″-lactone-6′-acetate as well as open chain sophorolipids with either acetate or butyrate groups substituted on the C-6s, *i,e.,* the primary hydroxy at the reducing and non-reducing glucose of sophorose.

The HPAEC-PAD and GC-MS analysis confirmed the monosaccharide composition of the natural sophorolipids as glucose and that glucose is the only monosaccharide present. Furthermore, the type of the glycosidic linkage in sophorolipids and sophorose was confirmed by GC-MS as a β (1→2)-link, whereas the linkage in isomaltose was identified as α (1→6)-link.

The valuable sugar sophorose was isolated from the lactone waste stream as a pure form in gram scale quantities using a very simple solvent extraction method, requiring only water; the crude products were separated using a charcoal: celite column. Evidence has been provided, which suggested that sophorose is generated by an enzyme catalysed hydrolysis of sophorolipids.
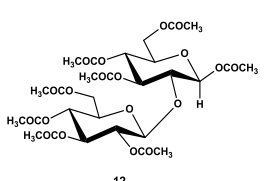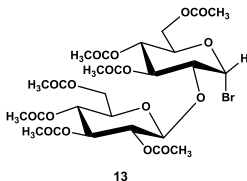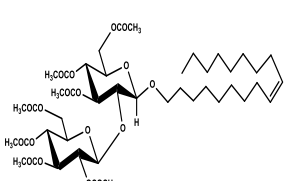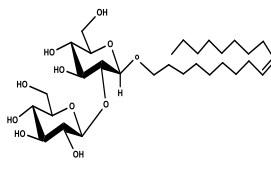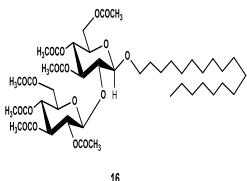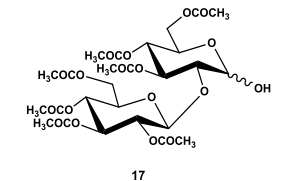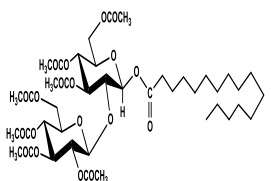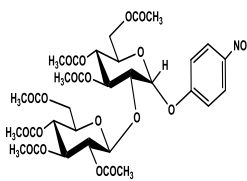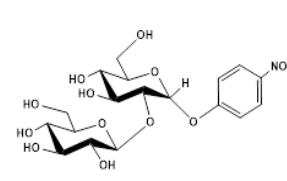
When treated with aqueous alkali, sophorose underwent epimerisation: the alkaline treatment of sophorose led to the formation of the new disaccharide 2-*O*-β-D-glucopyranosyl-D-mannose, which was successfully isolated in a pure form using the charcoal: celite column.

Moreover, the alkaline hydrolysis of the acid sophorolipids was carefully investigated in an attempt to prove that sophorose, isomaltose and glucose

were present in the lactone waste. These results were correlated with those obtained when utilizing sophorolipids as a carbon-feed source during the starvation period (lag phase) of a sophorolipid fermentation, which pointed to the presence of an enzyme that is capable of hydrolysing sophorolipids into glucolipid, sophorose, isomaltose and glucose.

In extending this work, sophorose was successfully employed in a sequence of chemical synthesis steps to produce a number of novel sophorolipids. The chemical structure of these novel sophorolipids are shown below in (Table 7-1):

Table 7-1: The chemical structures of novel sophorolipids

12

1′, 2″, 3′, 3″, 4′, 4″, 6′, 6″-octa-*O*-acetyl-β-D-sophorose

13

2″,3′,3″,4′,4″,6′,6″-hepta-*O*-acetyl-α-D-sophoryl bromide

Oleyl 2″, 3′, 3″, 4′, 4″, 6′, 6″-hepta-*O*-acetyl-β-oleyl-D-sophorose

15

oleyl β-D-sophoroside, CMC= 1.01 mM and γ_{CMC} =34.82 mN/m

16

stearyl 2″, 3′, 3″, 4′, 4″, 6′, 6″-hepta-*O*-acetyl-β-D-sophoroside

17

2″, 3′, 3″, 4′, 4″, 6′, 6″-hepta-*O*-acetyl-α/β-D-sophorose

18

2″, 3′, 3″, 4′, 4″, 6′, 6″-hepta-*O*-acetyl-1′-O-palmitoyl-β-D-sophoroside

19

2″, 3′, 3″, 4′, 4″, 6′, 6″-hepta-*O*-acetyl-α-(4-nitrophenyl)-D-sophorose

20

4-nitrophenyl-α-D-sophoroside

21 2″, 3′, 3″, 4′, 4″, 6′, 6″-hepta-*O*-acetyl-β-(4-nitrophenyl)-D-sophorose	**22** 4-nitrophenyl-β-D-sophoroside	**SL-Me-6,6-dibutyrate, 8** SL-Me-6′, 6″-dibutyrate, CMC= 0.40 mM and γ$_{CMC}$ =30.00 mN/m
SL-1′,6″-lactone-6′-acetate, 7 CMC= 0.31 mM and γ$_{CMC}$ =32.08 mN/m	**SL-1′,6″-Lactone, 6** CMC= 0.33 mM and γ$_{CMC}$ =32.15 mN/m	**SL-Et, 5** CMC= 0.72 mM and γ$_{CMC}$ =29.40 mN/m
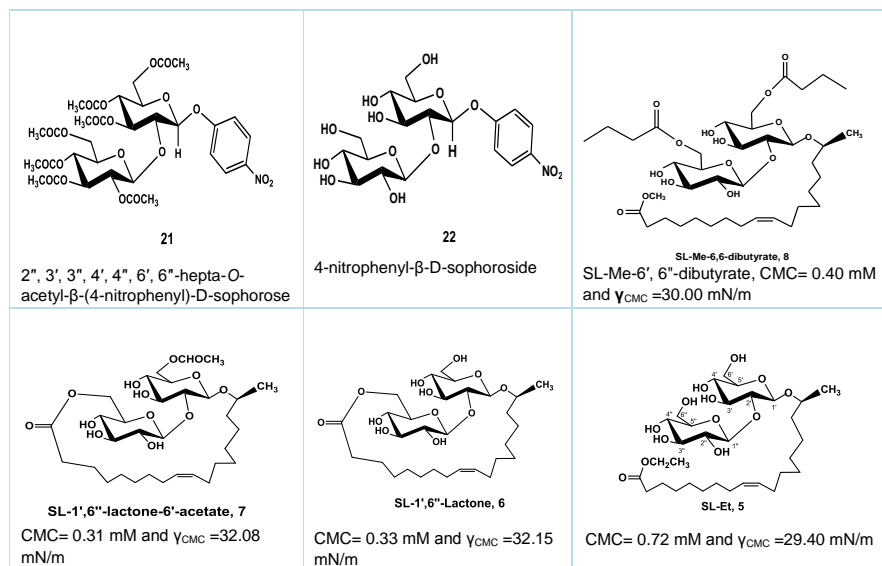
Once the novel sophorolipids has been produced and characterised, their potential applications were fully investigated. The interfacial surface properties were studied and it was found that the open chain alkyl ester derivatives namely methyl ester, ethyl ester and methyl ester-6',6"-sophorose dibutyrate have a reduced surface tension γ $_{CMC}$ values of 31.10, 29.40 and 30.00 mN/m of the parent sophorolipid and are more soluble in water with foam formation being observed. The lactone sophorolipid derivatives; 1′,4″-sophorolactone, 1′,6″-sophorolactone and 1′,6″-sophorolactone-6′-acetate also reduced the surface tension, γ $_{CMC}$ values of 31.60, 32.15 and 32.08 mN/m respectively and were more effective at reducing the surface tension of water than the acid sophorolipid and β-D-olely sophorose, but not effective as the alkylated ester derivatives. They are sparingly soluble in water with less foam formation being observed.

The lactone sophorolipids were found to be more active for many of the proposed applications than the acid form. The number of acetyl groups on the C-6s position of sophorose moiety proved to be important in influencing the surface activity of sophorolipids. The study concluded that the desirable

surface activity can be controlled by the adjustment of the hydrophilic/lipophilic balance of the methyl ester sophorolipids.

The enzyme substrate studies confirmed that the 4-nitrophenyl-α-D-sophoroside derivative has inhibitory activity against the α-glucosidase from *Saccharomyces cerevisiae* in the presence of the standard substrate 4-nitrophenyl-α-D-glucoside. It can act as a non-competitive inhibitor via reducing the rate of the hydrolysis reaction of the standard substrate.

Finally, the anticancer activity of the newly synthesised sophorolipids was investigated in a separate programme of work using MCF7 and PC3 cell lines. The MTT assay results confirmed that the sophorolipids possess antitumor activity as the IC_{50} results indicated that the purified compounds displayed potent growth inhibitory activity against these cell lines. After 96 h of incubation the tested sophorolipids influence cell viability in the following order:

2″,3′,3″,4′,4″,6′,6″-hepta-*O*-acetyl-β-oleyl-D-sophorose > 1′,6″-sophorolactone-6′-acetate > methyl ester-6′,6″-sophorose dibutyrate > 1′,6″-sophorolactone > methyl ester and the average IC_{50} (μM) values for MCF 7 cell line; 6.36, 10.00, 29.60, 52.70 and > 100 respectively, whereas the average IC_{50} (μM) values for PC 3 were; 5.62, 18.40, 57.80, 40.53 and > 100 respectively.

The MTT results indicated that the cell lines used were most sensitive to the 2″,3′,3″,4′,4″,6′,6″-hepta-*O*-acetyl-β-oleyl-D-sophorose, which was capable of causing the death of MCF7 & PC3 cells giving an IC_{50} value of 5.82 μM and 4.78 μM at 96 h, respectively. Whereas the results for the β-octacetate-D-sophorose derivative revealed that there is no cytotoxicity against cell lines, which again is in sharp contrast to the results, which was observed for the corresponding acetylated sophorolipid, 2″,3′,3″,4′,4″,6′,6″-hepta-*O*-acetyl-D-sophorose. Therefore, sophorolipids represent a distinctive and novel class of drugs, which maybe a significant promising therapy against different type of cancers.

7.1 Future work

Further work is required to isolate the active enzyme(s) present in the sophorolipid spent fermentation liquor, and which can metabolise (hydrolyses) sophorolipids under the condition of starvation. This work requires multiple extraction and purification processes to be conducted on both sophorolipids' cells and the fermentation liquor. The first step of the purification process, involves the cells disruption/cell lysis to isolate the protein of interest using the following methods: ultra-sonication, homogenization under high pressure and freezing & thawing. If the protein of interest is secreted into the fermentation liquor, a common process is to isolate the protein by precipitation using an increased amount of ammonium sulphate and then collecting different protein fractions after precipitation and subjecting them for dialysis to remove the ammonium sulphate. The precipitated protein fractions can be characterised and separated based on charge or hydrophobicity using an ion-exchange or affinity chromatographic techniques.

Other further studies are required to define the precise mechanisms involved in the cytotoxic effect induced by the sophorolipids using different cancer cell lines and studying the cytotoxic effect of sophorolipids on healthy cell-lines too.

Some novel sophorolipids have been prepared in this work, however, further work is again required to modify the chemical structure of natural sophorolipids to produce more novel derivatives using the enzymatic synthesis pathway or starting from sophorose as a substrate and using chemical modification then it would be of interest to study their antimicrobial activity.

It would also be of interest to explore the synthesis of novel gemini (dimeric) sophorolipids as a new variety of glycolipid biosurfactants. Gemini surfactants are composed of two hydrophobic parts (aliphatic chain or aromatic moiety) and two polar head groups (two cationic/anionic or sugar moiety).

206

A proposed synthetic gemini sophorolipid is shown in figure (7-1). These can be synthesised starting from sophorose as the amphiphilic head group connected by a spacer group (linking units) or via a chemical modification of the natural sophorolipids into oligomeric surfactants. The spacer group may be hydrophobic (aliphatic chain or aromatic) or hydrophilic (polyether). Gemini surfactants are more effective than the corresponding traditional surfactants in reducing the surface tension of water and possess better foaming, wetting and cleansing properties.
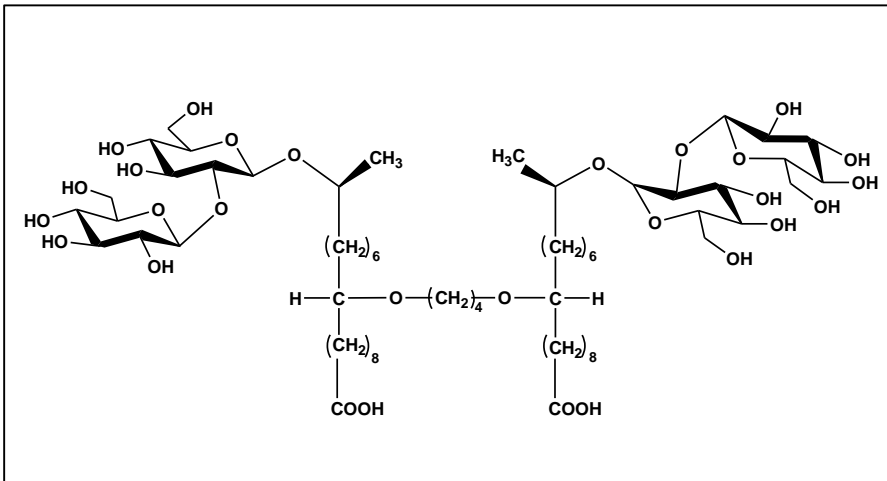
Figure 7-1: The chemical structure of a proposed gemini sophorolipid

8. References and publication

8. References

(1) Finnerty, W. R. Biosurfactants in environmental biotechnology. *Current Opinion in Biotechnology* **1994**, *5*, 291-295.

(2) Mulligan, C. N. Environmental applications for biosurfactants. *Environmental Pollution* **2005**, *133*, 183-198.

(3) Nelson, R. Application of surfactants in the petroleum industry. *Journal of the American Oil Chemists Society* **1982**, *59*, 823A-826A.

(4) Mishra, M.; Muthuprasanna, P.; Prabha, K. S.; Rani, P. S.; Satish, I. A.; Ch, I. S.; Arunachalam, G.; Shalini, S. *Basics and Potential Applications of Surfactants*-a Review. **2009**, online available at: http://citeseerx.ist.psu.edu/ /viewdoc/summary/doi=10.1.1.545.7183.

(5) Mann, R.; Bidwell, J. The acute toxicity of agricultural surfactants to the tadpoles of four Australian and two exotic frogs. *Environmental pollution* **2001**, *114*, 195-205.

(6) Mann, R. M.; Boddy, M. R. Biodegradation of a nonylphenol ethoxylate by the autochthonous microflora in lake water with observations on the influence of light. *Chemosphere* **2000**, *41*, 1361-1369.

(7) Rosenberg, E.; Ron, E. High-and low-molecular-mass microbial surfactants. *Applied microbiology and biotechnology* **1999**, *52*, 154-162.

(8) Desai, J. D.; Banat, I. M. Microbial production of surfactants and their commercial potential. *Microbiology and Molecular biology reviews* **1997**, *61*, 47-64.

(9) Saharan, B.; Sahu, R.; Sharma, D. A review on biosurfactants: fermentation, current developments and perspectives. *Genetic Engineering and Biotechnology Journal* **2011**, *2011*, 1-14.

(10) Guerra-Santos, L.; Käppeli, O.; Fiechter, A. Pseudomonas aeruginosa biosurfactant production in continuous culture with glucose as carbon source. *Applied and Environmental Microbiology* **1984**, *48*, 301-305.

(11) Hisatsuka, K.-i.; Nakahara, T.; Sano, N.; Yamada, K. Formation of rhamnolipid by Pseudomonas aeruginosa and its function in hydrocarbon fermentation. *Agricultural and Biological Chemistry* **1971**, *35*, 686-692.

(12) Banat, I. M.; Makkar, R. S.; Cameotra, S. Potential commercial applications of microbial surfactants. *Applied Microbiology and Biotechnology* **2000**, *53*, 495-508.

(13) Greek, B. F. Detergent industry ponders products for a new decade. *Chemical & Engineering News* **1990**, *68*, 37-41.

(14) Inès, M.; Dhouha, G. Glycolipid biosurfactants: Potential related biomedical and biotechnological applications. *Carbohydrate Research* **2015**, *416*, 59-69.

(15) Yoo, D.S.; Lee, B.S.; Kim, E.K. Characteristics of microbial biosurfactant as an antifungal agent against plant pathogenic fungus. *Journal of Microbiology and Biotechnology* **2005**, *15*, 1164-1169.

(16) Lee, Y.-J.; Choi, J.-K.; Kim, E.-K.; Youn, S.-H.; Yang, E.-J. Field experiments on mitigation of harmful algal blooms using a Sophorolipid-Yellow clay mixture and effects on marine plankton. *Harmful Algae* **2008**, *7*, 154-162.

(17) Isoda, H.; Kitamoto, D.; Shinmoto, H.; Matsumura, M.; Nakahara, T. Microbial extracellular glycolipid induction of differentiation and inhibition of the protein kinase C activity of human promyelocytic leukemia cell line HL60. *Bioscience, Biotechnology, and Biochemistry* **1997**, *61*, 609-614.

(18) Chen, J.; Song, X.; Zhang, H.; Qu, Y. Production, structure elucidation and anticancer properties of sophorolipid from Wickerhamiella domercqiae. *Enzyme and Microbial Technology* **2006**, *39*, 501-506.

(19) Anderson, D.; Stefani, A. The degradation of acidic polysaccharides during structural analysis involving permethylation. *Analytica Chimica Acta* **1979**, *105*, 147-152.

(20) Tadros, T. F.: *Applied Surfactants: principles and applications*; John Wiley & Sons, **2006**.

(21) Tadros, T. F.: *Encyclopedia of Colloid and Interface Science*; Springer, **2013**.

(22) Joshi, S.; Bharucha, C.; Desai, A. J. Production of biosurfactant and antifungal compound by fermented food isolate Bacillus subtilis 20B. *Bioresource Technology* **2008**, *99*, 4603-4608.

(23) Greek, B. Sales of detergents growing despite recession. *Chemical & Engineering News* **1991**, *69*, 25-&.

(24) Bognolo, G. Biosurfactants as emulsifying agents for hydrocarbons. *Colloids and Surfaces A: Physicochemical and Engineering Aspects* **1999**, *152*, 41-52.

(25) Saerens, K. M.; Roelants, S. L.; Van Bogaert, I. N.; Soetaert, W. Identification of the UDP-glucosyltransferase gene UGTA1, responsible for the first glucosylation step in the sophorolipid biosynthetic pathway of Candida bombicola ATCC 22214. *FEMS Yeast Research* **2011**, *11*, 123-132.

(26) Saerens, K. M.; Zhang, J.; Saey, L.; Van Bogaert, I. N.; Soetaert, W. Cloning and functional characterization of the UDP-glucosyltransferase UgtB1 involved in sophorolipid production by Candida bombicola and creation of a glucolipid-producing yeast strain. *Yeast* **2011**, *28*, 279-292.

(27) Breithaupt, T.; Light, R. Affinity chromatography and further characterization of the glucosyltransferases involved in hydroxydocosanoic acid sophoroside production in Candida bogoriensis. *Journal of Biological Chemistry* **1982**, *257*, 9622-9628.

(28) Esders, T. W.; Light, R. J. Glucosyl-and acetyltransferases involved in the biosynthesis of glycolipids from Candida bogoriensis. *Journal of Biological Chemistry* **1972**, *247*, 1375-1386.

(29) Bucholtz, M.; Light, R. Acetylation of 13-sophorosyloxydocosanoic acid by an acetyltransferase purified from Candida bogoriensis. *Journal of Biological Chemistry* **1976**, *251*, 424-430.

(30) Ito, S.; Kinta, M.; Inoue, S. Growth of Yeasts on n-Alkanes: Inhibition by a Lactonic Sophorolipid Produced by. *Agricultural and Biological Chemistry* **1980**, *44*, 2221-2223.

(31) Inoue, S.; Ito, S. Sophorolipids from Torulopsis bombicola as microbial surfactants in alkane fermentations. *Biotechnology Letters* **1982**, *4*, 3-8.

(32) Otto, R.; Daniel, H.-J.; Pekin, G.; Müller-Decker, K.; Fürstenberger, G.; Reuss, M.; Syldatk, C. Production of sophorolipids from whey. *Applied Microbiology and Biotechnology* **1999**, *52*, 495-501.

(33) Casas, J.; García-Ochoa, F. Sophorolipid production by Candida bombicola: Medium composition and culture methods. *Journal of Bioscience and Bioengineering* **1999**, *88*, 488-494.

(34) Rahman, K.; Rahman, T. J.; McClean, S.; Marchant, R.; Banat, I. M. Rhamnolipid Biosurfactant Production by Strains of Pseudomonas aeruginosa Using Low-Cost Raw Materials. *Biotechnology Progress* **2002**, *18*, 1277-1281.

(35) Neto, D. C.; Meira, J. A.; de Araújo, J. M.; Mitchell, D. A.; Krieger, N. Optimization of the production of rhamnolipids by Pseudomonas aeruginosa UFPEDA 614 in solid-state culture. *Applied microbiology and biotechnology* **2008**, *81*, 441-448.

(36) Chen, J.; Song, X.; Zhang, H.; Qu, Y. B.; Miao, J. Y. Sophorolipid produced from the new yeast strain Wickerhamiella domercqiae induces apoptosis in H7402 human liver cancer cells. *Applied Microbiology and Biotechnology* **2006**, *72*, 52-59.

(37) Asmer, H.-J.; Lang, S.; Wagner, F.; Wray, V. Microbial production, structure elucidation and bioconversion of sophorose lipids. *Journal of the American Oil Chemists' Society* **1988**, *65*, 1460-1466.

(38) Hall, P. J.; Haverkamp, J.; Van Kralingen, C. G.; Schmidt, M.: Sepharose lipid surfactants and nonionic surfactants. *Google Patents*, **1996**.

210

(39) Felse, P. A.; Shah, V.; Chan, J.; Rao, K. J.; Gross, R. A. Sophorolipid biosynthesis by Candida bombicola from industrial fatty acid residues. *Enzyme and Microbial Technology* **2007**, *40*, 316-323.

(40) Kitamoto, D.; Yanagishita, H.; Shinbo, T.; Nakane, T.; Kamisawa, C.; Nakahara, T. Surface active properties and antimicrobial activities of mannosylerythritol lipids as biosurfactants produced by Candida antarctica. *Journal of Biotechnology* **1993**, *29*, 91-96.

(41) Morita, T.; Konishi, M.; Fukuoka, T.; Imura, T.; Kitamoto, D. Production of glycolipid biosurfactants, mannosylerythritol lipids, by Pseudozyma siamensis CBS 9960 and their interfacial properties. *Journal of Bioscience and Bioengineering* **2008**, *105*, 493-502.

(42) Jarvis, F.; Johnson, M. A glyco-lipide produced by Pseudomonas aeruginosa. *Journal of the American Chemical Society* **1949**, *71*, 4124-4126.

(43) Lang, S.; Philp, J. C. Surface-active lipids in rhodococci. *Antonie van leeuwenhoek* **1998**, *74*, 59-70.

(44) Kakinuma, A.; Ouchida, A.; Shima, T.; Sugino, H.; Isono, M.; Tamura, G.; Arima, K. Confirmation of the structure of surfactin by mass spectrometry. *Agricultural and Biological Chemistry* **1969**, *33*, 1669-1671.

(45) Arima, K.; Kakinuma, A.; Tamura, G. Surfactin, a crystalline peptidelipid surfactant produced by Bacillussubtilis: Isolation, characterization and its inhibition of fibrin clot formation. *Biochemical and Biophysical Research Communications* **1968**, *31*, 488-494.

(46) Käppeli, O.; Finnerty, W. Partition of alkane by an extracellular vesicle derived from hexadecane-grown Acinetobacter. *Journal of Bacteriology* **1979**, *140*, 707-712.

(47) Käppeli, O.; Walther, P.; Mueller, M.; Fiechter, A. Structure of the cell surface of the yeast Candida tropicalis and its relation to hydrocarbon transport. *Archives of Microbiology* **1984**, *138*, 279-282.

(48) Beebe, J. L.; Umbreit, W. Extracellular lipid of Thiobacillus thiooxidans. *Journal of Bacteriology* **1971**, *108*, 612.

(49) Rosenberg, E.; Rubinovitz, C.; Legmann, R.; Ron, E. Purification and chemical properties of Acinetobacter calcoaceticus A2 biodispersan. *Applied and Environmental Microbiology* **1988**, *54*, 323-326.

(50) Cirigliano, M. C.; Carman, G. M. Isolation of a bioemulsifier from Candida lipolytica. *Applied and Environmental Microbiology* **1984**, *48*, 747-750.

(51) Lipid library resources, online available at :http://lipidlibrary.aocs.org/.

(52) Chamanrokh, P.; Assadi, M. M.; Amoabediny, G.; Rashedi, H. Cleaning oil-contaminated vessel by emulsan producers (autochthonous bacteria). *Iranian Journal of Environmental Health Science & Engineering* **2010**, *7*, 209-222.

(53) Gorin, P.; Spencer, J.; Tulloch, A. Hydroxy fatty acid glycosides of sophorose from Torulopsis magnoliae. *Canadian Journal of Chemistry* **1961**, *39*, 846-855.

(54) Tulloch, A.; Spencer, J.; Deinema, M. A new hydroxy fatty acid sophoroside from Candida bogoriensis. *Canadian Journal of Chemistry* **1968**, *46*, 345-348.

(55) Spencer, J.; Gorin, P.; Tulloch, A. Torulopsis bombicola sp. n. *Antonie van Leeuwenhoek* **1970**, *36*, 129-133.

(56) Van Bogaert, I. N. A.; Zhang, J.; Soetaert, W. Microbial synthesis of sophorolipids. *Process Biochemistry* **2011**, *46*, 821-833.

(57) The World's Largest Fungal Culture Collection, online available at: http://www.cbs.knaw.nl/collections/Biolomics.

(58) Davila, A.; Marchal, R.; Monin, N.; Vandecasteele, J. Identification and determination of individual sophorolipids in fermentation products by gradient elution high-performance liquid chromatography with evaporative light-scattering detection. *Journal of Chromatography A* **1993**, *648*, 139-149.

(59) Develter, D. W.; Lauryssen, L. M. Properties and industrial applications of sophorolipids. *European journal of Lipid Science and Technology* **2010**, *112*, 628-638.

(60) Shah, V.; Doncel, G. F.; Seyoum, T.; Eaton, K. M.; Zalenskaya, I.; Hagver, R.; Azim, A.; Gross, R. Sophorolipids, microbial glycolipids with anti-human immunodeficiency virus and sperm-immobilizing activities. *Antimicrobial Agents and Chemotherapy* **2005**, *49*, 4093-4100.

(61) Göbbert, U.; Lang, S.; Wagner, F. Sophorose lipid formation by resting cells of Torulopsis bombicola. *Biotechnology Letters* **1984**, *6*, 225-230.

(62) Davila, A.-M.; Marchal, R.; Vandecasteele, J.-P. Sophorose lipid production from lipidic precursors: predictive evaluation of industrial substrates. *Journal of Industrial Microbiology* **1994**, *13*, 249-257.

(63) Lottermoser, K.; Schunck, W. h.; Asperger, O. Cytochromes P450 of the sophorose lipid-producing yeast Candida apicola: Heterogeneity and polymerase chain reaction-mediated cloning of two genes. *Yeast* **1996**, *12*, 565-575.

(64) Van Bogaert, I. N.; Demey, M.; Develter, D.; Soetaert, W.; Vandamme, E. J. Importance of the cytochrome P450 monooxygenase CYP52 family for the sophorolipid-producing yeast Candida bombicola. *FEMS Yeast Research* **2009**, *9*, 87-94.

(65) Van Bogaert, I. N.; Roelants, S.; Develter, D.; Soetaert, W. Sophorolipid production by Candida bombicola on oils with a special fatty acid composition and their consequences on cell viability. *Biotechnology Letters* **2010**, *32*, 1509-1514.

(66) Van Bogaert, I. N.; Saerens, K.; De Muynck, C.; Develter, D.; Soetaert, W.; Vandamme, E. J. Microbial production and application of sophorolipids. *Applied Microbiology and Biotechnology* **2007**, *76*, 23-34.

(67) Van Bogaert, I.; Fleurackers, S.; Van Kerrebroeck, S.; Develter, D.; Soetaert, W. Production of new-to-nature sophorolipids by cultivating the yeast Candida bombicola on unconventional hydrophobic substrates. *Biotechnology and Bioengineering* **2011**, *108*, 734-741.

(68) Lang, S.; Katsiwela, E.; Wagner, F. Antimicrobial effects of biosurfactants. *Lipid/Fett* **1989**, *91*, 363-366.

(69) Halling, P. J. Thermodynamic predictions for biocatalysis in nonconventional media: theory, tests, and recommendations for experimental design and analysis. *Enzyme and microbial technology* **1994**, *16*, 178-206.

(70) Furuta, T.; Igarashi, K.; Hirata, Y.: Low-foaming detergent compositions. *US Patent* 20,040,171,512, **2004**.

(71) Kawano, J.; Utsugi, T.; Inoue, S.; Hayashi, S.: Powdered compressed cosmetic material. *Google Patents*, **1981**.

(72) Mager, H.; Röthlisberger, R.; Wzgner, F. Use of sophorose-lipid lactone for the treatment of dandruffs and body odour. *European patent* **1987**, *209783*.

(73) Shao, L.; Song, X.; Ma, X.; Li, H.; Qu, Y. Bioactivities of sophorolipid with different structures against human esophageal cancer cells. *Journal of Surgical Research* **2012**, *173*, 286-291.

(74) Marchal R, L. J., Sulzer C, Davila AM Production of sophorolipid acetate acids from oils or esters. *US Patent 5900366* **1999**.

(75) Pesce, L. A biotechnological method for the regeneration of hydrocarbons from dregs and muds, on the base of biosurfactants. *World patent* **2002**, *2*, 062495.

(76) Ducreux, J.; Ballerini, D.; Baviere, M.; Bocard, C.; Monin, N.: Composition containing a surface active compound and glycolipids and decontamination process for a porous medium polluted by hydrocarbons. *Google Patents*, **1997**.

(77) Takashi, N.; Yoji, A.; Kazuo, N.; Tatsu, N.; Sumiko, T.; Jotaro, N. Composition for high-density cold storage transportation. *Japanese patent* **2001**, *2001131538*.

(78) Pellecier, F.; André, P. Cosmetic use of sophorolipids as subcutaneous adipose cushion regulation agents and slimming application. *World patent,* **2004**, *108063*, 208.

(79) Shah, V.; Doncel, G. F.; Seyoum, T.; Eaton, K. M.; Zalenskaya, I.; Hagver, R.; Azim, A.; Gross, R. Sophorolipids, microbial glycolipids with anti-human immunodeficiency virus and sperm-immobilizing activities. *Antimicrobial Agents and Chemotherapy* **2005**, *49*, 4093-4100.

(80) Bluth, M. H.; Kandil, E.; Mueller, C. M.; Shah, V.; Lin, Y.-Y.; Zhang, H.; Dresner, L.; Lempert, L.; Nowakowski, M.; Gross, R. Sophorolipids block lethal effects of septic shock in rats in a cecal ligation and puncture model of experimental sepsis*. *Critical care medicine* **2006**, *34*, E188.

(81) Sleiman, J. N.; Kohlhoff, S. A.; Roblin, P. M.; Wallner, S.; Gross, R.; Hammerschlag, M. R.; Zenilman, M. E.; Bluth, M. H. Sophorolipids as antibacterial agents. *Annals of Clinical & Laboratory Science* **2009**, *39*, 60-63.

(82) Lo, C.-M.; Ju, L.-K. Sophorolipids-induced cellulase production in cocultures of Hypocrea jecorina Rut C30 and Candida bombicola. *Enzyme and Microbial Technology* **2009**, *44*, 107-111.

(83) Gross, R.; Shah, V. Anti-herpes virus properties of various forms of sophorolipids. *World patent WO2007US63701* **2007**.

(84) Singh, S.; Patel, P.; Jaiswal, S.; Prabhune, A.; Ramana, C.; Prasad, B. A direct method for the preparation of glycolipid–metal nanoparticle conjugates: sophorolipids as reducing and capping agents for the synthesis of water re-dispersible silver nanoparticles and their antibacterial activity. *New Journal of Chemistry* **2009**, *33*, 646-652.

(85) Develter, D. W.; Fleurackers, S. J. Sophorolipids and rhamnolipids. *Surfactants from Renewable Resources* **2010**, 213.

(86) Dekoster, C. G.; Heerma, W.; Pepermans, H. A.; Groenewegen, A.; Peters, H.; Haverkamp, J. Tandem mass spectrometry and nuclear magnetic resonance spectroscopy studies of Candida bombicola sophorolipids and product formed on hydrolysis by cutinase. *Analytical biochemistry* **1995**, *230*, 135-148.

(87) Rau, U.; Heckmann, R.; Wray, V.; Lang, S. Enzymatic conversion of a sophorolipid into a glucose lipid. *Biotechnology letters* **1999**, *21*, 973-977.

(88) Hu, Y.; Ju, L. K. Lipase-Mediated Deacetylation and Oligomerization of Lactonic Sophorolipids. *Biotechnology progress* **2003**, *19*, 303-311.

(89) Allingham, R. Sophoroside esters in prepared food products. *US patent* **1971**, *3622344*.

(90) Zhang, L.; Somasundaran, P.; Singh, S. K.; Felse, A. P.; Gross, R. Synthesis and interfacial properties of sophorolipid derivatives. *Colloids and Surfaces A: Physicochemical and Engineering Aspects* **2004**, *240*, 75-82.

(91) Bisht, K. S.; Gross, R. A.; Kaplan, D. L. Enzyme-mediated regioselective acylations of sophorolipids. *The Journal of Organic Chemistry* **1999**, *64*, 780-789.

(92) Recke, V. K.; Gerlitzki, M.; Hausmann, R.; Syldatk, C.; Wray, V.; Tokuda, H.; Suzuki, N.; Lang, S. Enzymatic production of modified 2-dodecyl-sophorosides (biosurfactants) and their characterization. *European Journal of Lipid Science and Technology* **2013**, *115*, 452-463.

(93) Carr, J. A.; Bisht, K. S. Enzyme-catalyzed regioselective transesterification of peracylated sophorolipids. *Tetrahedron* **2003**, *59*, 7713-7724.

(94) Zerkowski, J. A.; Solaiman, D. K.; Ashby, R. D.; Foglia, T. A. Head group-modified sophorolipids: Synthesis of new cationic, zwitterionic, and anionic surfactants. *Journal of Surfactants and Detergents* **2006**, *9*, 57-62.

(95) Kurtzman, C. P.; Price, N. P.; Ray, K. J.; Kuo, T.-M. Production of sophorolipid biosurfactants by multiple species of the Starmerella (Candida) bombicola yeast clade. *FEMS microbiology letters* **2010**, *311*, 140-146.

(96) Solaiman, D. K.; Ashby, R. D.; Nuñez, A.; Foglia, T. A. Production of sophorolipids by Candida bombicola grown on soy molasses as substrate*,**. *Biotechnology letters* **2004**, *26*, 1241-1245.

(97) Nuñez, A.; Ashby, R.; Foglia, T. A.; Solaiman, D. K. LC/MS analysis and lipase modification of the sophorolipids produced by Rhodotorula bogoriensis**. *Biotechnology letters* **2004**, *26*, 1087-1093.

(98) Solaiman, D. K.; Ashby, R. D.; Zerkowski, J. A.; Foglia, T. A. Simplified soy molasses-based medium for reduced-cost production of sophorolipids by Candida bombicola. *Biotechnology letters* **2007**, *29*, 1341-1347.

(99) Nunez, A.; Ashby, R.; Foglia, T.; Solaiman, D. Analysis and characterization of sophorolipids by liquid chromatography with atmospheric pressure chemical ionization. *Chromatographia* **2001**, *53*, 673-677.

(100) Ashby, R. D.; Solaiman, D. K.; Foglia, T. A. Property control of sophorolipids: influence of fatty acid substrate and blending. *Biotechnology letters* **2008**, *30*, 1093-1100.

(101) Ratsep, P.; Shah, V. Identification and quantification of sophorolipid analogs using ultra-fast liquid chromatography–mass spectrometry. *Journal of Microbiological Methods* **2009**, *78*, 354-356.

(102) Cavalero, D. A.; Cooper, D. G. The effect of medium composition on the structure and physical state of sophorolipids produced by Candida bombicola ATCC 22214. *Journal of Biotechnology* **2003**, *103*, 31-41.

(103) Ma, X.-j.; Li, H.; Shao, L.-j.; Shen, J.; Song, X. Effects of nitrogen sources on production and composition of sophorolipids by Wickerhamiella domercqiae var. sophorolipid CGMCC 1576. *Applied Microbiology and Biotechnology* **2011**, *91*, 1623-1632.

(104) Shin, J. D.; Lee, J.; Kim, Y. B.; Han, I.-s.; Kim, E.-K. Production and characterization of methyl ester sophorolipids with 22-carbon-fatty acids. *Bioresource Technology* **2010**, *101*, 3170-3174.

(105) Hu, Y.; Ju, L.-K. Purification of lactonic sophorolipids by crystallization. *Journal of biotechnology* **2001**, *87*, 263-272.

(106) Daverey, A.; Pakshirajan, K. Production, characterization, and properties of sophorolipids from the yeast Candida bombicola using a low-cost fermentative medium. *Applied Biochemistry and biotechnology* **2009**, *158*, 663-674.

(107) Daverey, A.; Pakshirajan, K. Sophorolipids from Candida bombicola using mixed hydrophilic substrates: production, purification and characterization. *Colloids and surfaces B: Biointerfaces* **2010**, *79*, 246-253.

(108) Blake, J.; Richards, G. A critical re-examination of problems inherent in compositional analysis of hemicelluloses by gas-liquid chromatography. *Carbohydrate Research* **1970**, *14*, 375-387.

(109) Vliegenthart, J.; Gerwig, G.; Kamerling, J. Determination of the D and L configuration of neutral monosaccharides by high-resolution capillary GLC. *Carbohydrate Research* **1978**, *62*, 349-357.

(110) Rocklin, R. D.; Pohl, C. A. Determination of carbohydrates by anion exchange chromatography with pulsed amperometric detection. *Journal of Liquid Chromatography* **1983**, *6*, 1577-1590.

(111) Cataldi, T. R.; Margiotta, G.; Zambonin, C. G. Determination of sugars and alditols in food samples by HPAEC with integrated pulsed amperometric detection using alkaline eluents containing barium or strontium ions. *Food Chemistry* **1998**, *62*, 109-115.

(112) Cataldi, T. R.; Campa, C.; De Benedetto, G. E. Carbohydrate analysis by high-performance anion-exchange chromatography with pulsed amperometric detection: The potential is still growing. *Fresenius' Journal of Analytical Chemistry* **2000**, *368*, 739-758.

(113) El-Rassi, Z.: *Carbohydrate analysis by modern chromatography and electrophoresis*; Elsevier, **2002**; Vol. 66.

(114) Corradini, C.; Cavazza, A.; Bignardi, C. High-performance anion-exchange chromatography coupled with pulsed electrochemical detection as a powerful tool to evaluate carbohydrates of food interest: principles and applications. *International Journal of Carbohydrate Chemistry* **2012**, *2012*.

(115) Lee, Y. C. High-performance anion-exchange chromatography for carbohydrate analysis. *Analytical Biochemistry* **1990**, *189*, 151-162.

(116) A, H. High performance anion exchange chromatography with pulsed amperometric detection a powerful tool for the analysis of dietary fiber and complex carbohydrates. *New York: Marcel Dekker, Incorporated; 1999.*

(117) Ruiz-Matute, A. I.; Hernandez-Hernandez, O.; Rodríguez-Sánchez, S.; Sanz, M. L.; Martínez-Castro, I. Derivatization of carbohydrates for GC and GC–MS analyses. *Journal of Chromatography B* **2011**, *879*, 1226-1240.

(118) Medeiros, P. M.; Simoneit, B. R. Analysis of sugars in environmental samples by gas chromatography–mass spectrometry. *Journal of Chromatography A* **2007**, *1141*, 271-278.

(119) Gómez-González, S.; Ruiz-Jiménez, J.; Priego-Capote, F.; Luque de Castro, M. a. D. Qualitative and Quantitative Sugar Profiling in Olive Fruits, Leaves, and Stems by Gas Chromatography− Tandem Mass Spectrometry (GC-MS/MS) after Ultrasound-Assisted Leaching. *Journal of Agricultural and Food Chemistry* **2010**, *58*, 12292-12299.

(120) Gerwig, G. J.; Kamerling, J. P.; Vliegenthart, J. F. Determination of the absolute configuration of monosaccharides in complex carbohydrates by capillary GLC. *Carbohydrate research* **1979**, *77*, 1-7.

(121) Albersheim, P.; Nevins, D. J.; English, P. D.; Karr, A. A method for the analysis of sugars in plant cell-wall polysaccharides by gas-liquid chromatography. *Carbohydrate Research* **1967**, *5*, 340-345.

(122) Stellner, K.; Saito, H.; Hakomori, S.-I. Determination of aminosugar linkages in glycolipids by methylation: aminosugar linkages of ceramide pentasaccharides of rabbit erythrocytes and of Forssman antigen. *Archives of Biochemistry and Biophysics* **1973**, *155*, 464-472.

(123) Lama, L.; Nicolaus, B.; Calandrelli, V.; Manca, M. C.; Romano, I.; Gambacorta, A. Effect of growth conditions on endo-and exopolymer biosynthesis in Anabaena cylindrica 10 C. *Phytochemistry* **1996**, *42*, 655-659.

(124) Poli, A.; Anzelmo, G.; Nicolaus, B. Bacterial exopolysaccharides from extreme marine habitats: production, characterization and biological activities. *Marine Drugs* **2010**, *8*, 1779-1802.

(125) Large, D. G.; Warren, C. D.: *Glycopeptides and Related Compounds: Synthesis, Analysis, and Applications*; CRC Press, **1997**.

(126) Purdie, T.; Irvine, J. C. CIX.—The stereoisomeric tetramethyl methylglucosides and tetramethyl glucose. *Journal of the Chemical Society, Transactions* **1904**, *85*, 1049-1070.

(127) Denham, W. S., Woodhouse HJ. The methylation of cellulose. *J. Chem. Soc.* **1913**, *103*, 1735–1741.

(128) HAKOMORI, S.-I. A rapid permethylation of glycolipid, and polysaccharide catalyzed by methylsulfinyl carbanion in dimethyl sulfoxide. *The Journal of Biochemistry* **1964**, *55*, 205-208.

(129) Brimacombe, J.; Jones, B.; Stacey, M.; Willard, J. Alkylation of carbohydrates using sodium hydride. *Carbohydrate Research* **1966**, *2*, 167-169.

(130) Ciucanu, I.; Kerek, F. A simple and rapid method for the permethylation of carbohydrates. *Carbohydrate Research* **1984**, *131*, 209-217.

(131) Ciucanu, I.; Costello, C. E. Elimination of oxidative degradation during the per-O-methylation of carbohydrates. *Journal of the American Chemical Society* **2003**, *125*, 16213-16219.

(132) Chakladar, S.; Wang, Y.; Clark, T.; Cheng, L.; Ko, S.; Vocadlo, D. J.; Bennet, A. J. A mechanism-based inactivator of glycoside hydrolases involving formation of a transient non-classical carbocation. *Nature Communications* **2014**, *5*.

(133) Clarke, A.; Bray, M.; Strating, H., Types of glycoside hydrolyase, *Carbohydrate Research* **1988**, *12*, 20-26.

(134) Sinnott, M. L. Catalytic mechanism of enzymic glycosyl transfer. *Chemical Reviews* **1990**, *90*, 1171-1202.

(135) Davies, G.; Henrissat, B. Structures and mechanisms of glycosyl hydrolases. *Structure* **1995**, *3*, 853-859.

(136) Rye, C. S.; Withers, S. G. Glycosidase mechanisms. *Current opinion in chemical biology* **2000**, *4*, 573-580.

(137) McCarter, J. D.; Withers, S. G. 5-Fluoro glycosides: a new class of mechanism-based inhibitors of both α-and β-glucosidases. *Journal of the American Chemical Society* **1996**, *118*, 241-242.

(138) Zechel, D. L.; Withers, S. G. Glycosidase mechanisms: anatomy of a finely tuned catalyst. *Accounts of Chemical Research* **2000**, *33*, 11-18.

(139) Vuong, T. V.; Wilson, D. B. Glycoside hydrolases: catalytic base/nucleophile diversity. *Biotechnology and Bioengineering* **2010**, *107*, 195-205.

(140) Poomtien, J.; Thaniyavarn, J.; Pinphanichakarn, P.; Jindamorakot, S.; Morikawa, M. Production and Characterization of a Biosurfactant from Cyberlindnera samutprakarnensis JP52T. *Bioscience, Biotechnology, and Biochemistry* **2013**, *77*, 2362-2370.

(141) Cuvier, A.-S.; Berton, J.; Stevens, C. V.; Fadda, G. C.; Babonneau, F.; Van Bogaert, I. N.; Soetaert, W.; Pehau-Arnaudet, G.; Baccile, N. pH-triggered formation of nanoribbons from yeast-derived glycolipid biosurfactants. *Soft matter* **2014**, *10*, 3950-3959.

(142) Bisht, K. S.; Gao, W.; Gross, R. A. Glycolipids from Candida bombicola: polymerization of a 6-O-acryloyl sophorolipid derivative. *Macromolecules* **2000**, *33*, 6208-6210.

(143) Dubois, M.; Gilles, K. A.; Hamilton, J. K.; Rebers, P.; Smith, F. Colorimetric method for determination of sugars and related substances. *Analytical Chemistry* **1956**, *28*, 350-356.

(144) Jourdier, E.; Ben Chaabane, F.: PROCESS FOR THE PRODUCTION OF SOPHOROSE STARTING FROM SOPHOROLIPIDS. *US Patent,* 20,150,336,999, **2015**.

(145) Vogel, A. I. Textbook of Practical Organic Chemistry 5th Ed. *Prentice Hall* **1996**.

(146) Pet, W. a. H. *Chem.Ind.* **1955,** *12*,125-129.

(147) Whelam, H. a. *J.Chem.Soc.(Lond)* **1958**, *23*, 1342-1350.

(148) Koeppen, B. Some observations on the synthesis of sophorose. *Carbohydrate Research* **1968**, *7*, 410-413.

(149) Redemann, C.; Niemann, C. Acetobromoglucose. *Organic Syntheses* **1998**, *Vol. III*, 11-14.

(150) Migrdichious, V. *Organic Syntheses* **1998**, *Vol. III*, 52.

(151) Schmidt, R. R. New Methods for the Synthesis of Glycosides and Oligosaccharides—Are There Alternatives to the Koenigs-Knorr Method?[New Synthetic Methods (56)]. *Angewandte Chemie International Edition in English* **1986**, *25*, 212-235.

(152) Garegg, P.; Konradsson, P.; Kvarnström, I.; Norberg, T.; Svensson, S.; Wigilius, B. Studies on Koenigs-Knorr glycosidations. *Acta Chem. Scand. B* **1985**, *39*, 41-50.

(153) Crich, D. Mechanism of a chemical glycosylation reaction. *Accounts of Chemical Research* **2010**, *43*, 1144-1153.

(154) Van Doren, H. A.; van der Geest, R.; Kellogg, R. M.; Wynberg, H. Synthesis and liquid crystalline properties of the n-alkyl 1-thio-α-d-glucopyranosides, a new homologous series of carbohydrate mesogens. *Carbohydrate Research* **1989**, *194*, 71-77.

(155) Mabic, S.; Benezra, C.; Lepoittevin, J.-P. Direct synthesis of mono-glycosylated catechols from glycosylacetates or imidates using BF 3. OEt 2 as catalyst. *Tetrahedron letters* **1993**, *34*, 4531-4534.

(156) Sokolov, V.; Zakharov, V.; Studentsov, E. Stereoselectivity of Reactions at the Glycoside Center of Carbohydrates: VII. Synthesis of Aryl α-and-β-D-Glucopyranosides by Helferich, Catalyzed by Boron Trifluoride Etherate. *Russian Journal of General Chemistry* **2002**, *72*, 806-811.

(157) Seela, F.; Winkeler, D. Preferred β-Glycoside Formation by Phase Transfer Catalysis in the Synthesis of D-Arabinofuranosyl-7-deazapurine Nucleosides. *Angewandte Chemie International Edition in English* **1979**, *18*, 536-536.

(158) Chrétien, F.; Di Cesare, P.; Gross, B. Synthesis of thiodisaccharides using phase-transfer catalysis. *Journal of the Chemical Society, Perkin Transactions 1* **1988**, 3297-3300.

(159) Cao, S.; Tropper, F. D.; Roy, R. Stereoselective phase transfer catalyzed syntheses of glycosyloxysuccinimides and their transformations into glycoprobes. *Tetrahedron* **1995**, *51*, 6679-6686.

(160) Ma, X.; Li, H.; Song, X. Surface and biological activity of sophorolipid molecules produced by Wickerhamiella domercqiae var. sophorolipid CGMCC 1576. *Journal of Colloid and Interface Science* **2012**, *376*, 165-172.

(161) Faustino, C. M. C.; Calado, A. R. T.; Garcia-Rio, L. Dimeric and monomeric surfactants derived from sulfur-containing amino acids. *Journal of Colloid and Interface Science* **2010**, *351*, 472-477.

(162) Marchant, R.; Banat, I. M. Microbial biosurfactants: challenges and opportunities for future exploitation. *Trends in Biotechnology* **2012**, *30*, 558-565.

(163) Tulloch, A.; Spencer, J.; Gorin, P. The fermentation of long-chain compounds by torulopsis magnoliae: i. structures of the hydroxy fatty acids obtained by the fermentation of fatty acids and hydrocarbons. *Canadian Journal of Chemistry* **1962**, *40*, 1326-1338.

(164) Ribeiro, I. A.; Bronze, M. R.; Castro, M. F.; Ribeiro, M. H. Design of selective production of sophorolipids by Rhodotorula bogoriensis through nutritional requirements. *Journal of Molecular Recognition* **2012**, *25*, 630-640.

(165) Tulloch, A.; Hill, A.; Spencer, J. Structure and reactions of lactonic and acidic sophorosides of 17-hydroxyoctadecanoic acid. *Canadian Journal of Chemistry* **1968**, *46*, 3337-3351.

(166) Davila, A.-M.; Marchal, R.; Vandecasteele, J.-P. Kinetics and balance of a fermentation free from product inhibition: sophorose lipid production by Candida bombicola. *Applied Microbiology and Biotechnology* **1992**, *38*, 6-11.

(167) Hommel, R.; Weber, L.; Weiss, A.; Himmelreich, U.; Rilke, O.; Kleber, H.-P. Production of sophorose lipid by Candida (Torulopsis) apicola grown on glucose. *Journal of Biotechnology* **1994**, *33*, 147-155.

(168) Recke, V. K.; Beyrle, C.; Gerlitzki, M.; Hausmann, R.; Syldatk, C.; Wray, V.; Tokuda, H.; Suzuki, N.; Lang, S. Lipase-catalyzed acylation of microbial mannosylerythritol lipids (biosurfactants) and their characterization. *Carbohydrate Research* **2013**, *373*, 82-88.

(169) Fox, A.; Morgan, S.; Gilbart, J.; Biermann, C.; McGinnis, G. Analysis of Carbohydrates by GLC and MS. *Analysis of Carbohydrates by GLC and MS* **1989**.

(170) Falus, G.; Nowakowski, M.; Bluth, M.; Aikens, J.: Purified Ethyl Ester Sophorolipid for the Treatment of Sepsis. *Google Patents*, **2011**.

(171) Azim, A.; Shah, V.; Doncel, G. F.; Peterson, N.; Gao, W.; Gross, R. Amino acid conjugated sophorolipids: a new family of biologically active functionalized glycolipids. *Bioconjugate Chemistry* **2006**, *17*, 1523-1529.

(172) Gao, W.; Hagver, R.; Shah, V.; Xie, W.; Gross, R. A.; Ilker, M. F.; Bell, C.; Burke, K. A.; Coughlin, E. B. Glycolipid polymer synthesized from natural lactonic sophorolipids by ring-opening metathesis polymerization. *Macromolecules* **2007**, *40*, 145-147.

(173) Hu, Y.; Ju, L.-K. Sophorolipid production from different lipid precursors observed with LC-MS. *Enzyme and Microbial Technology* **2001**, *29*, 593-601.

(174) Bajaj, V.; Tilay, A.; Annapure, U. Enhanced production of bioactive sophorolipids by Starmerella bombicola NRRL Y-17069 by design of experiment approach with successive purification and characterization. *Journal of Oleo Science* **2012**, *61*, 377-386.

(175) Mandels, M.; Parrish, F. W.; Reese, E. T. Sophorose as an inducer of cellulase in Trichoderma viride. *Journal of Bacteriology* **1962**, *83*, 400-408.

(176) Francis, G.; Kerem, Z.; Makkar, H. P.; Becker, K. The biological action of saponins in animal systems: a review. *British journal of Nutrition* **2002**, *88*, 587-605.

(177) Attele, A. S.; Wu, J. A.; Yuan, C.-S. Ginseng pharmacology: multiple constituents and multiple actions. *Biochemical Pharmacology* **1999**, *58*, 1685-1693.

(178) Freudenberg, K.; Toepffer, H.; Andersen, C. C. Zur Kenntnis der Aceton-Zucker, XV.: Versuche zur Synthese von Disacchariden. *Berichte der deutschen chemischen Gesellschaft (A and B Series)* **1928**, *61*, 1750-1760.

(179) Thompson, A.; Anno, K.; Wolfrom, M.; Inatome, M. Acid reversion products from D-glucose. *Journal of the American Chemical Society* **1954**, *76*, 1309-1311.

(180) COXON, B.; FLETCHER Jr, H. G. Simplified preparation of sophorose (2-O-β-d-glucopyranosyl-d-glucose). *The Journal of Organic Chemistry* **1961**, *26*, 2892-2894.

(181) Clancy, M. 823. Sophorose and its derivatives. *Journal of the Chemical Society (Resumed)* **1960**, *25*, 4213-4217.

(182) WOOD JR, H. B.; Allerton, R.; DIEHL, H. W.; FLETCHER JR, H. G. Stevioside. I. The structure of the glucose moieties. *The Journal of Organic Chemistry* **1955**, *20*, 875-883.

(183) Hoffmann, N.; Pietruszka, J.; Söffing, C. From sophorose lipids to natural product synthesis. *Advanced Synthesis & Catalysis* **2012**, *354*, 959-963.

(184) Fleurackers, S. J. On the use of waste frying oil in the synthesis of sophorolipids. *EuropeanJournal of Lipid Science and Technology* **2006**, *108*, 5-12.

(185) Weber, A.; Zeiner, T. Purification of Biosurfactants 9. *Biosurfactants: Production and Utilization—Processes, Technologies, and Economics* **2014**, *159*, 129.

(186) Whelan, W.; Bailey, J.; Roberts, P. 260. The mechanism of carbohydrase action. Part I. The preparation and properties of maltodextrin substrates. *Journal of the Chemical Society (Resumed)* **1953**, 1293-1298.

(187) LINBERG, B.; WICKBERG, B. Separation of methylated sugars on carbon columns. *Acta. Chem. Scand.* **1954**, *8*, 205-301.

(188) SALEM, A.; Johnson, J. Influence of various oligosaccharides on staling of bread. *Food Technology* **1965**, *19*, 849-&.

(189) Miller, G. L. Micro column chromatographic method for analysis of oligosaccharides. *Analytical Biochemistry* **1960**, *1*, 133-140.

(190) Abe, T.; Horiuchi, K.; Kikuchi, H.; Aritsuka, T.; Takata, Y.; Fukushi, E.; Fukushi, Y.; Kawabata, J.; Ueno, K.; Onodera, S. Structural confirmation of oligosaccharides newly isolated from sugar beet molasses. *Chemistry Central Journal* **2012**, *6*, 89.

(191) Van Bogaert, I. N.; Zhang, J.; Soetaert, W. Microbial synthesis of sophorolipids. *Process Biochemistry* **2011**, *46*, 821-833.

(192) Gakhokidze, R. A. Saccharinic acids. *Russian Chemical Reviews* **1980**, *49*, 222.

(193) Knill, C. J.; Kennedy, J. F. Degradation of cellulose under alkaline conditions. *Carbohydrate Polymers* **2003**, *51*, 281-300.

(194) Lobry de Bruyn, C. Action of dilute alkalis on the carbohydrates. *Rec. Trav. Chim.* **1895**, *14*, 156-165.

(195) Kobayashi, H.; Shibata, N.; Konno, S.; Hisamicha, K.; Suzuki, S. Epimerization of reducing terminal groups of (1→ 2)-linked d-gluco-and d-manno-disaccharides in aqueous sodium hydroxide. *Carbohydrate research* **1992**, *229*, 369-375.

(196) Van Bogaert, I. N.; Holvoet, K.; Roelants, S. L.; Li, B.; Lin, Y. C.; Van de Peer, Y.; Soetaert, W. The biosynthetic gene cluster for sophorolipids: a biotechnological interesting biosurfactant produced by Starmerella bombicola. *Molecular microbiology* **2013**, *88*, 501-509.

(197) Adachi, S.; Kobayashi, T. Synthesis of esters by immobilized-lipase-catalyzed condensation reaction of sugars and fatty acids in water-miscible organic solvent. *Journal of bioscience and bioengineering* **2005**, *99*, 87-94.

(198) Koenigs, W.; Knorr, E. Ueber einige Derivate des Traubenzuckers und der Galactose. *Berichte der deutschen chemischen Gesellschaft* **1901**, *34*, 957-981.

(199) Mydock, L. K.; Demchenko, A. V. Mechanism of chemical O-glycosylation: from early studies to recent discoveries. *Organic & biomolecular chemistry* **2010**, *8*, 497-510.

(200) Demchenko, A. V. General aspects of the glycosidic bond formation. *Handbook of Chemical Glycosylation* **2008**, *9*,1-27.

(201) Zhu, X.; Schmidt, R. R. New Principles for Glycoside-Bond Formation. *Angewandte Chemie International Edition* **2009**, *48*, 1900-1934.

(202) Nigudkar, S. S.; Demchenko, A. V. Stereocontrolled 1, 2-cis glycosylation as the driving force of progress in synthetic carbohydrate chemistry. *Chemical Science* **2015**, *6*, 2687-2704.

(203) Hanessian, S.; Guindon, Y. Chemistry of the glycosidic linkage. Direct conversion of glycosides into 1-thioglycosides by use of [alkyl (or aryl) thio] trimethylsilanes. *Carbohydrate Research* **1980**, *86*, C3-C6.

(204) Toshima, K.; Tatsuta, K. Recent progress in O-glycosylation methods and its application to natural products synthesis. *Chemical reviews* **1993**, *93*, 1503-1531.

(205) Peng, P.; Schmidt, R. R. An Alternative Reaction Course in O-Glycosidation with O-Glycosyl Trichloroacetimidates as Glycosyl Donors and Lewis Acidic Metal Salts as Catalyst: Acid–Base Catalysis with Gold Chloride-Glycosyl Acceptor Adducts. *Journal of the American Chemical Society* **2015**, *137*, 12653-12659.

(206) Takeo, K. i. Koenigs-Knorr reaction of methyl 4, 6-O-benzylidene-beta-D-glucopyranoside with 2, 3, 4, 6-tetra-o-acetyl-alpha-D-glucopyranosyl bromide. *Carbohydrate Research* **1979,** *70*, 25-32.

(207) Takeo, K. i. Synthesis of benzyl?-and?-sophorosides, and of benzyl?-laminarabioside. *Carbohydrate Research* **1980**, *86*, 151-157.

223

(208) Kanchanapoom, T.; Kasai, R.; Picheansoonthon, C.; Yamasaki, K. Megastigmane, aliphatic alcohol and benzoxazinoid glycosides from Acanthus ebracteatus. *Phytochemistry* **2001**, *58*, 811-817.

(209) US national libray of medicine, online available at: https://www.nlm.nih.gov.

(210) Silverstein, R. M.; Webster, F. X.; Kiemle, D. J.; Bryce, D. L.: *Spectrometric identification of organic compounds*; *John Wiley & Sons*, **2014**.

(211) Yan, L.; Kahne, D. Generalizing glycosylation: synthesis of the blood group antigens Lea, Leb, and Lex using a standard set of reaction conditions. *Journal of the American Chemical Society* **1996**, *118*, 9239-9248.

(212) Cooper, D. G.; Paddock, D. Production of a biosurfactant from Torulopsis bombicola. *Applied and environmental microbiology* **1984**, *47*, 173-176.

(213) Rau, U.; Hammen, S.; Heckmann, R.; Wray, V.; Lang, S. Sophorolipids: a source for novel compounds. *Industrial Crops and Products* **2001**, *13*, 85-92.

(214) Daniel, H.-J.; Otto, R.; Binder, M.; Reuss, M.; Syldatk, C. Production of sophorolipids from whey: development of a two-stage process with Cryptococcus curvatus ATCC 20509 and Candida bombicola ATCC 22214 using deproteinized whey concentrates as substrates. *Applied Microbiology and Biotechnology* **1999**, *51*, 40-45.

(215) Liu, X.-L.; Zeng, G.-M.; Tang, L.; Zhong, H.; Wang, R.-Y.; Fu, H.-Y.; Liu, Z.-F.; Hung, H.-l.; Zhang, J.-C. Effects of dirhamnolipid and SDS on enzyme production from Phanerochaete chrysosporium in submerged fermentation. *Process Biochemistry* **2008**, *43*, 1300-1303.

(216) Helle, S. S.; Duff, S. J.; Cooper, D. G. Effect of surfactants on cellulose hydrolysis. *Biotechnology and Bioengineering* **1993**, *42*, 611-617.

(217) Shah, V.; Badia, D.; Ratsep, P. Sophorolipids having enhanced antibacterial activity. *Antimicrobial Agents and Chemotherapy* **2007**, *51*, 397-400.

(218) Fu, S. L.; Wallner, S. R.; Bowne, W. B.; Hagler, M. D.; Zenilman, M. E.; Gross, R.; Bluth, M. H. Sophorolipids and their derivatives are lethal against human pancreatic cancer cells. *Journal of Surgical Research* **2008**, *148*, 77-82.

(219) De Rienzo, M. A. D.; Banat, I. M.; Dolman, B.; Winterburn, J.; Martin, P. J. Sophorolipid biosurfactants: Possible uses as antibacterial and antibiofilm agent. *NewBiotechnology* **2015**.

(220) Zhang, Y.; Han, G.; Fan, B.; Zhou, Y.; Zhou, X.; Wei, L.; Zhang, J. Green tea (−)-epigallocatechin-3-gallate down-regulates VASP expression and inhibits breast cancer cell migration and invasion by attenuating Rac1 activity. *European Journal of Pharmacology* **2009**, *606*, 172-179.

(221) Delbeke, E.; Roman, B.; Marin, G.; Van Geem, K.; Stevens, C. A new class of antimicrobial biosurfactants: quaternary ammonium sophorolipids. *Green Chemistry* **2015**, *17*, 3373-3377.

(222) Zhang, L.; Somasundaran, P.; Maltesh, C. Adsorption ofn-Dodecyl-β-d-maltoside on Solids. *Journal of Colloid and Interface Science* **1997**, *191*, 202-208.

(223) Shen, R.; Wang, S.; Ma, X.; Xian, J.; Li, J.; Zhang, L.; Wang, P. An easy colorimetric assay for glycosyltransferases. *Biochemistry (Moscow)* **2010**, *75*, 944-950.

(224) Cortés-Sánchez, A. d. J.; Hernández-Sánchez, H.; Jaramillo-Flores, M. E. Biological activity of glycolipids produced by microorganisms: New trends and possible therapeutic alternatives. *Microbiological Research* **2013**, *168*, 22-32.

(225) Kulakovskaya, E.; Baskunov, B.; Zvonarev, A. The Antibiotic and Membrane-damaging Activities of Cellobiose Lipids and Sophorose Lipids. *Journal of Oleo Science* **2014**, *63*, 701-707.

(226) Joshi-Navare, K.; Prabhune, A. A biosurfactant-sophorolipid acts in synergy with antibiotics to enhance their efficiency. *BioMedResearch International* **2013**.

(227) Types of Prostate Cancer. Online available at:. *http://www.cancerresearchuk.org/about-cancer/type/prostate-cancer/about/prostate-cancer-types#adeno*.

(228) Fackler, O. T.; Grosse, R. Cell motility through plasma membrane blebbing. *The Journal of Cell Biology* **2008**, *181*, 879-884.

8.1 Publication

1. Ammar, AL-Jasim, Mark Davis, Douglas Cossar, Timothy Miller, Paul Humphreys, and Andrew P. Laws. "Isolation of sophorose during sophorolipid production and studies of its stability in aqueous alkali: epimerisation of sophorose to 2-*O*-β-D-glucopyranosyl-D-mannose." *Carbohydrate Research* **2016**, *421*, 46-54.

226

9. Appendix I

Calibration curves of glucose and sophorose standards:

Glucose standard calibration curve

y = 2.8564x - 30.372
R² = 0.9926

Sophoros standandard calibration curve

y = 2.1444x - 1.7082
R² = 0.9993